Appendix 6B. Figures

Figure 6-1. Minimum Containment Sump pH Following a Design Basis LOCA

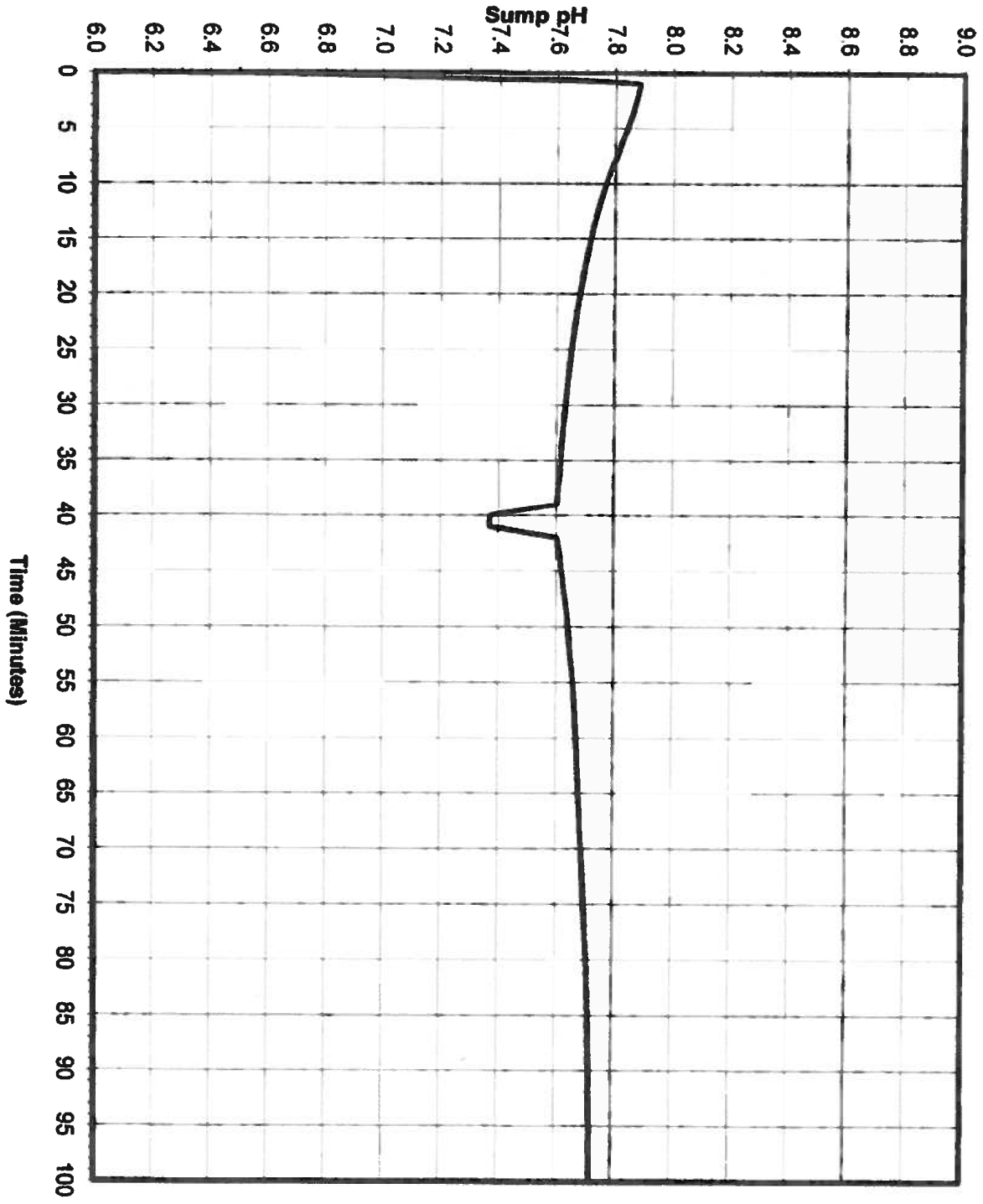

Figure 6-2. Sensitivity of Peak Pressure to Air Compression Ratio

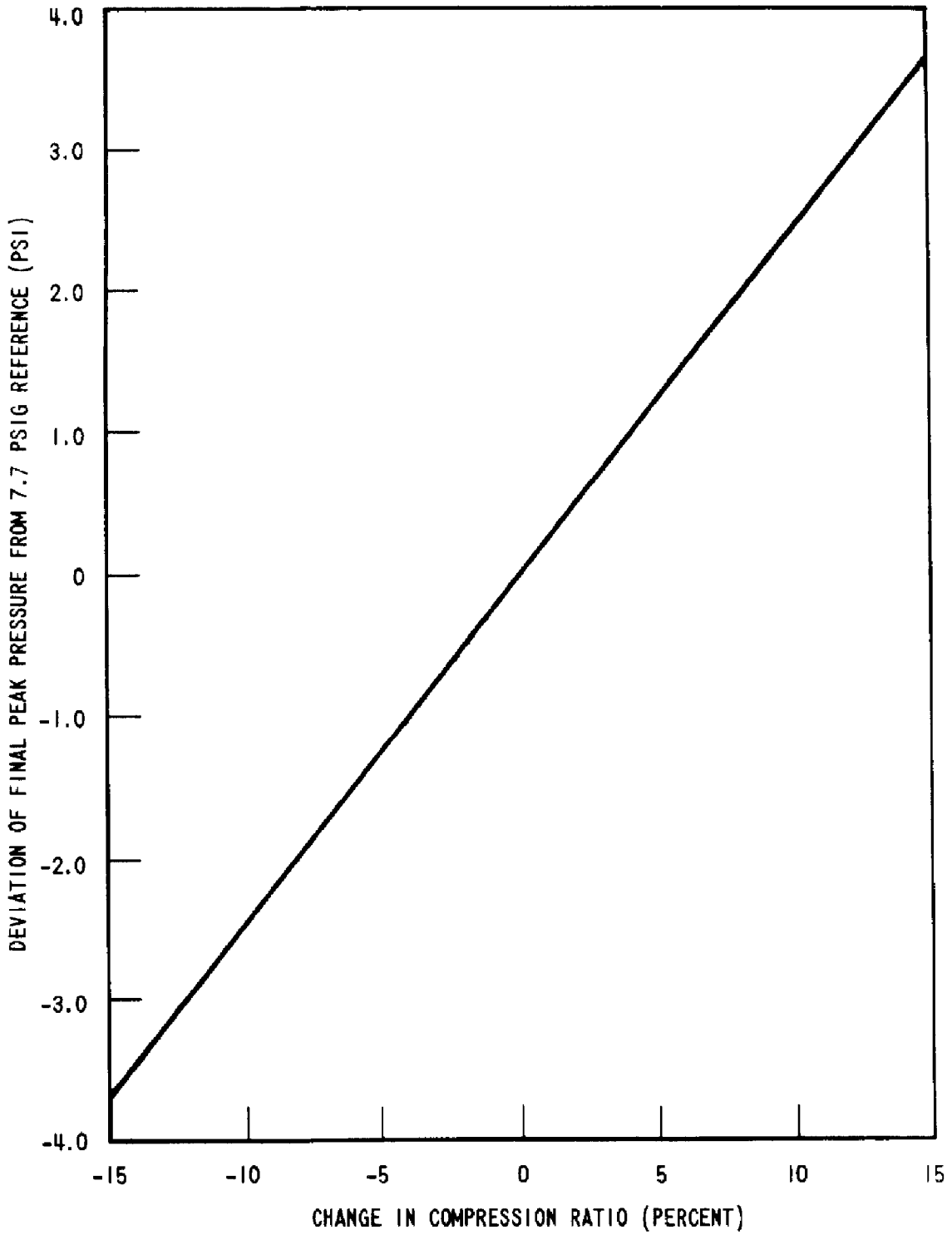

Figure 6-3. Steam Concentration in a Vertical Distribution Channel

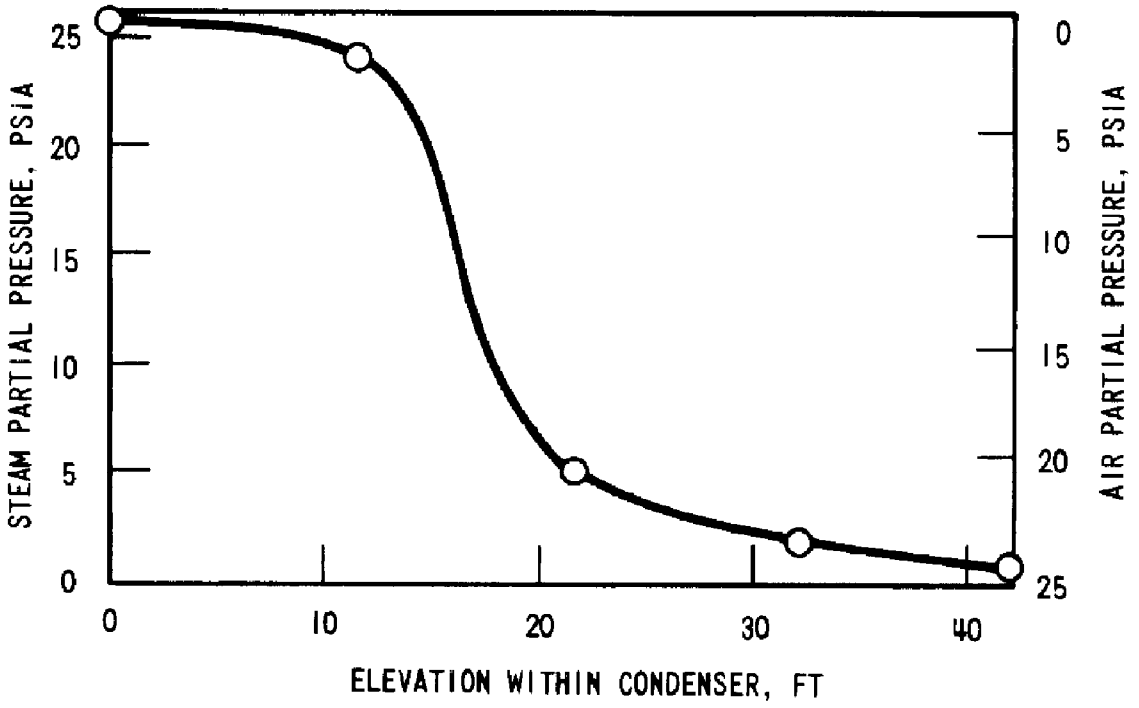

Figure 6-4. Peak Compression Pressure Versus Compression Ratio

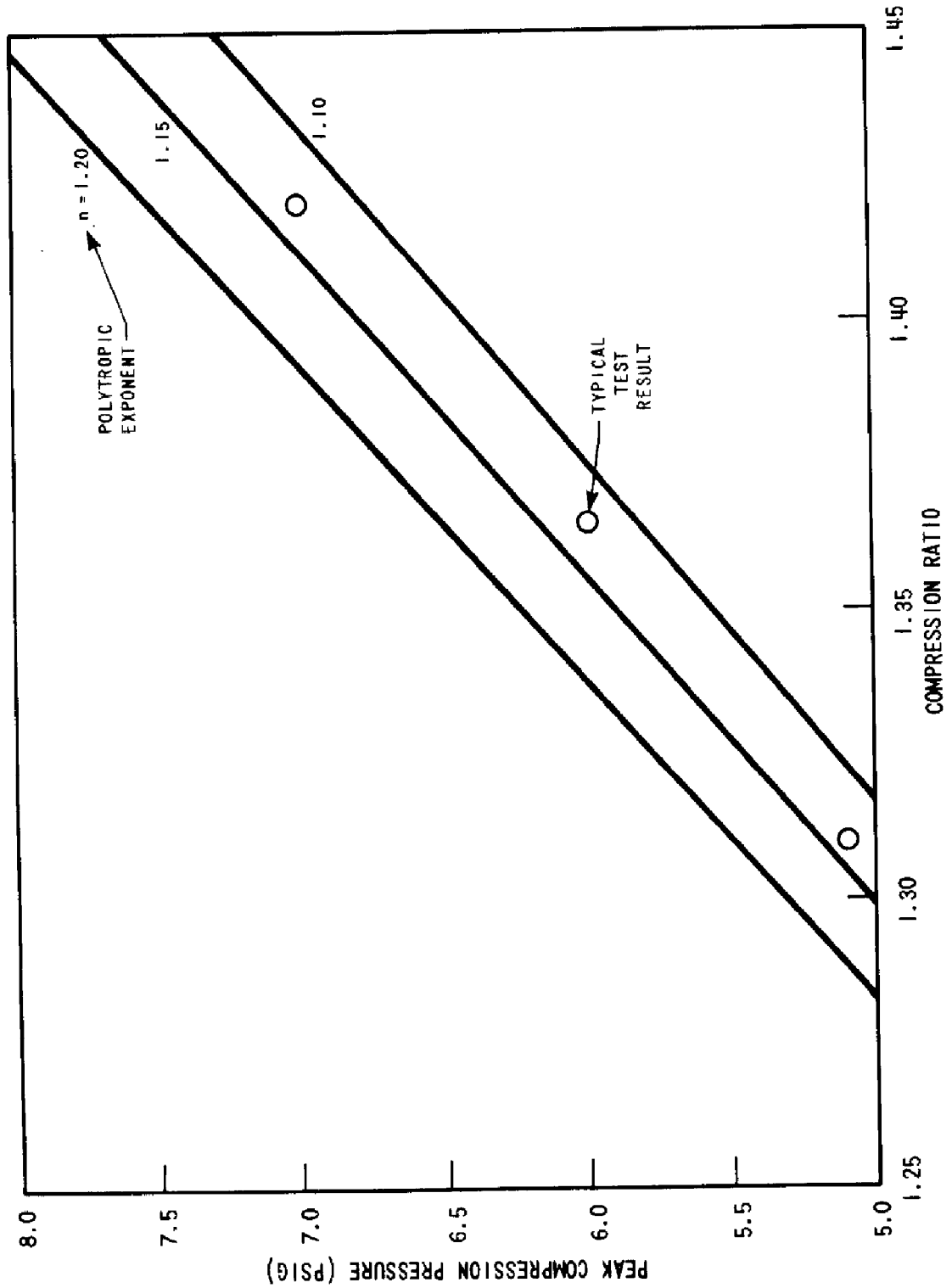

Figure 6-5. Upper Compartment Compression Pressure Versus Energy Release for Tests at 110% and 200% of Initial DBA Blowdown Rate

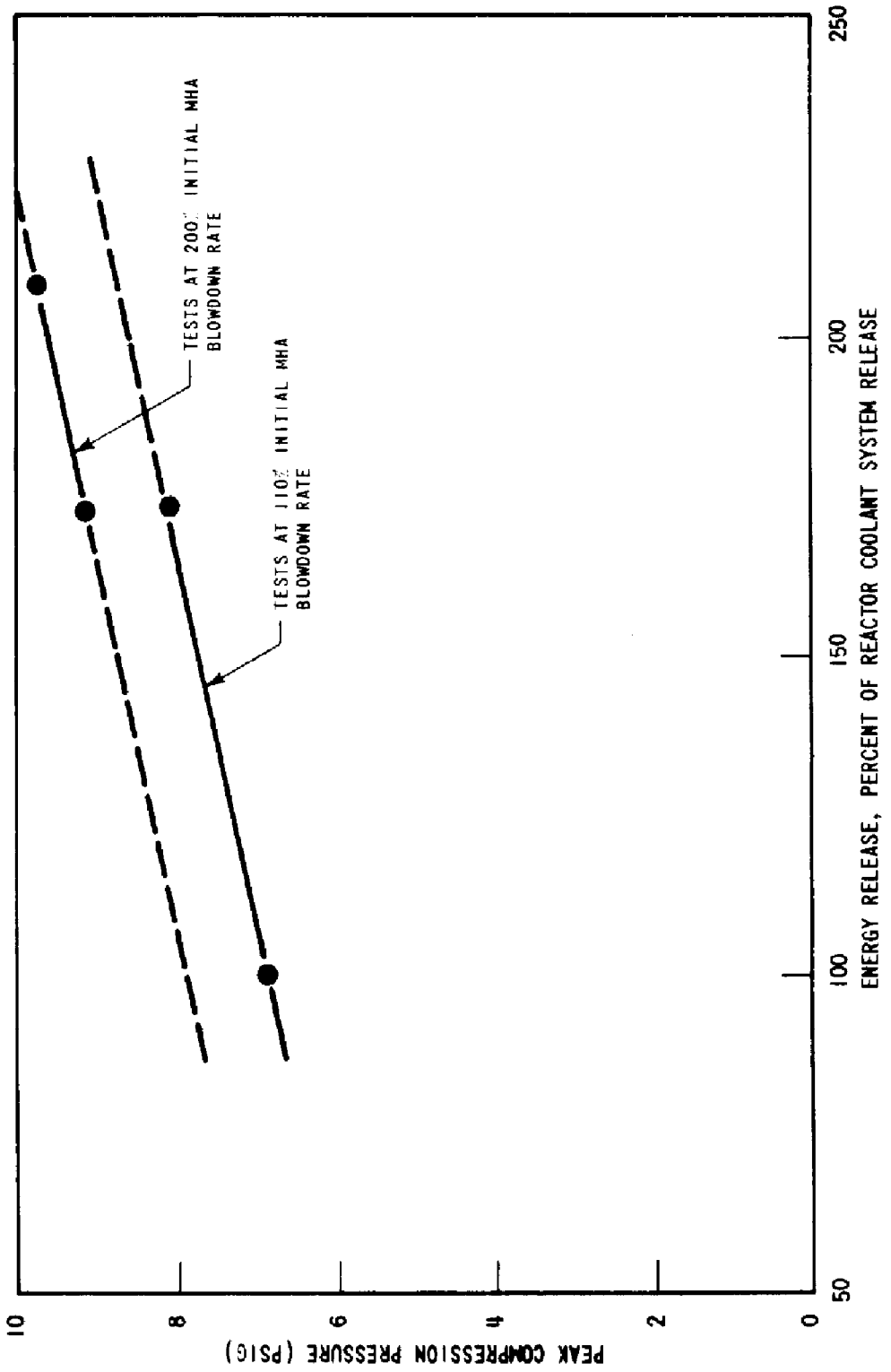

Figure 6-6. Peak Containment Pressure Transient – Pressure

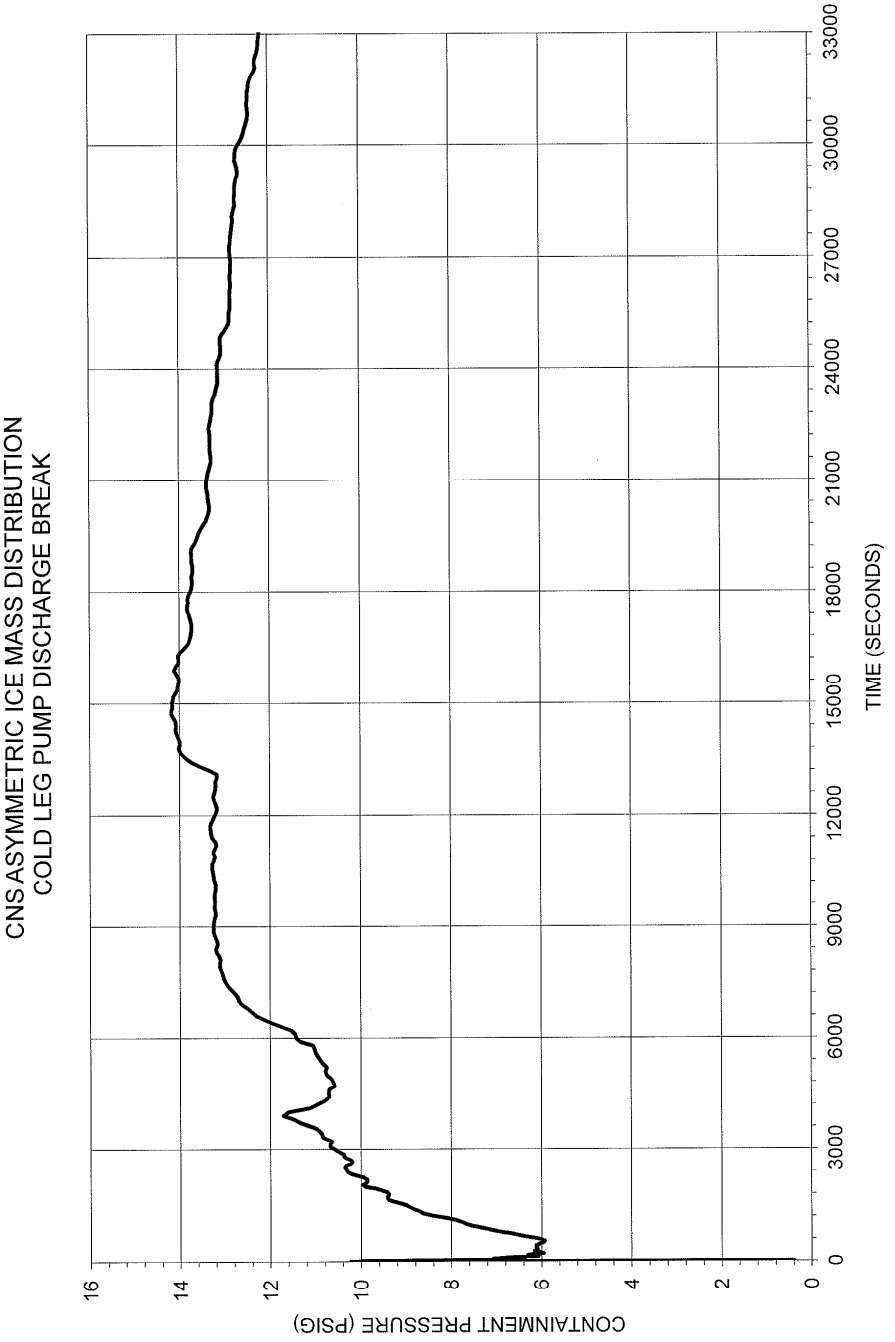

Figure 6-7. Peak Containment Pressure Transient - Upper Containment Temperature

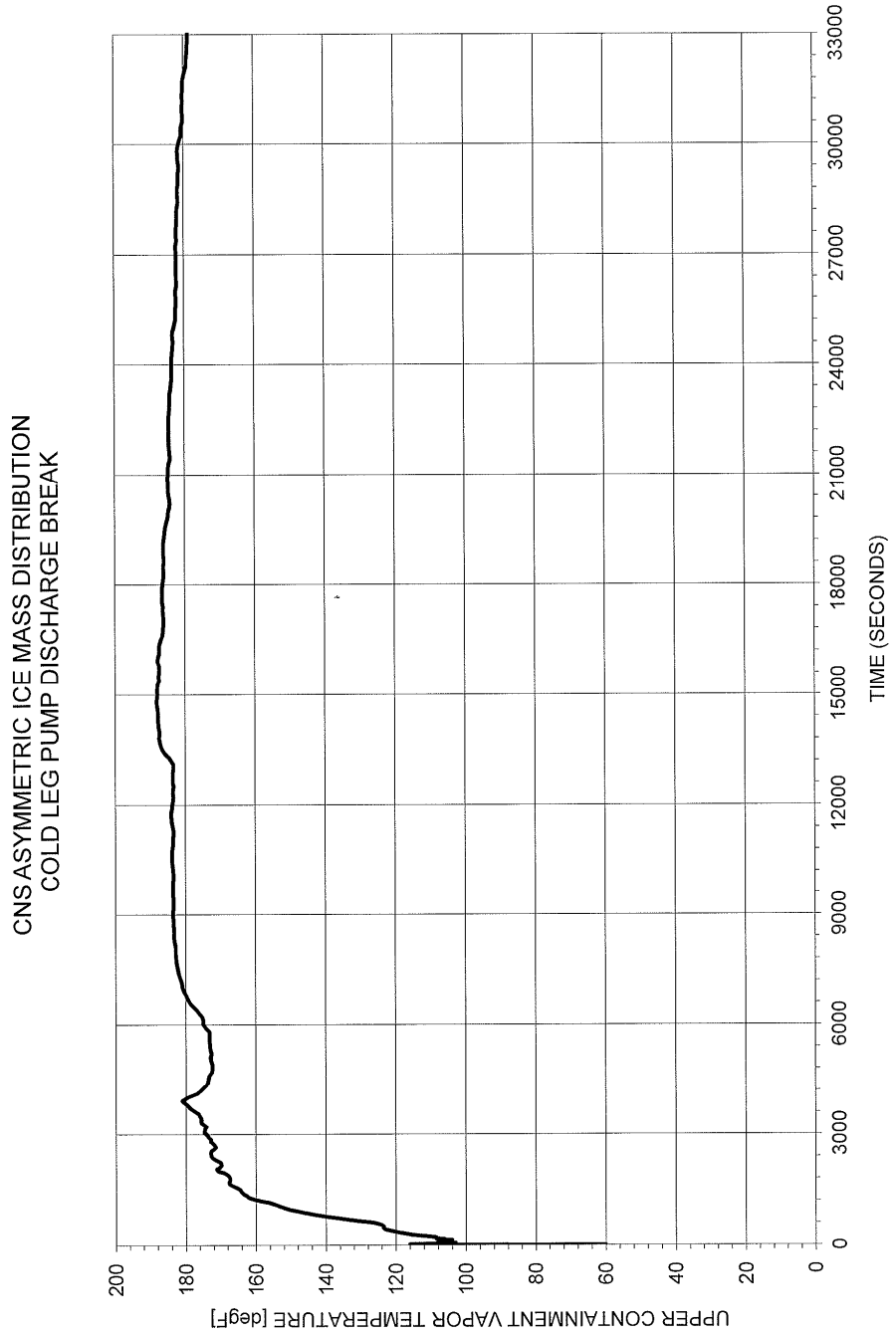

Figure 6-8. Peak Containment Pressure Transient - Lower Containment Temperature

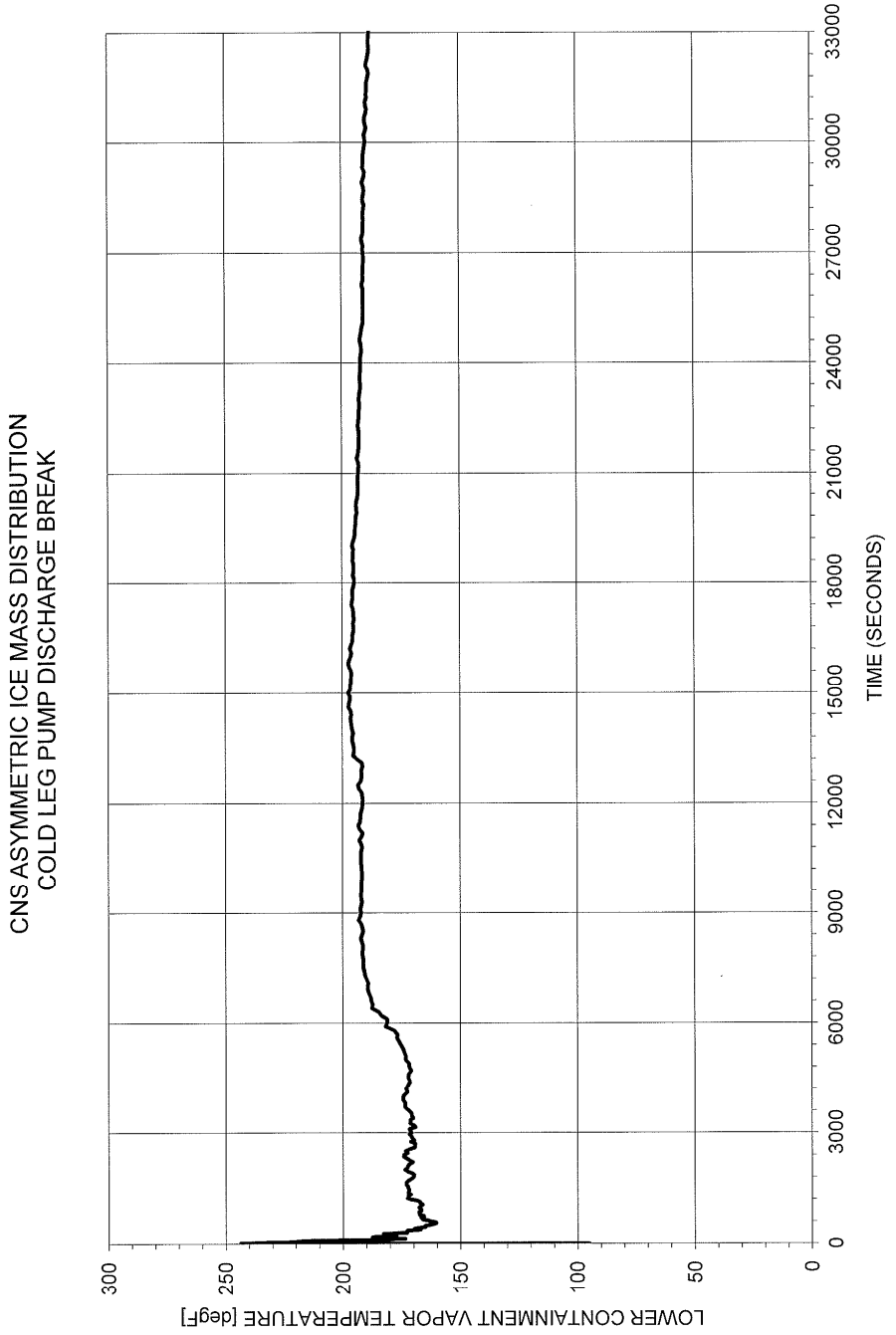

Figure 6-9. Peak Containment Pressure Transient - Sump Temperature

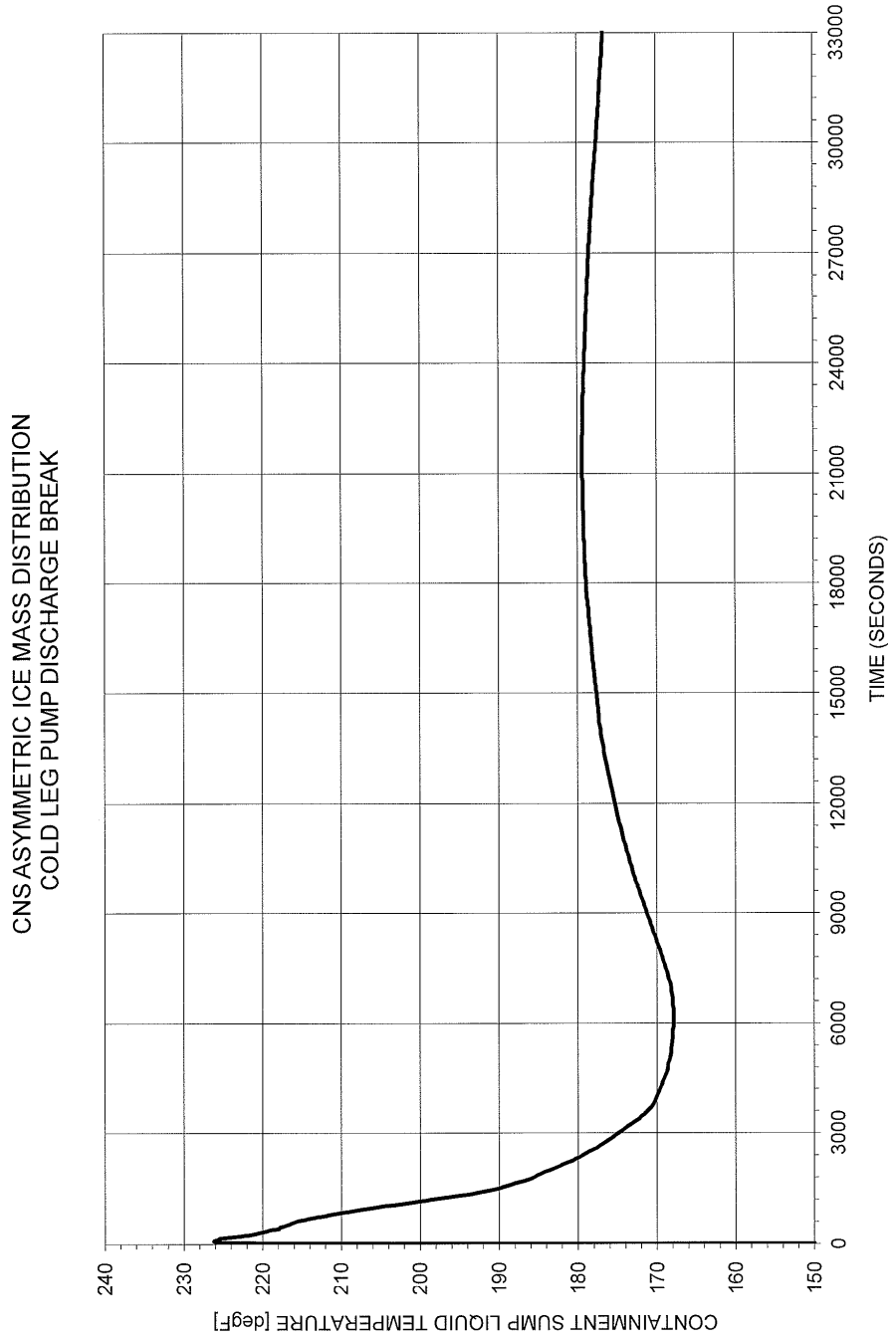

Figure 6-10. Peak Containment Pressure Transient - Ice Melted

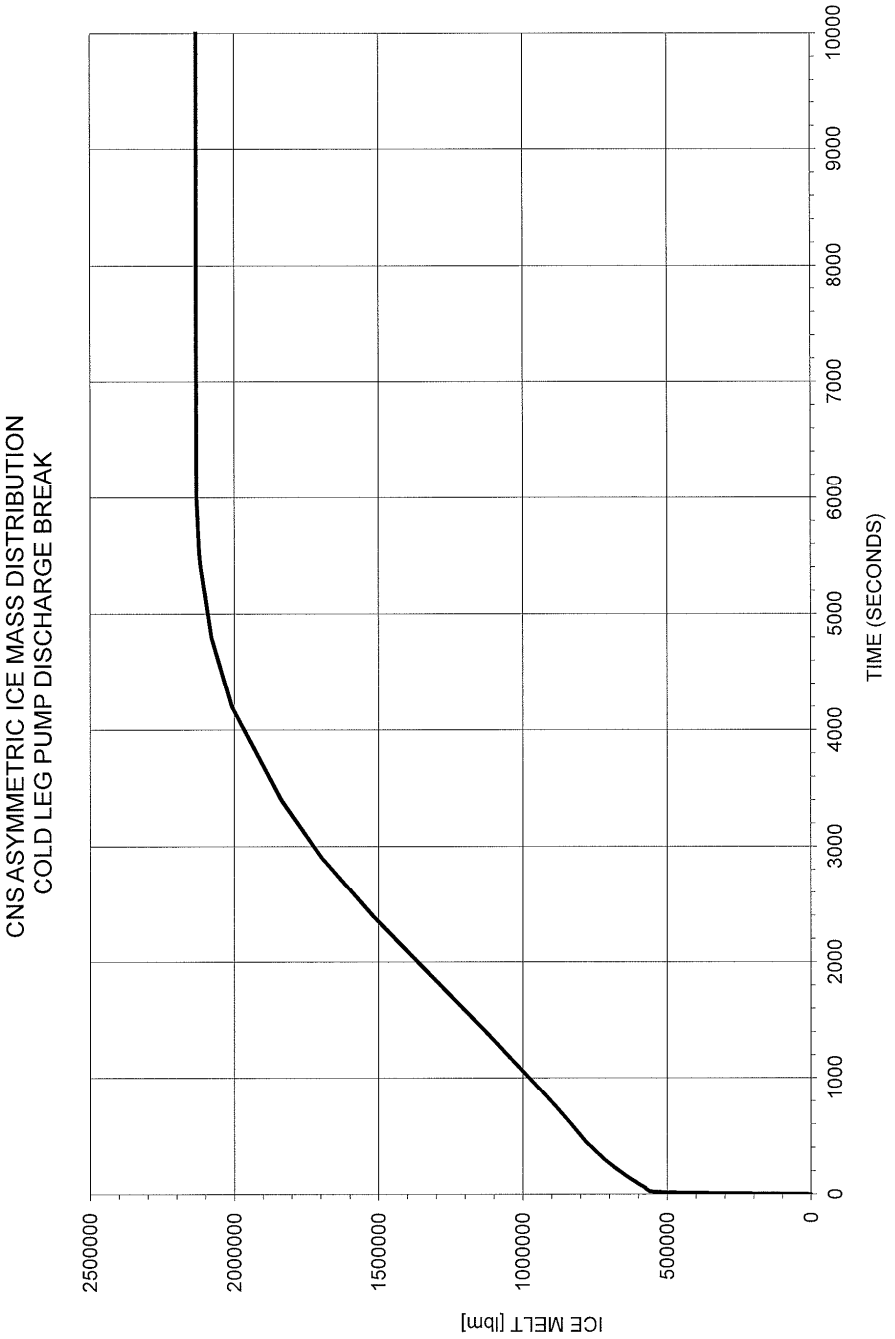

Figure 6-11. Containment Spray Return Drains from Air Return Pit Fans

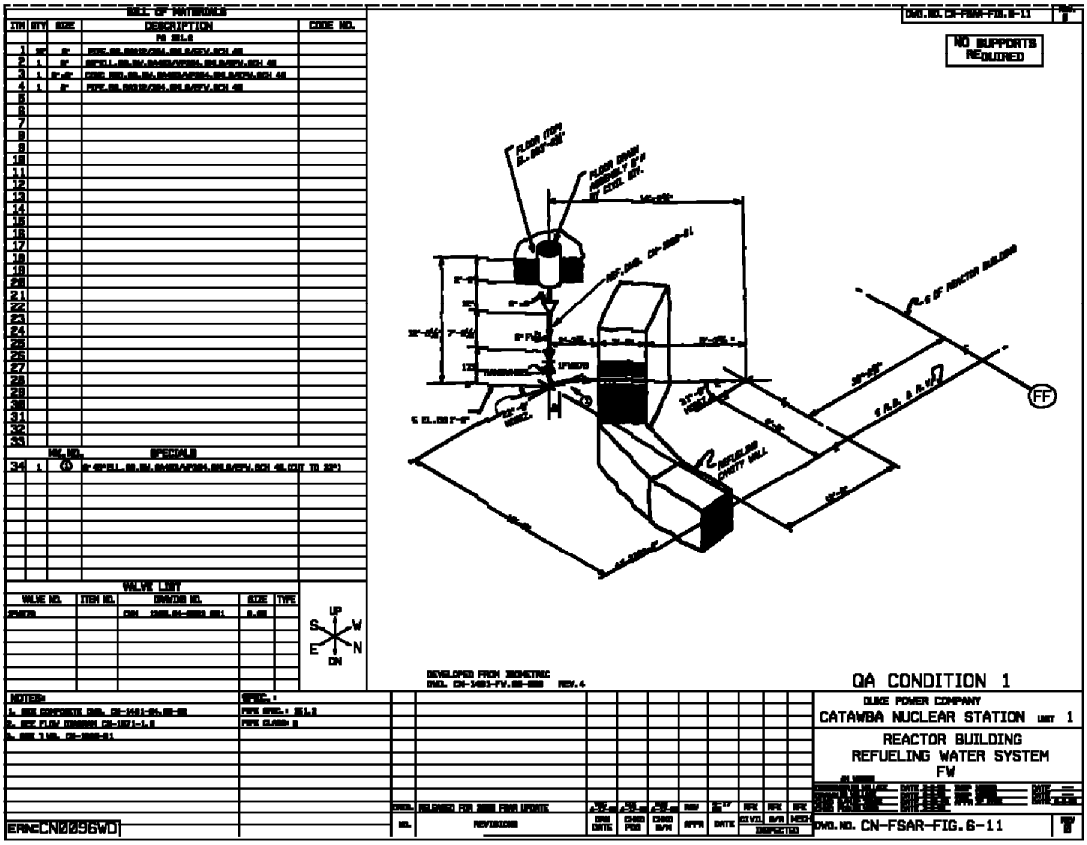

Figure 6-12. Containment Spray Return Drains from Air Return Pit Fans

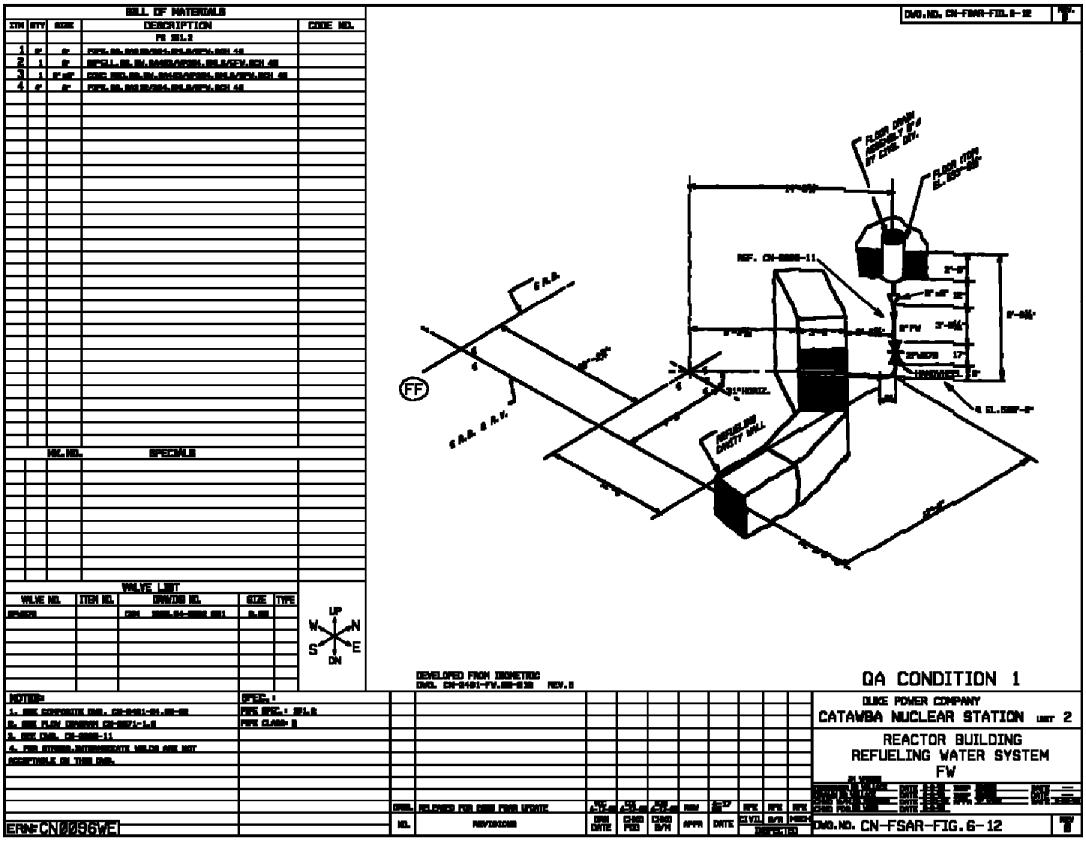

Figure 6-13. Drain Piping Arrangement Refueling Canal

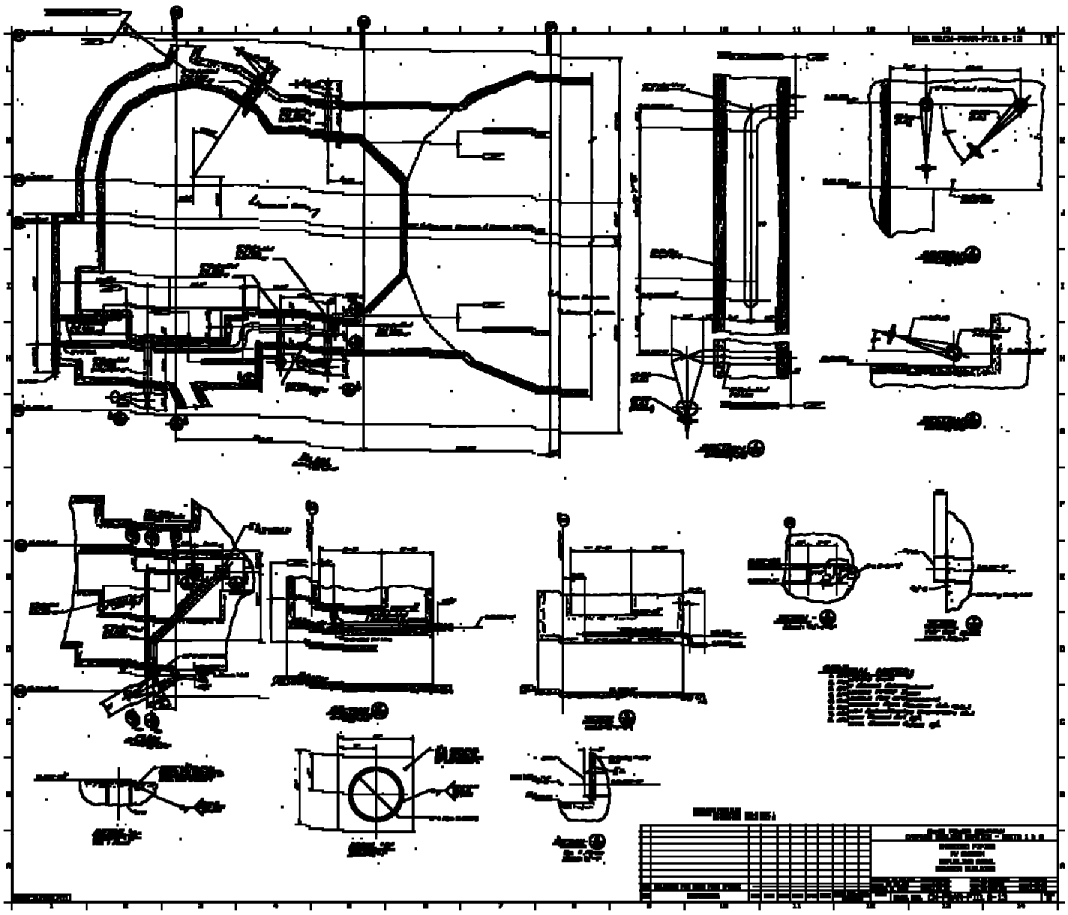

Figure 6-14. Ice Melted Versus Energy Release for Tests at Different Blowdown Rates

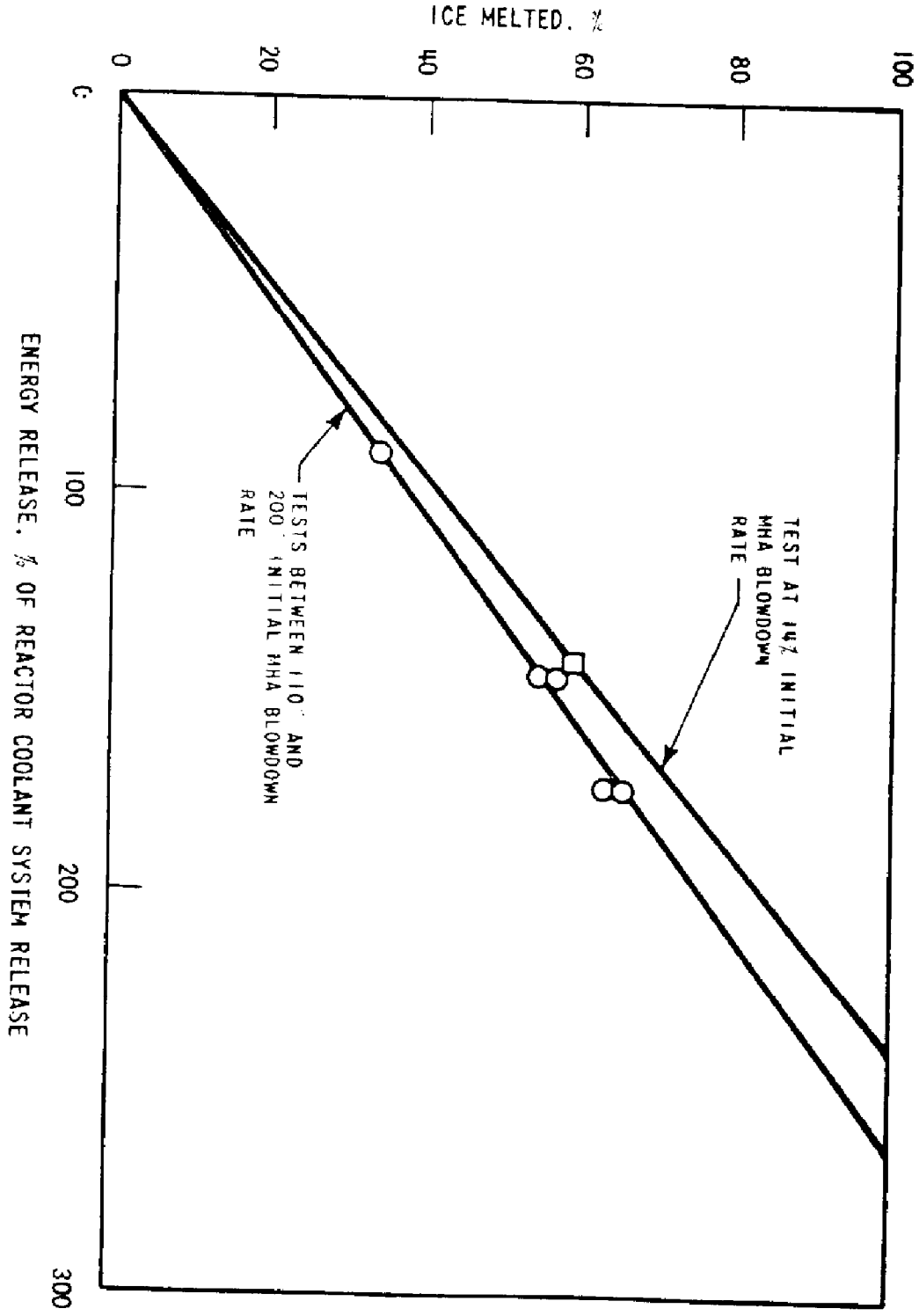

Figure 6-15. Upper Compartment Peak Compression Pressure Versus Blowdown Rate for Tests with 175% Energy Release

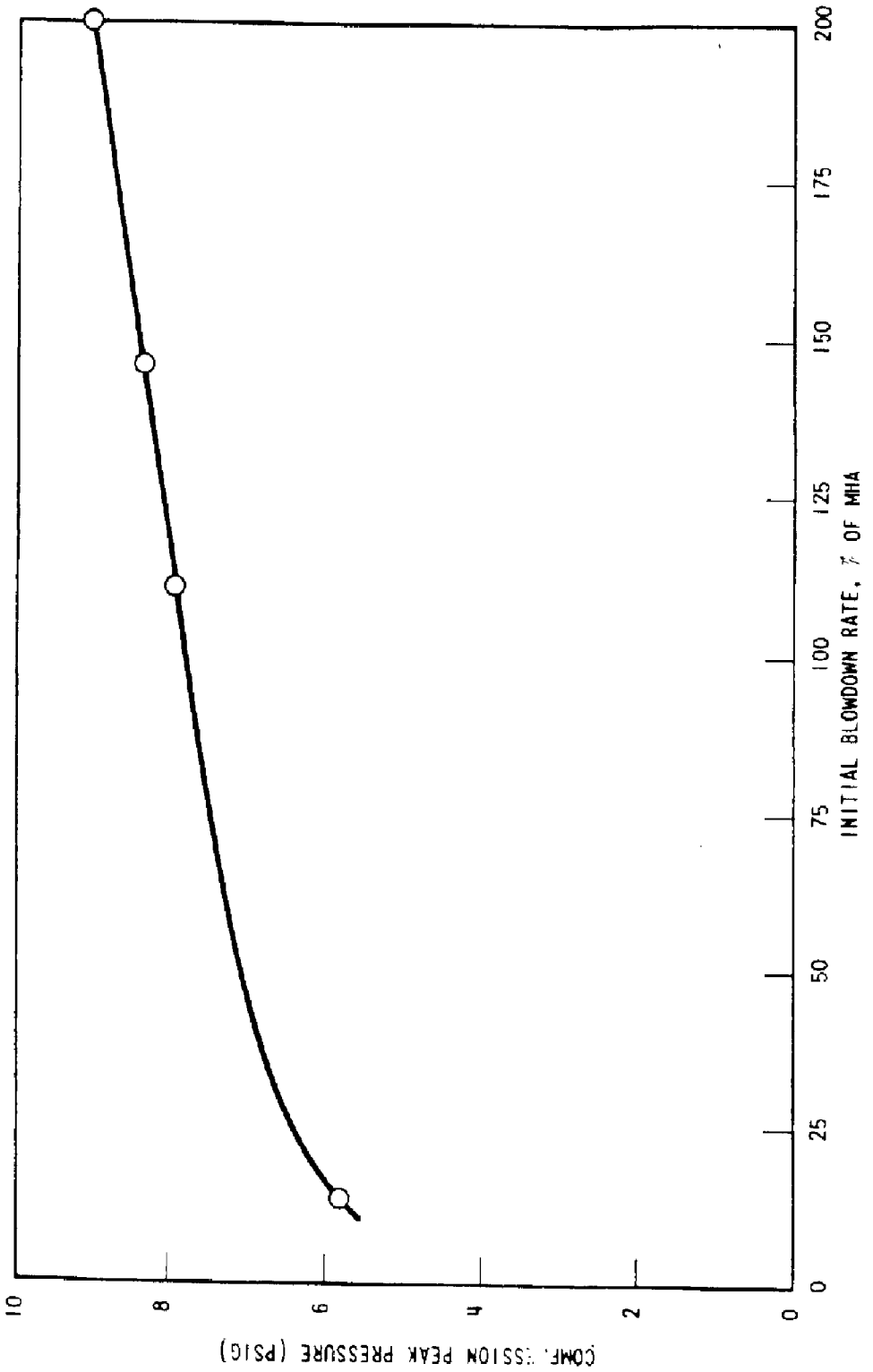

Figure 6-16. Peak Reverse Differential Pressure Transient

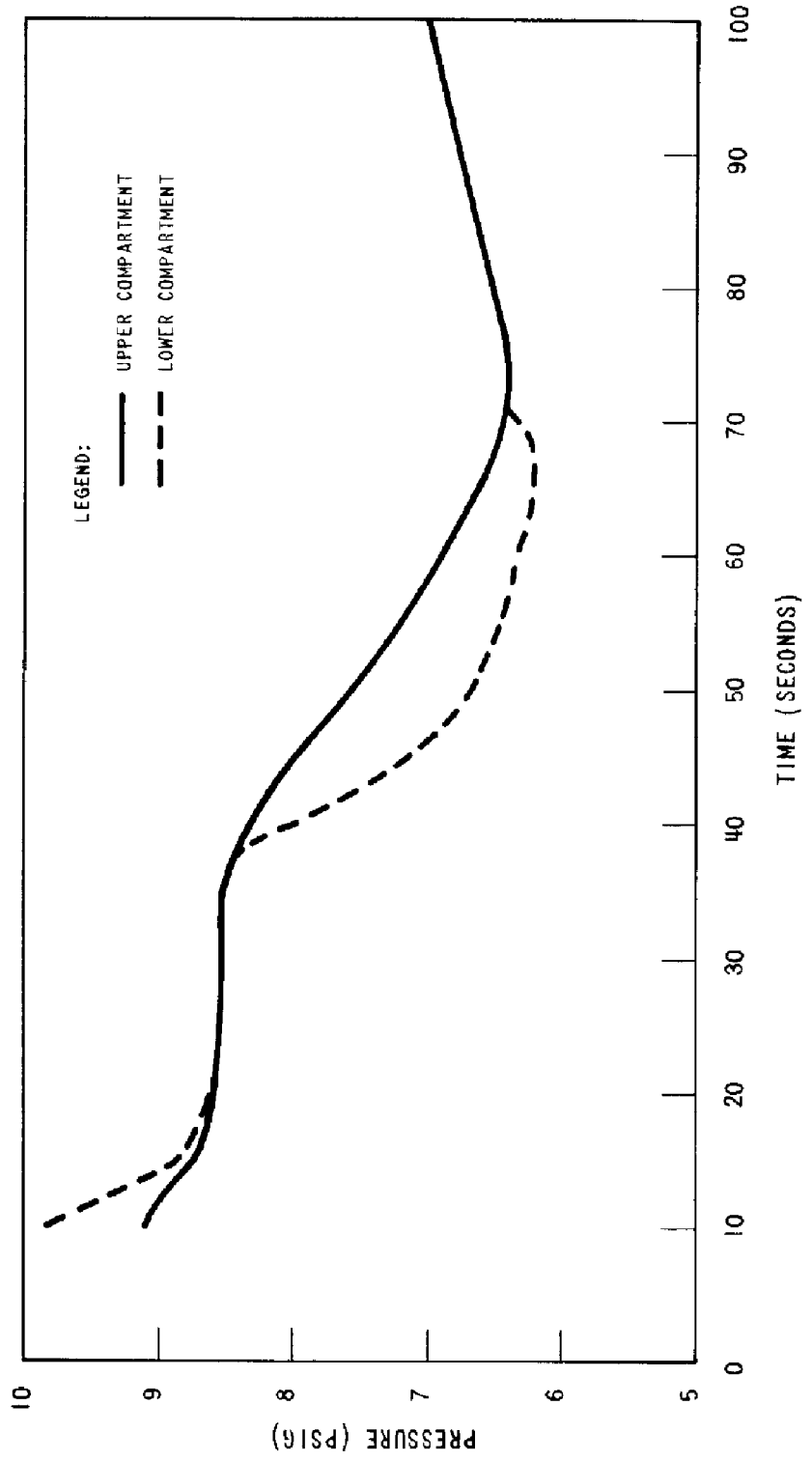

Figure 6-17. Peak Reverse Differential Pressure Transient

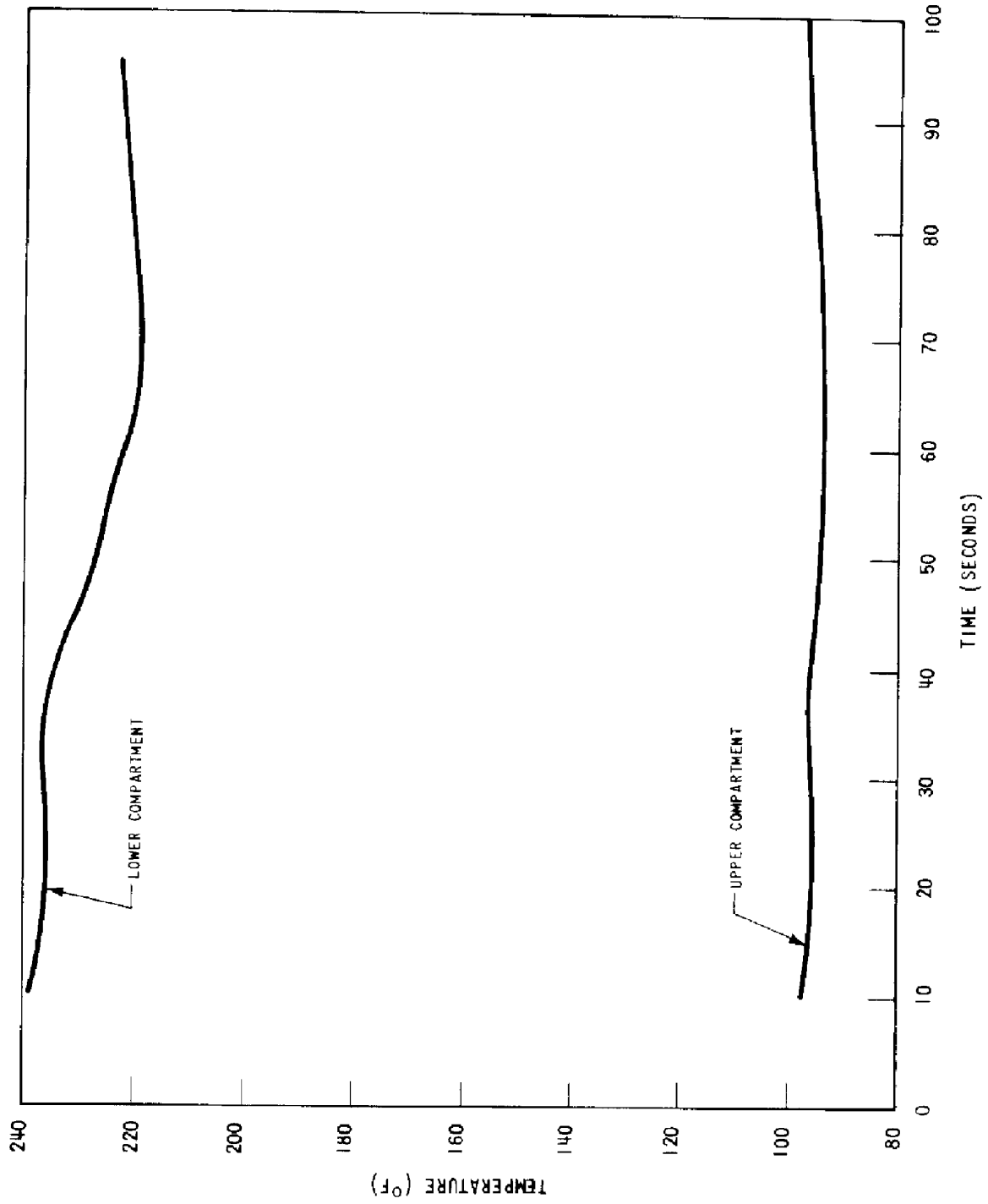

Figure 6-18. Pressure Increase Versus Deck Area from Deck Leakage Tests

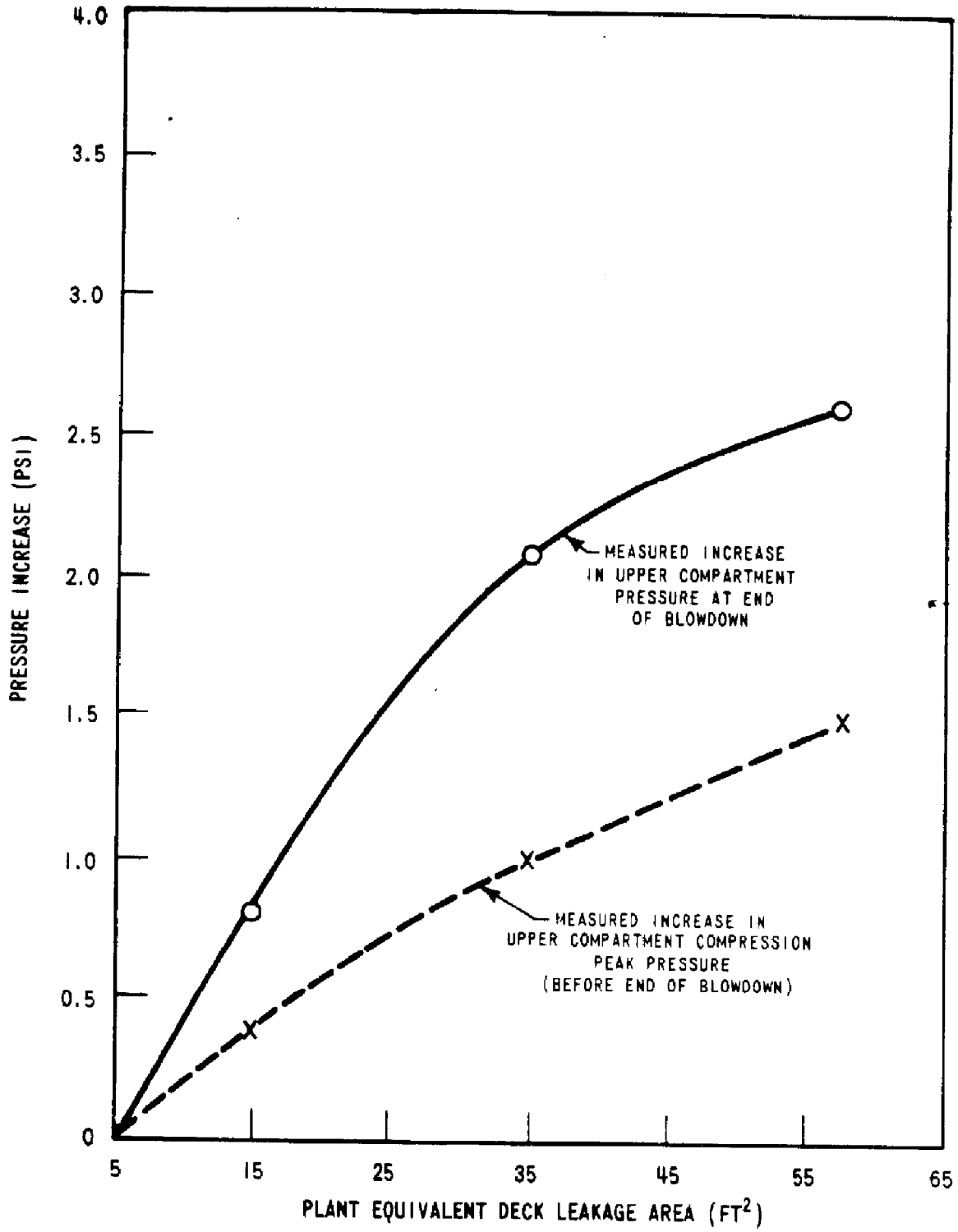

Figure 6-19. Energy Release at Time of Compression Peak Pressure from Full-Scale Section Test with 1-Foot Diameter Baskets

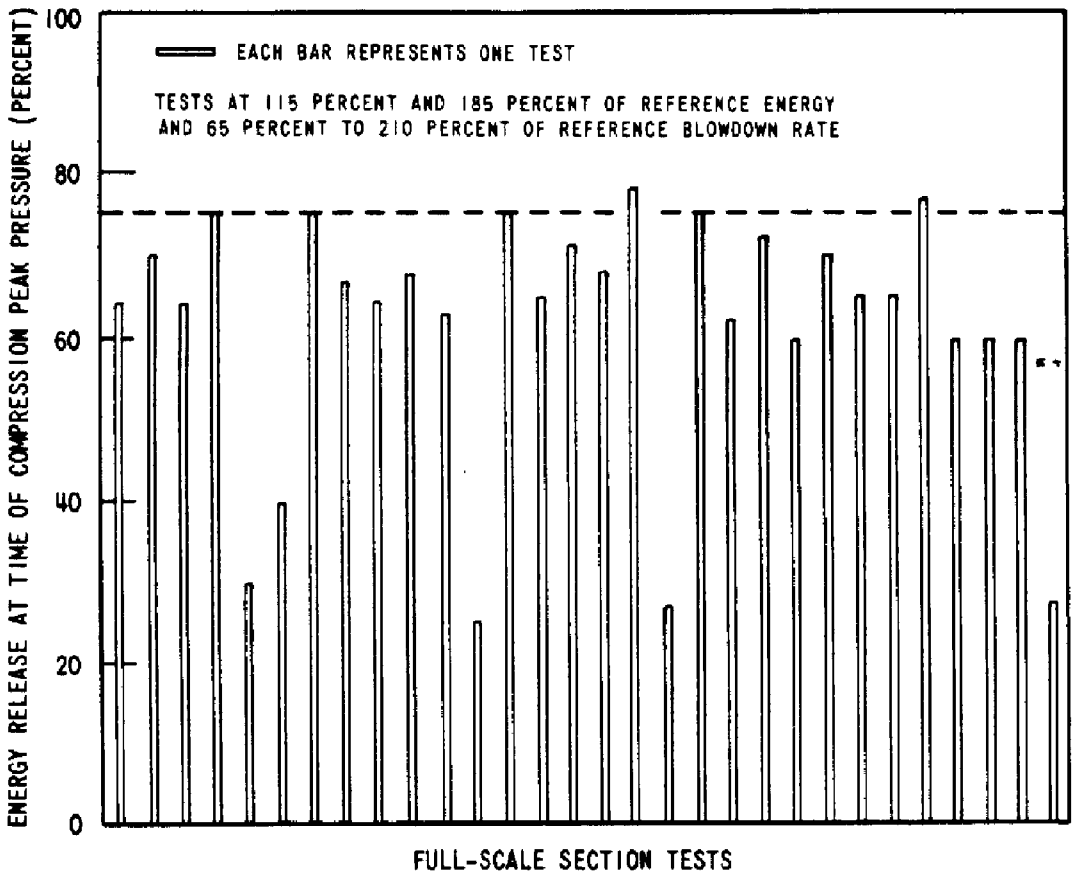

Figure 6-20. Peak Containment Temperature Transient - Lower Containment Temperature

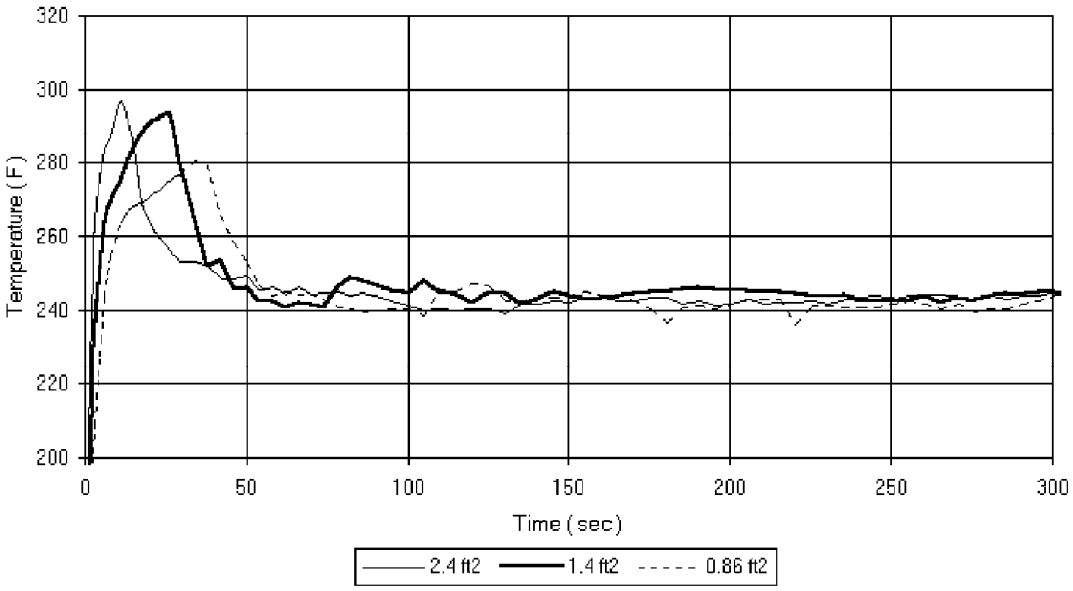

Figure 6-21. Peak Containment Temperature Transient - Break Compartment Temperature

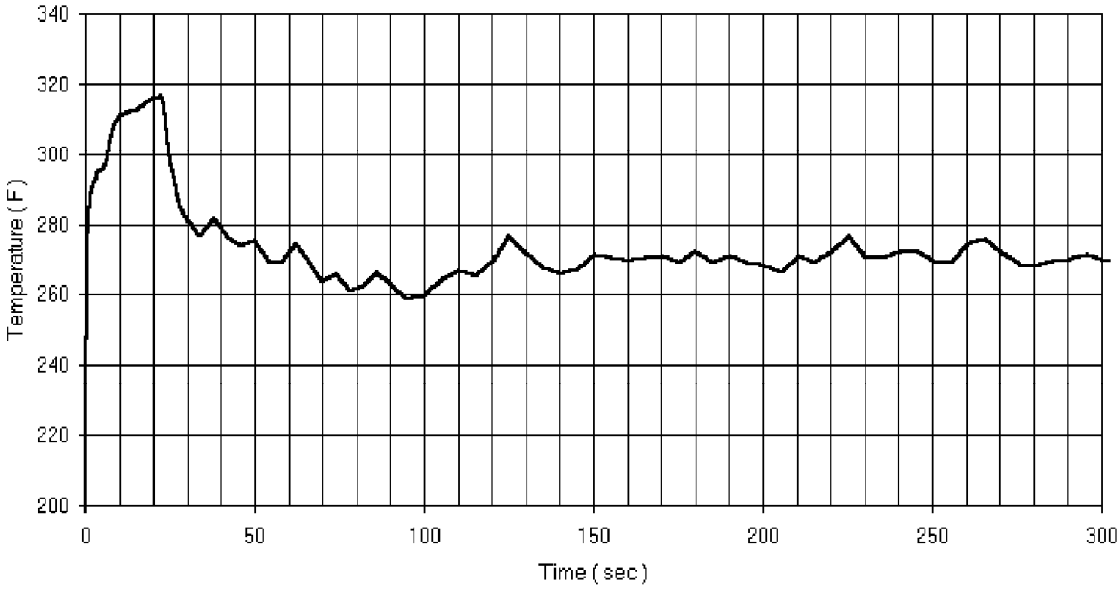

Figure 6-22. Deleted Per 1997 Update

Figure 6-23. Typical Upper and Lower Compartment Pressure Transient for Break Compartment Having a DEHL Break

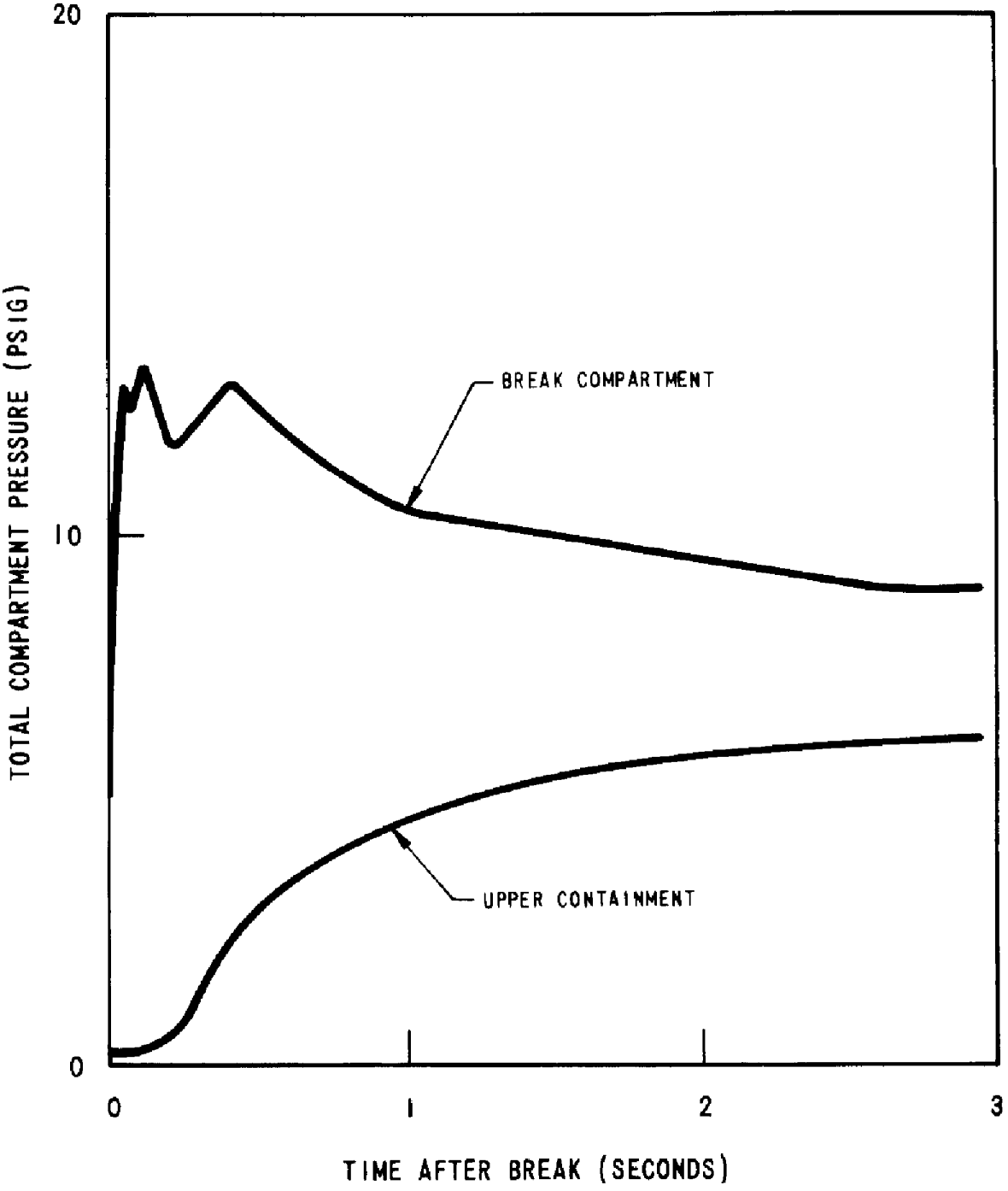

Figure 6-24. Typical Upper and Lower Compartment Pressure Transient for Break Compartment Having a DECL Break

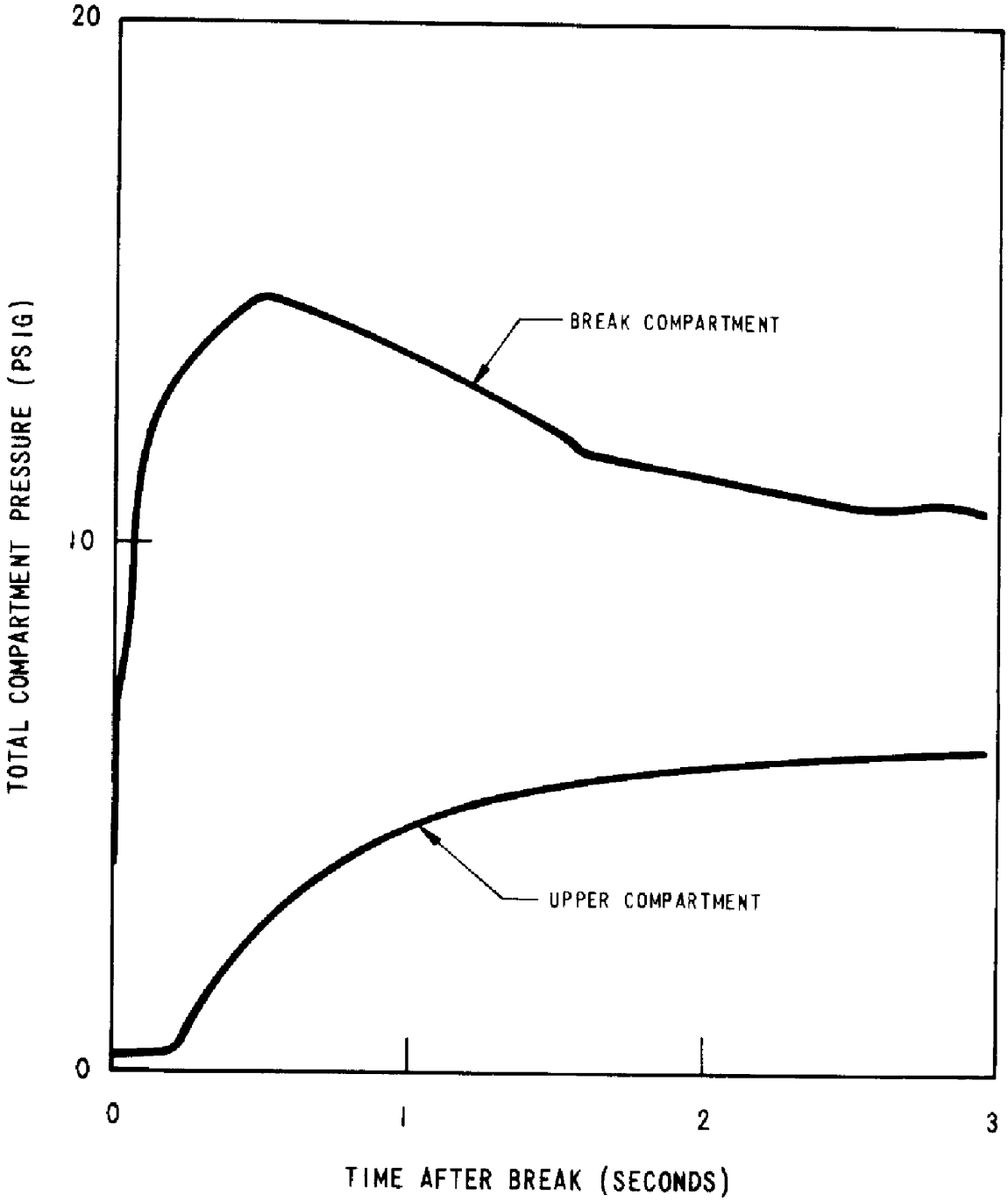

Figure 6-25. Plan at Equipment Rooms Elevation

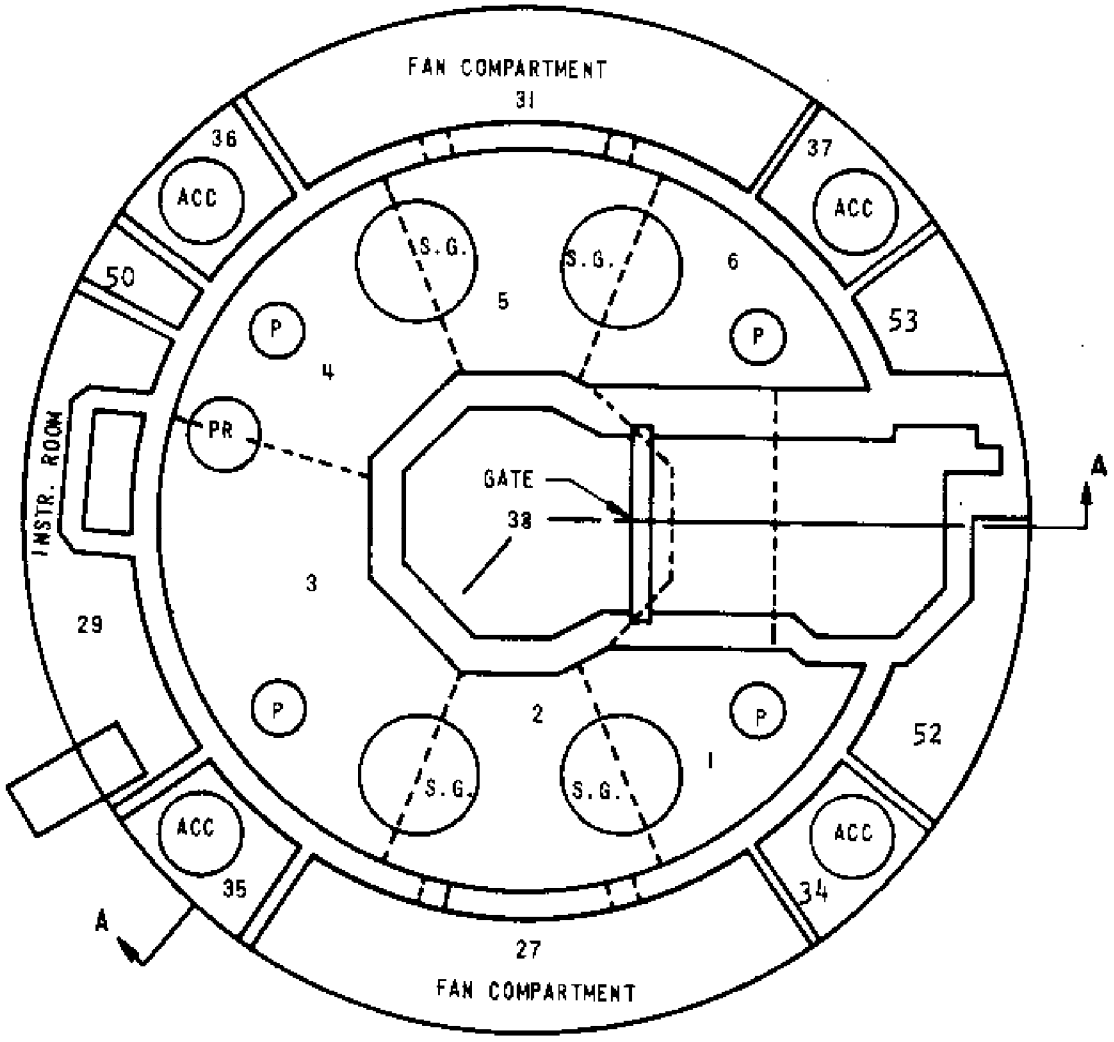

Figure 6-26. Compartment Section View

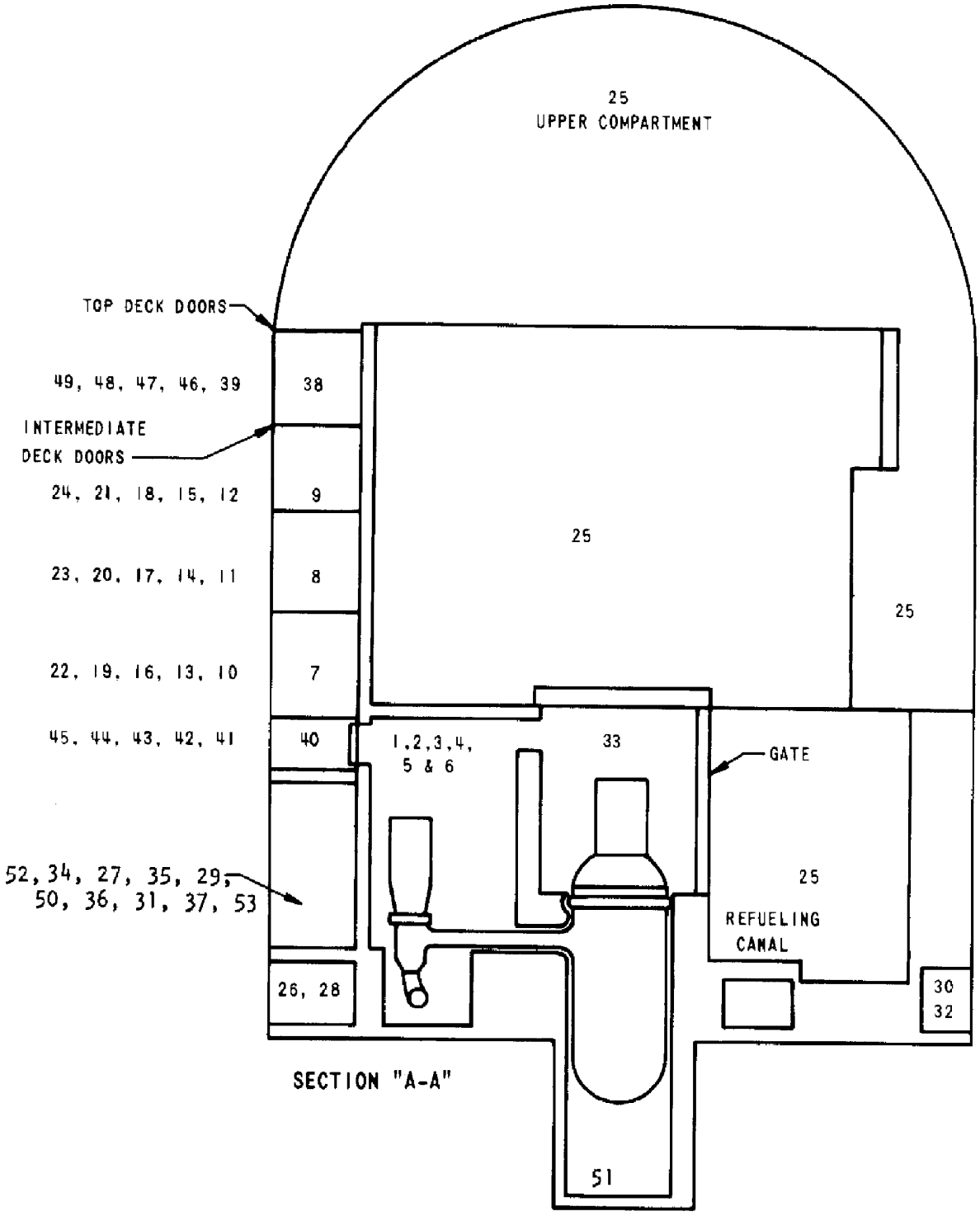

Figure 6-27. Plan View at Ice Condenser Elevation - Ice Condenser Compartments

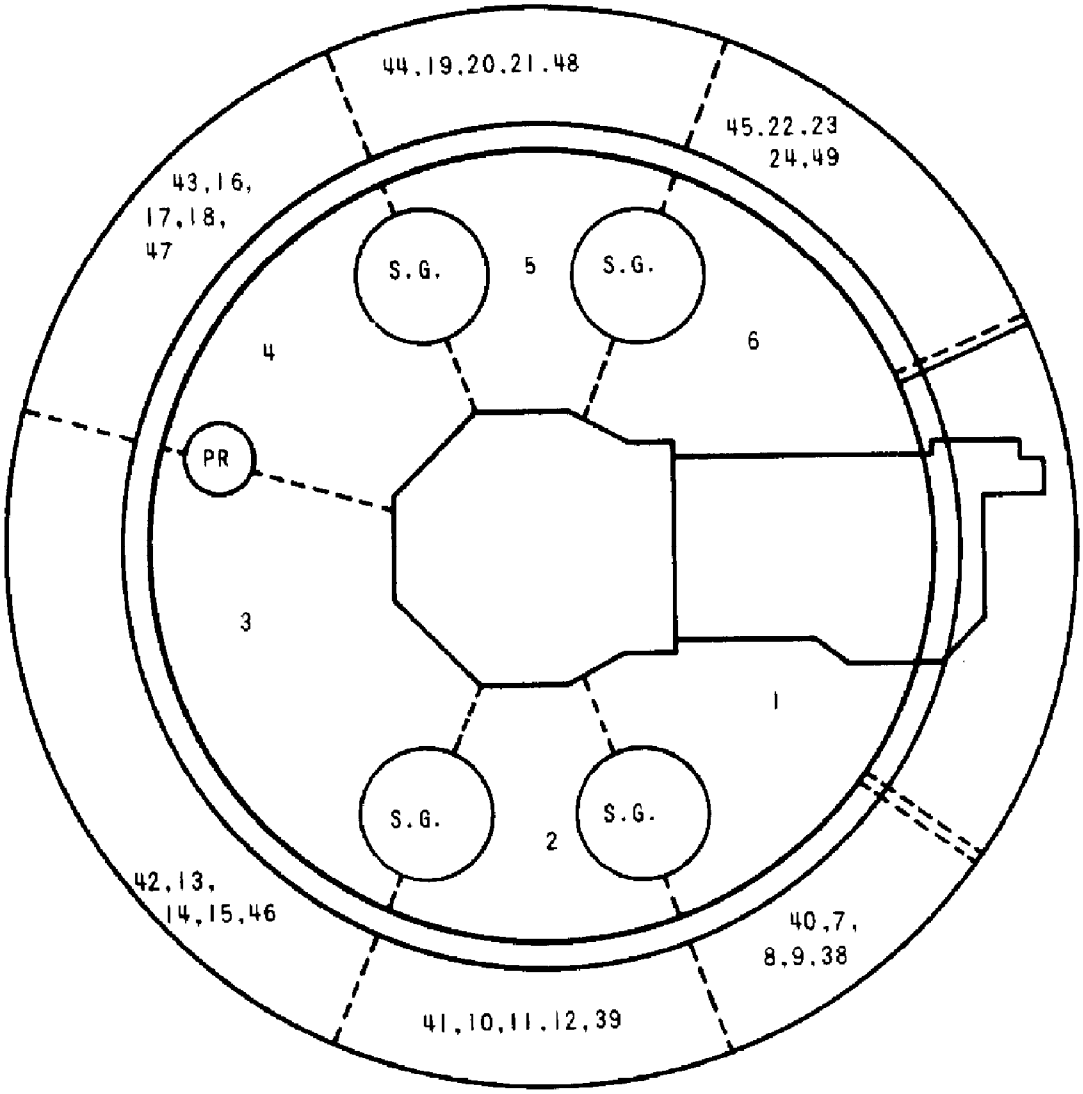

Figure 6-28. Layout of Containment Shell

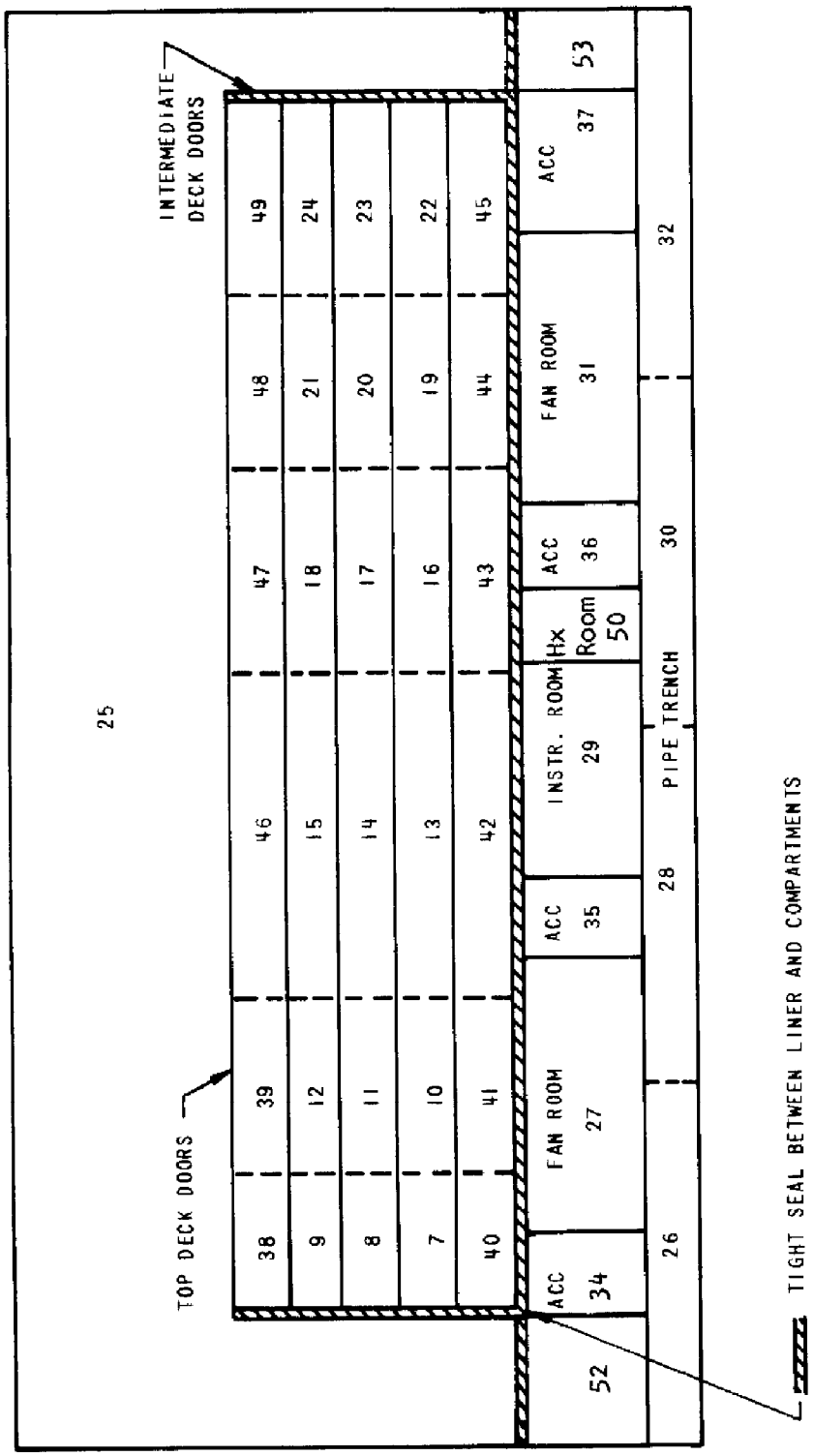

Figure 6-29. TMD Code Network

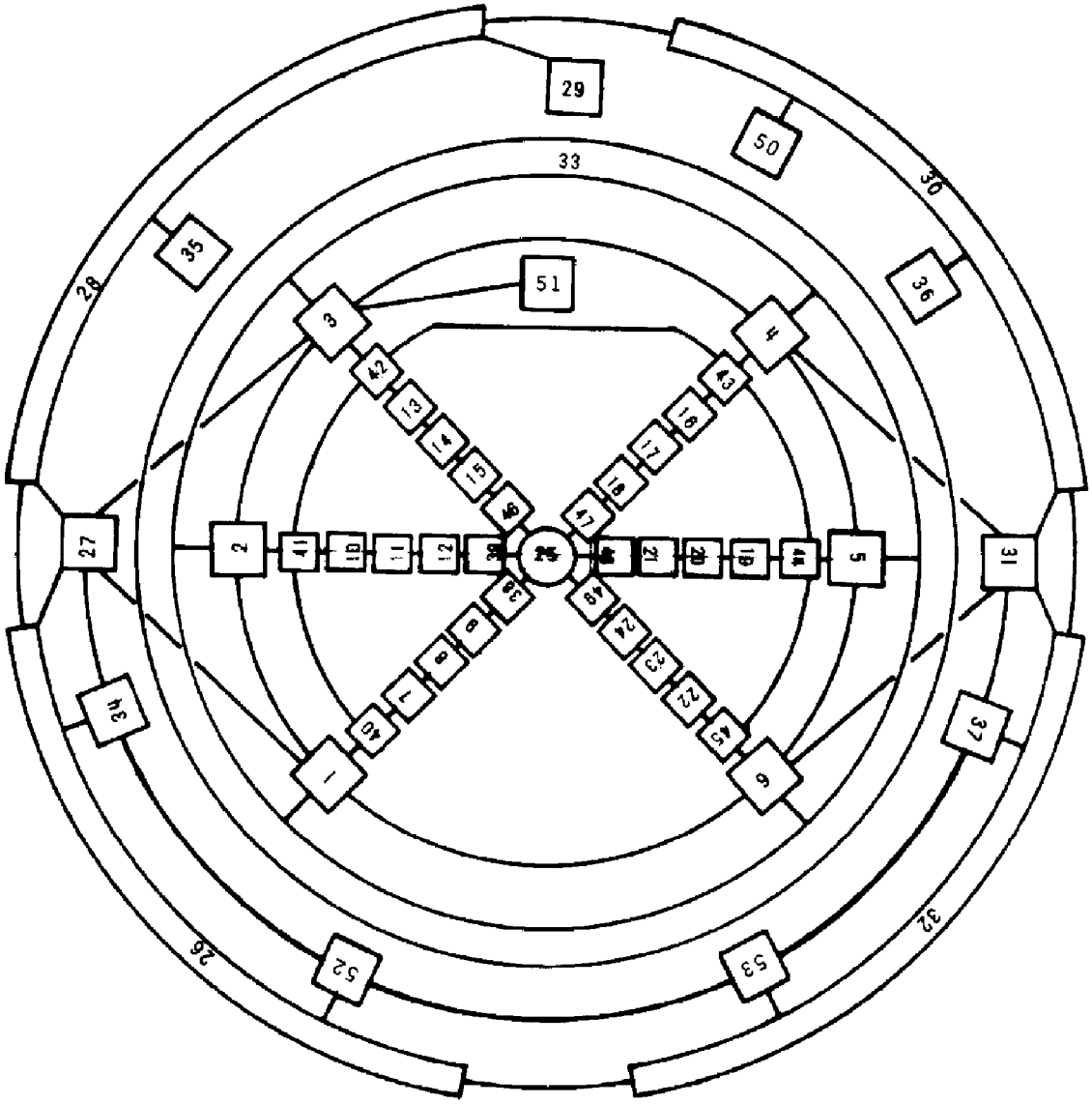

Figure 6-30. Nine Volume Nodalization of the Steam Generator Enclosure

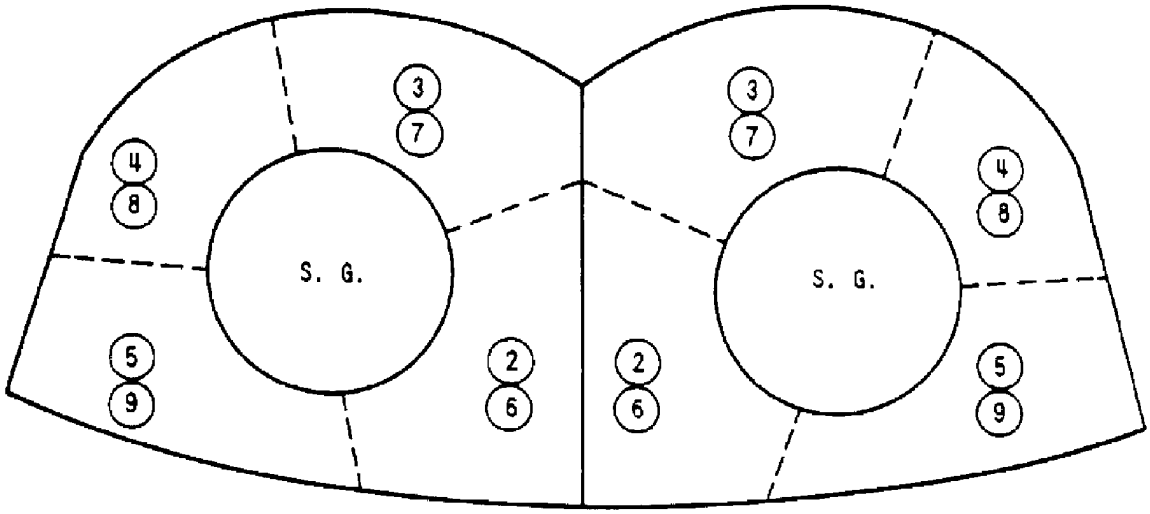

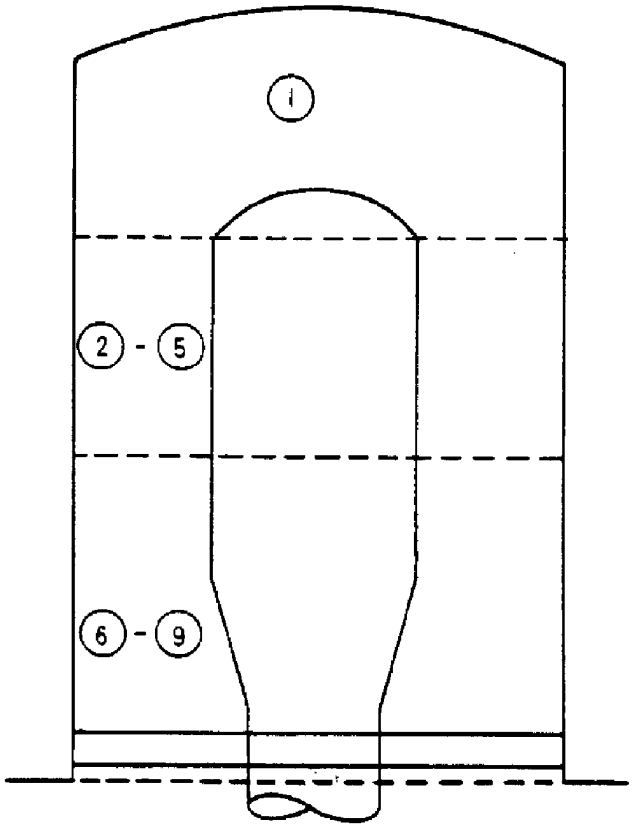

Figure 6-31. Double Ended Steam Line Break in Steam Generator Enclosure

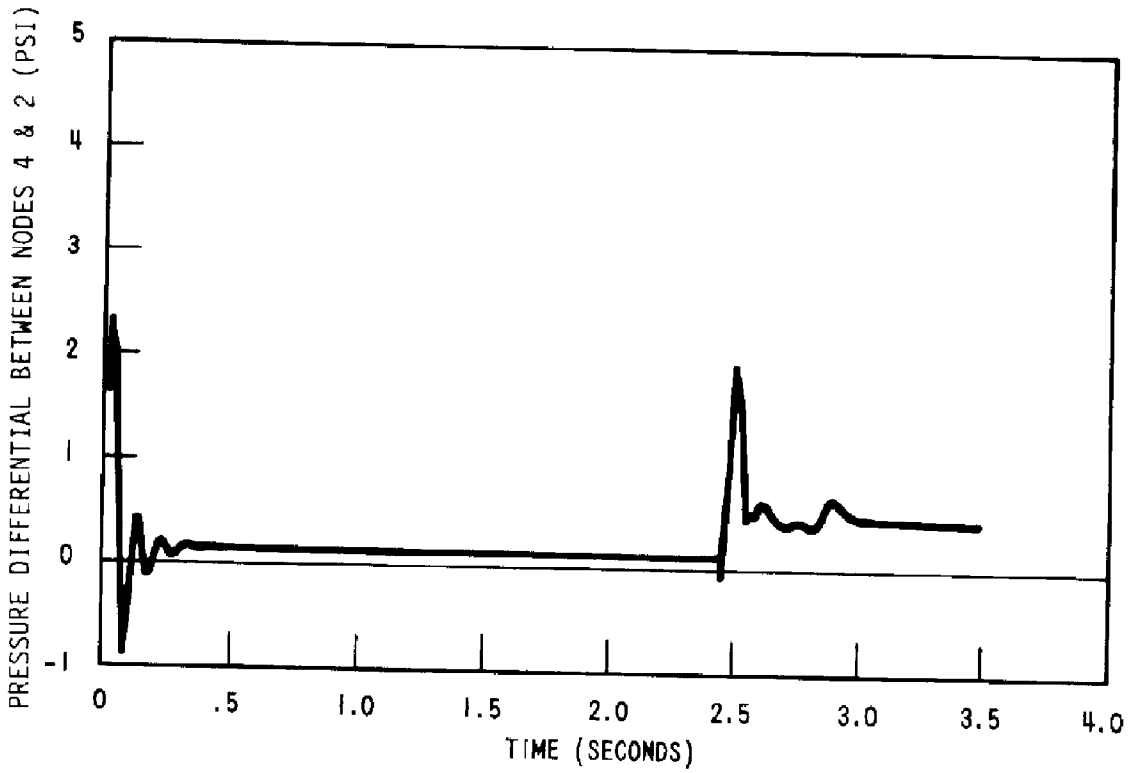

Figure 6-32. Double Ended Steam Line Break in Steam Generator Enclosure

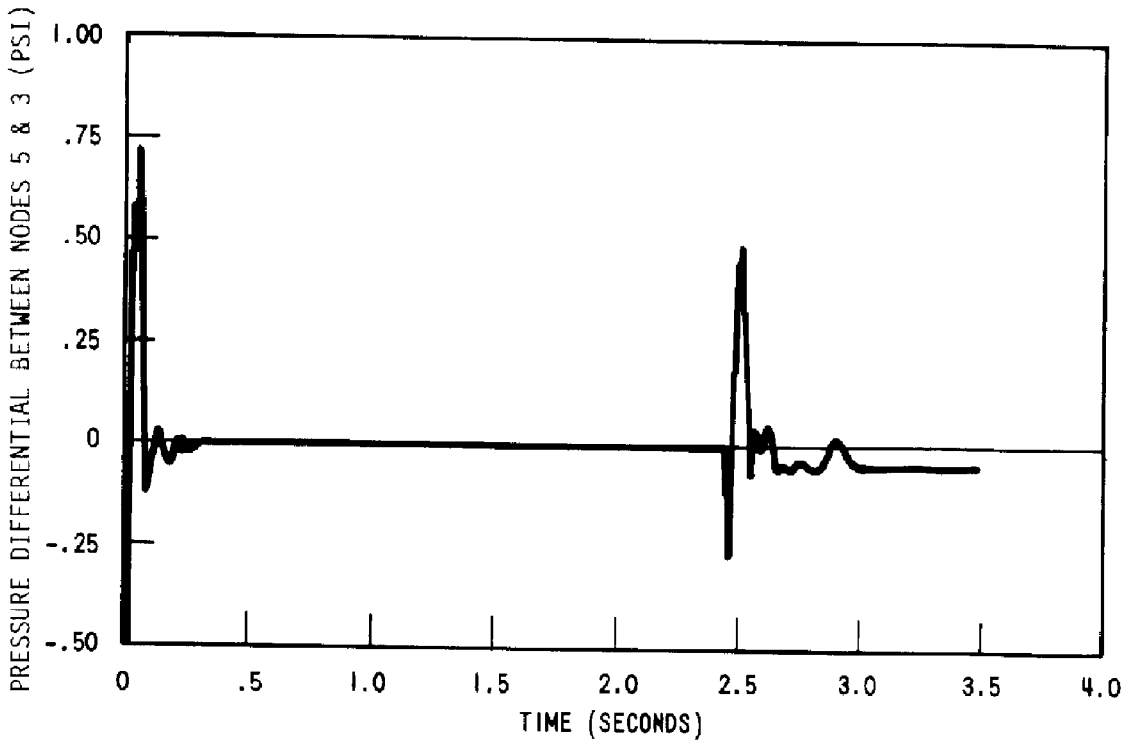

Figure 6-33. Double Ended Steam Line Break in Steam Generator Enclosure

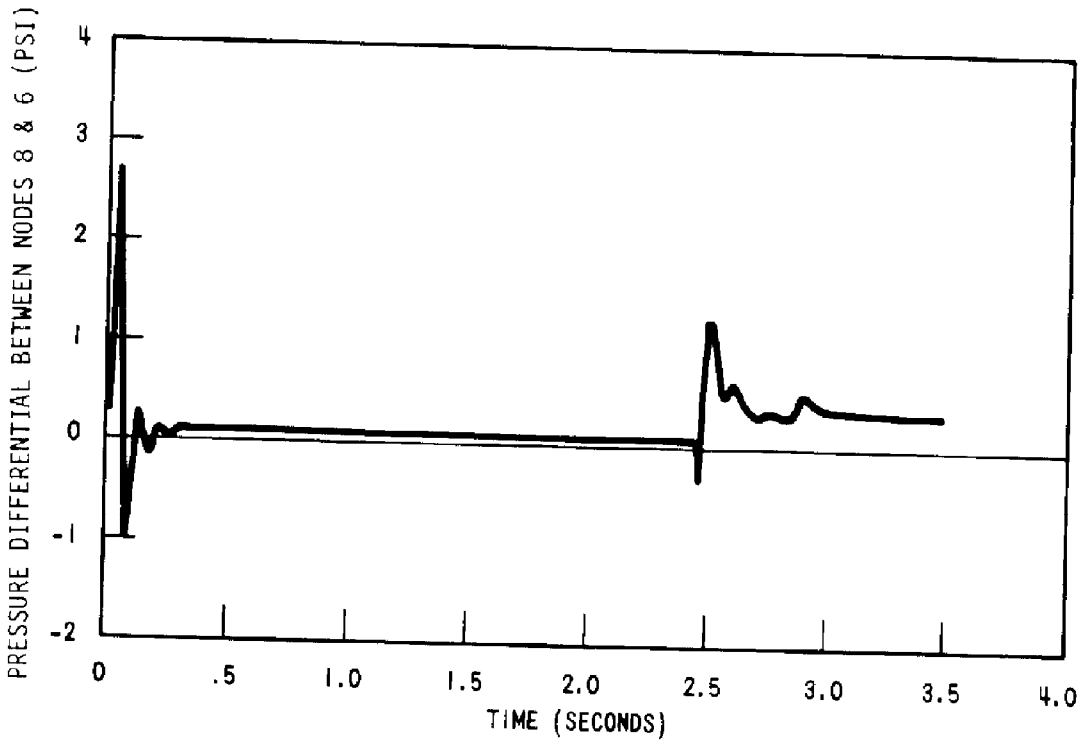

Figure 6-34. Double Ended Steam Line Break in Steam Generator Enclosure

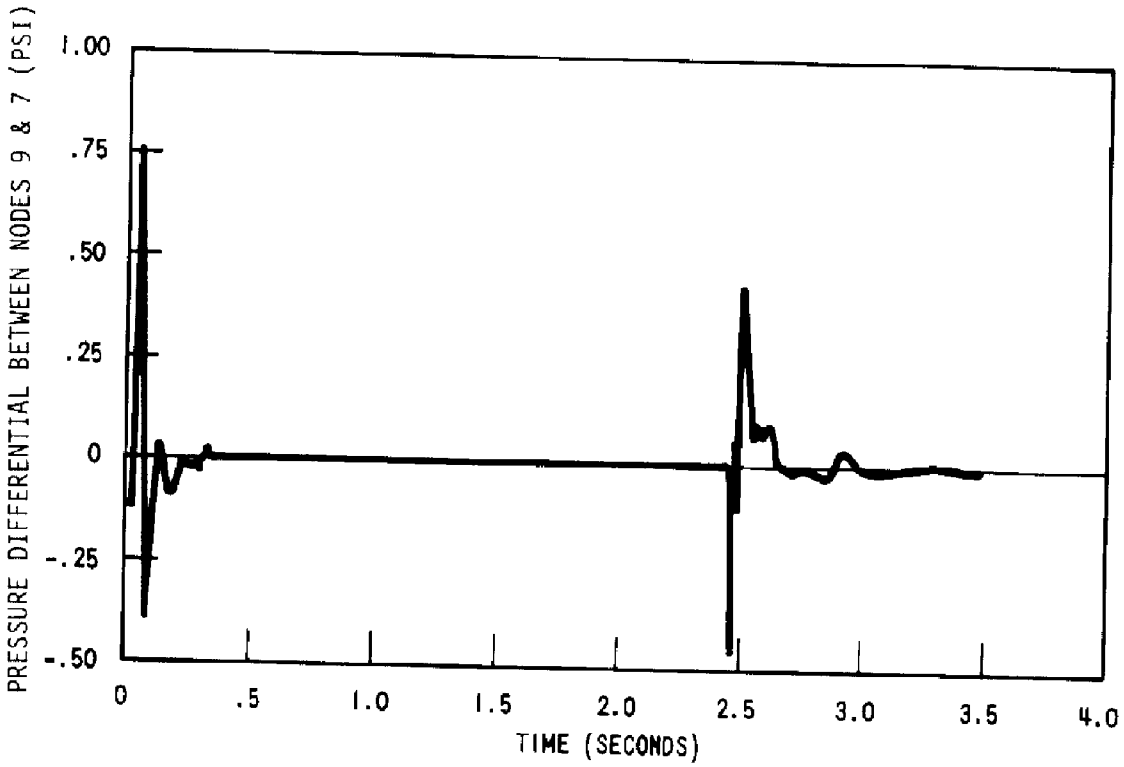

Figure 6-35. Double Ended Steam Line Break in Steam Generator Enclosure

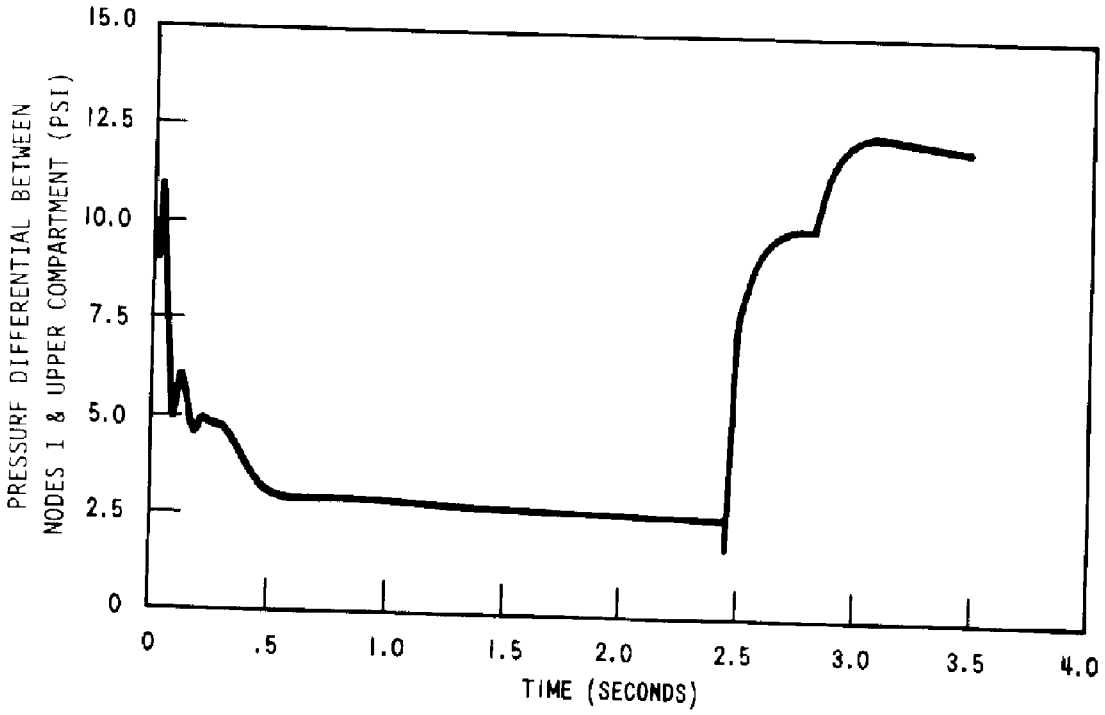

Figure 6-36. Two Volume Nodalization of the Steam Generator Enclosure

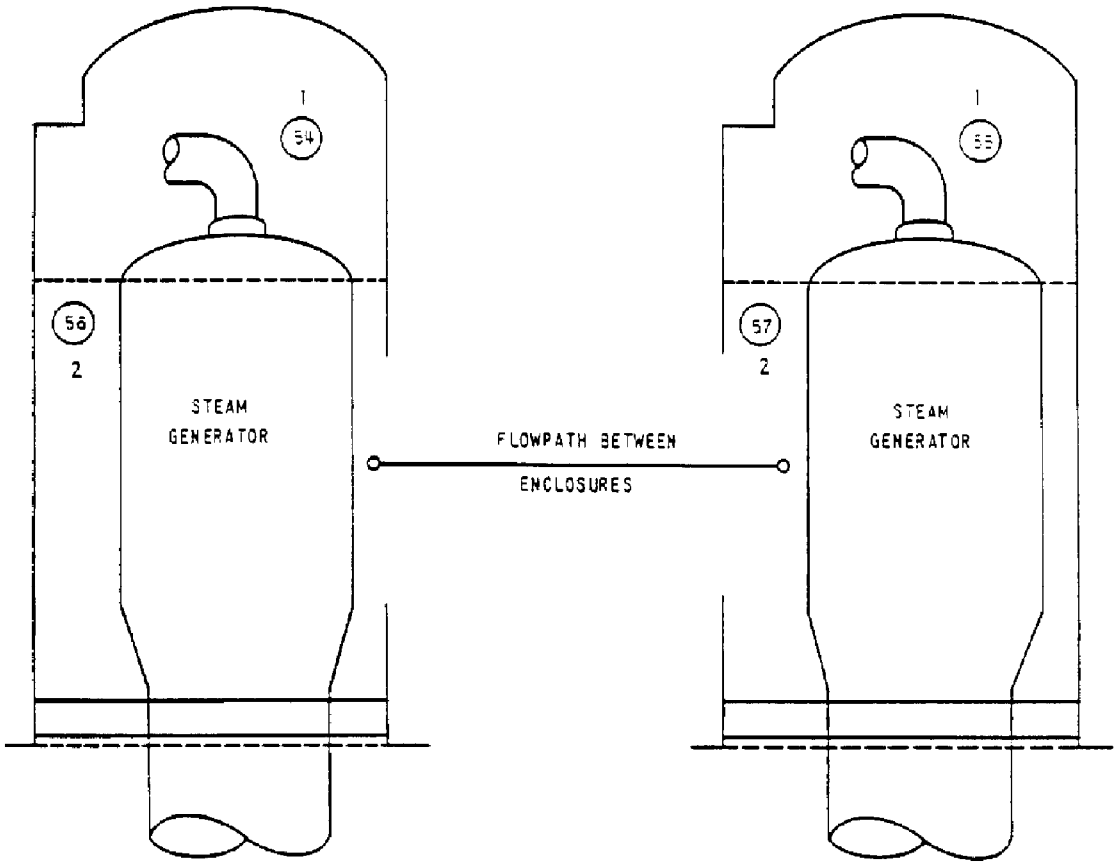

Figure 6-37. Two Volume Nodalization of the Pressurizer Enclosure

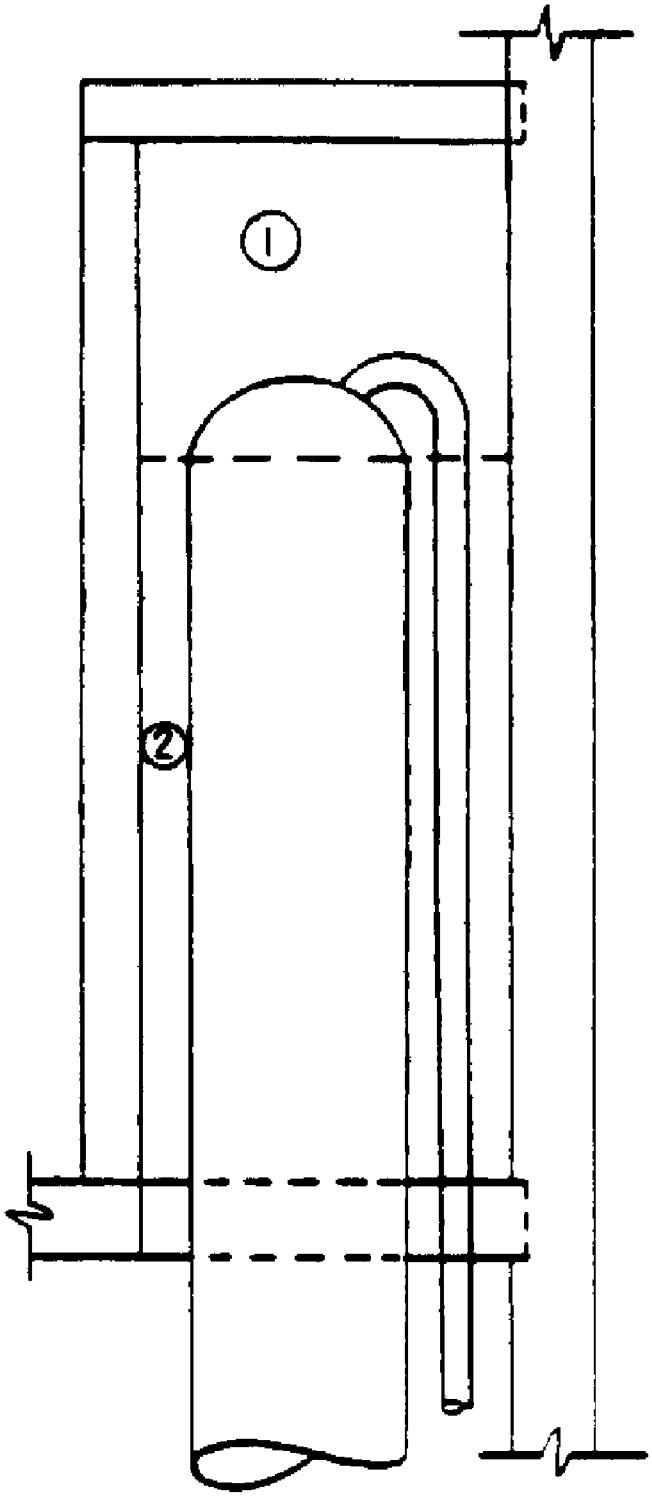

Figure 6-38. Four Volume Nodalization of the Pressurizer Enclosure

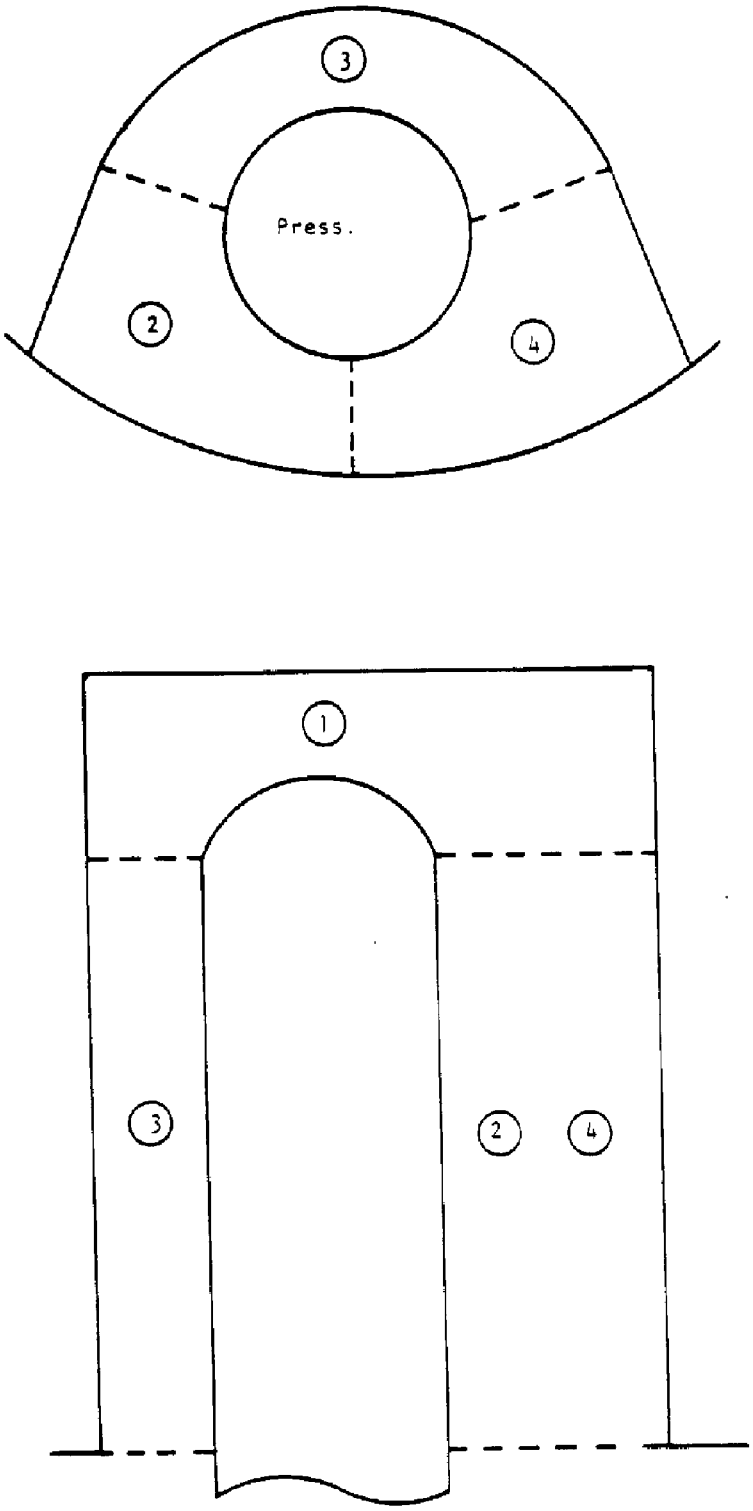

Figure 6-39. Developed View of the TMD Code Network for the Reactor Cavity Analysis

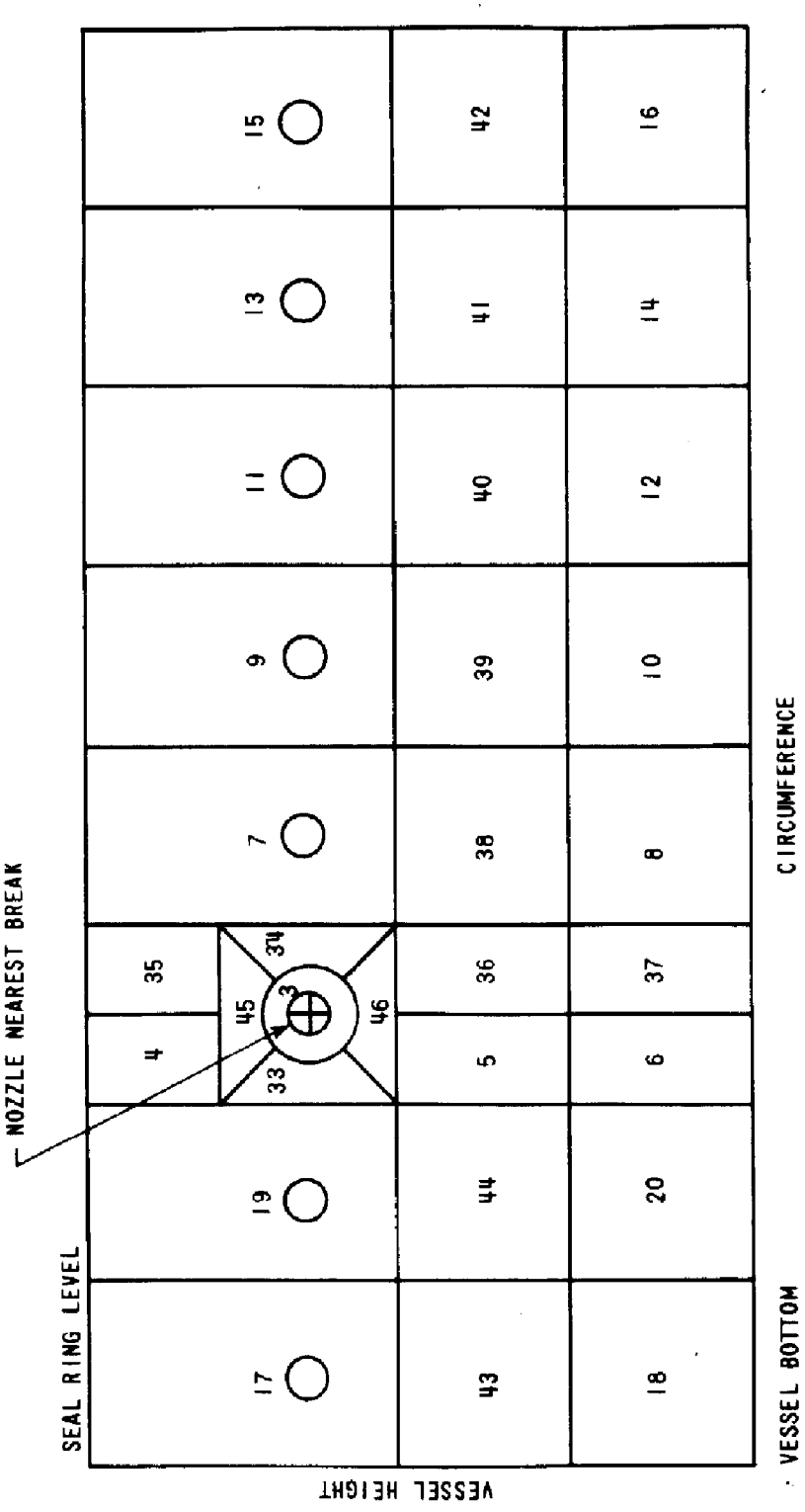

Figure 6-40. Flowpath Connections for the Reactor Cavity Analysis

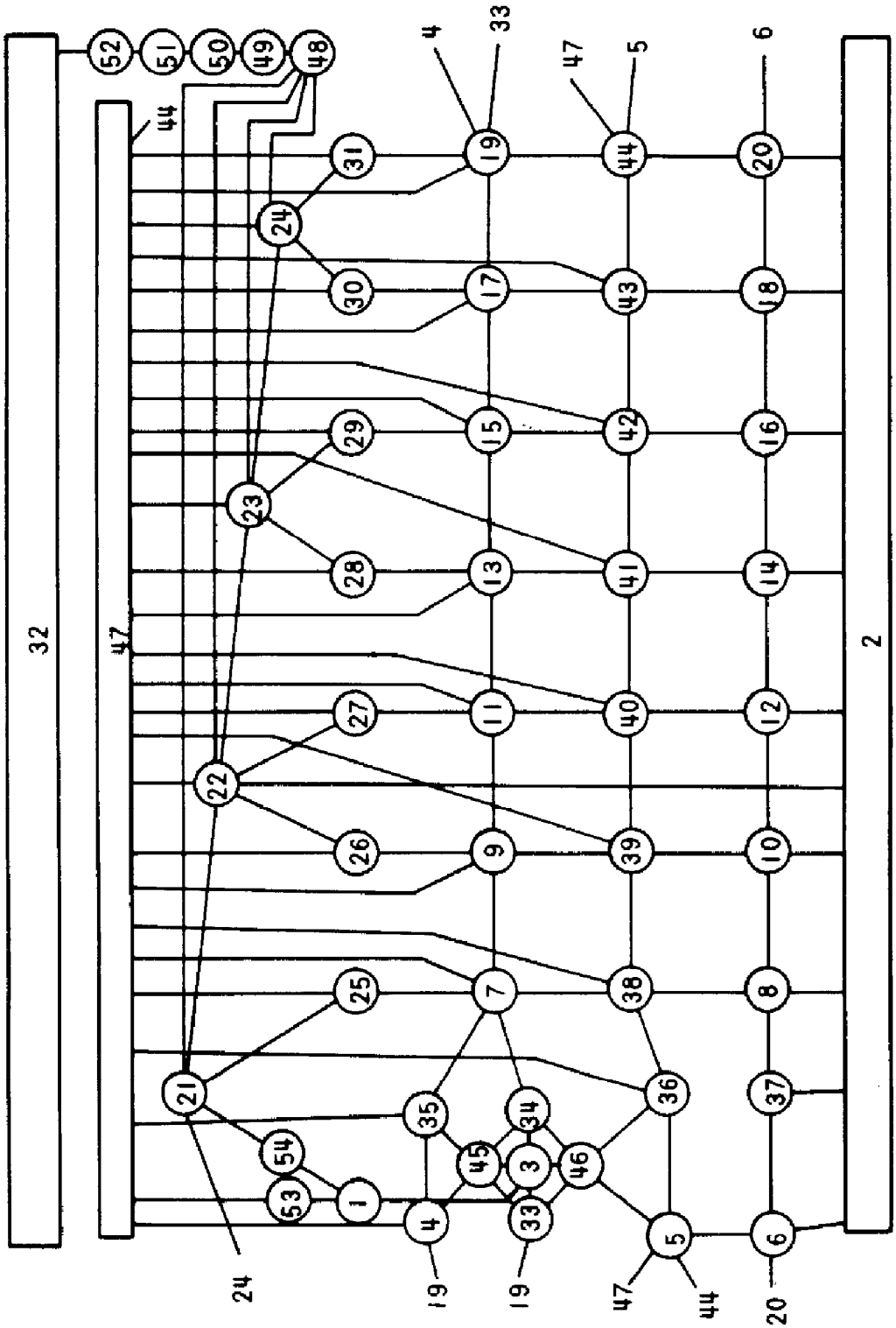

Figure 6-41. Containment Model for the Reactor Cavity Analysis

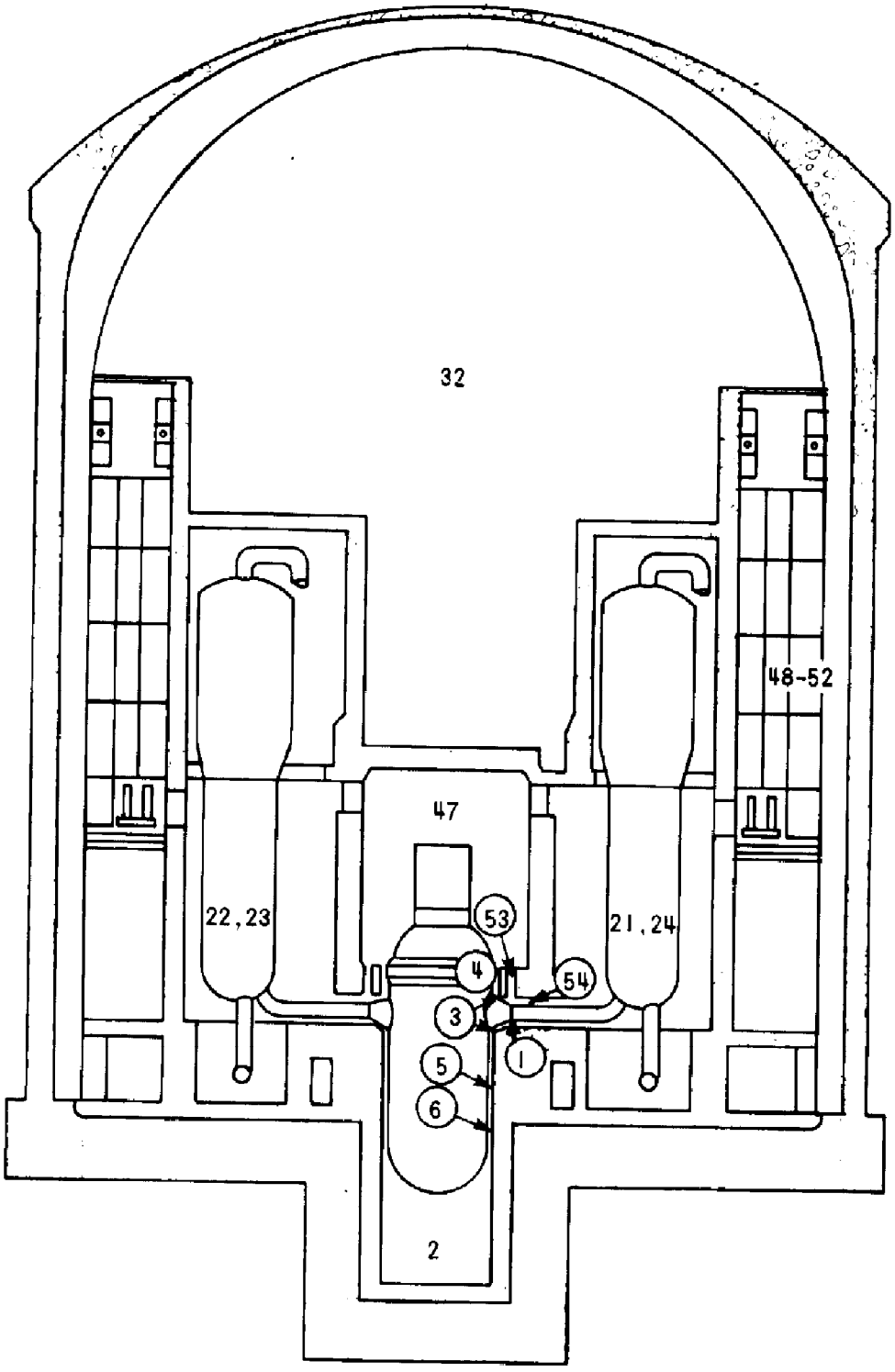

Figure 6-42. Reactor Vessel Nozzle Break Restraints

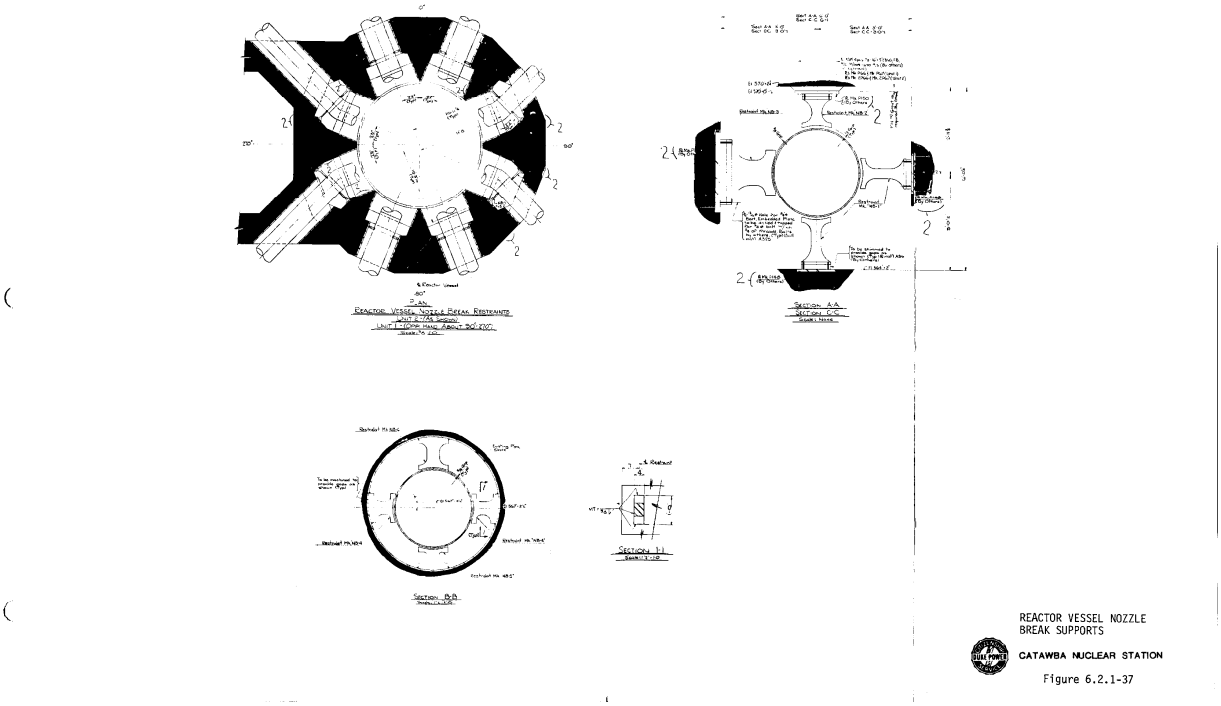

Figure 6-43. Reactor Cavity Analysis, Element 1

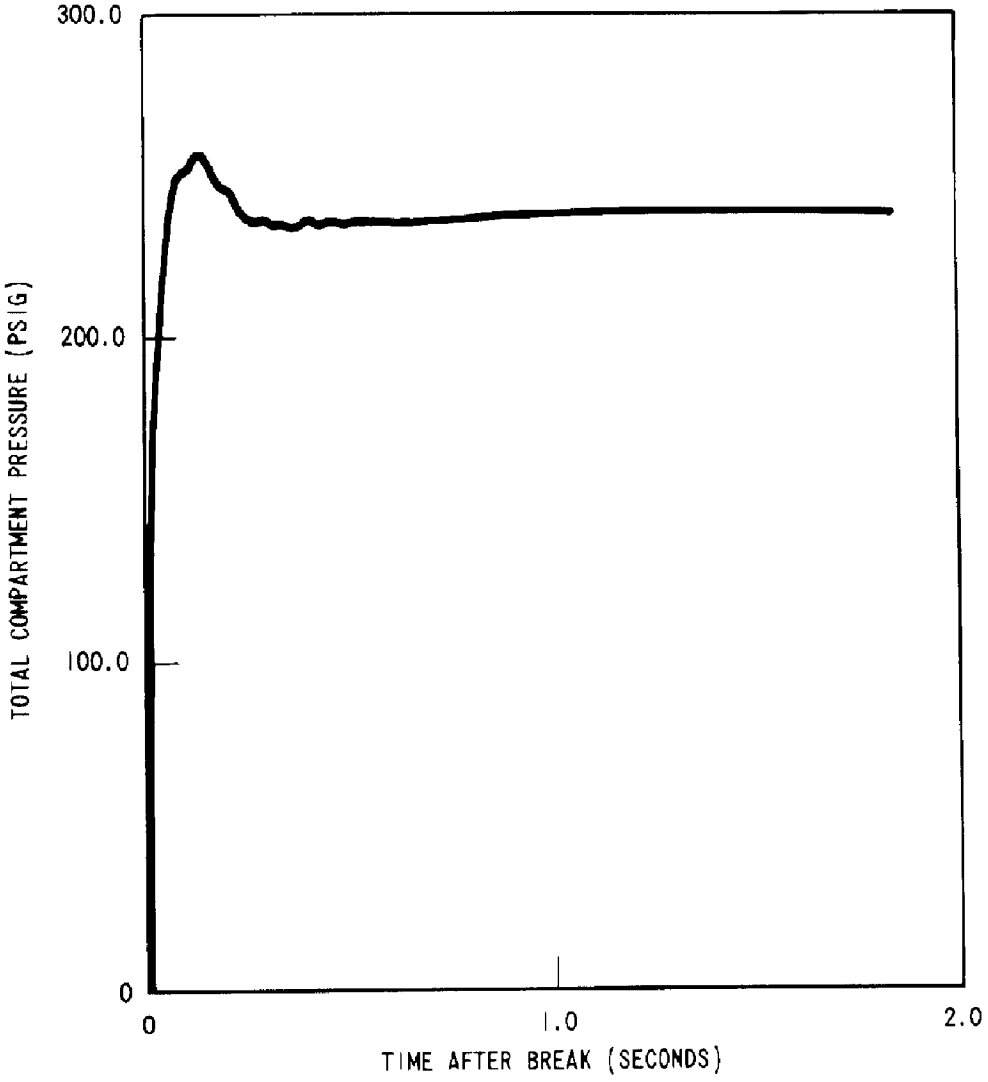

Figure 6-44. Reactor Cavity Analysis, Element 2

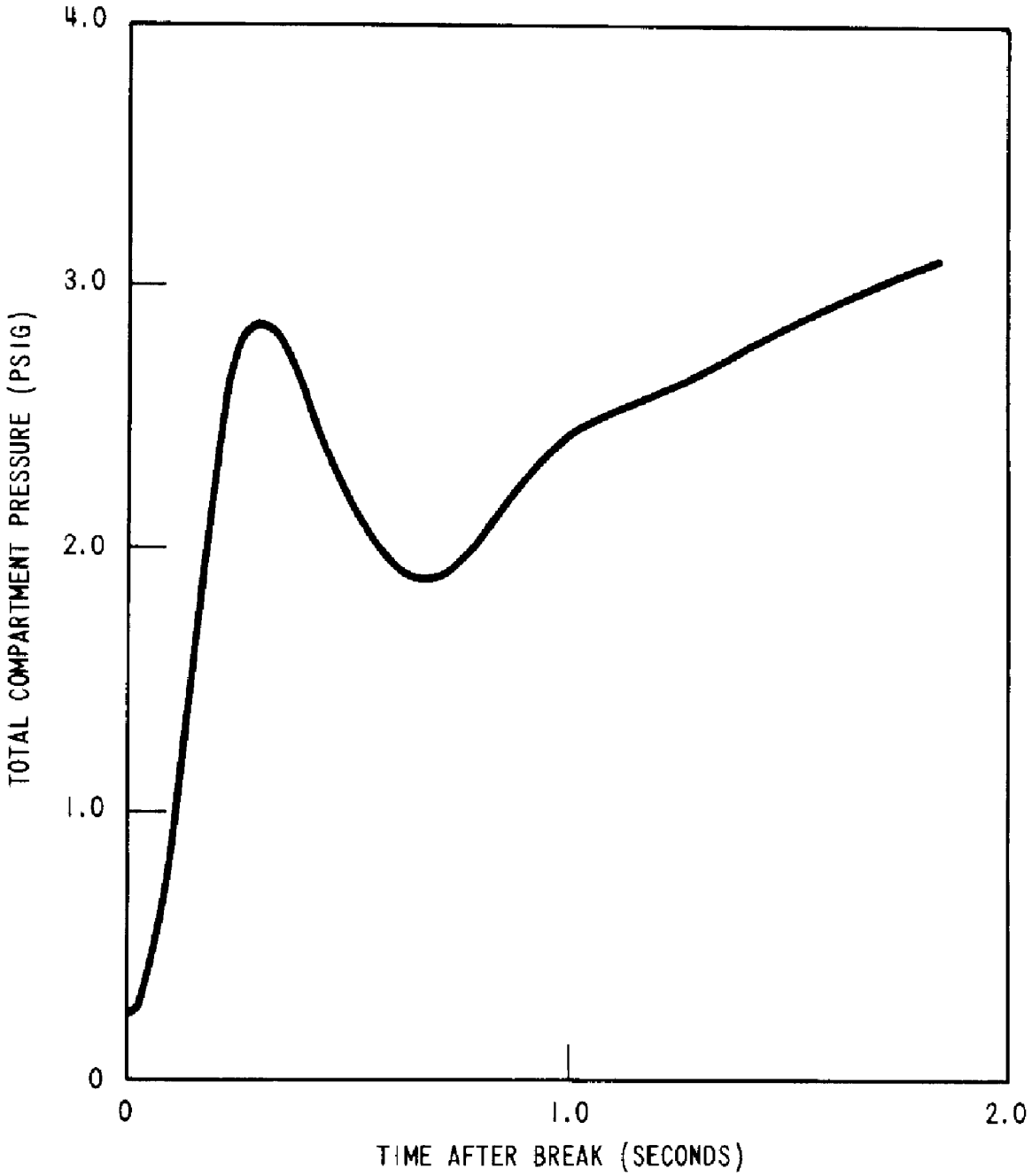

Figure 6-45. Reactor Cavity Analysis, Element 3

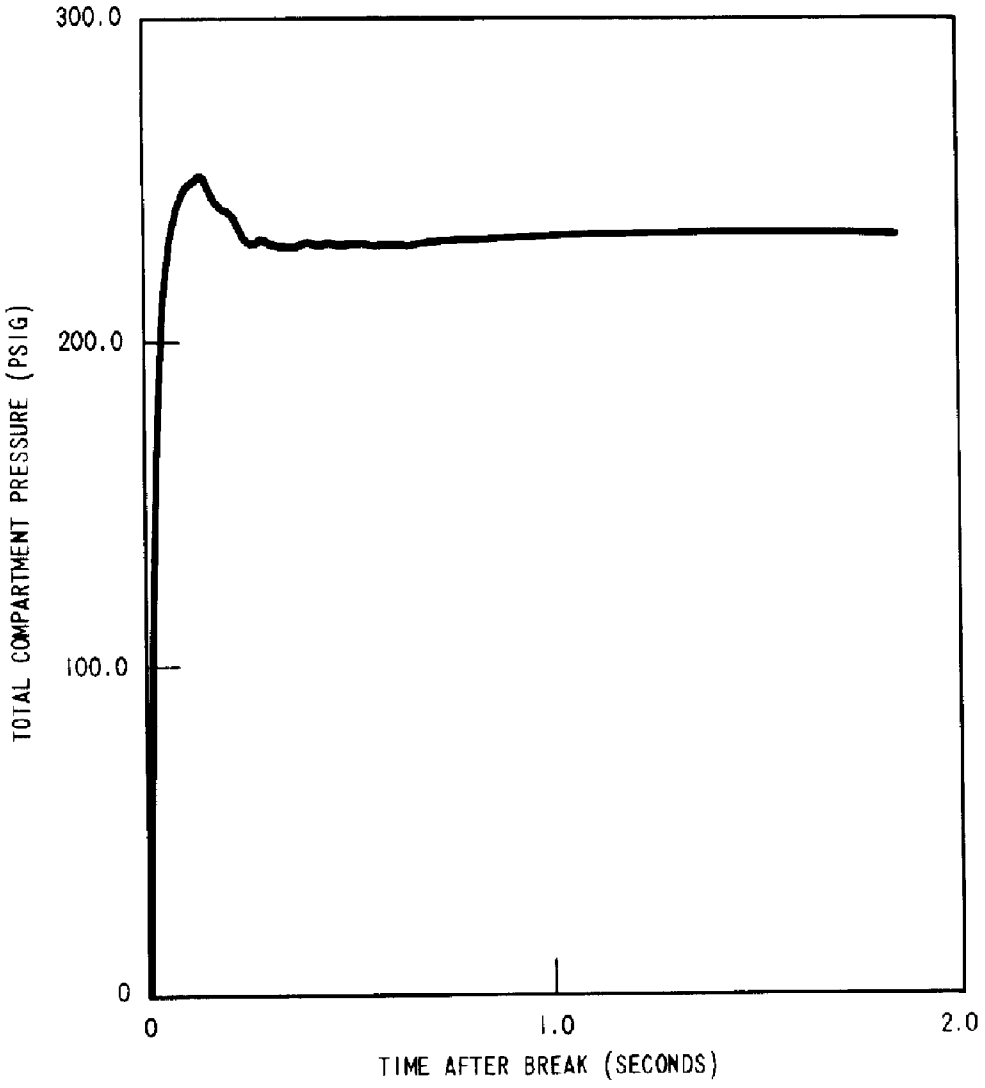

Figure 6-46. Reactor Cavity Analysis, Element 4

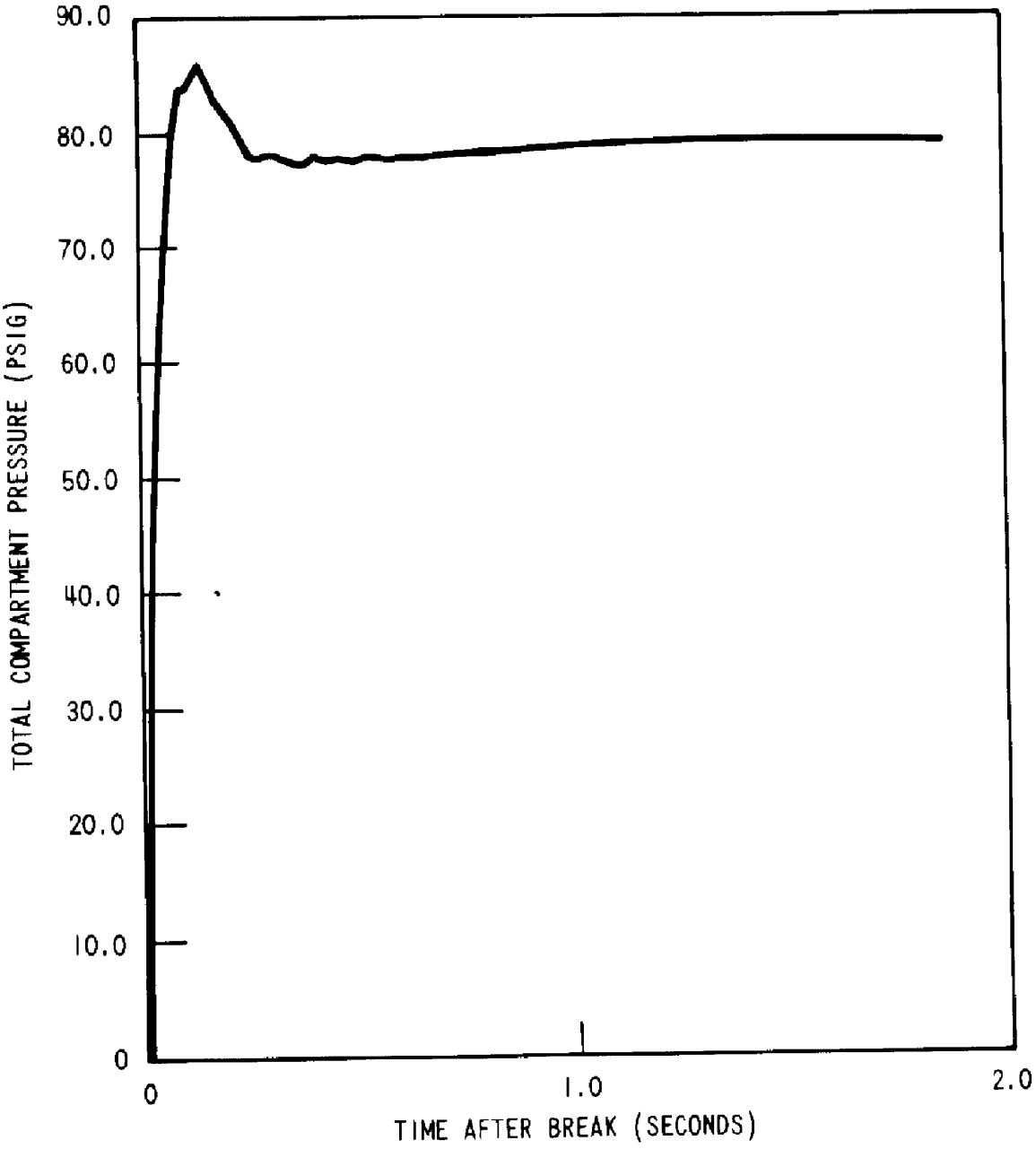

Figure 6-47. Reactor Cavity Analysis, Element 5

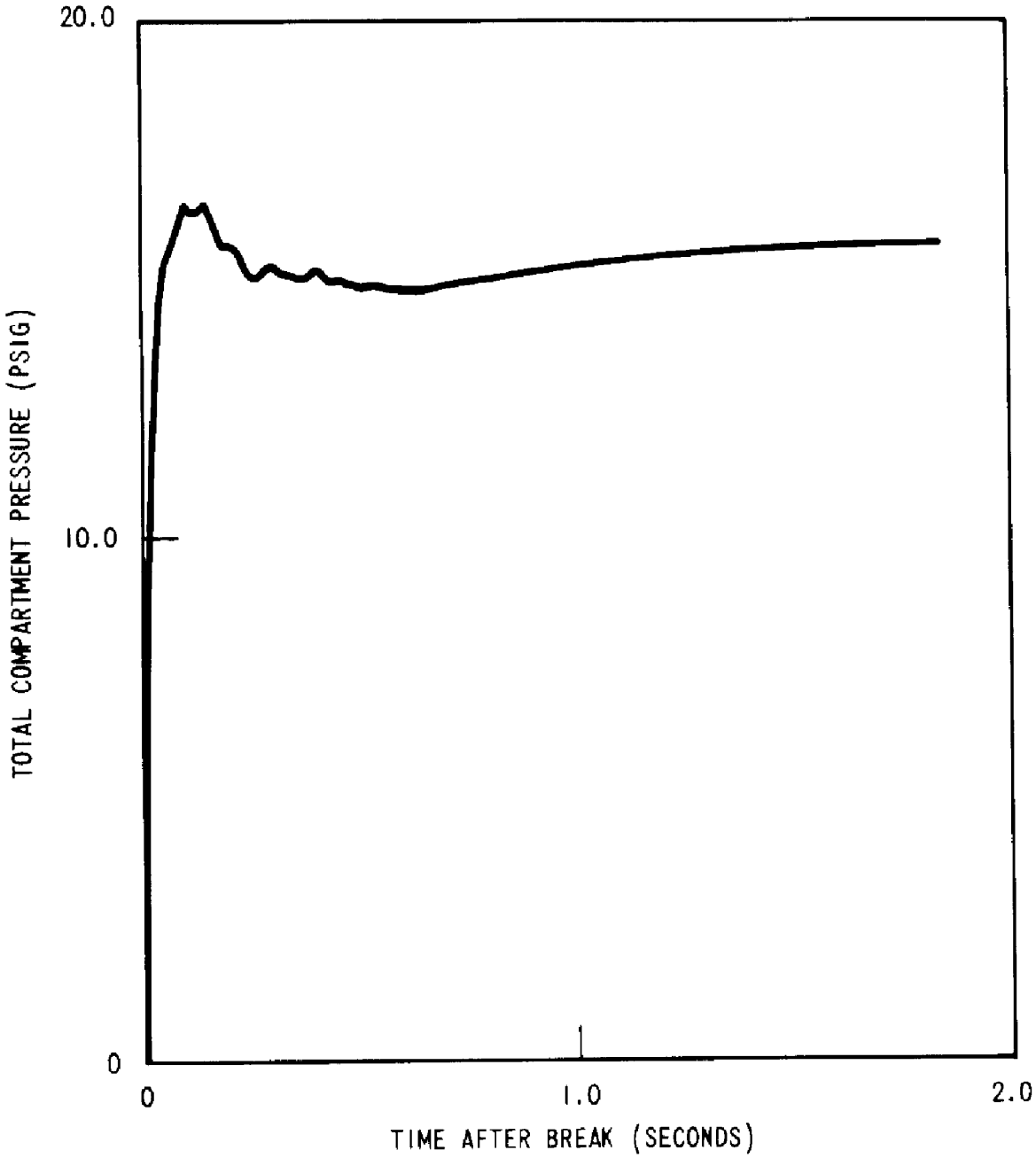

Figure 6-48. Reactor Cavity Analysis, Element 6

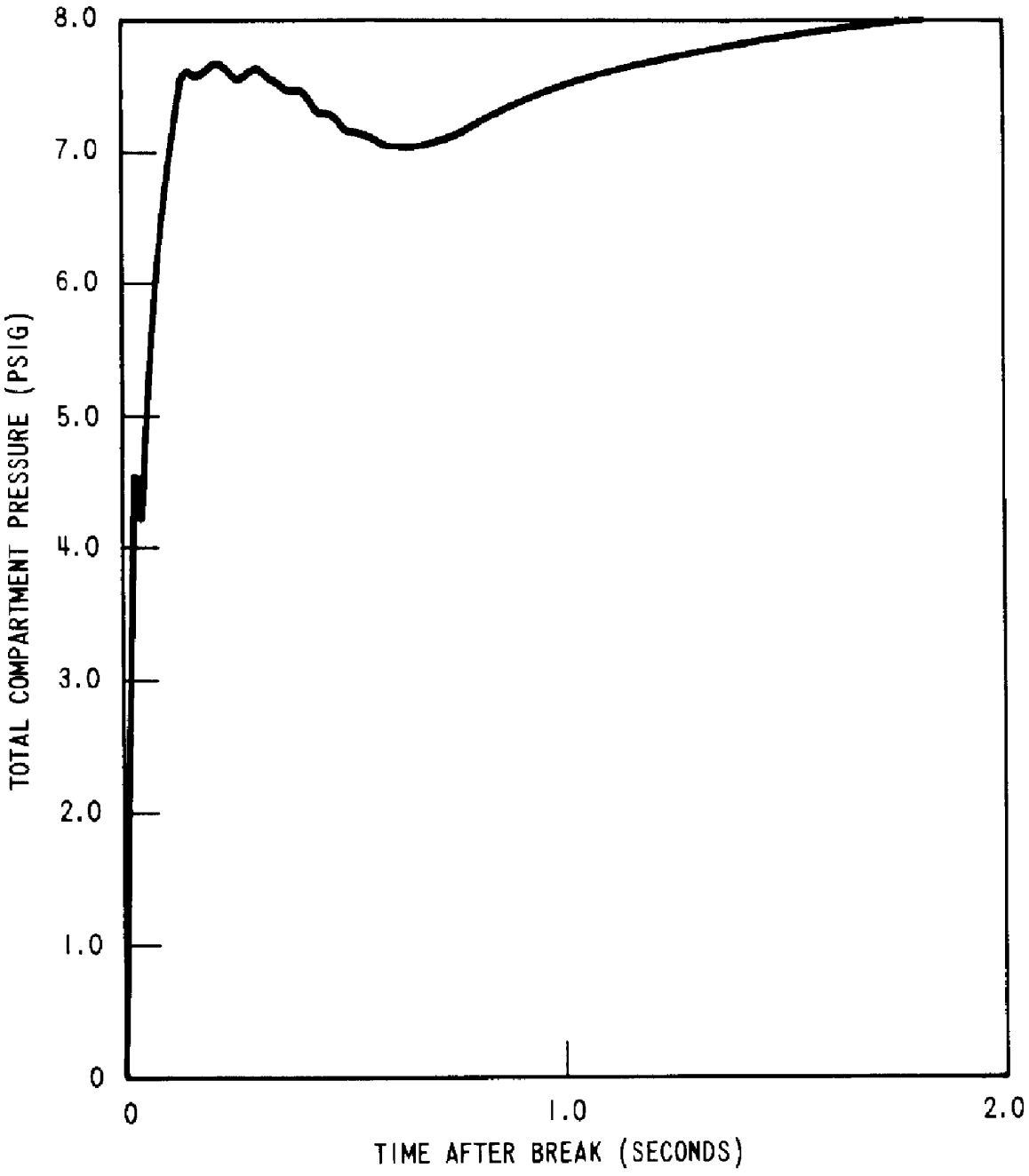

Figure 6-49. Reactor Cavity Analysis, Element 7

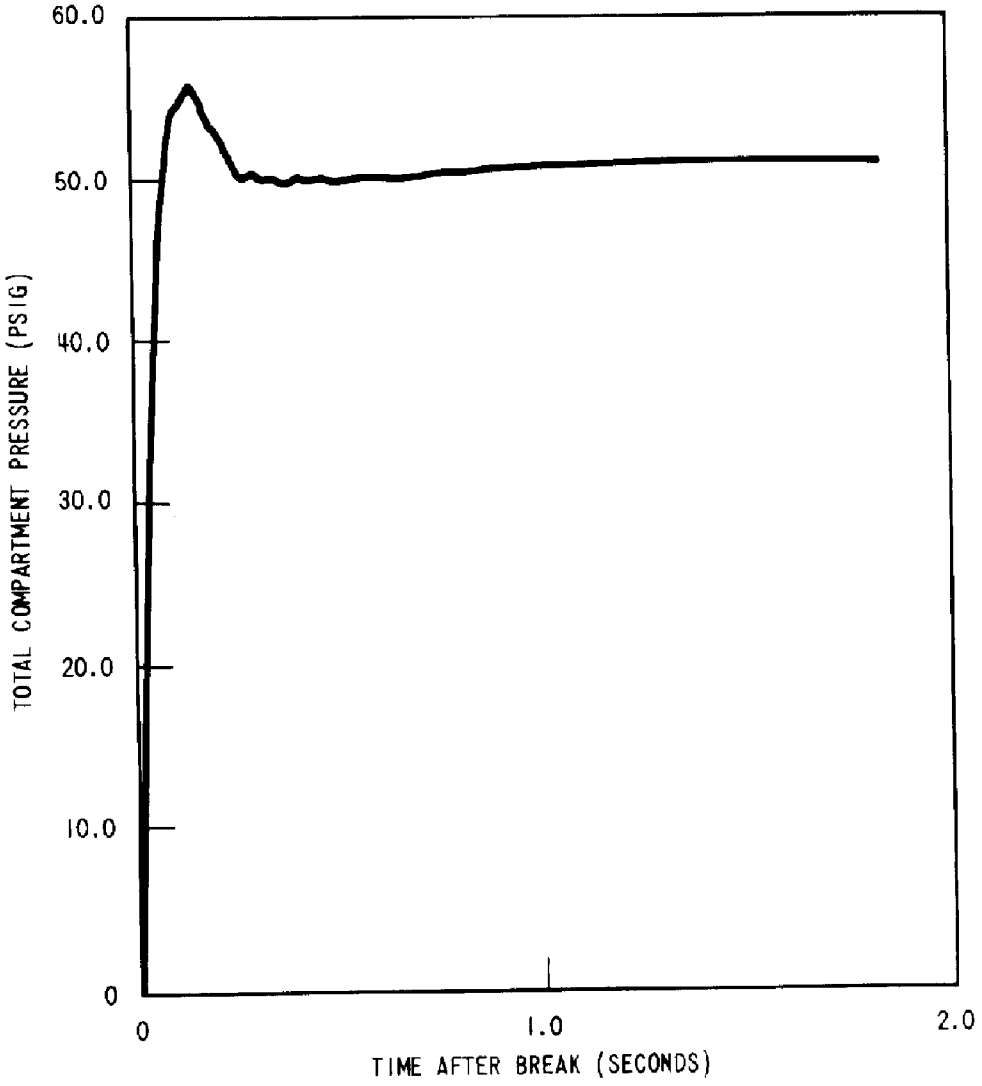

Figure 6-50. Reactor Cavity Analysis, Element 8

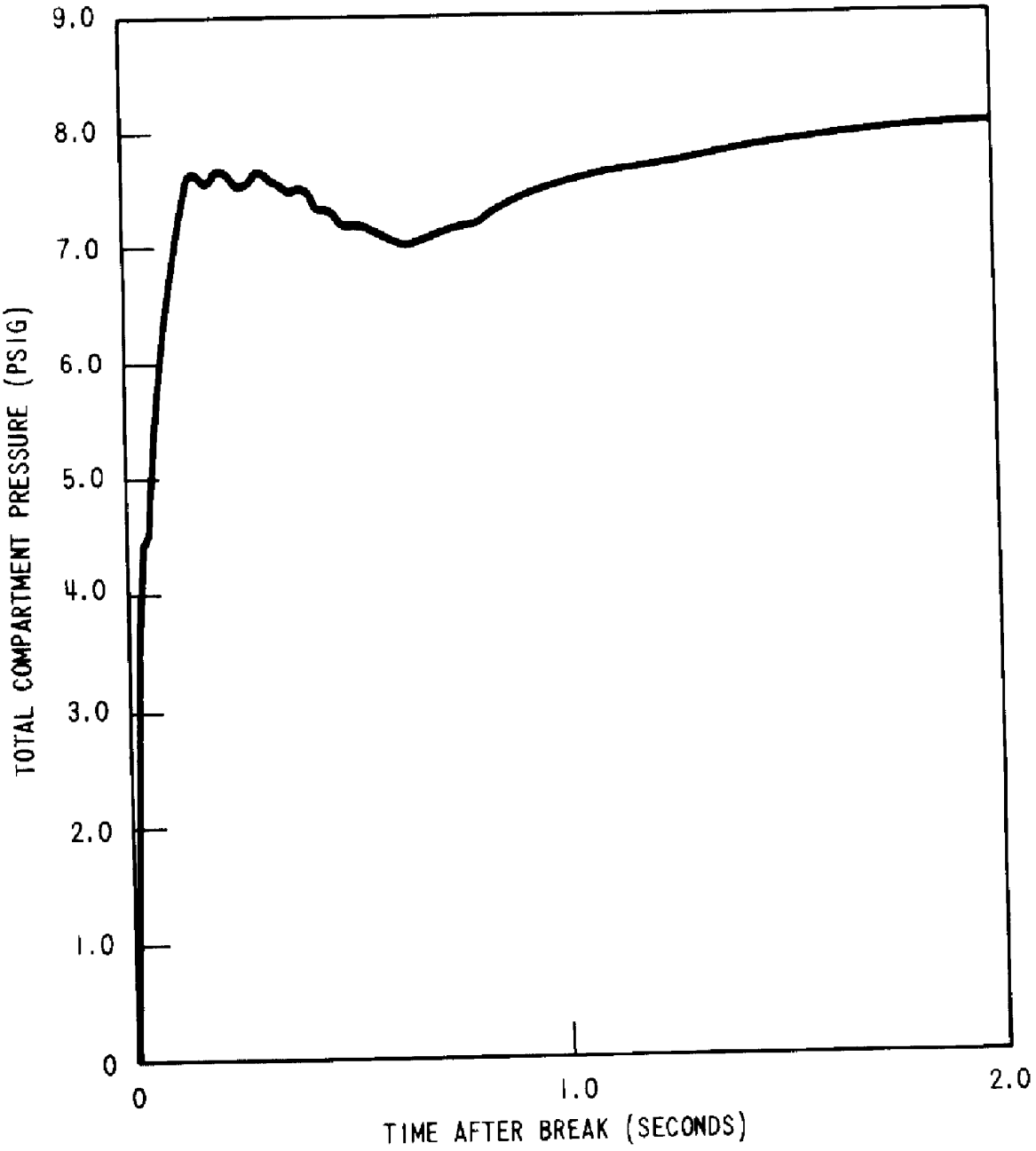

Figure 6-51. Reactor Cavity Analysis, Element 9

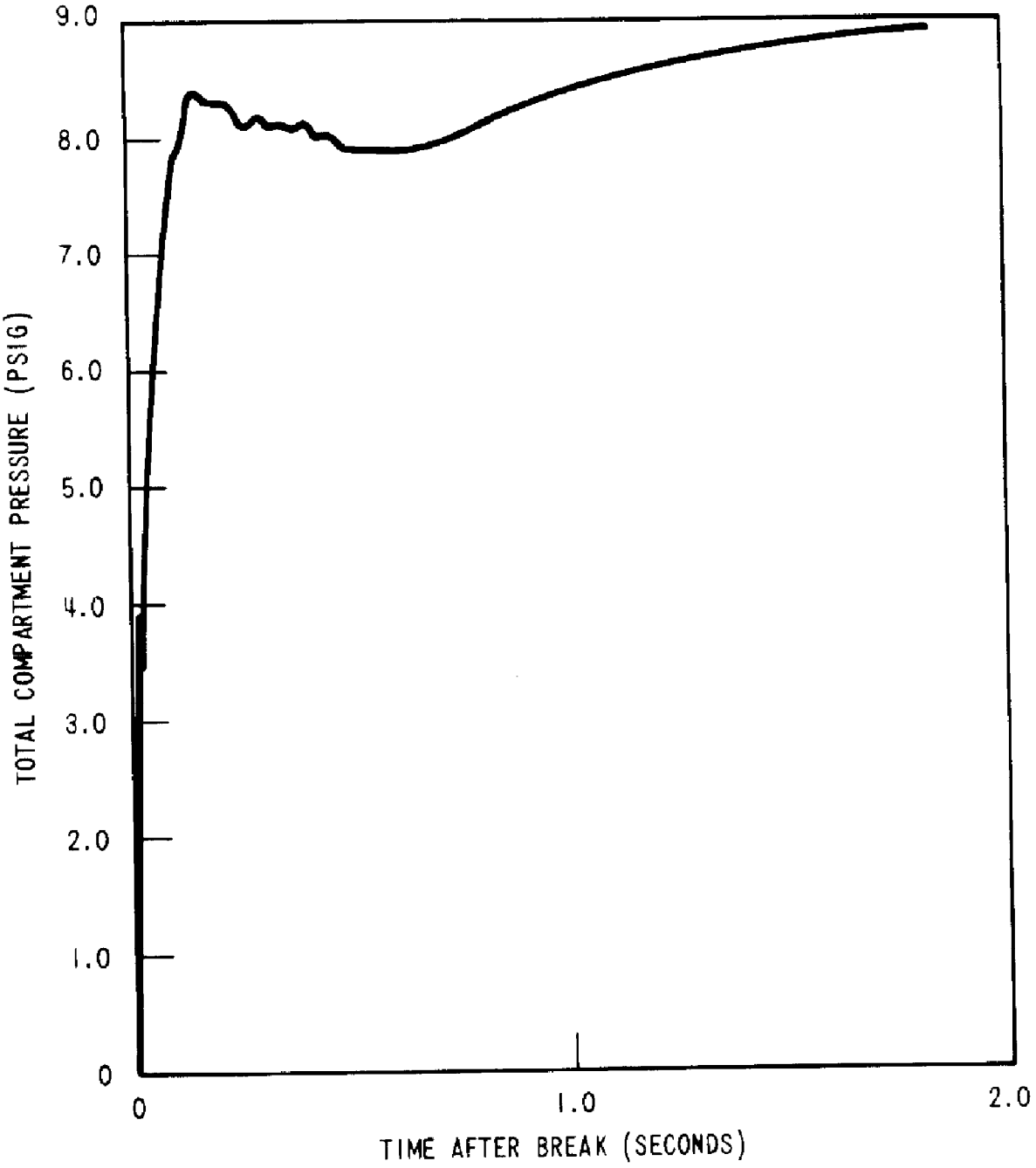

Figure 6-52. Reactor Cavity Analysis, Element 10

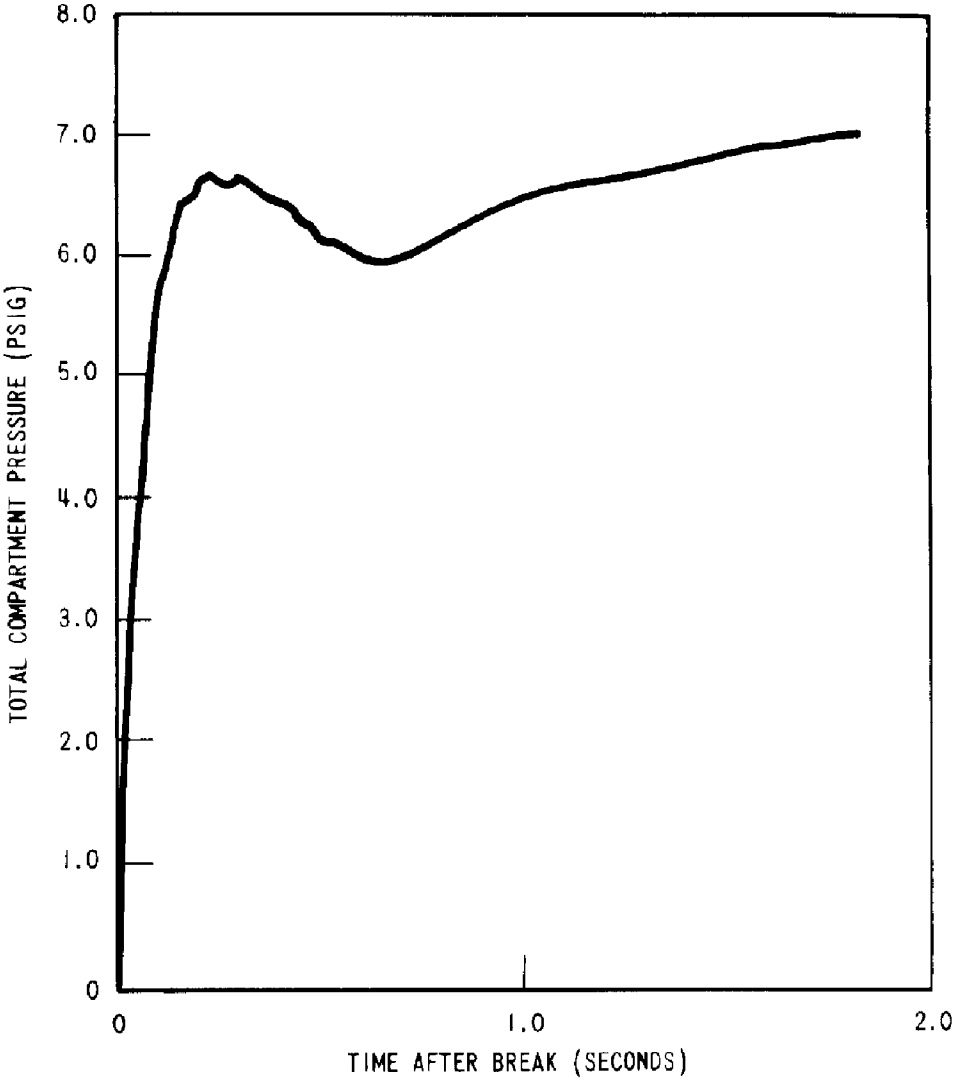

Figure 6-53. Reactor Cavity Analysis, Element 11

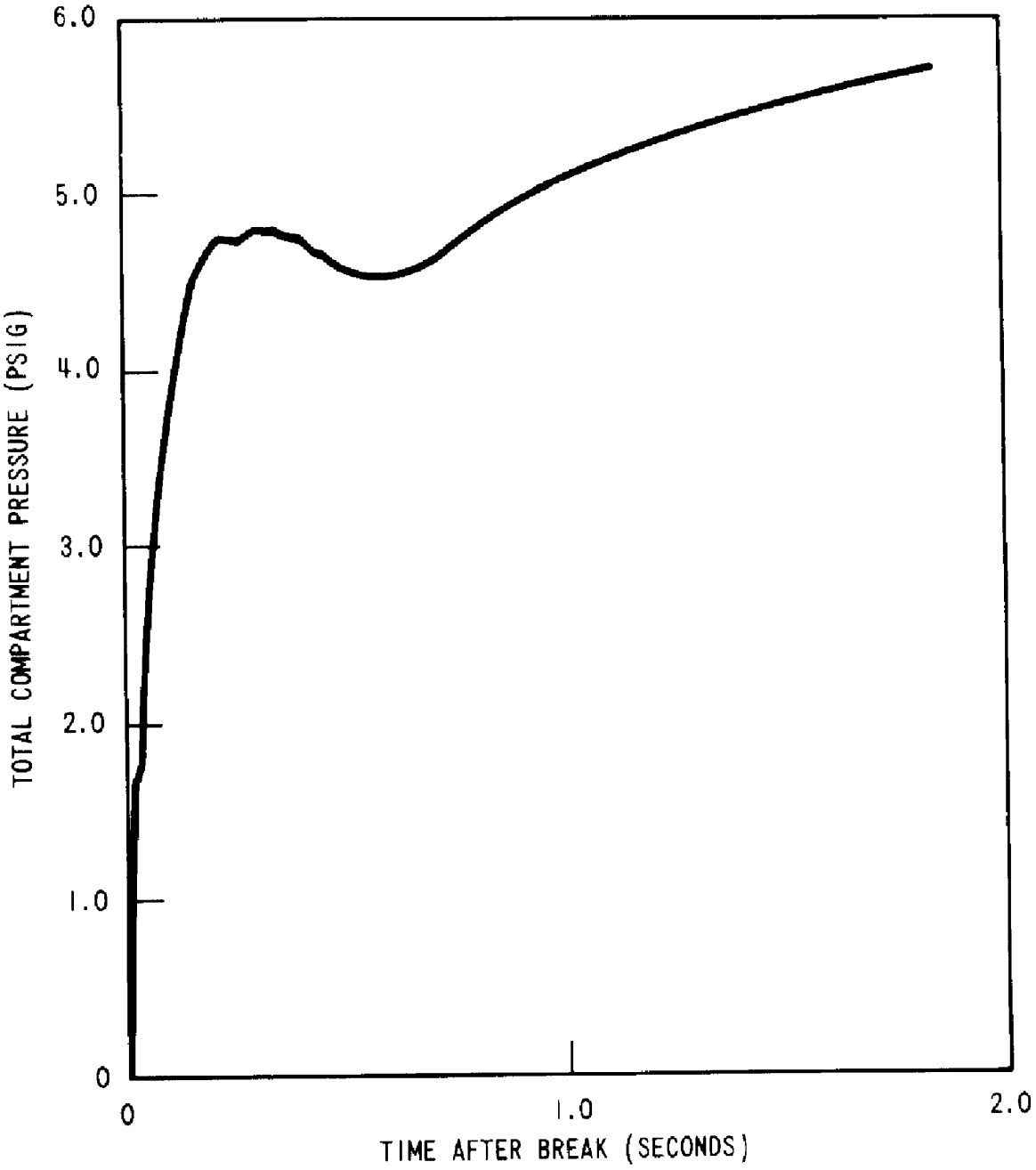

Figure 6-54. Reactor Cavity Analysis, Element 12

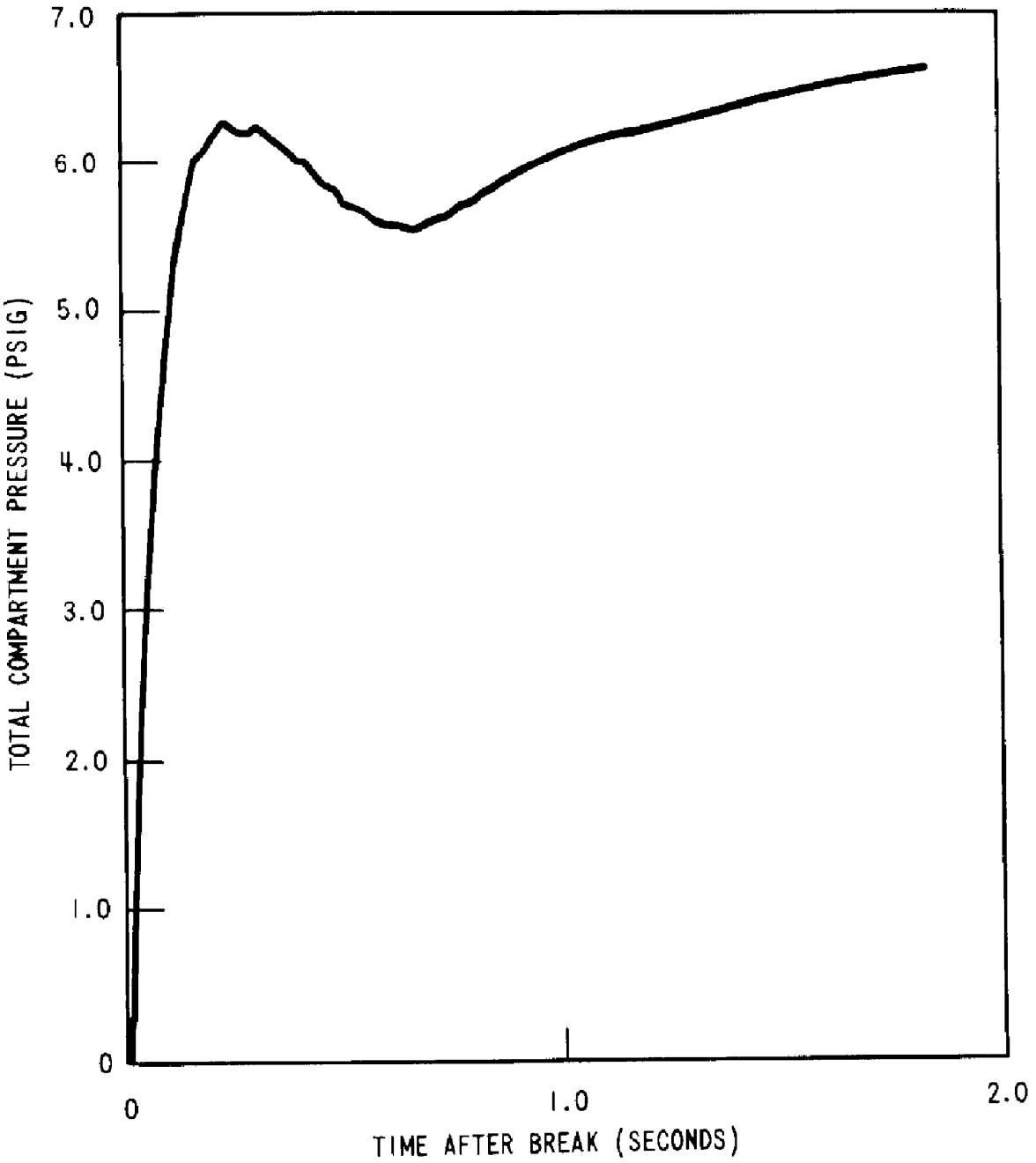

Figure 6-55. Reactor Cavity Analysis, Element 13

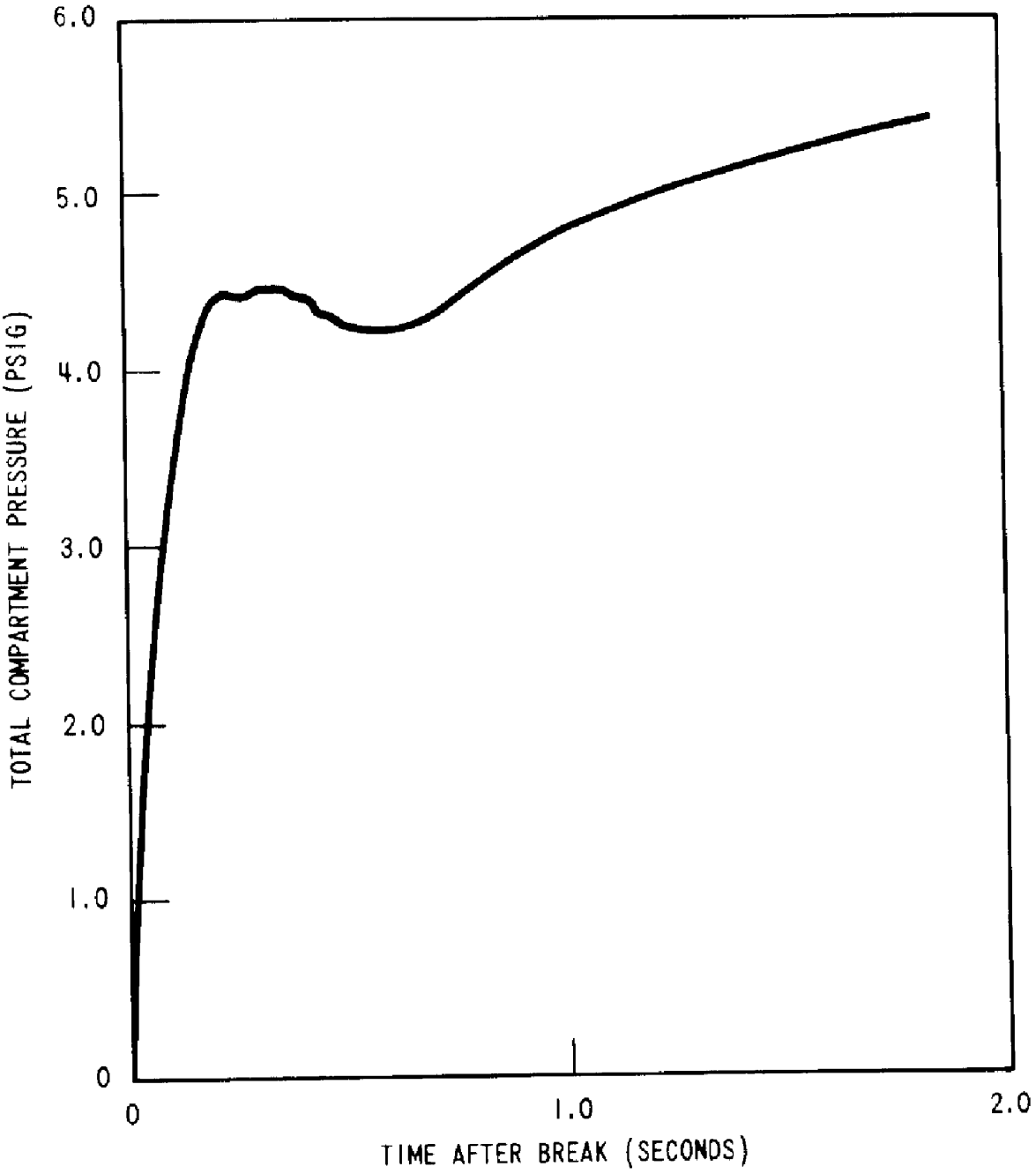

Figure 6-56. Reactor Cavity Analysis, Element 14

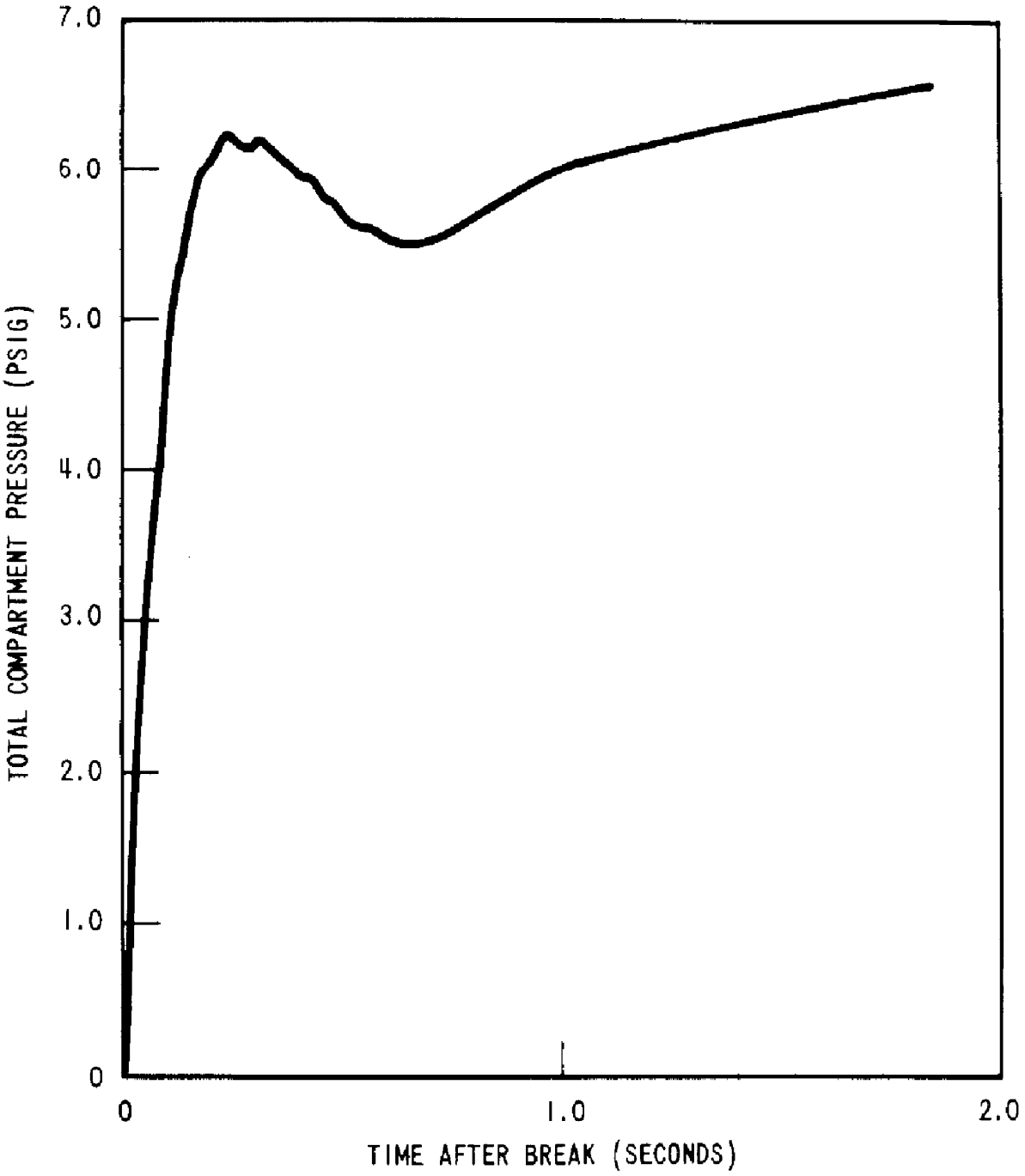

Figure 6-57. Reactor Cavity Analysis, Element 15

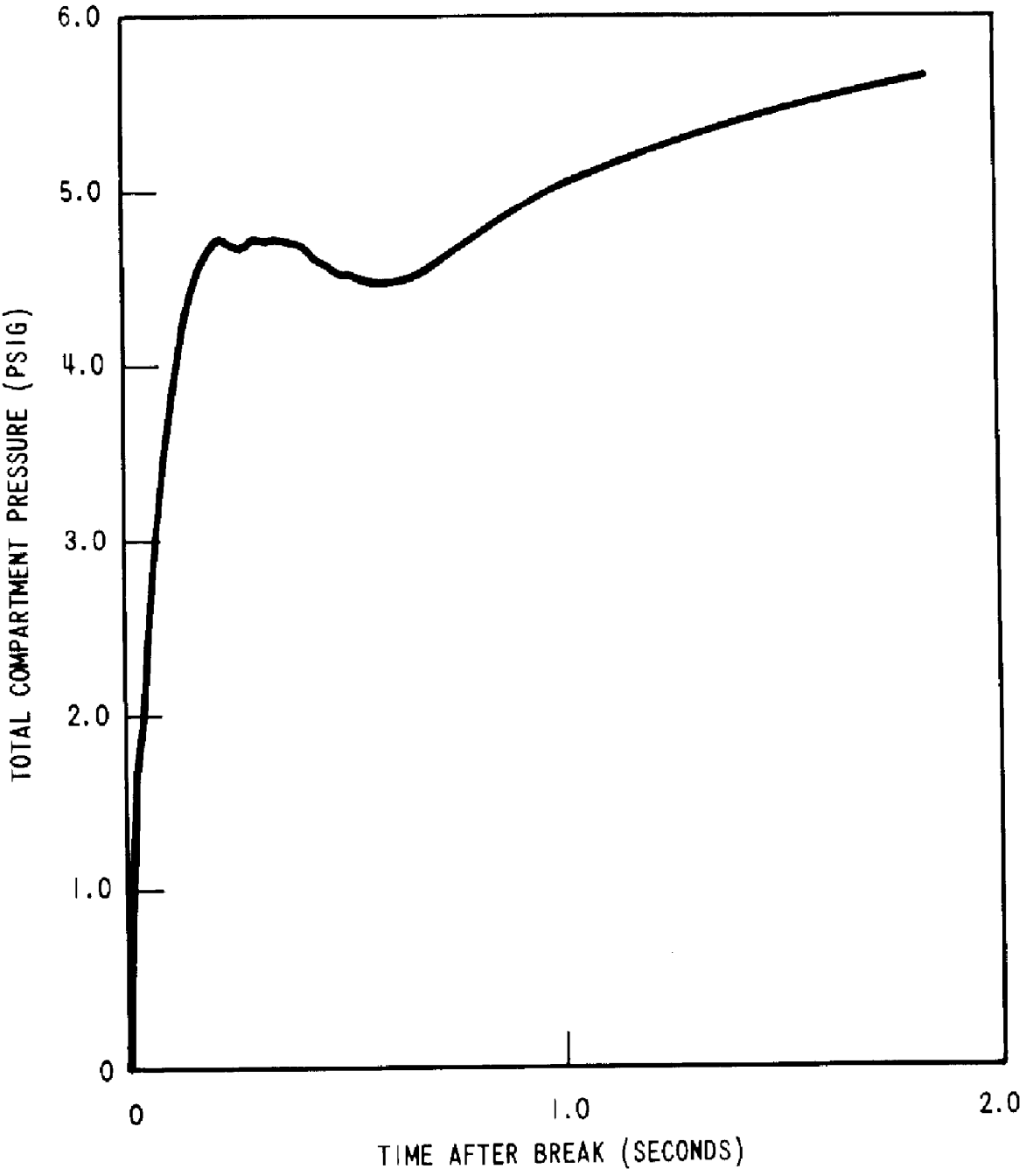

Figure 6-58. Reactor Cavity Analysis, Element 16

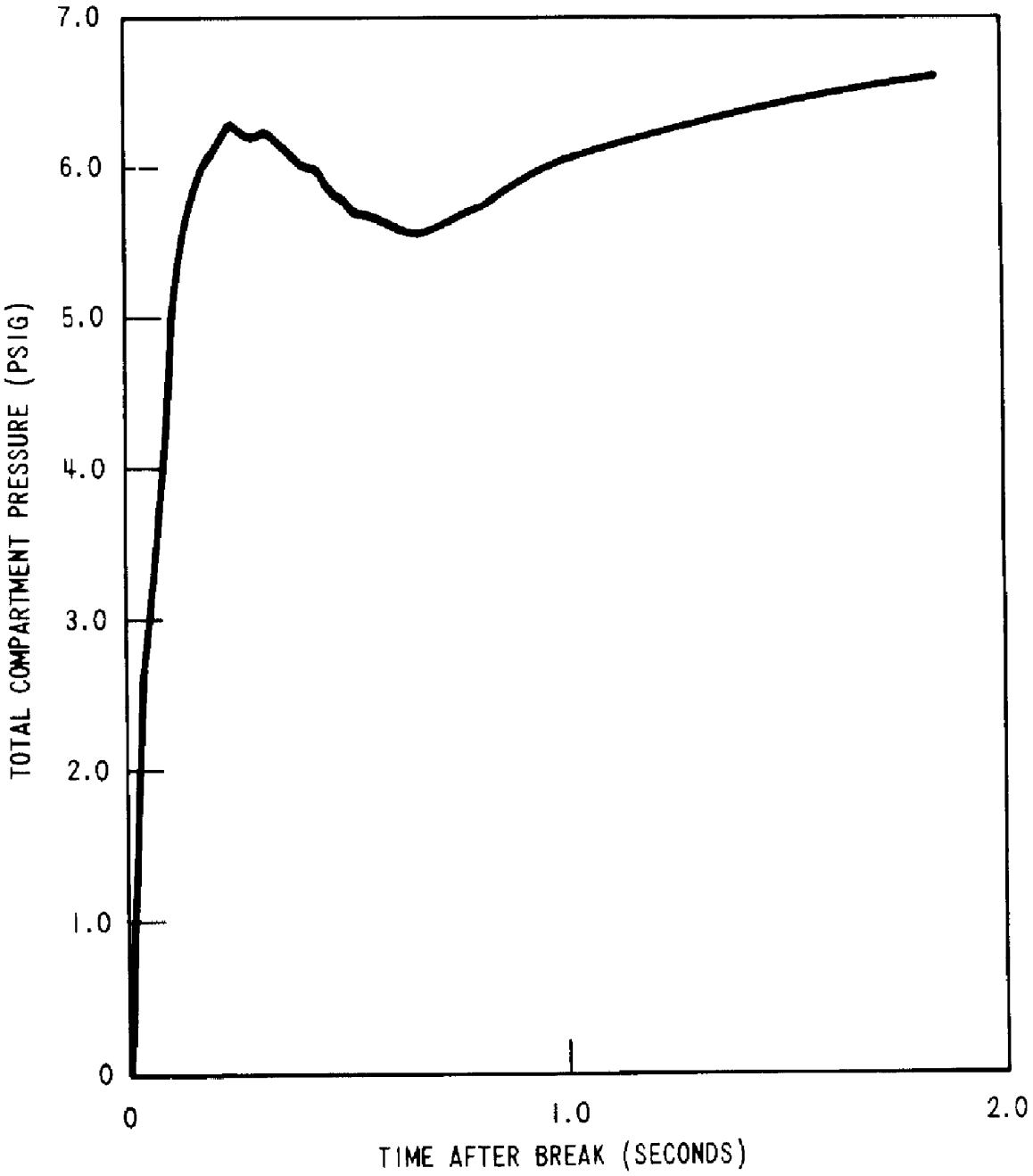

Figure 6-59. Reactor Cavity Analysis, Element 17

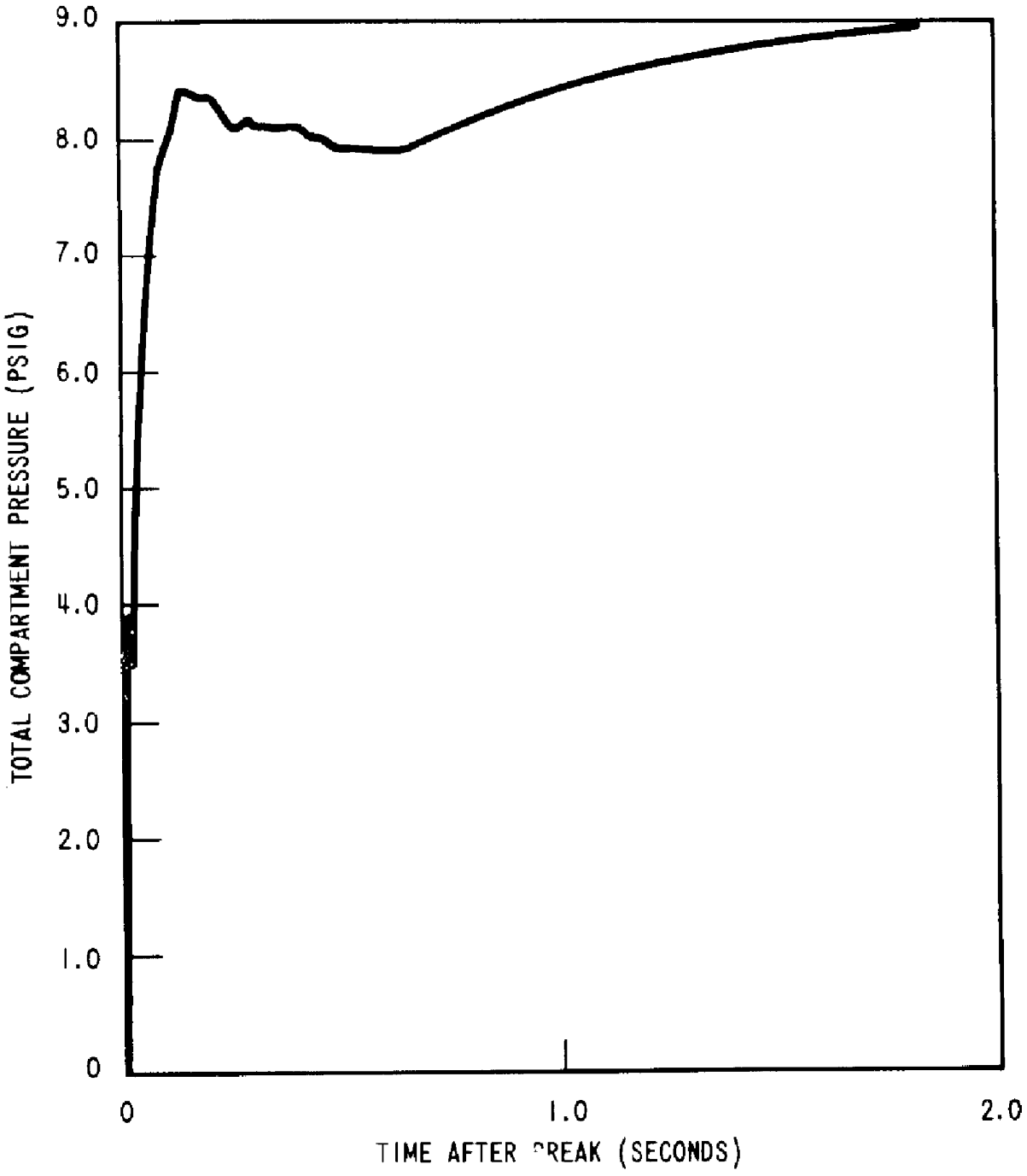

Figure 6-60. Reactor Cavity Analysis, Element 18

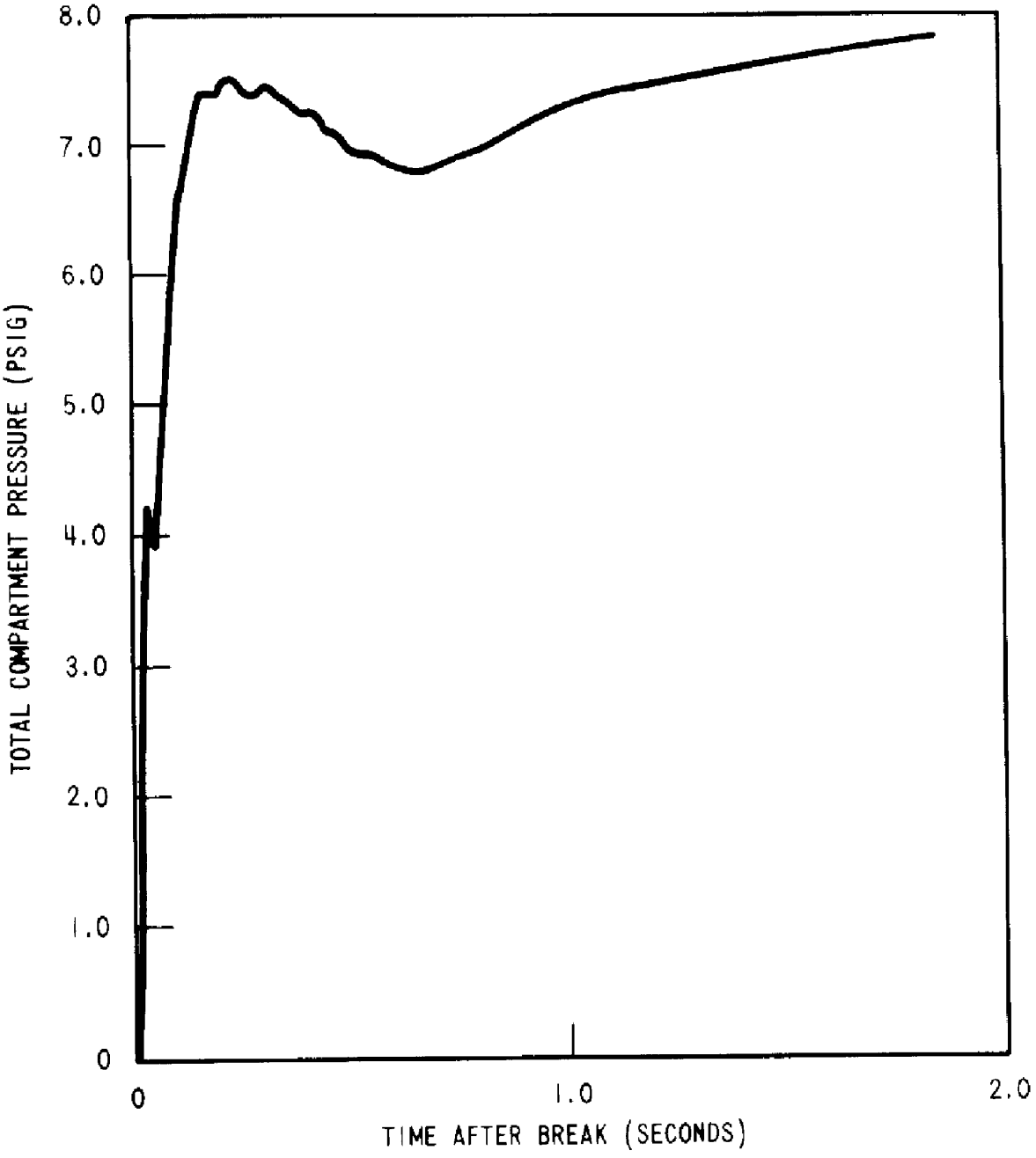

Figure 6-61. Reactor Cavity Analysis, Element 19

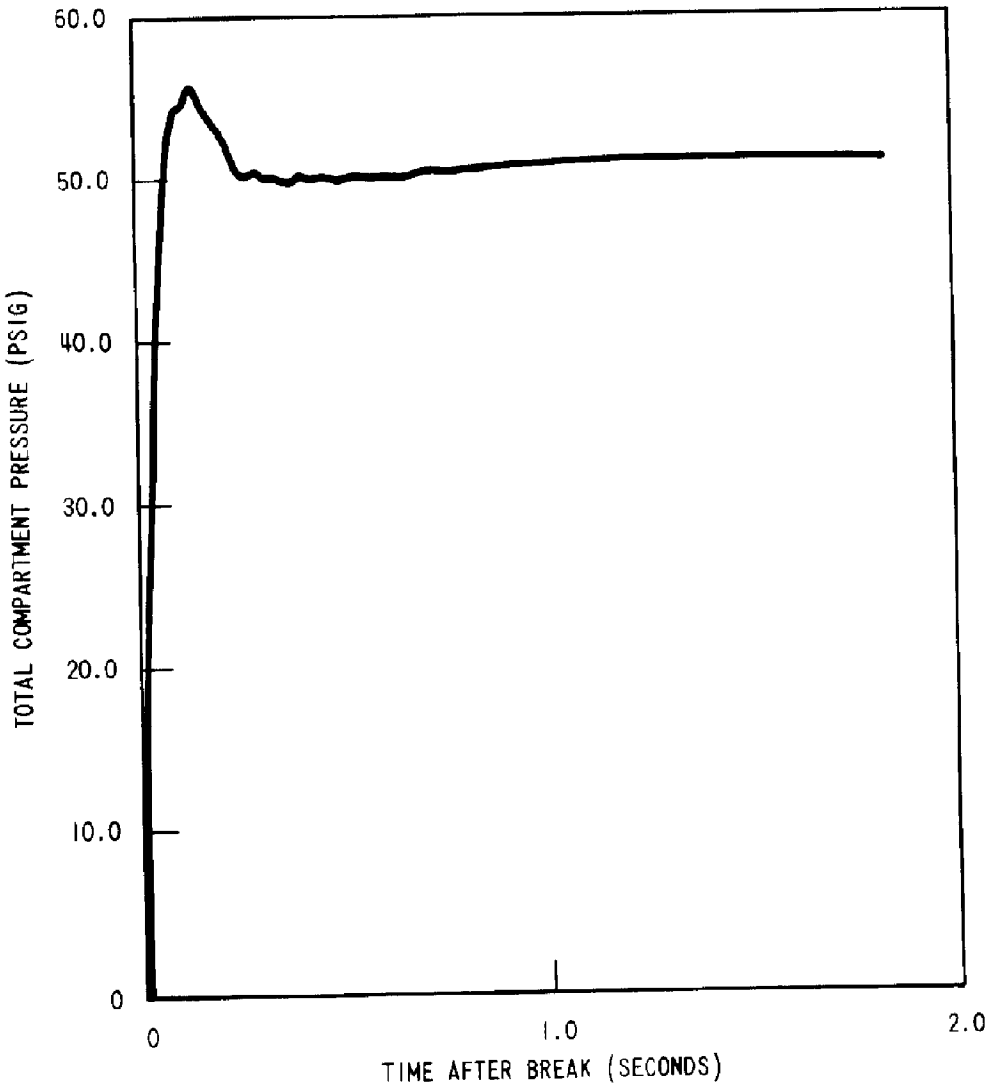

Figure 6-62. Reactor Cavity Analysis, Element 20

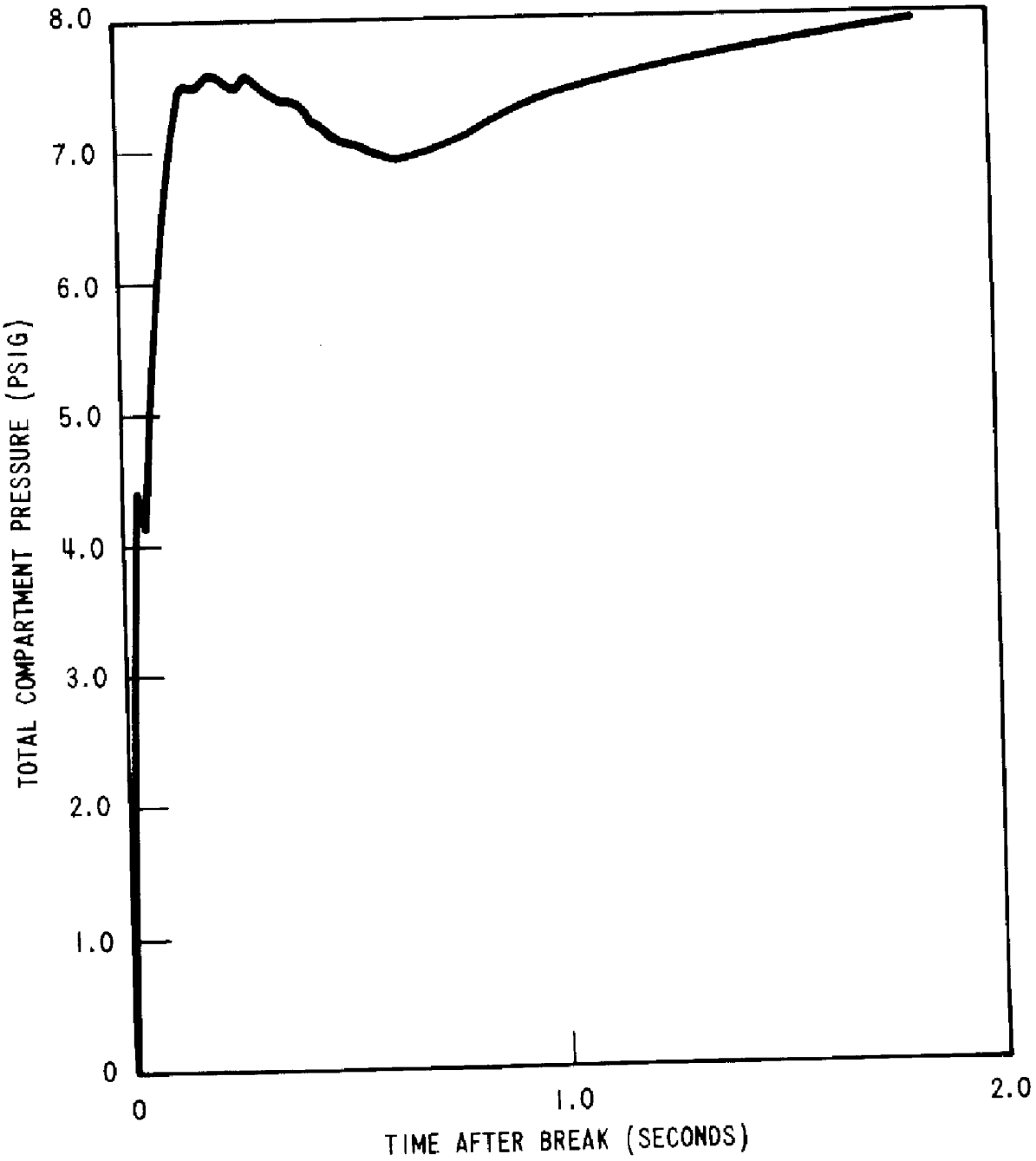

Figure 6-63. Reactor Cavity Analysis, Element 32

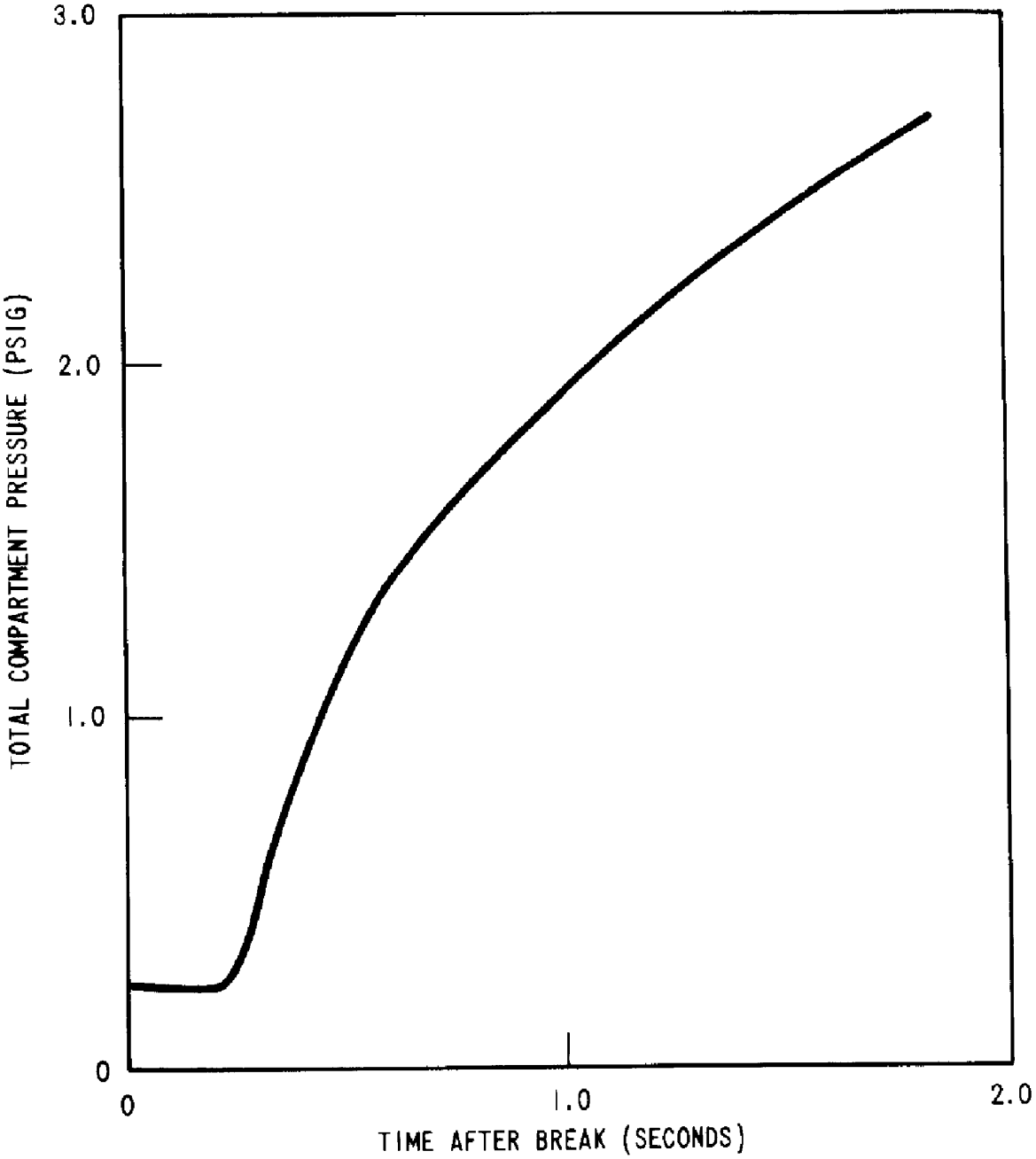

Figure 6-64. Reactor Cavity Analysis, Element 33

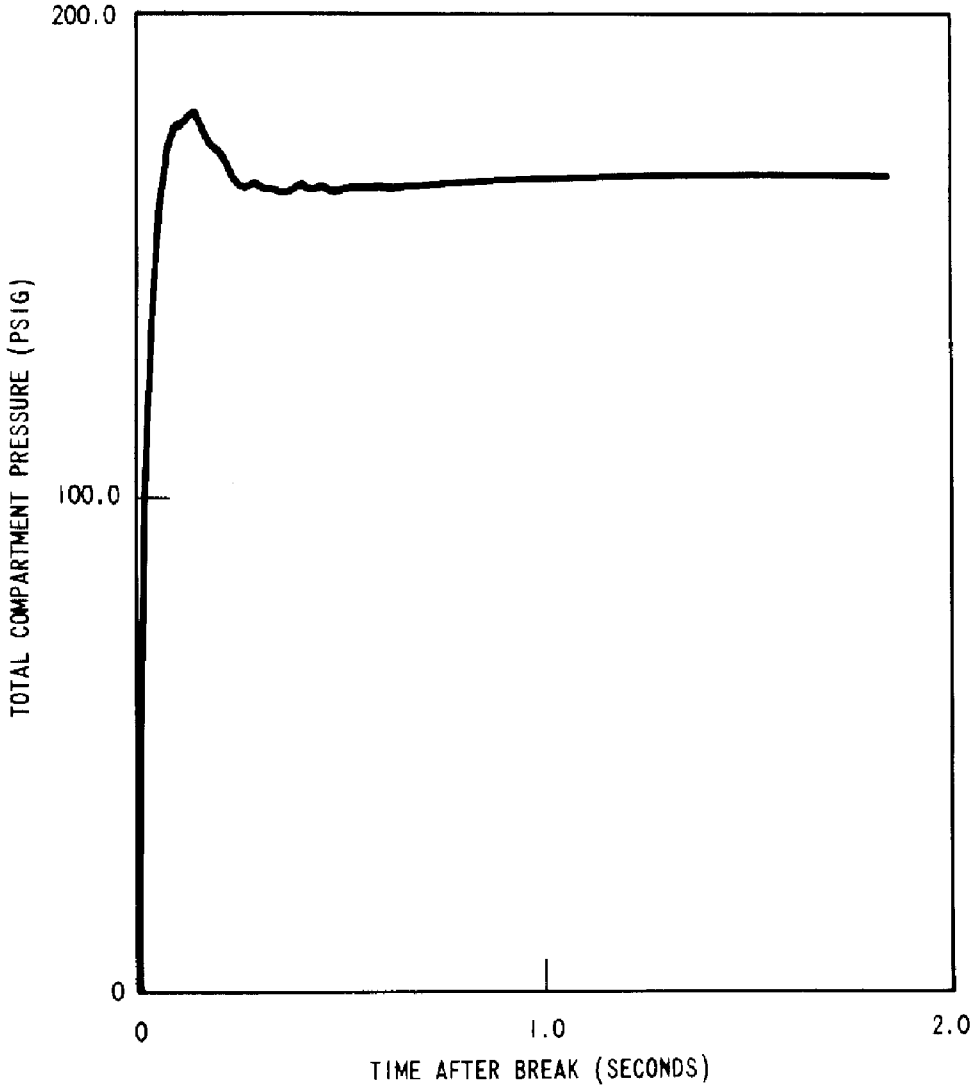

Figure 6-65. Reactor Cavity Analysis, Element 34

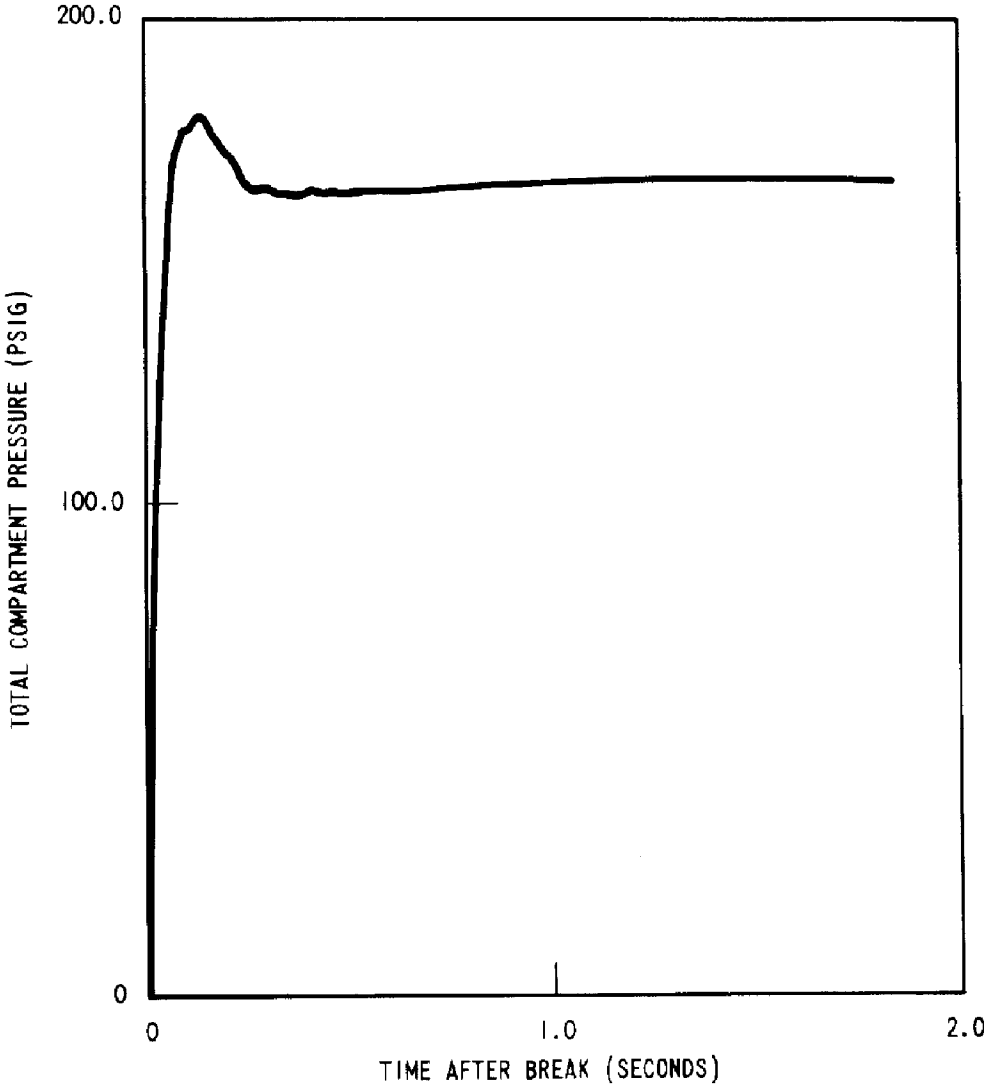

Figure 6-66. Reactor Cavity Analysis, Element 35

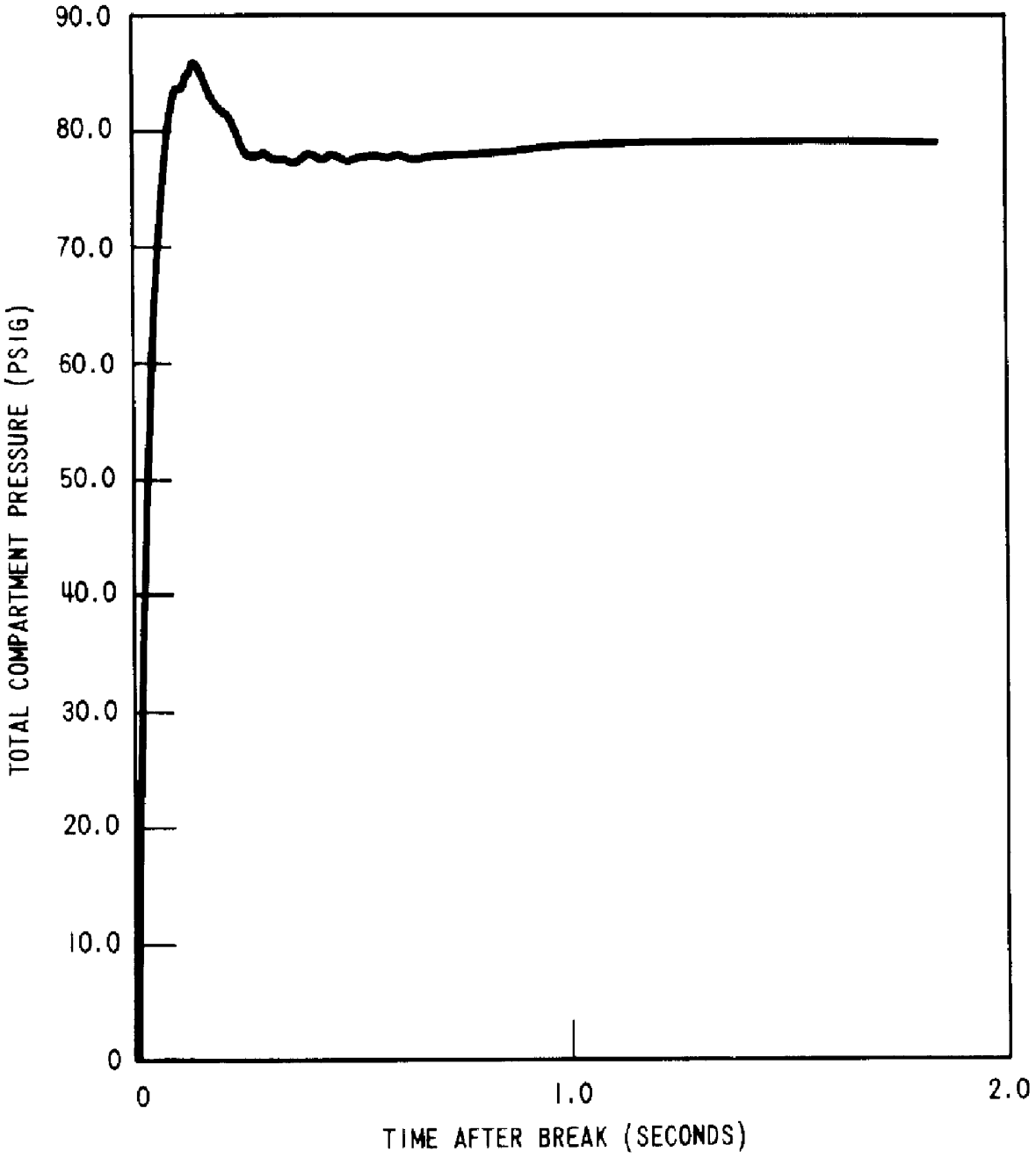

Figure 6-67. Reactor Cavity Analysis, Element 36

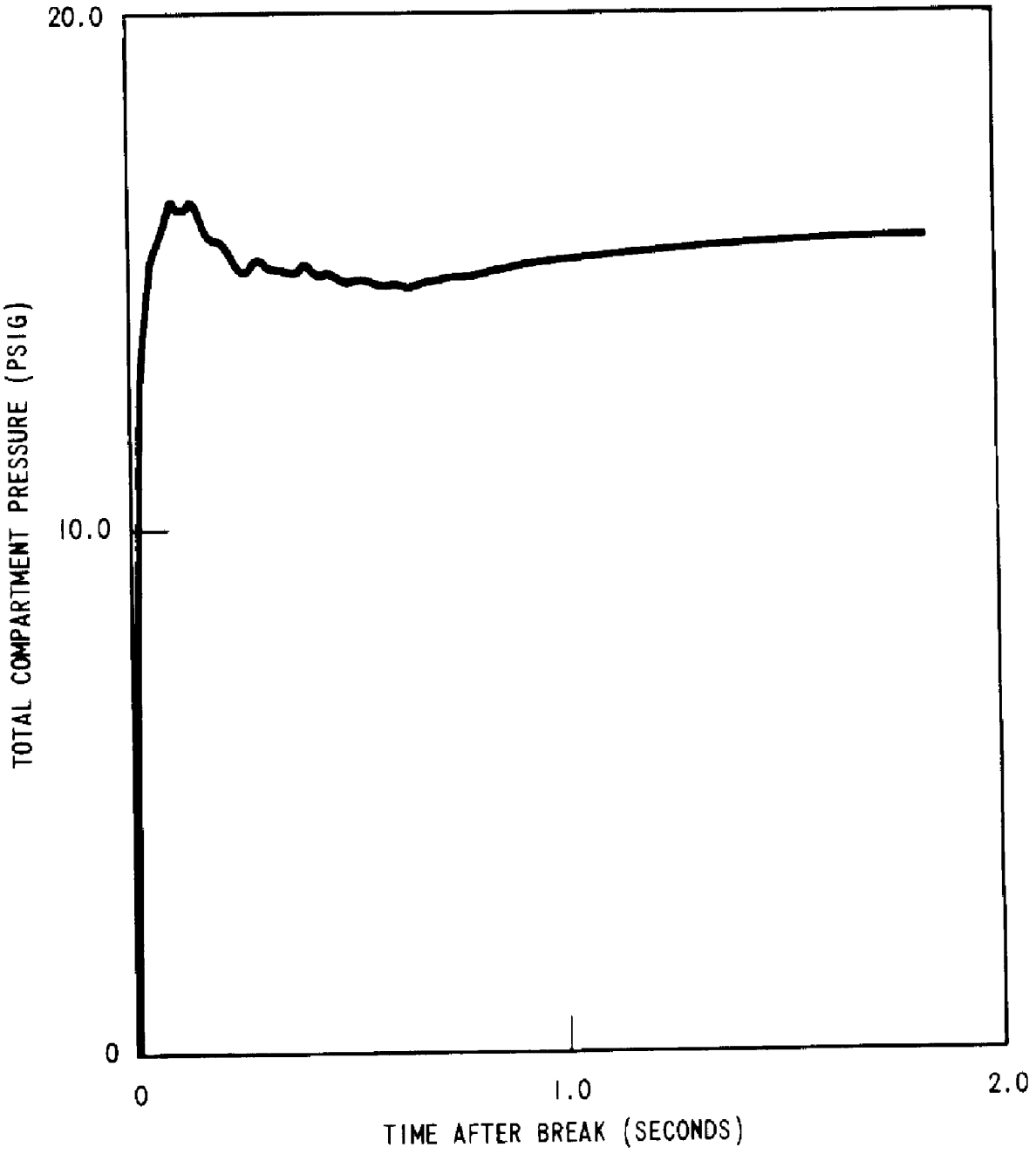

Figure 6-68. Reactor Cavity Analysis, Element 37

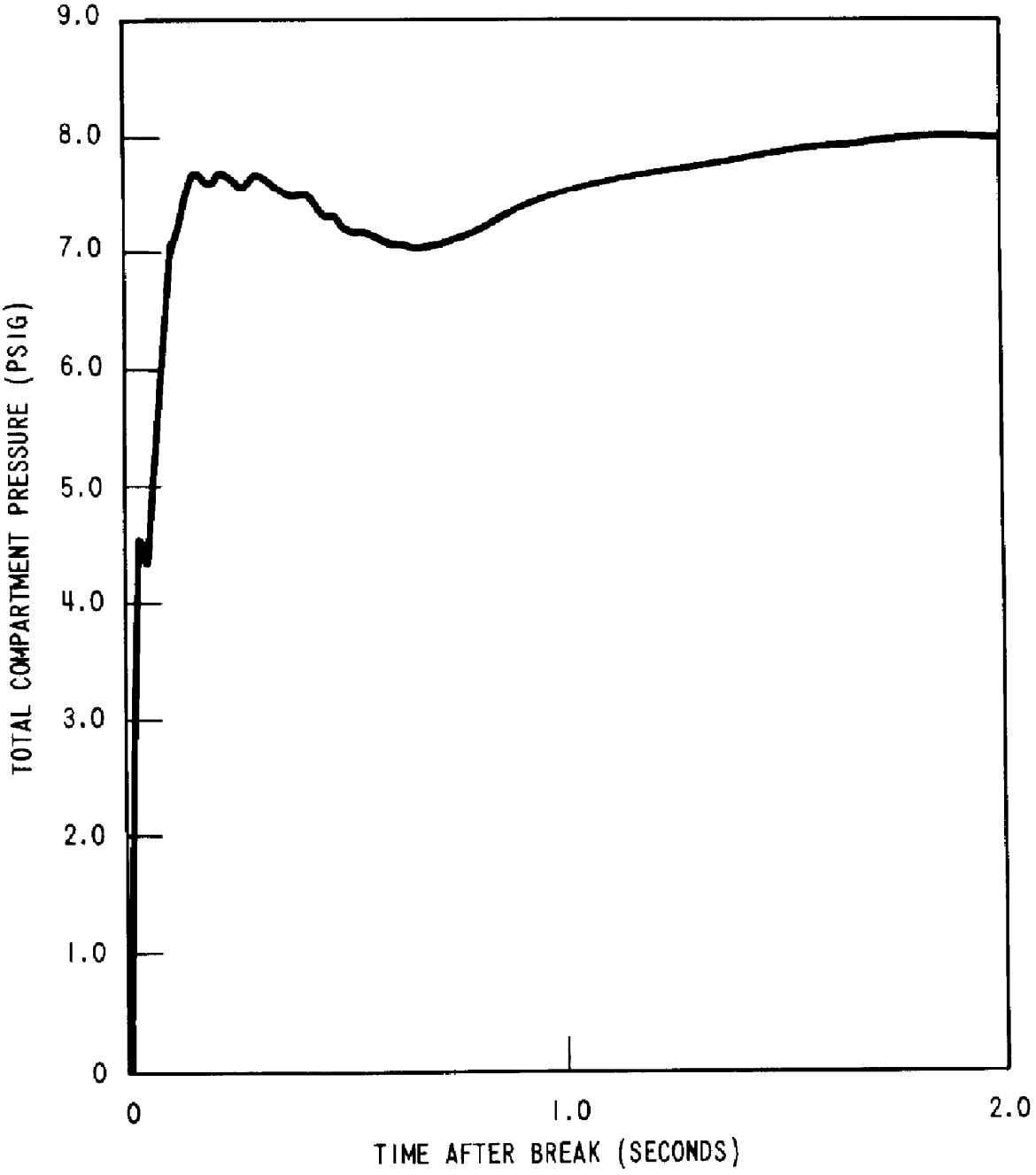

Figure 6-69. Reactor Cavity Analysis, Element 38

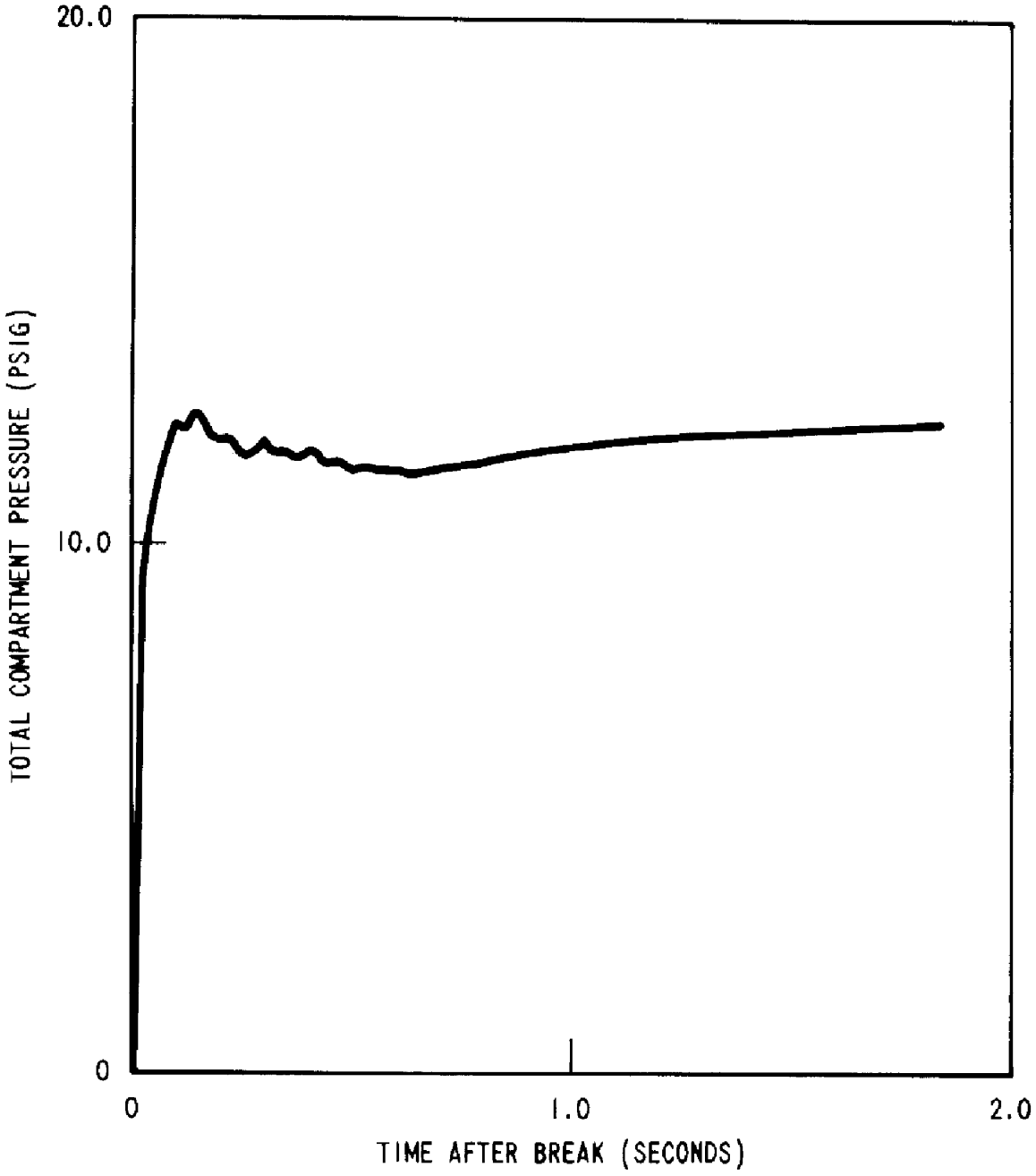

Figure 6-70. Reactor Cavity Analysis, Element 39

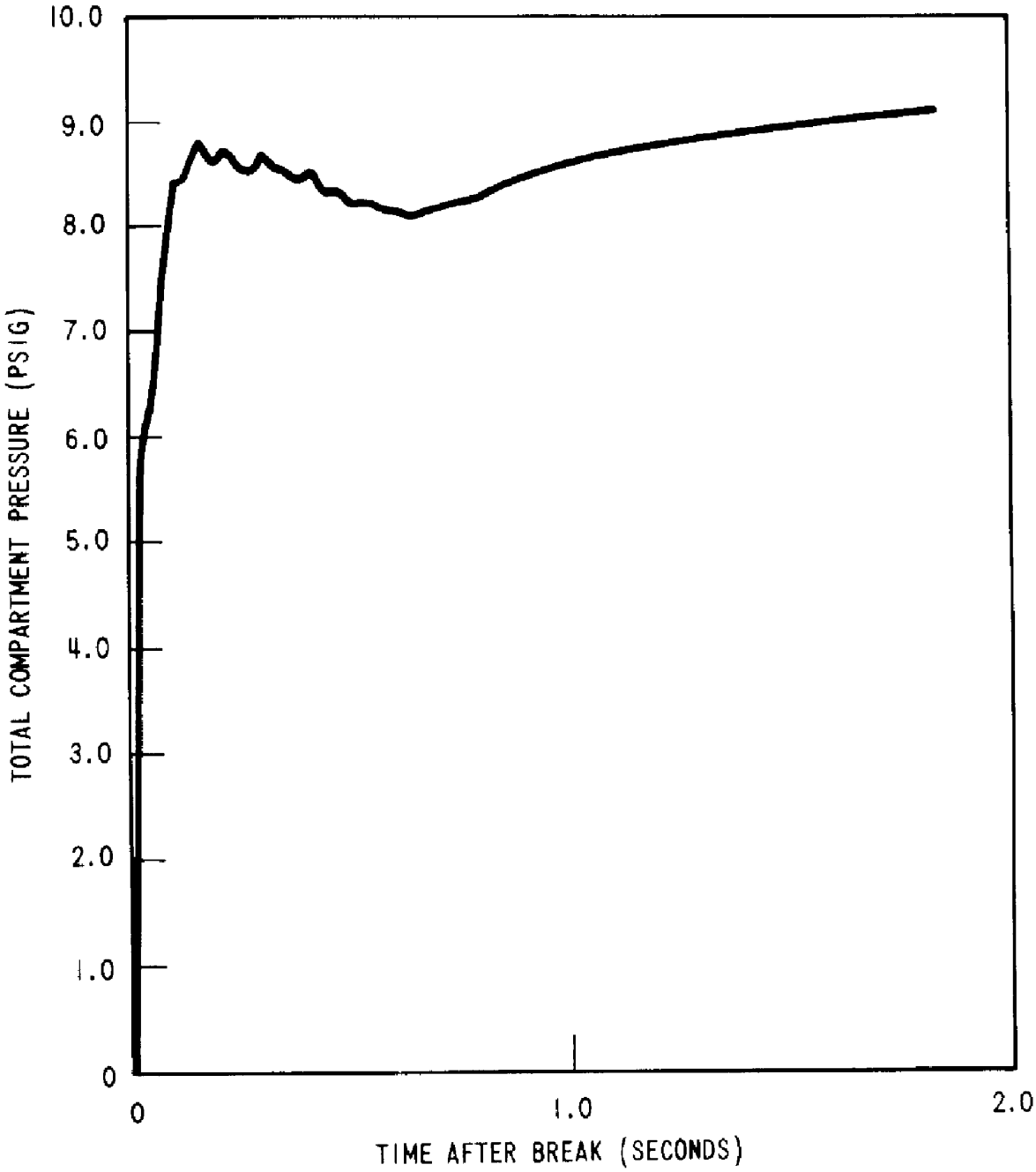

Figure 6-71. Reactor Cavity Analysis, Element 40

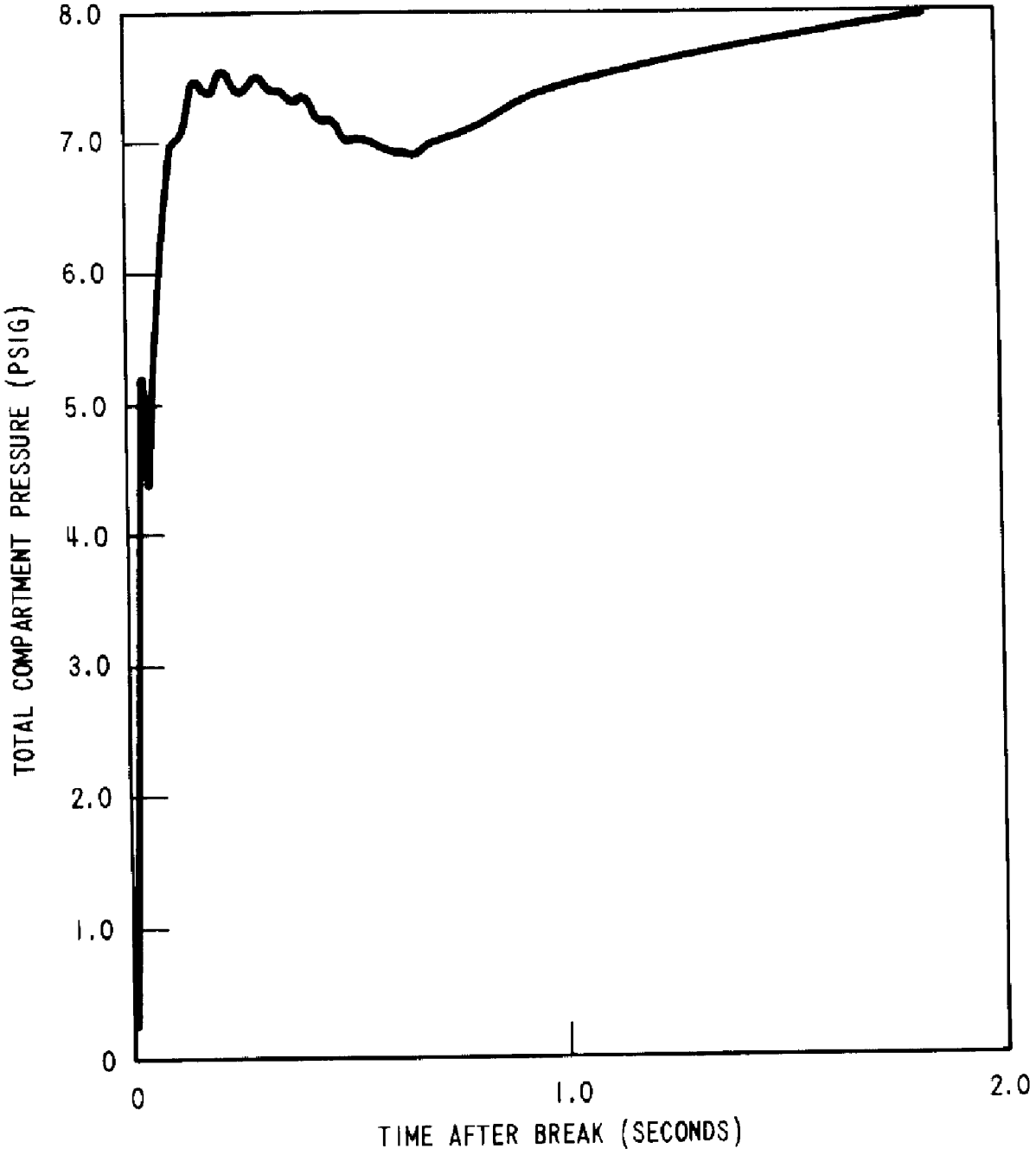

Figure 6-72. Reactor Cavity Analysis, Element 41

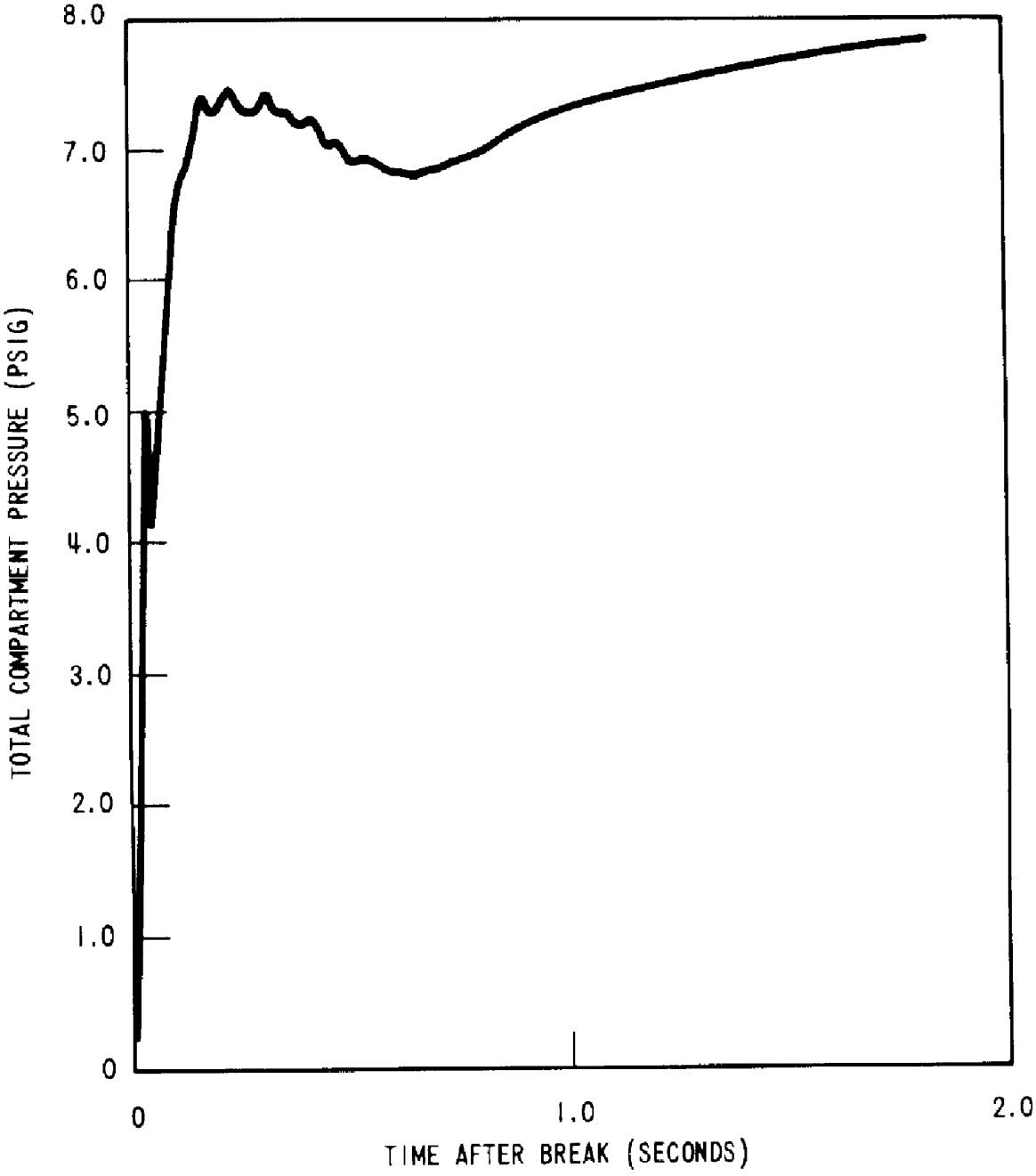

Figure 6-73. Reactor Cavity Analysis, Element 42

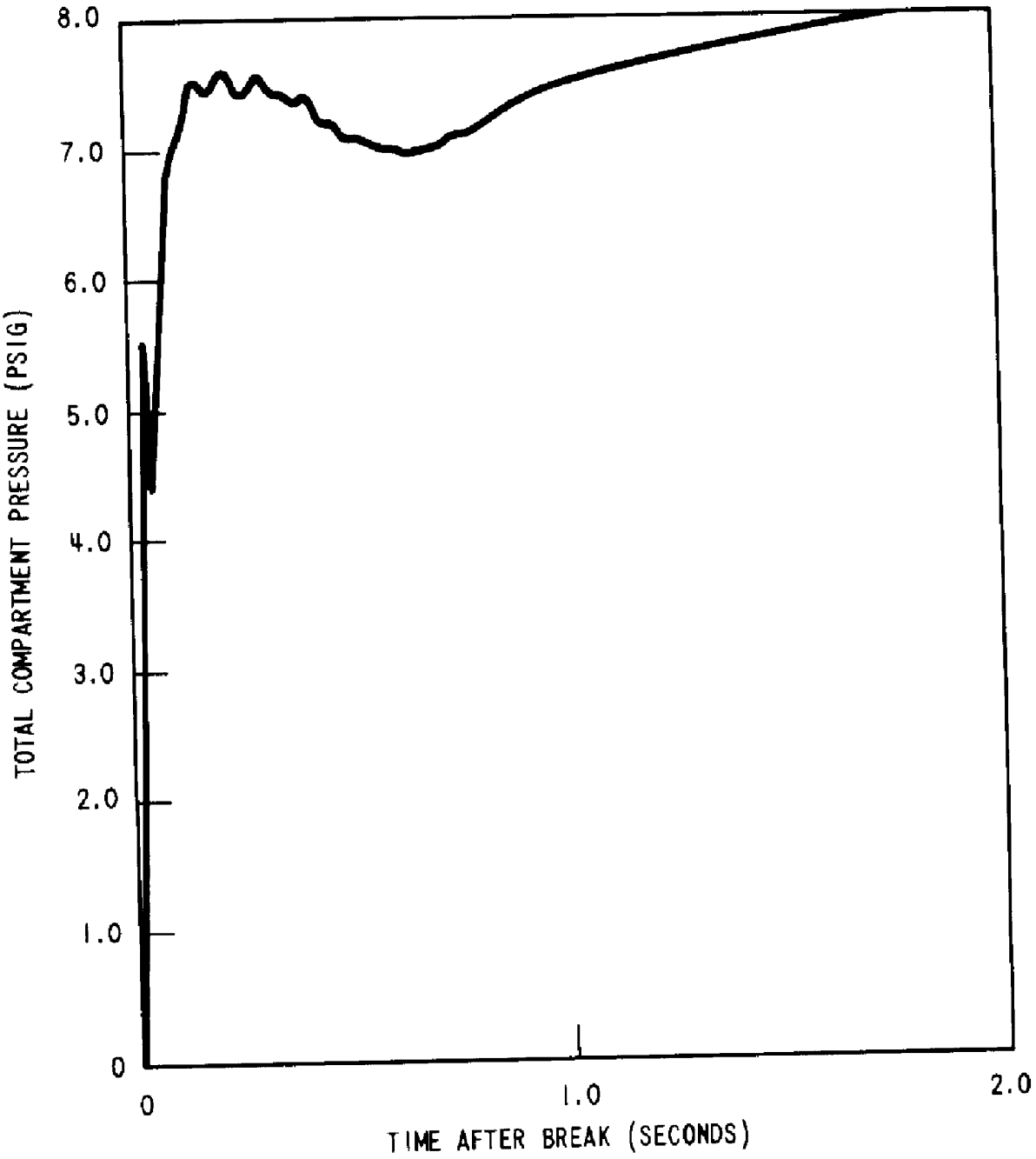

Figure 6-74. Reactor Cavity Analysis, Element 43

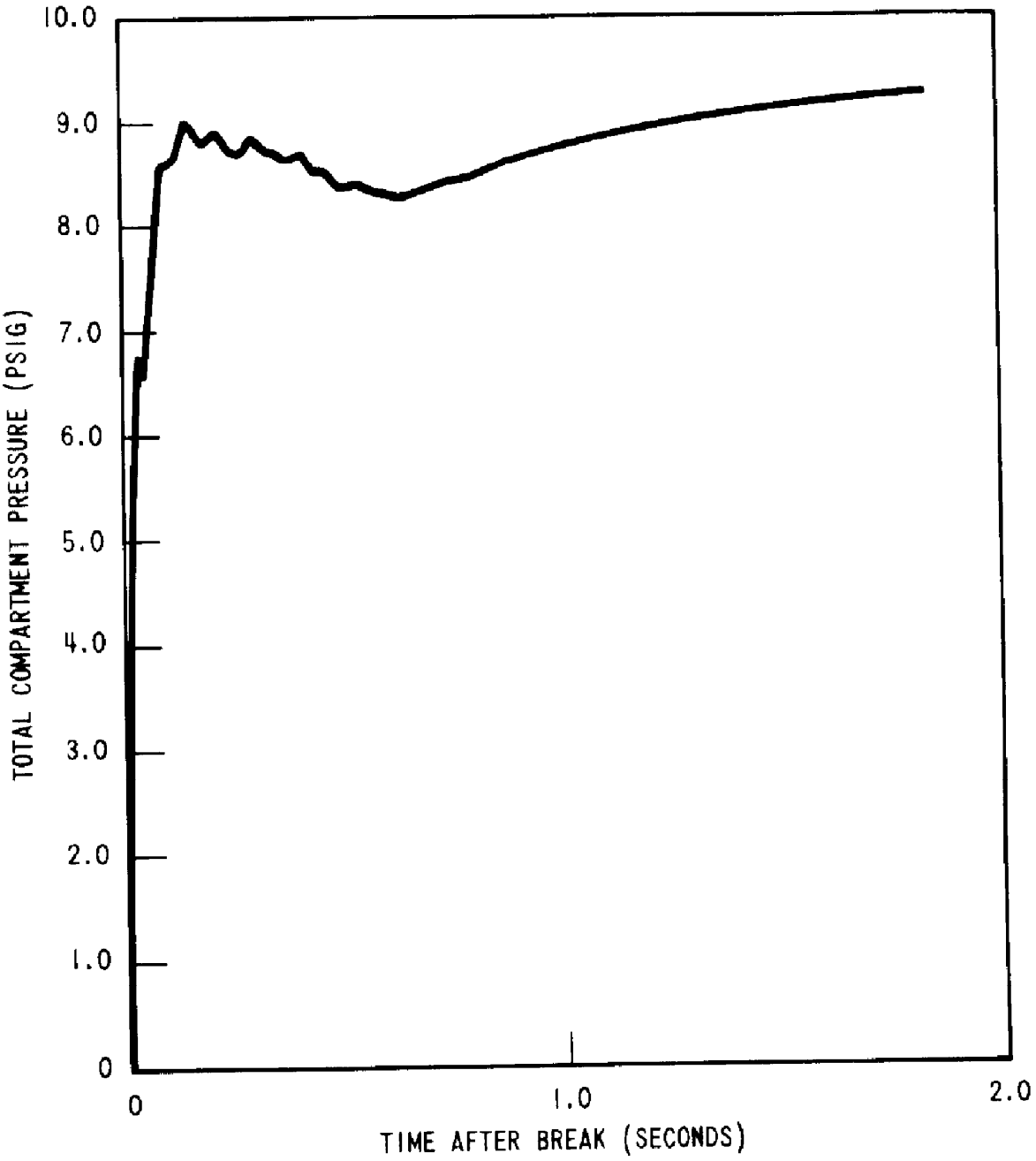

Figure 6-75. Reactor Cavity Analysis, Element 44

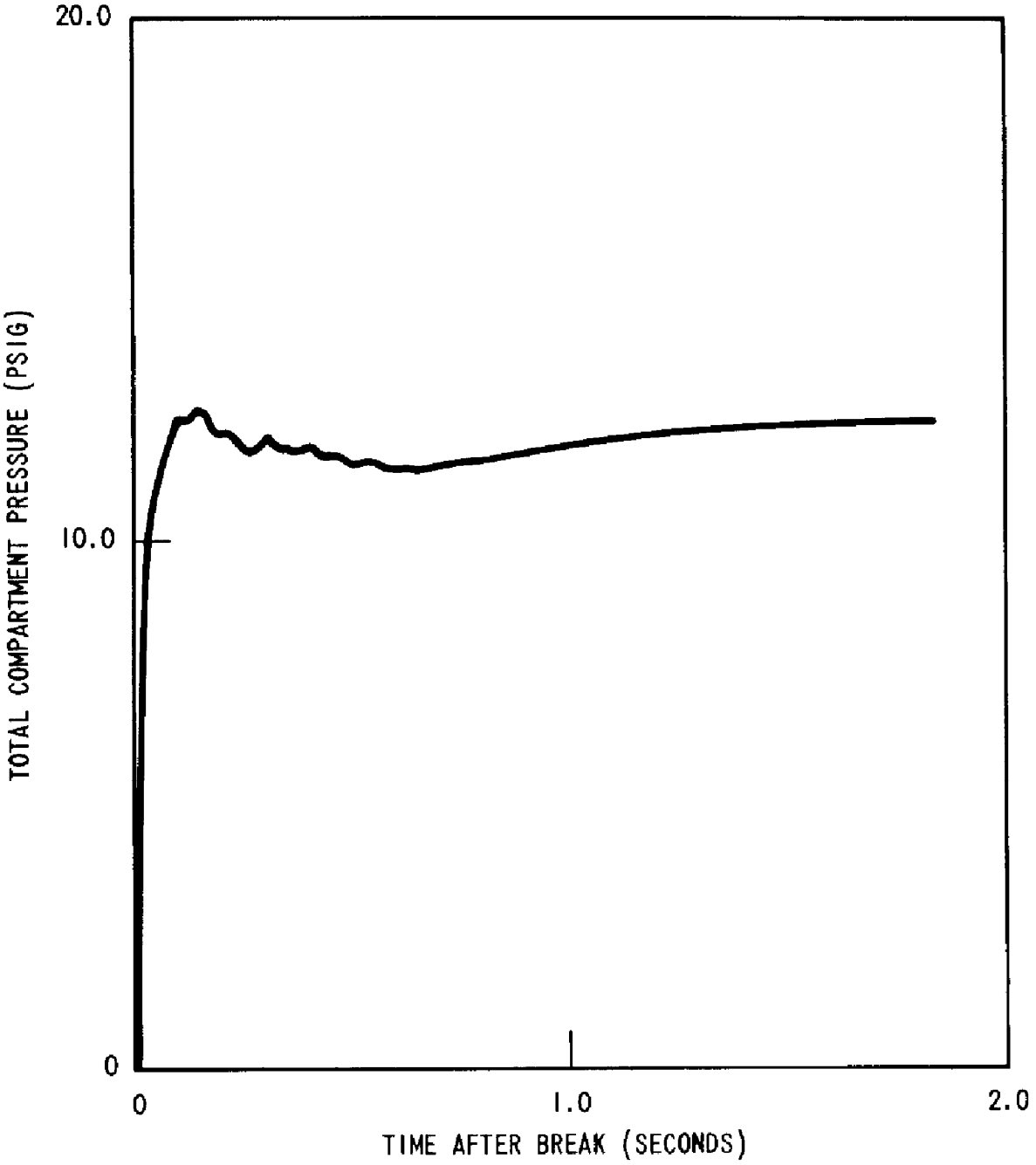

Figure 6-76. Reactor Cavity Analysis, Element 45

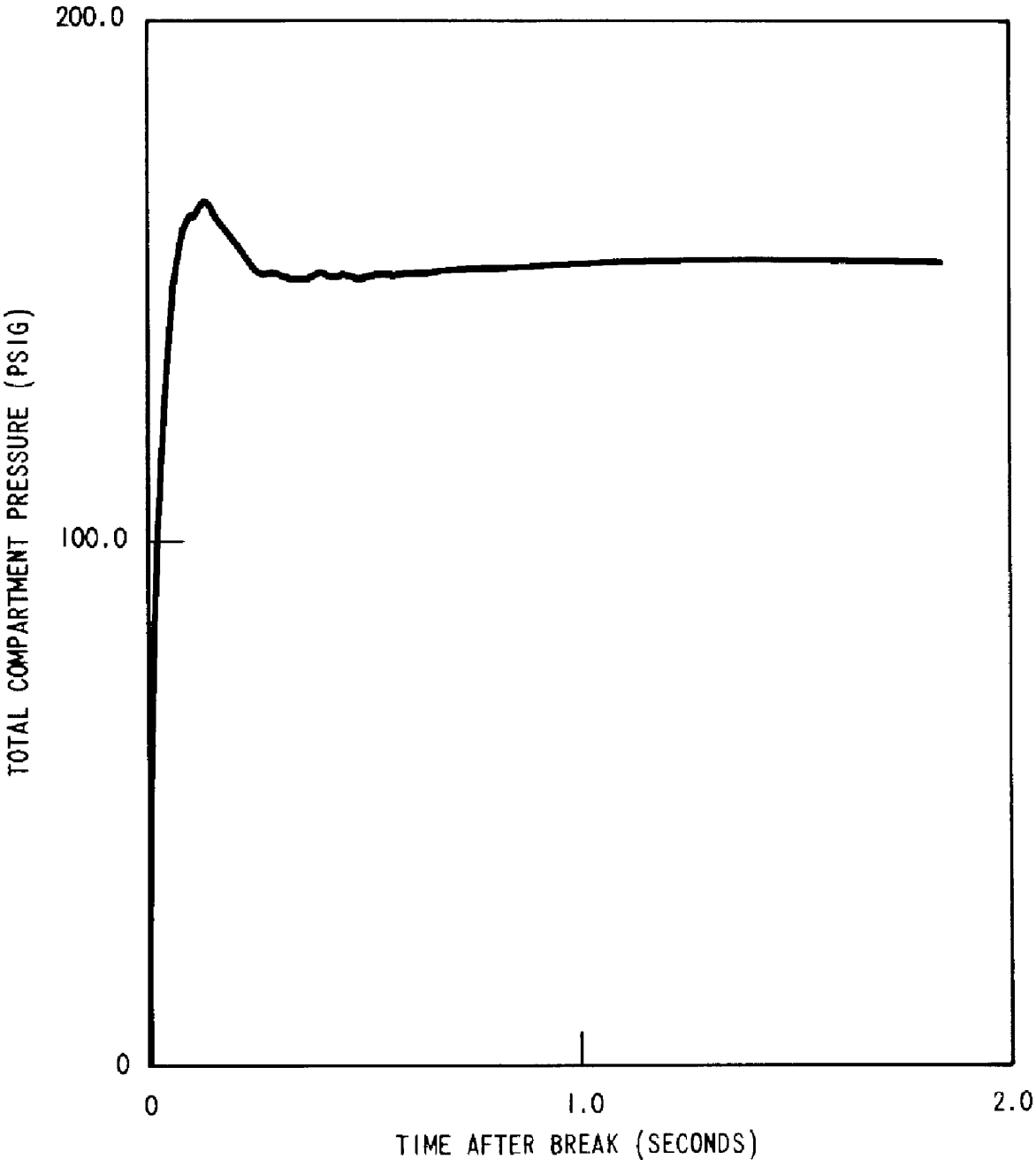

Figure 6-77. Reactor Cavity Analysis, Element 46

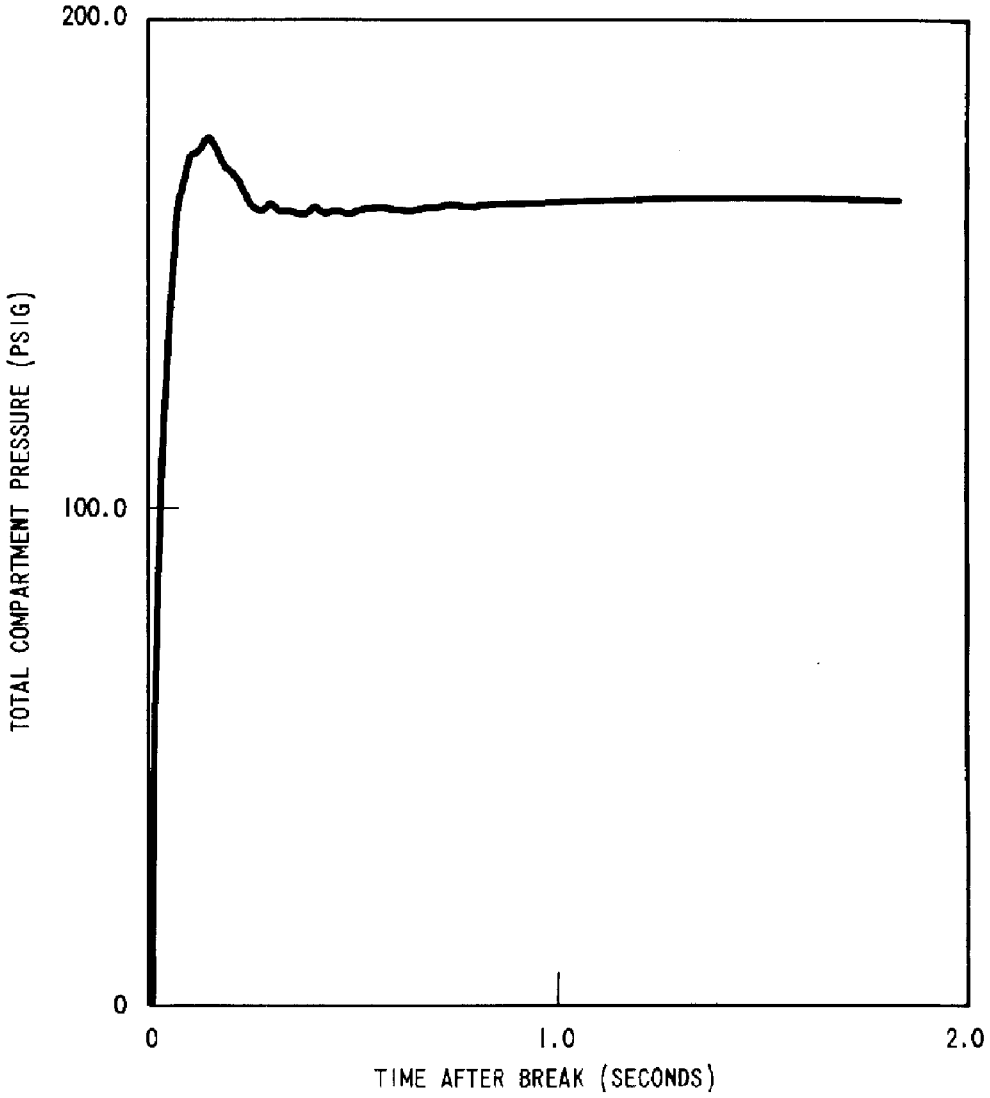

Figure 6-78. Reactor Cavity Analysis, Element 47

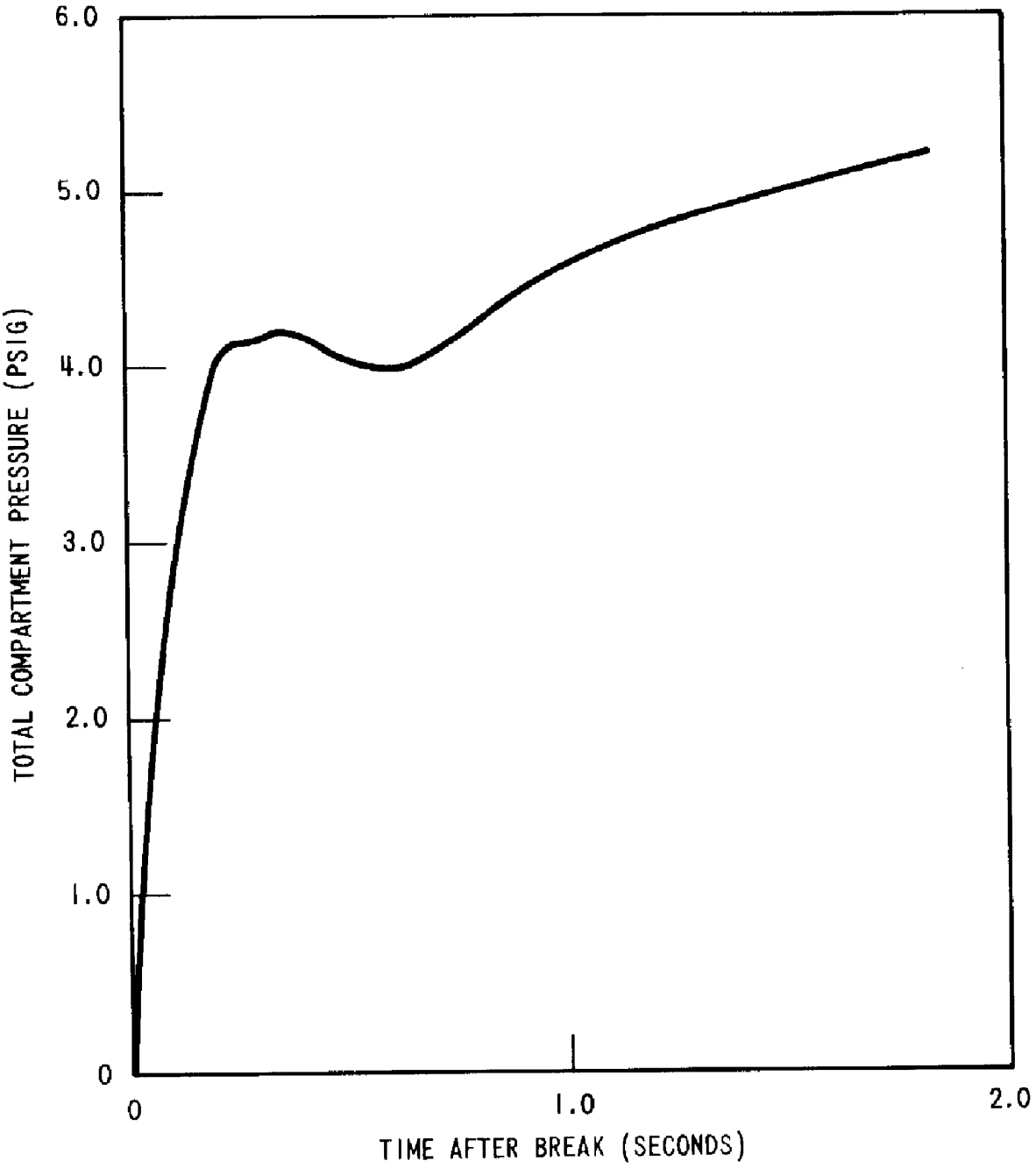

Figure 6-79. Reactor Cavity Analysis, Element 53

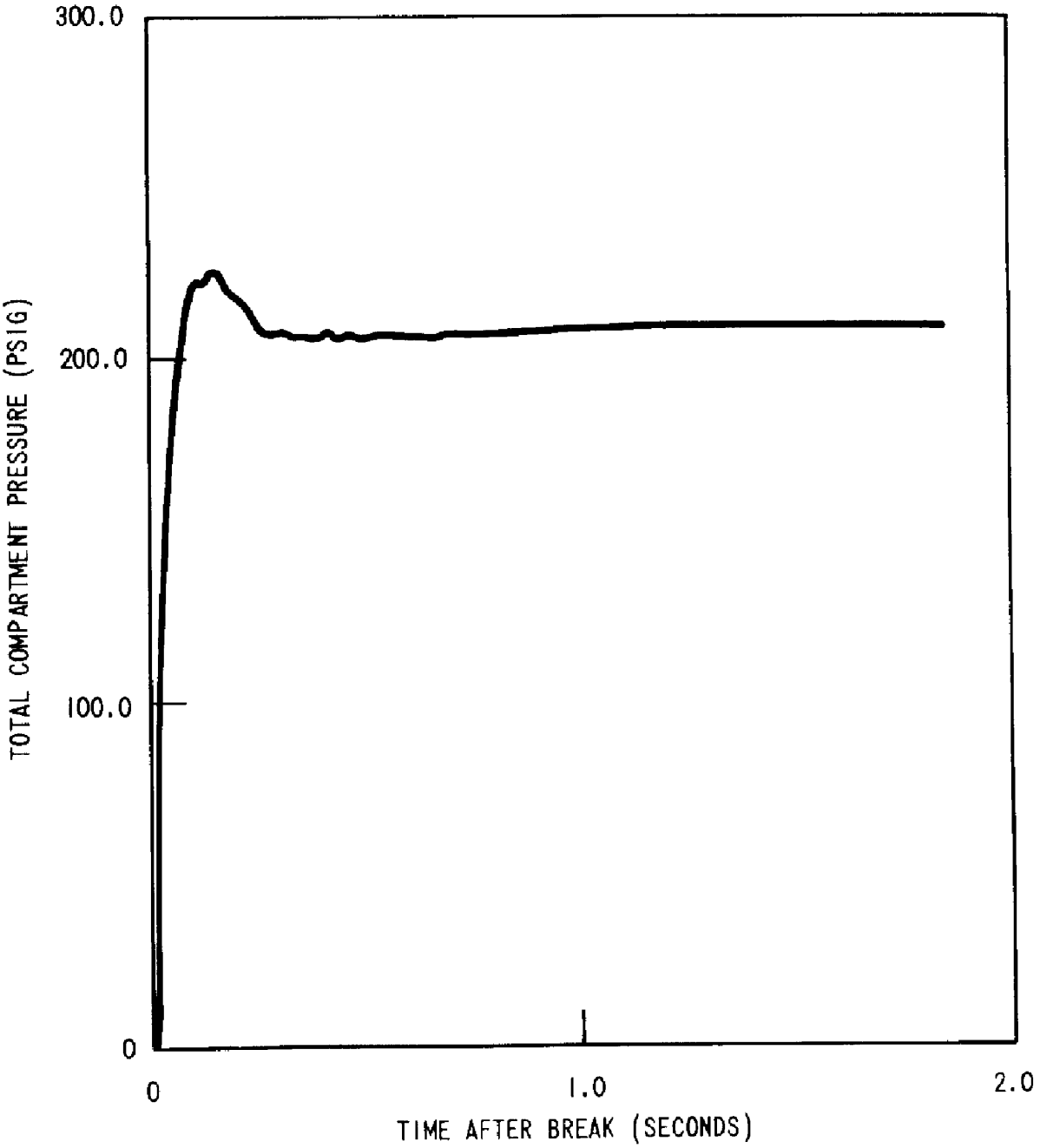

Figure 6-80. Reactor Cavity Analysis, Element 54

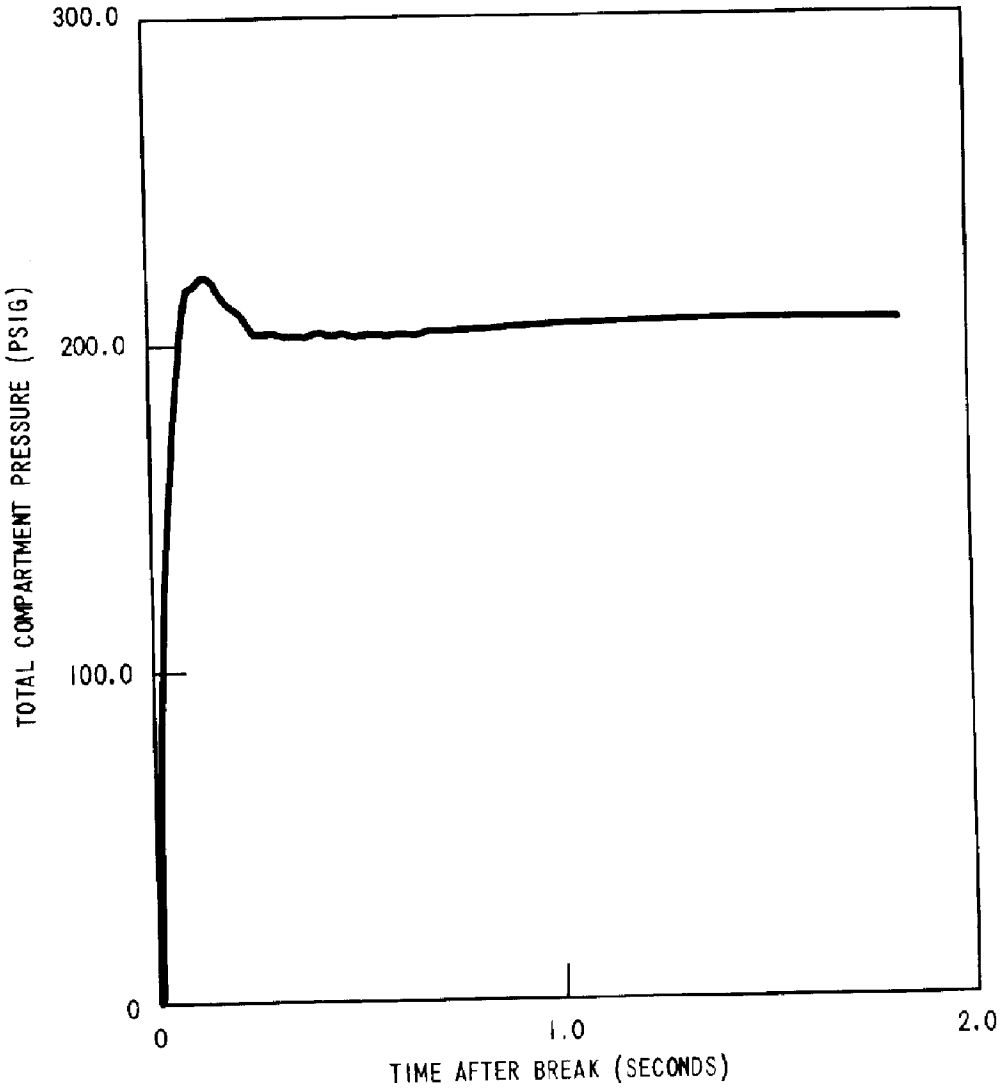

Figure 6-81. Hot Leg Double Ended Guillotine Break

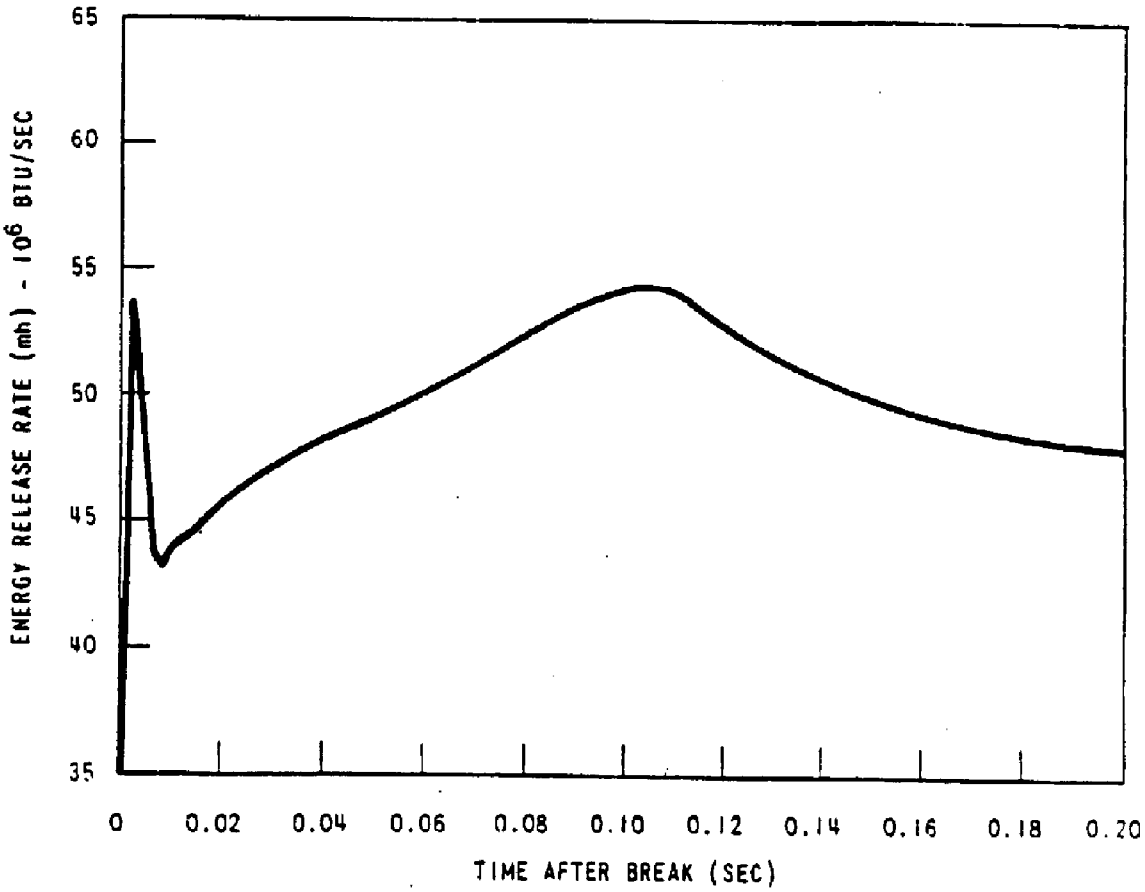

Figure 6-82. Hot Leg Double Ended Guillotine Break

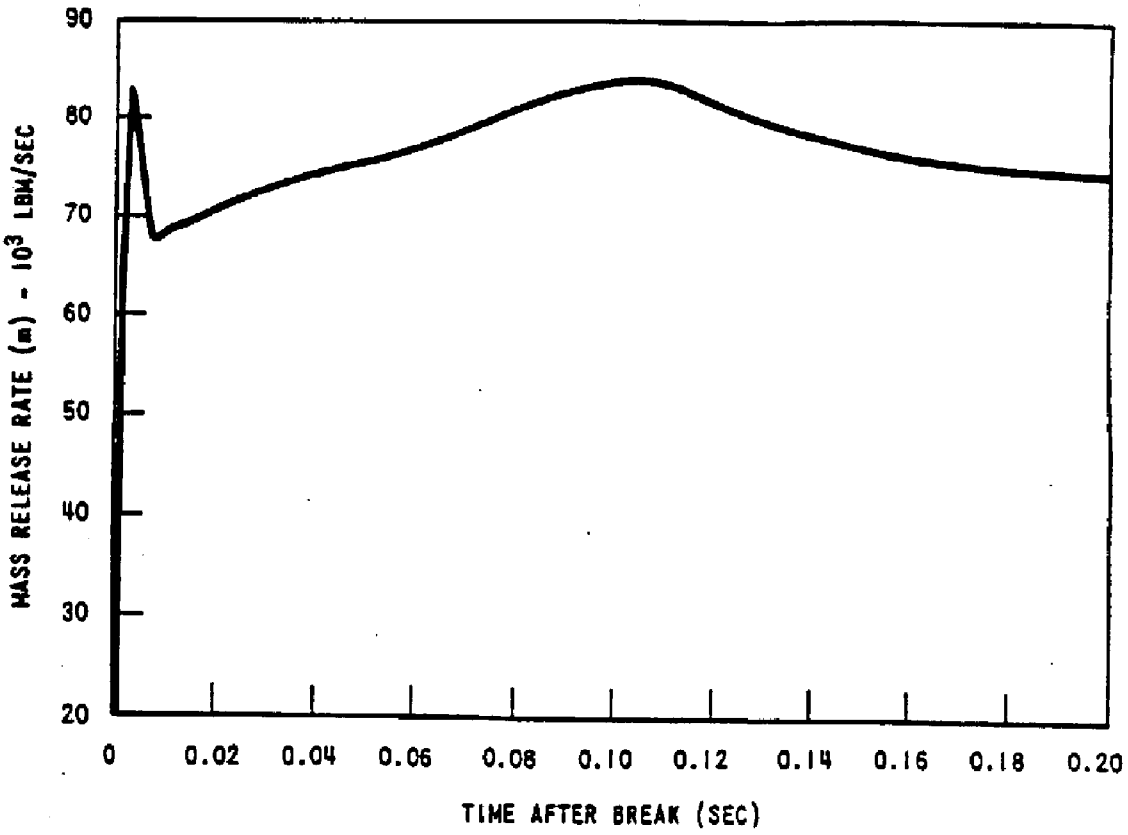

Figure 6-83. Cold Leg Double Ended Guillotine Break

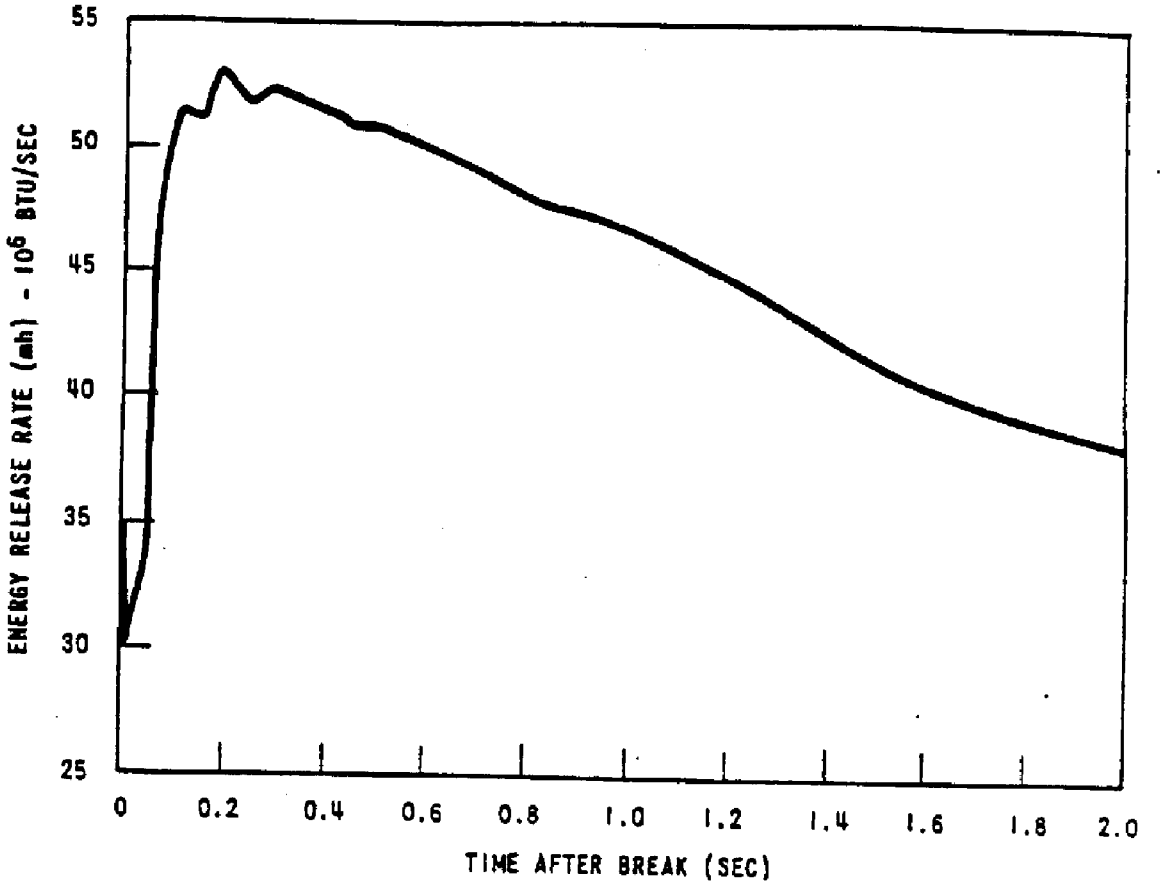

Figure 6-84. Cold Leg Double Ended Guillotine Break

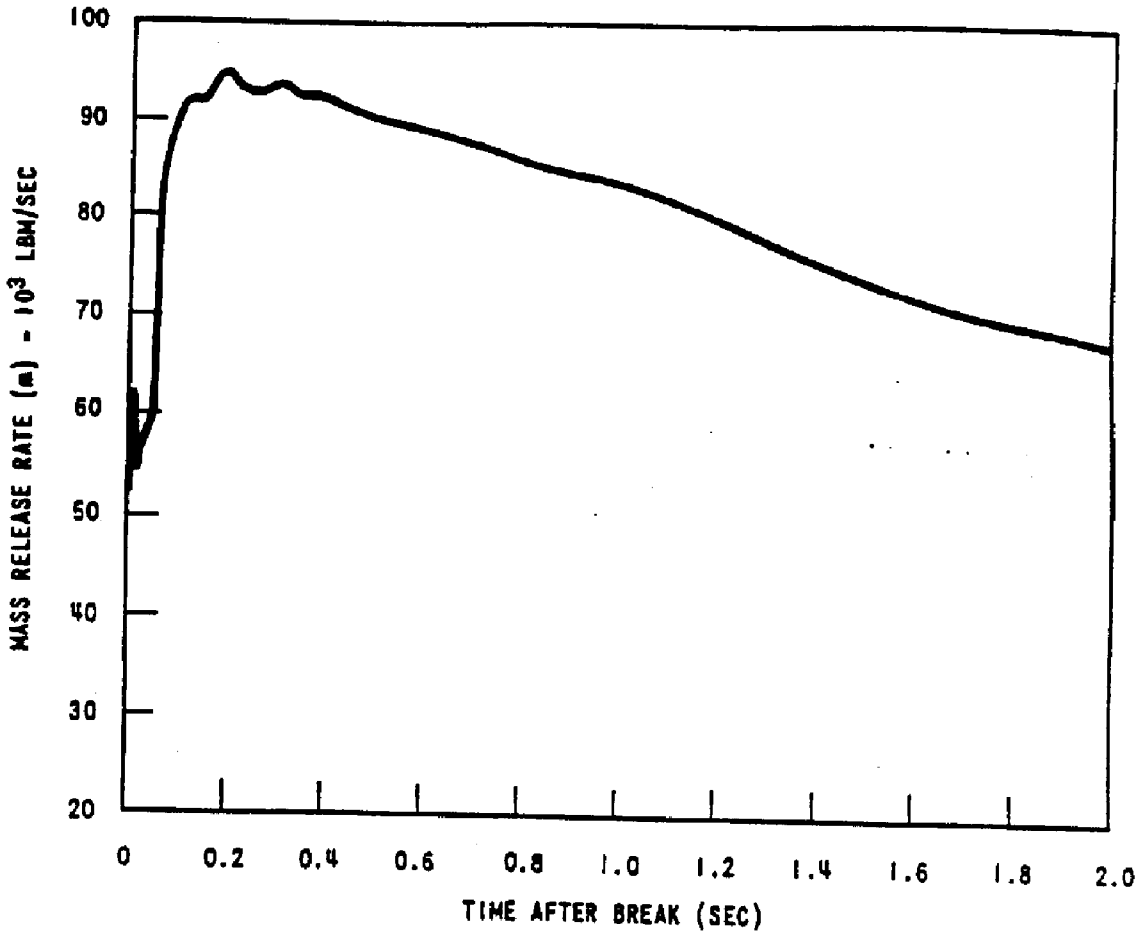

Figure 6-85. Hot Leg Single Ended Split Break

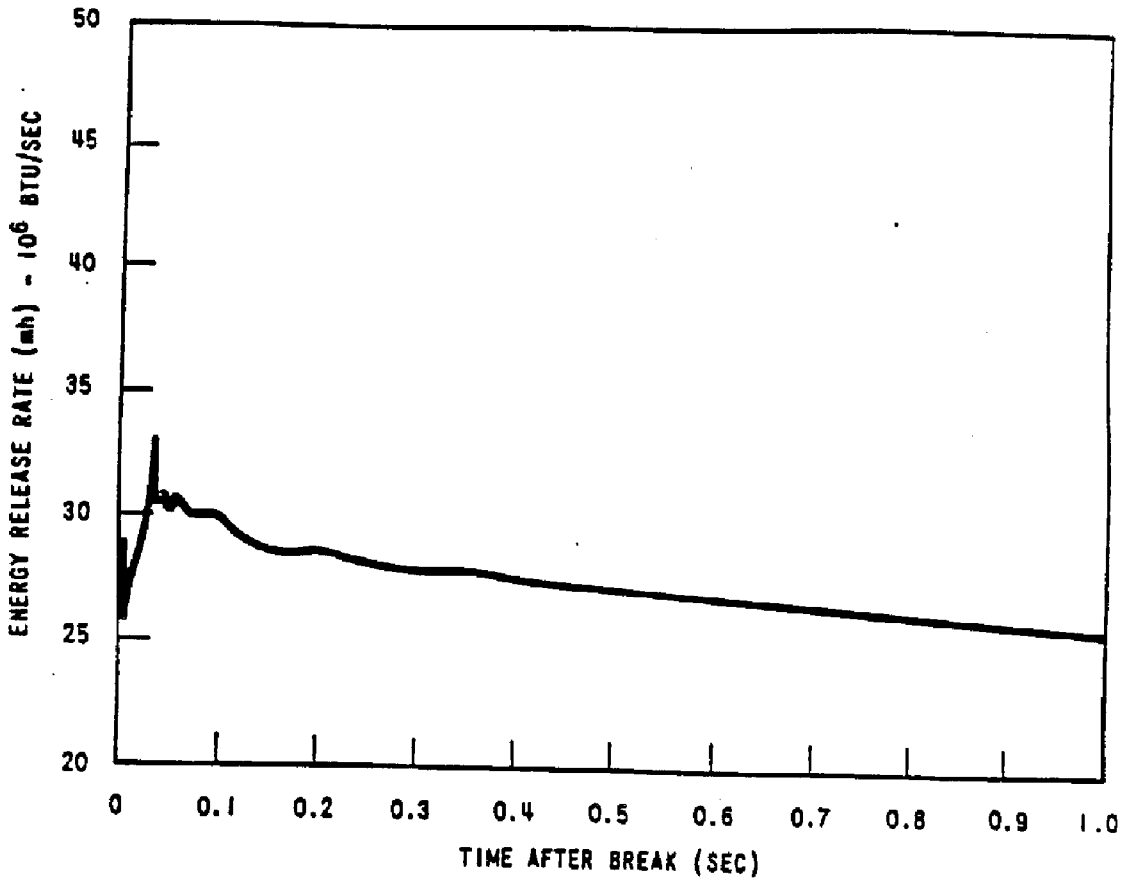

Figure 6-86. Hot Leg Single Ended Split Break

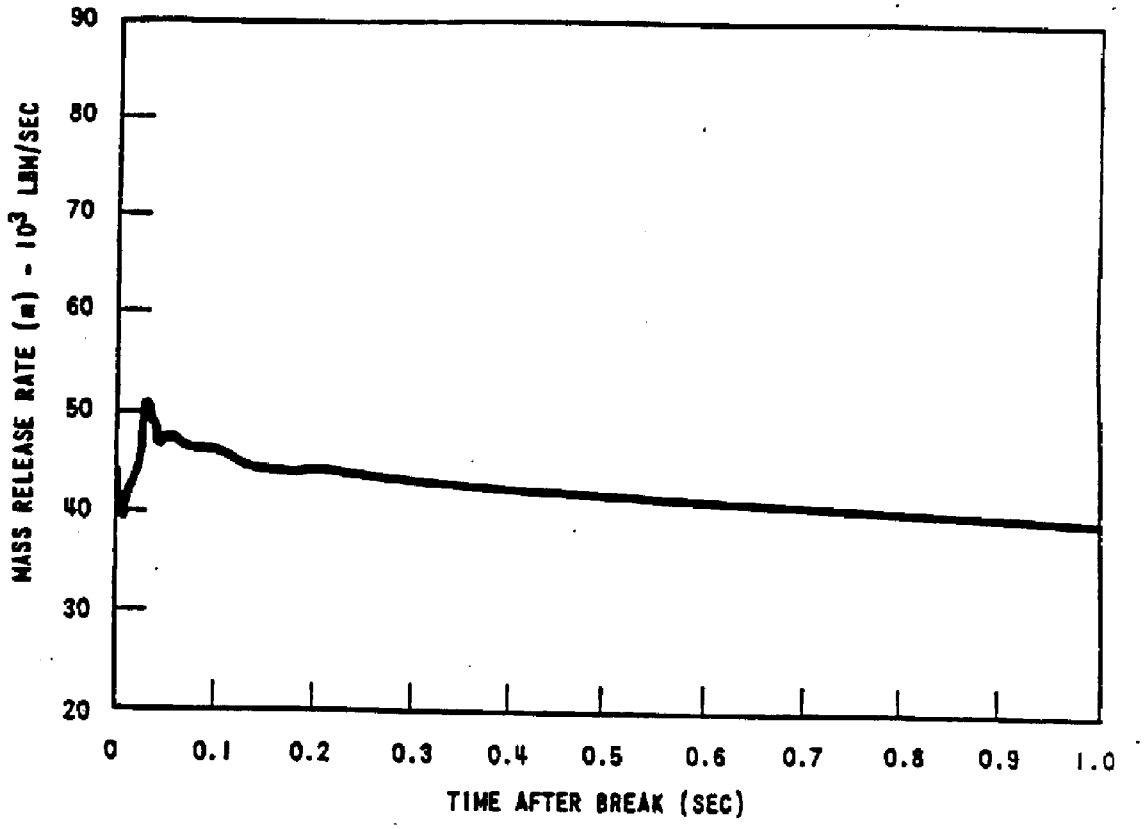

Figure 6-87. Cold Leg Single Ended Split Break

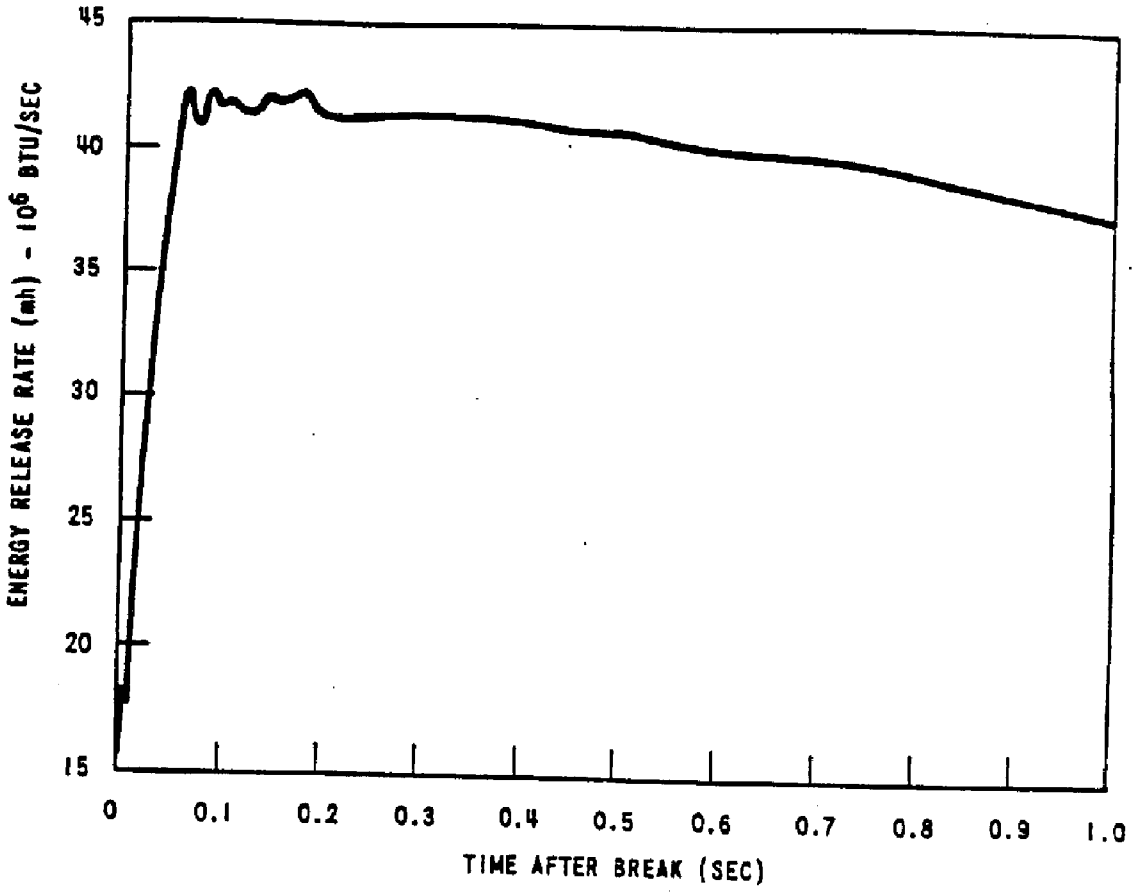

Figure 6-88. Cold Leg Single Ended Split Break

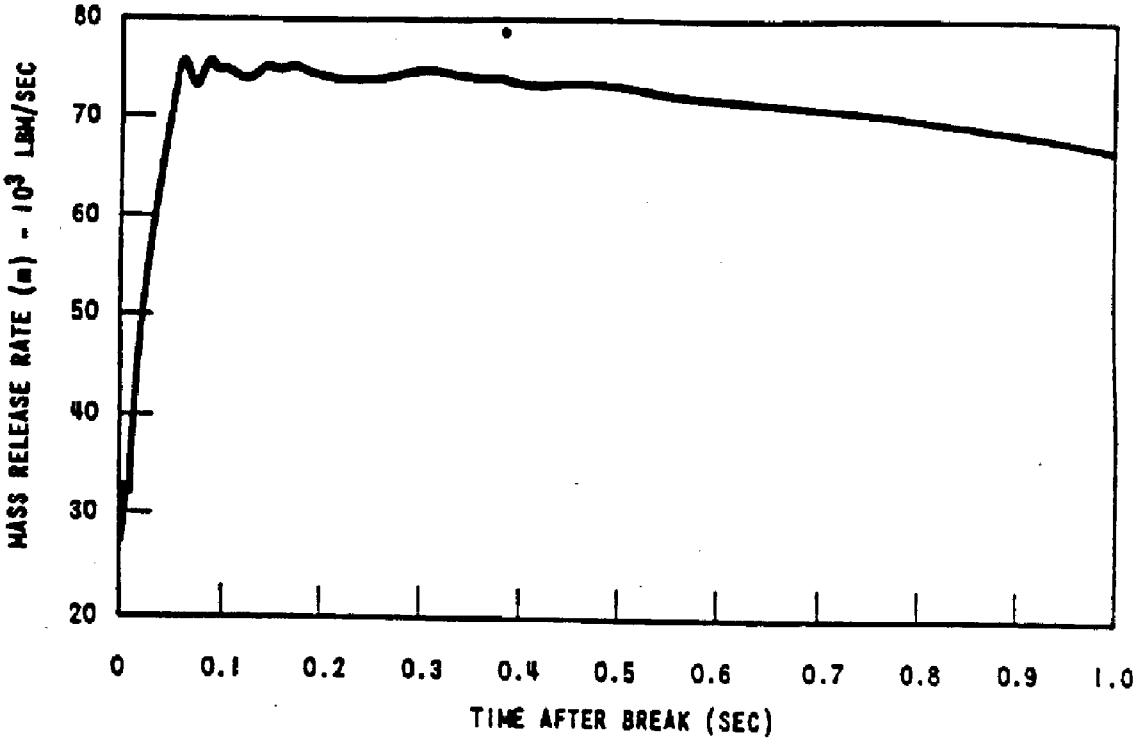

Figure 6-89. Comparison of Satan to Henry Fauske

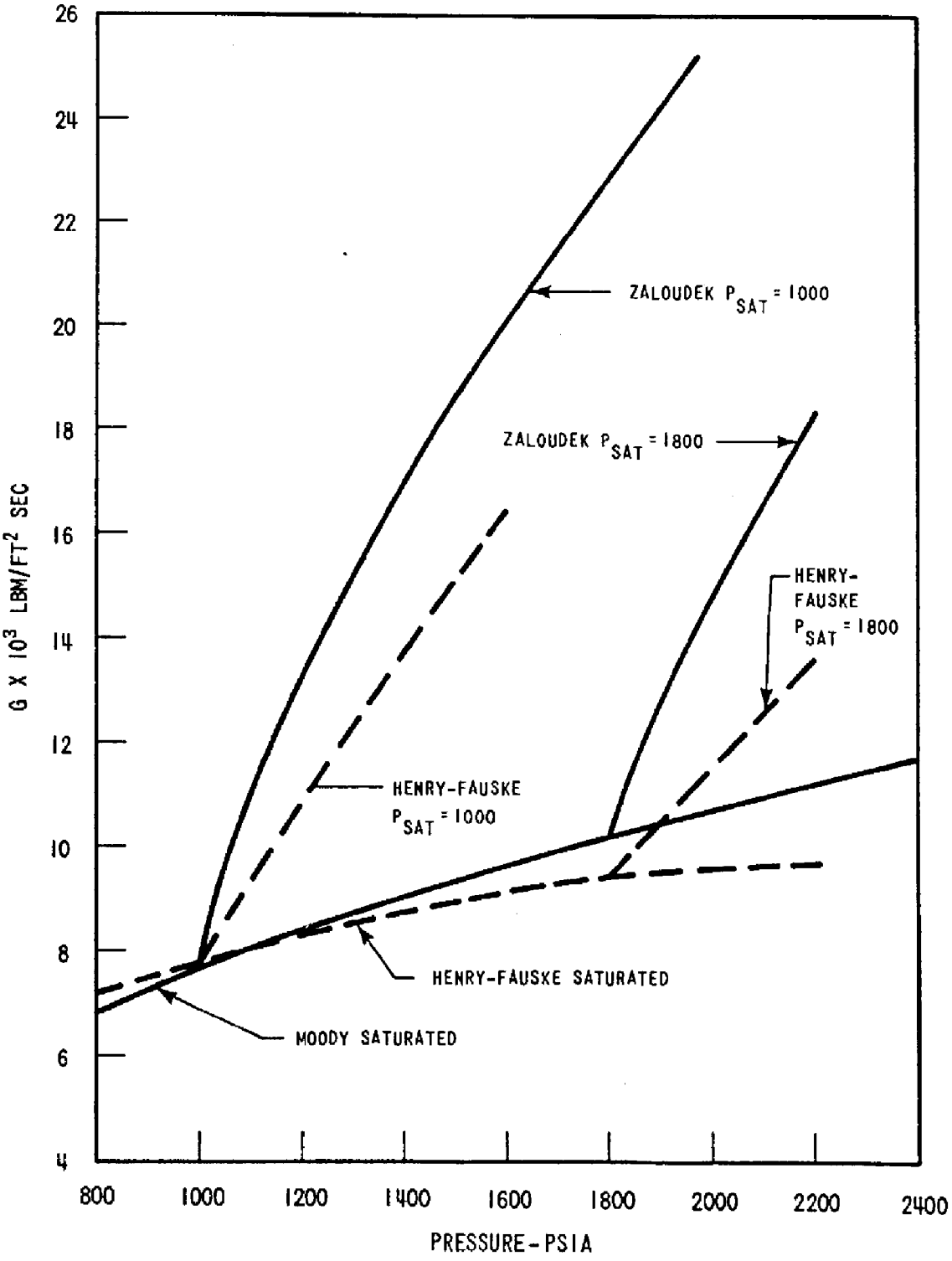

Figure 6-90. Comparison of Satan to Moody Subcooled

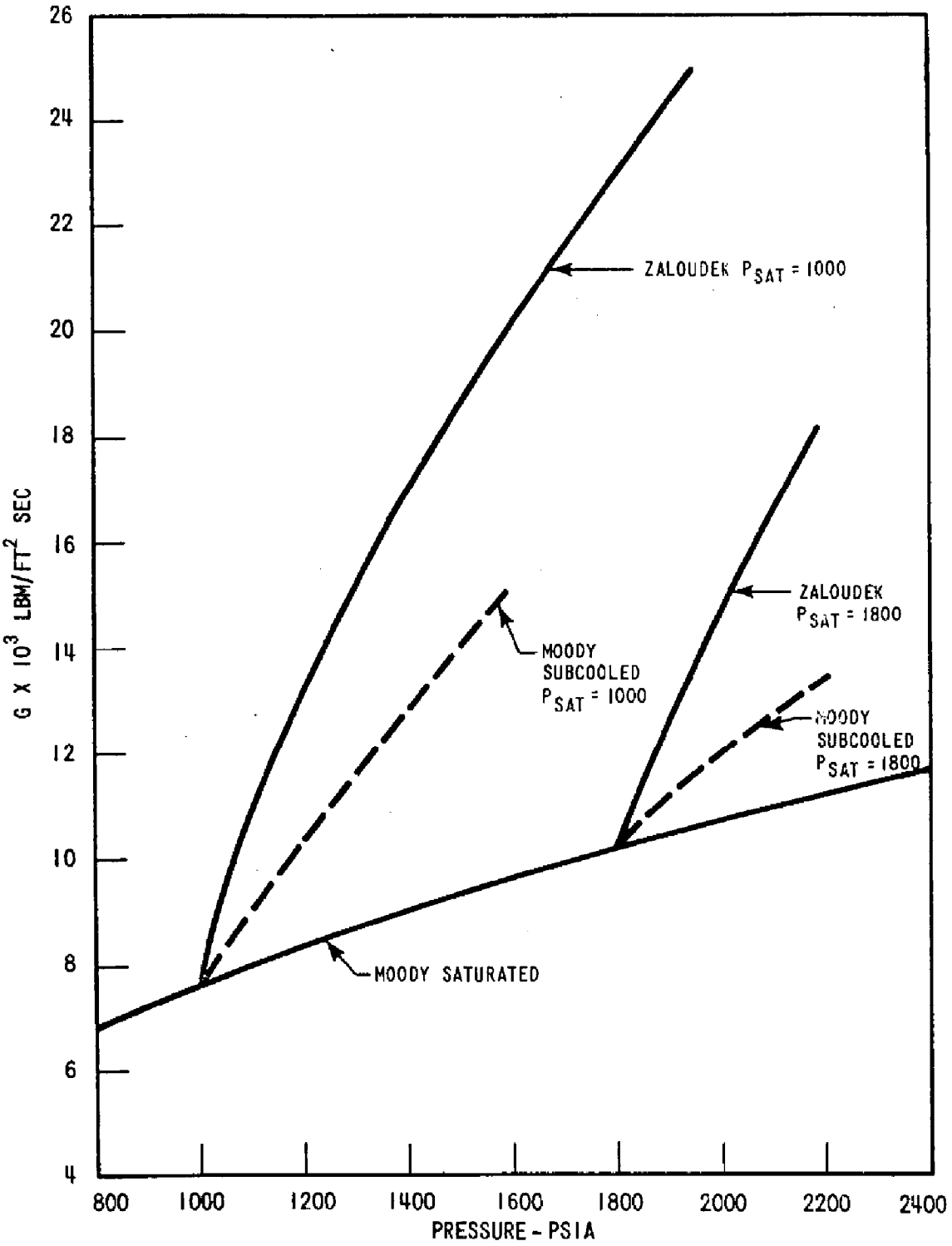

Figure 6-91. Zaloudek Measured Data Versus Modified Zaloudek Correlation

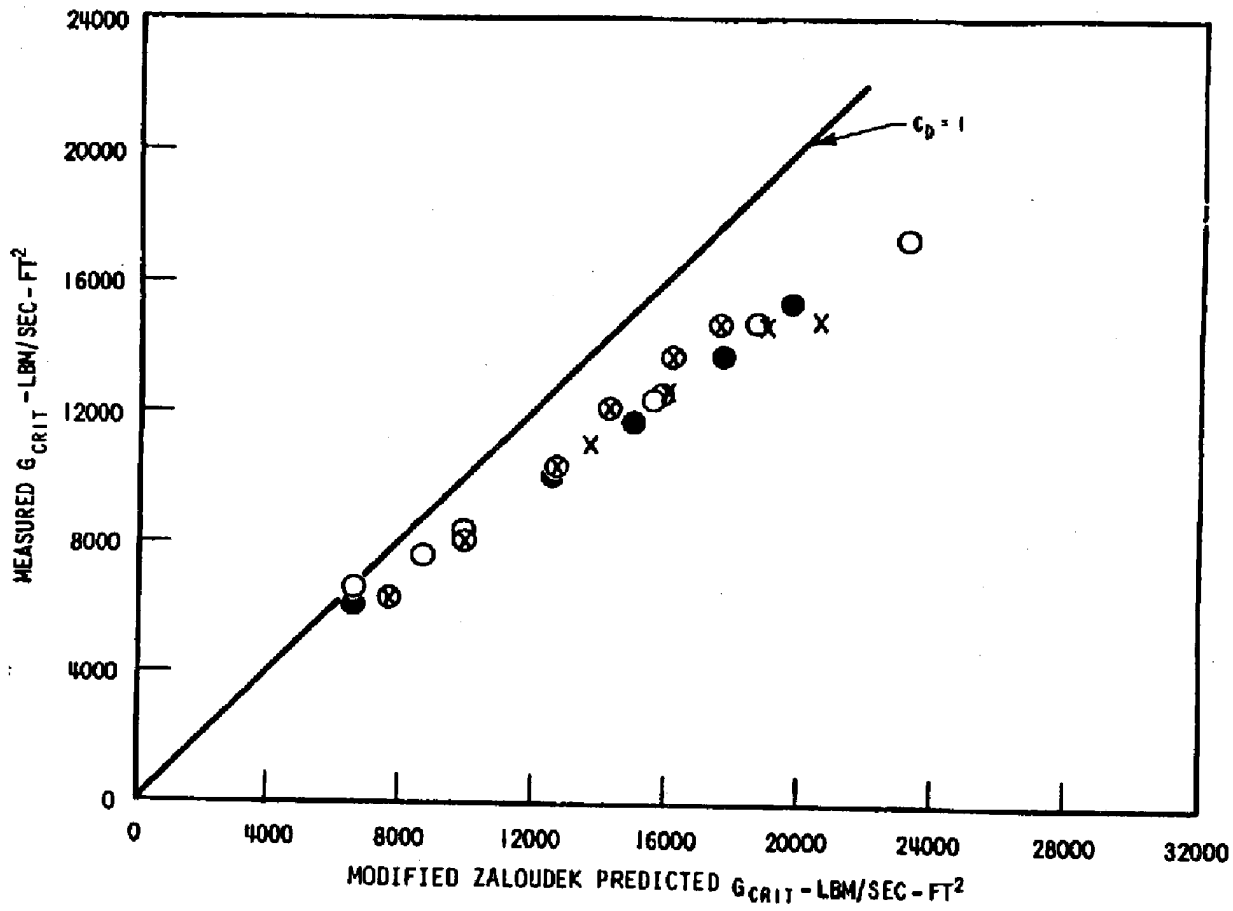

Figure 6-92. Zaloudek Short Tube Data

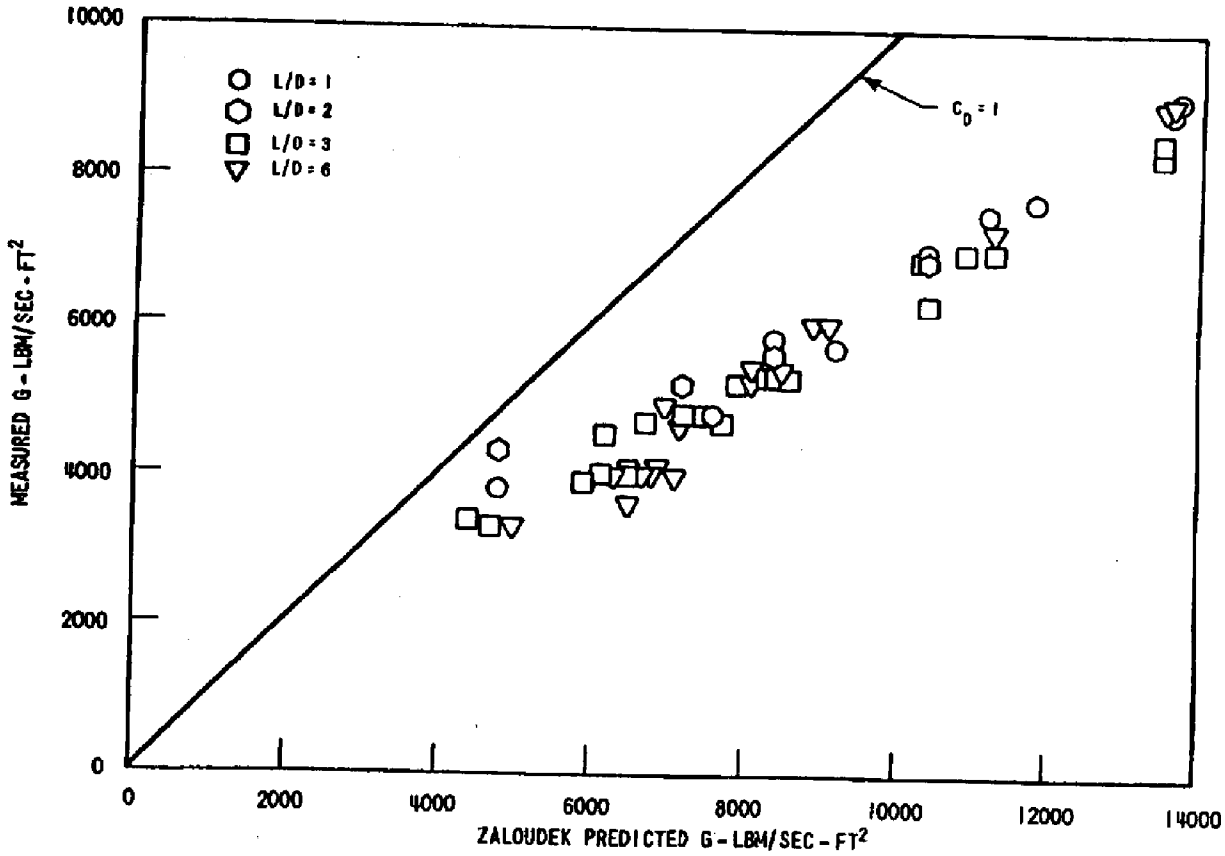

Figure 6-93. Exit Plane Quality as a Function of Upstream Pressure for Saturated Liquid

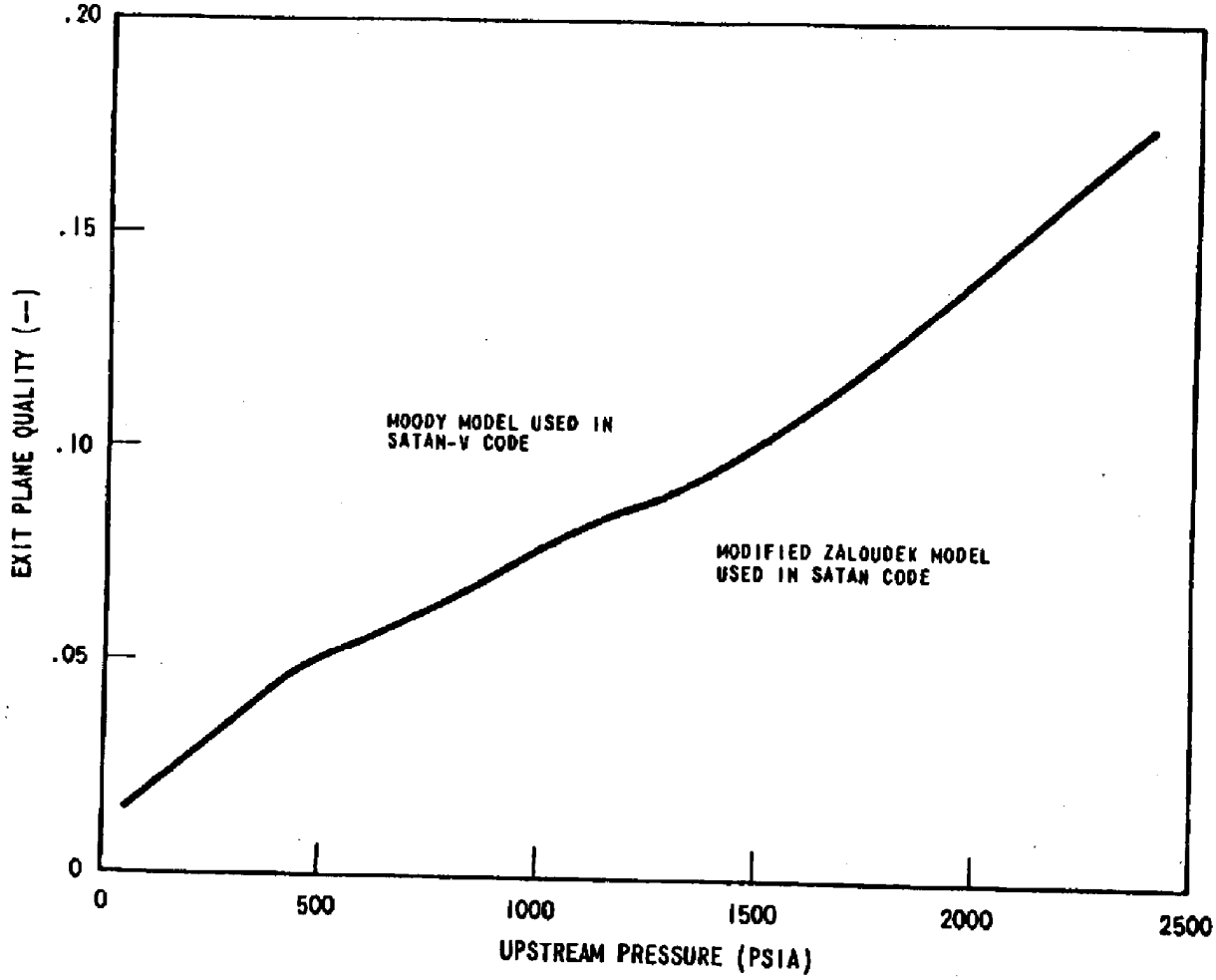

Figure 6-94. Henry ANL 7740 Data

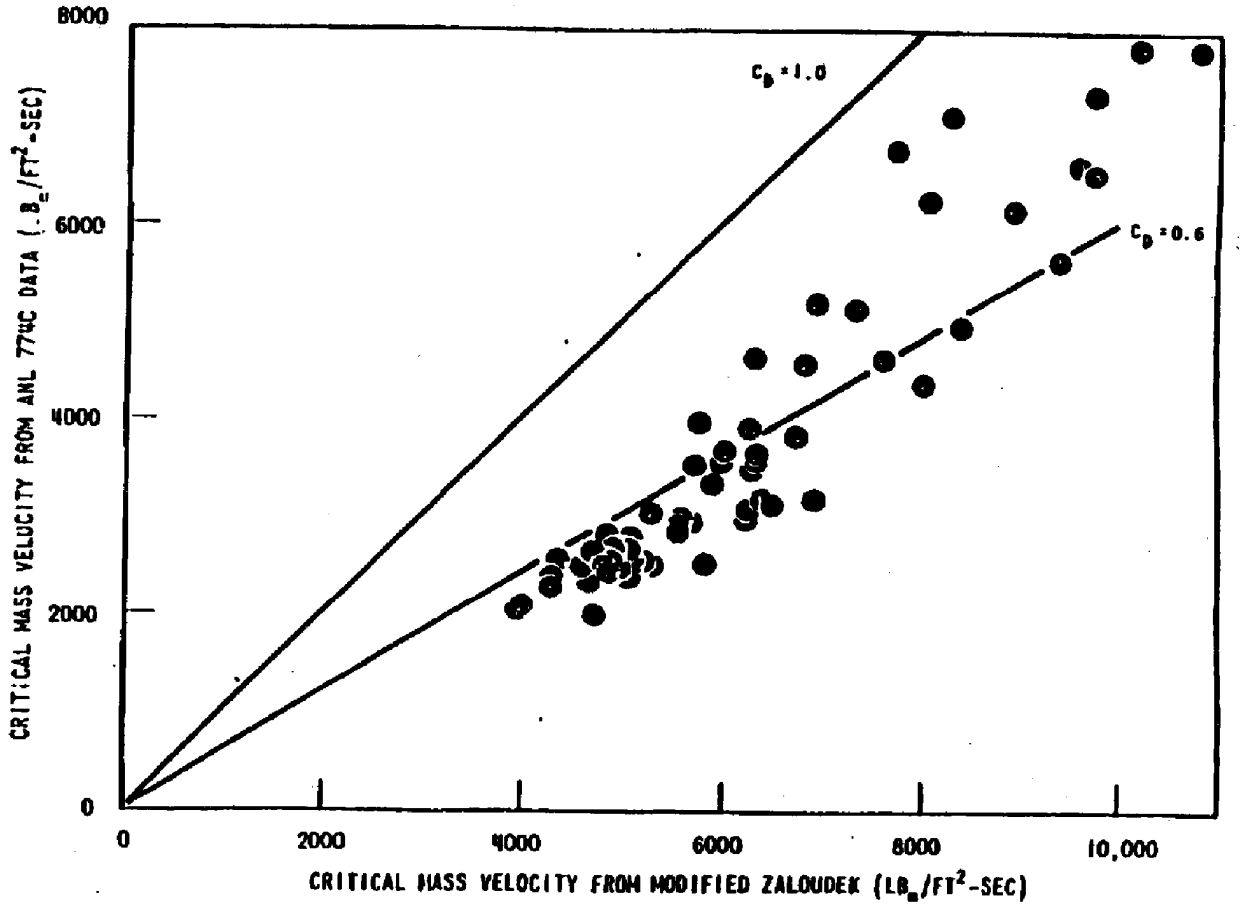

Figure 6-95. Loft Tests 809 and 813 Gage P-1

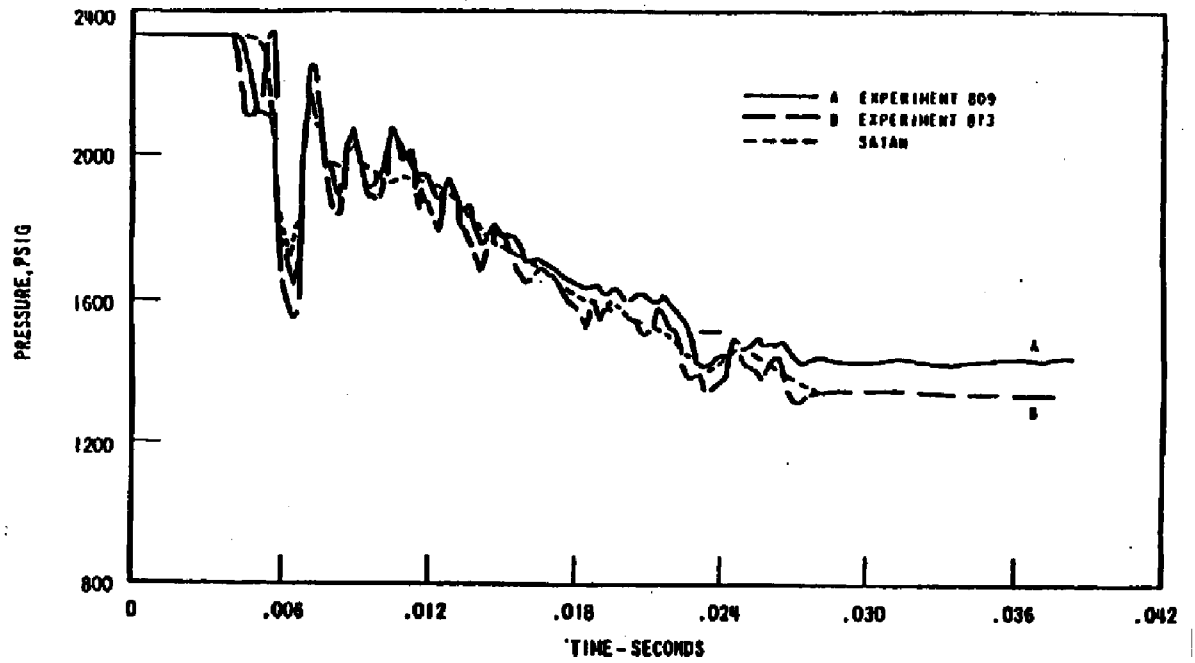

Figure 6-96. Deleted Per 2001 Update

Figure 6-97. Deleted Per 2001 Update

Figure 6-98. Deleted Per 2001 Update

Figure 6-99. Deleted Per 2001 Update

Figure 6-100. Deleted Per 2001 Update

Figure 6-101. Deleted Per 2001 Update

Figure 6-102. Illustration of Choked Flow Characteristics

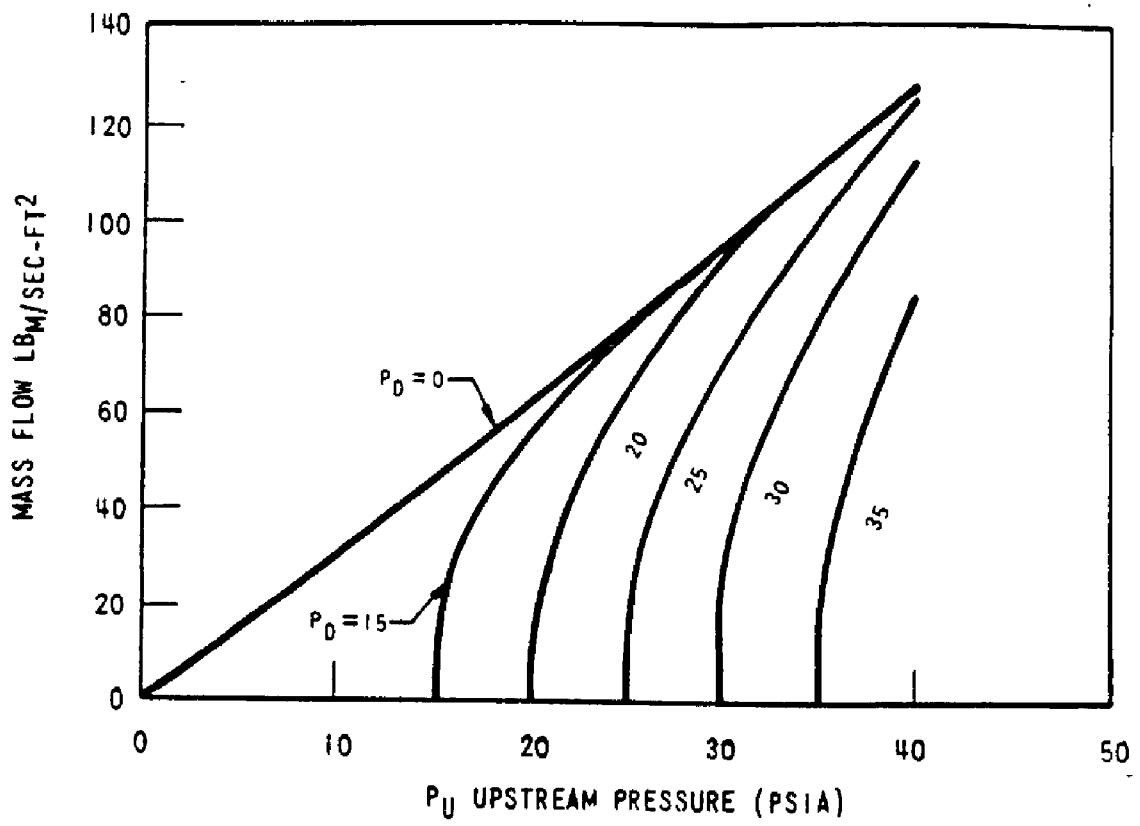

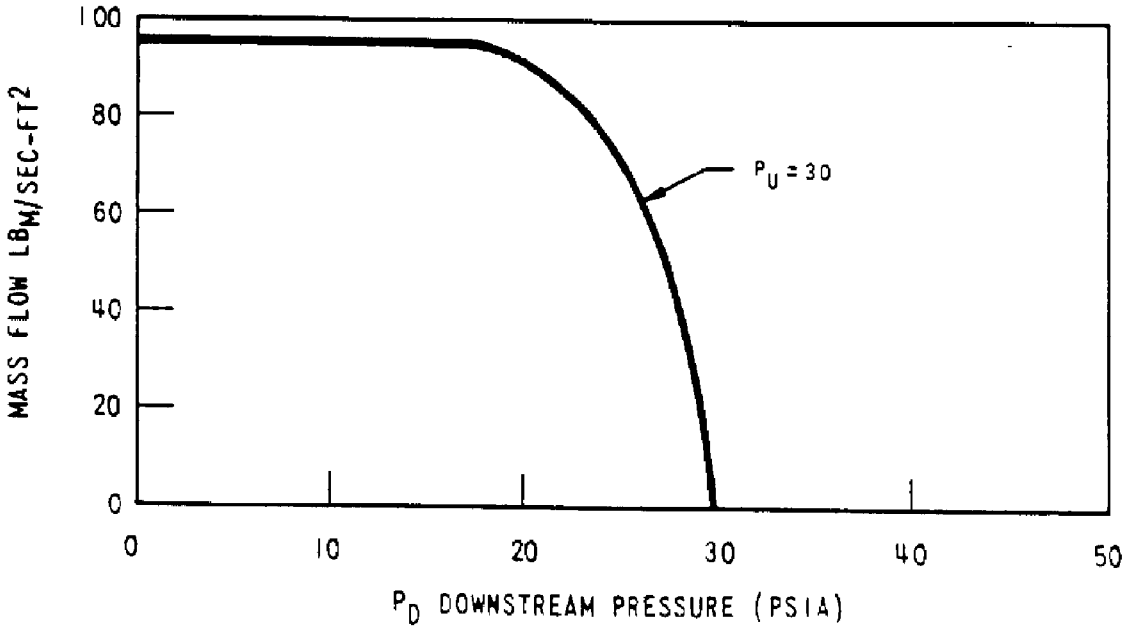

Figure 6-103. Flow Diagram of Containment Air Return Exchange & Hydrogen Skimmer System

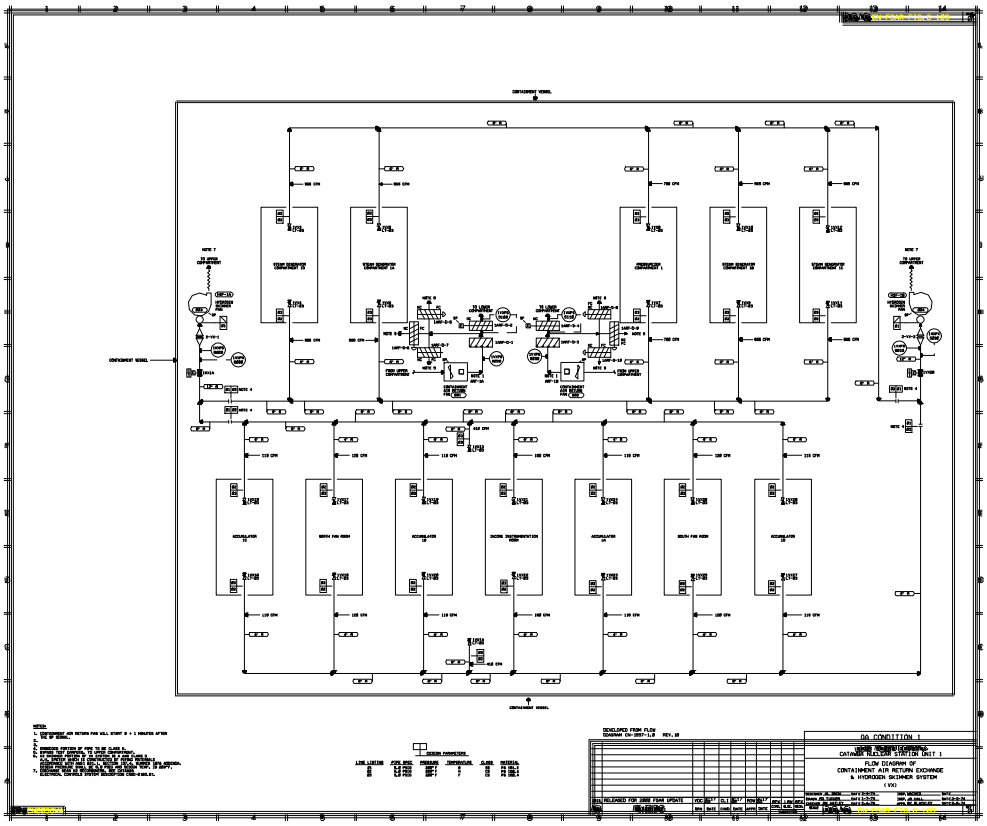

Figure 6-104. Reactor Building Plan at Elev. 565 + 3 Hydrogen Skimmer System

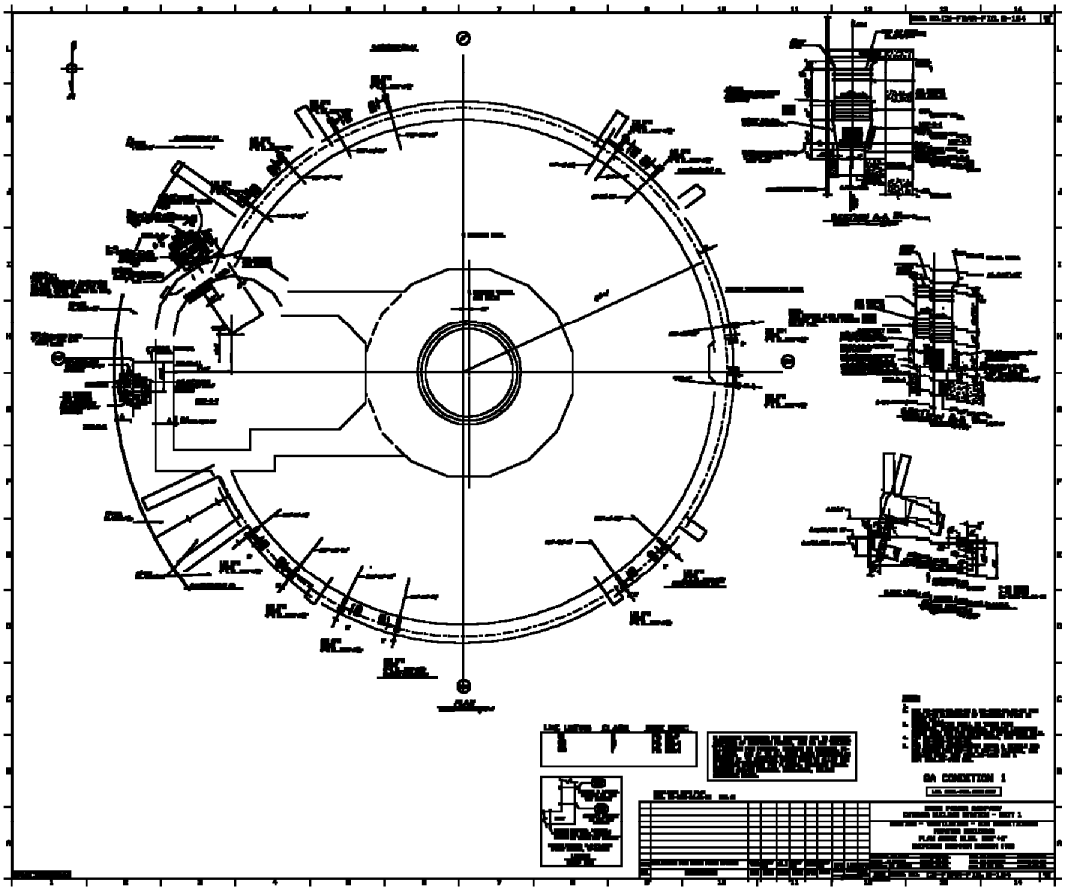

Figure 6-105. Reactor Building Hydrogen Skimmer System

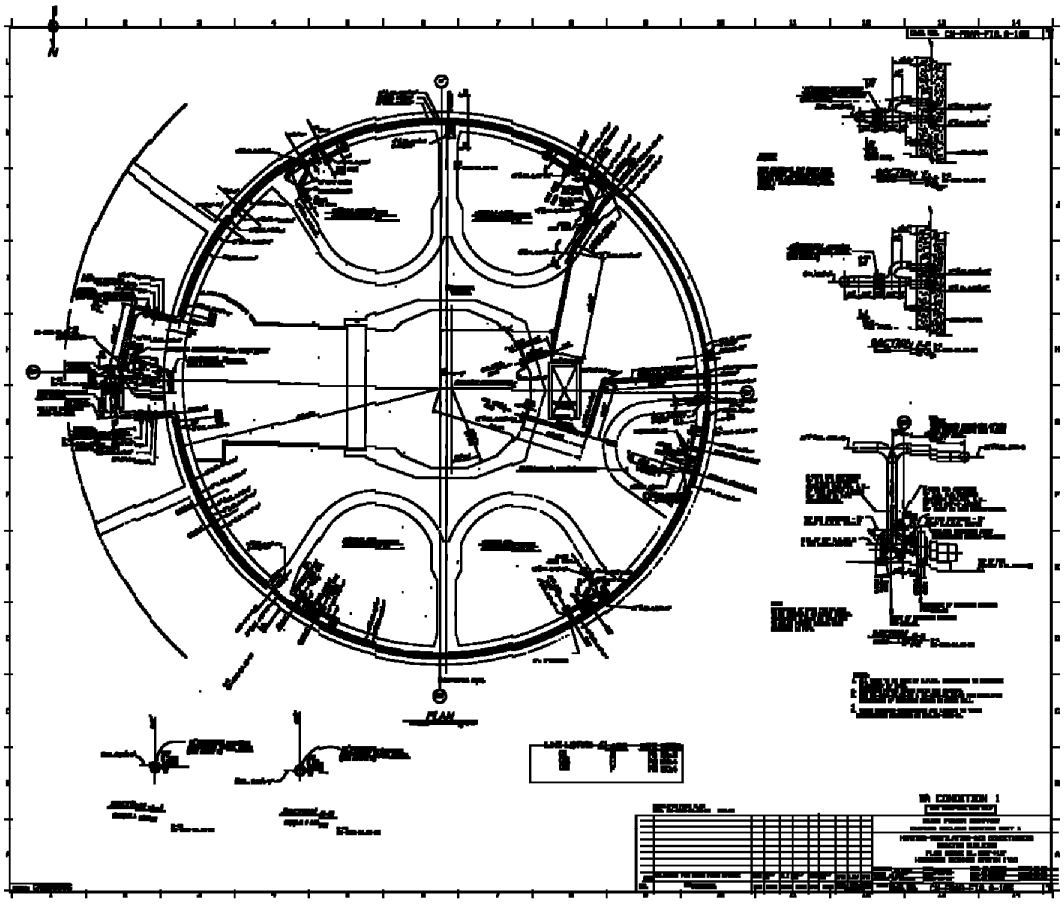

Figure 6-106. Containment Air Return Fan Performance Curve

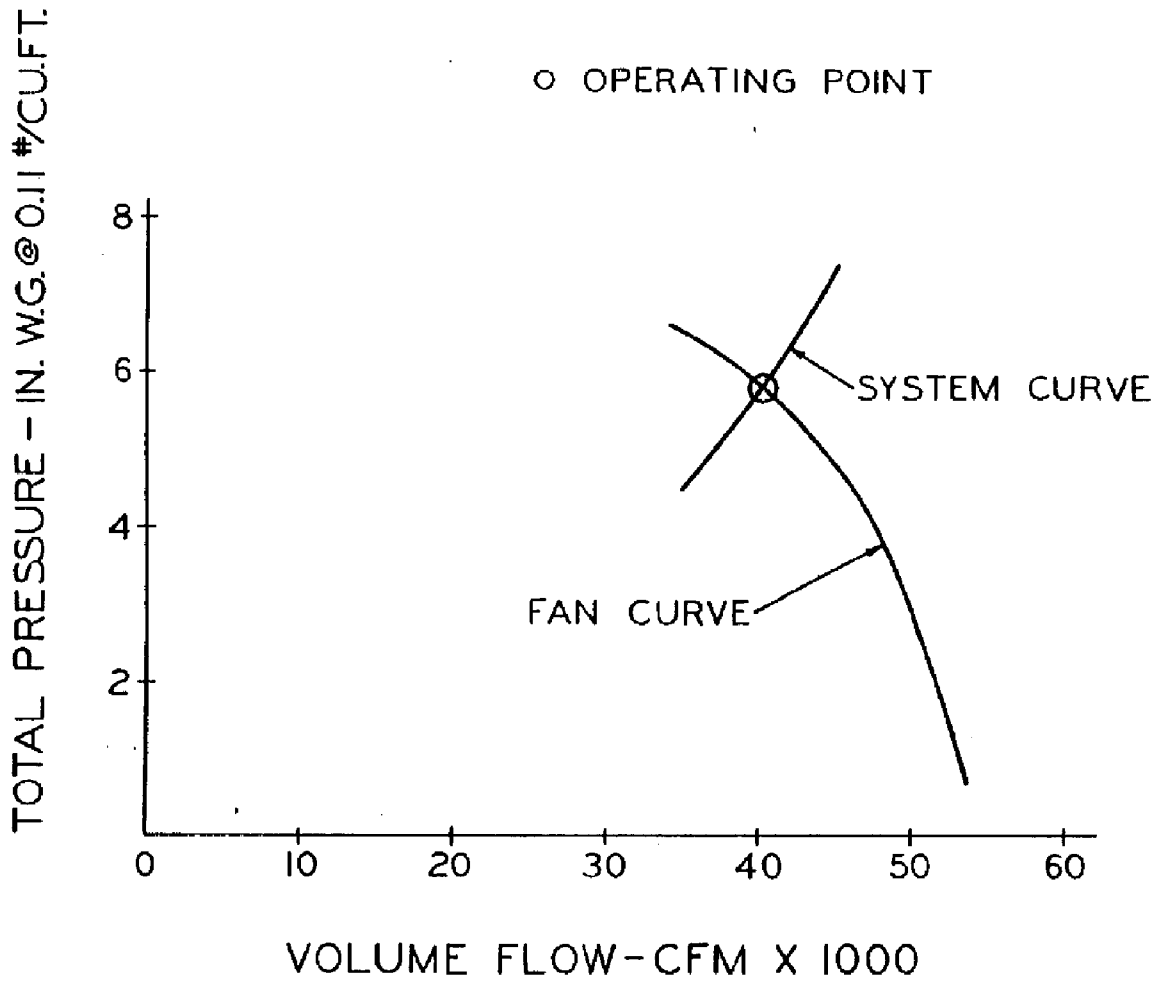

Figure 6-107. Hydrogen Skimmer Fan Performance Curve

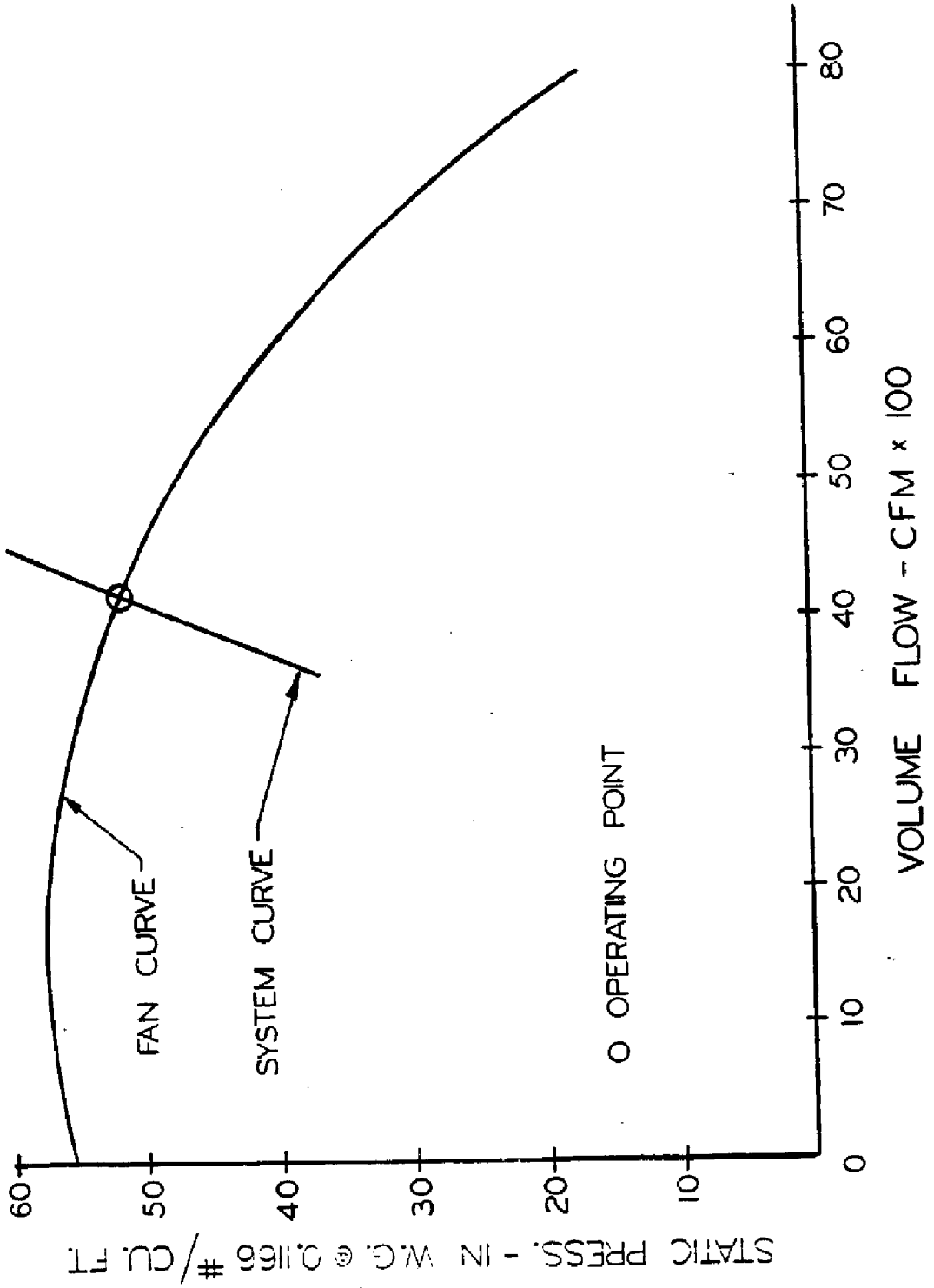

Figure 6-108. Areas of Potential Hydrogen Pockets

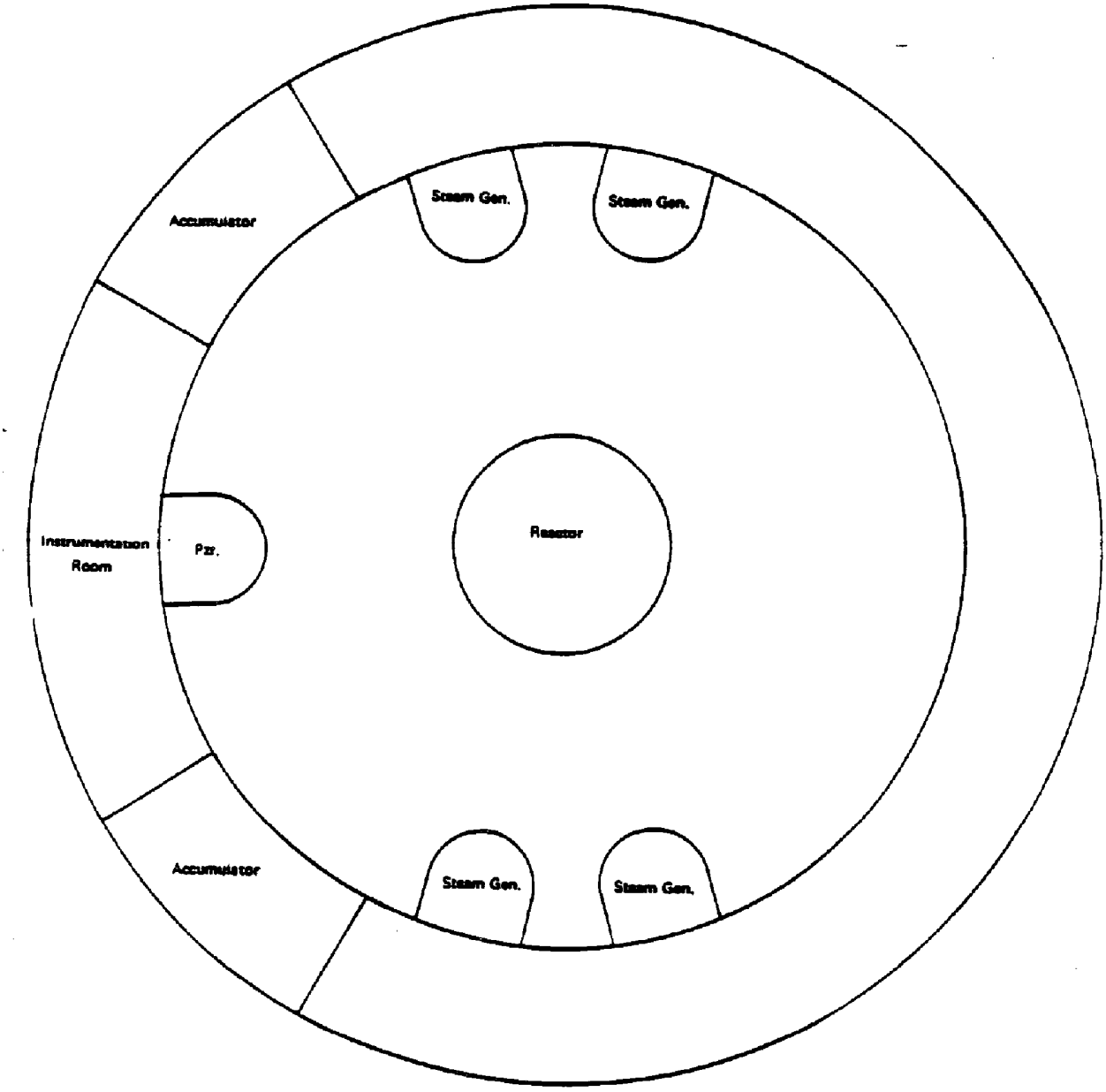

Figure 6-109. Flow Diagram of Containment Spray System

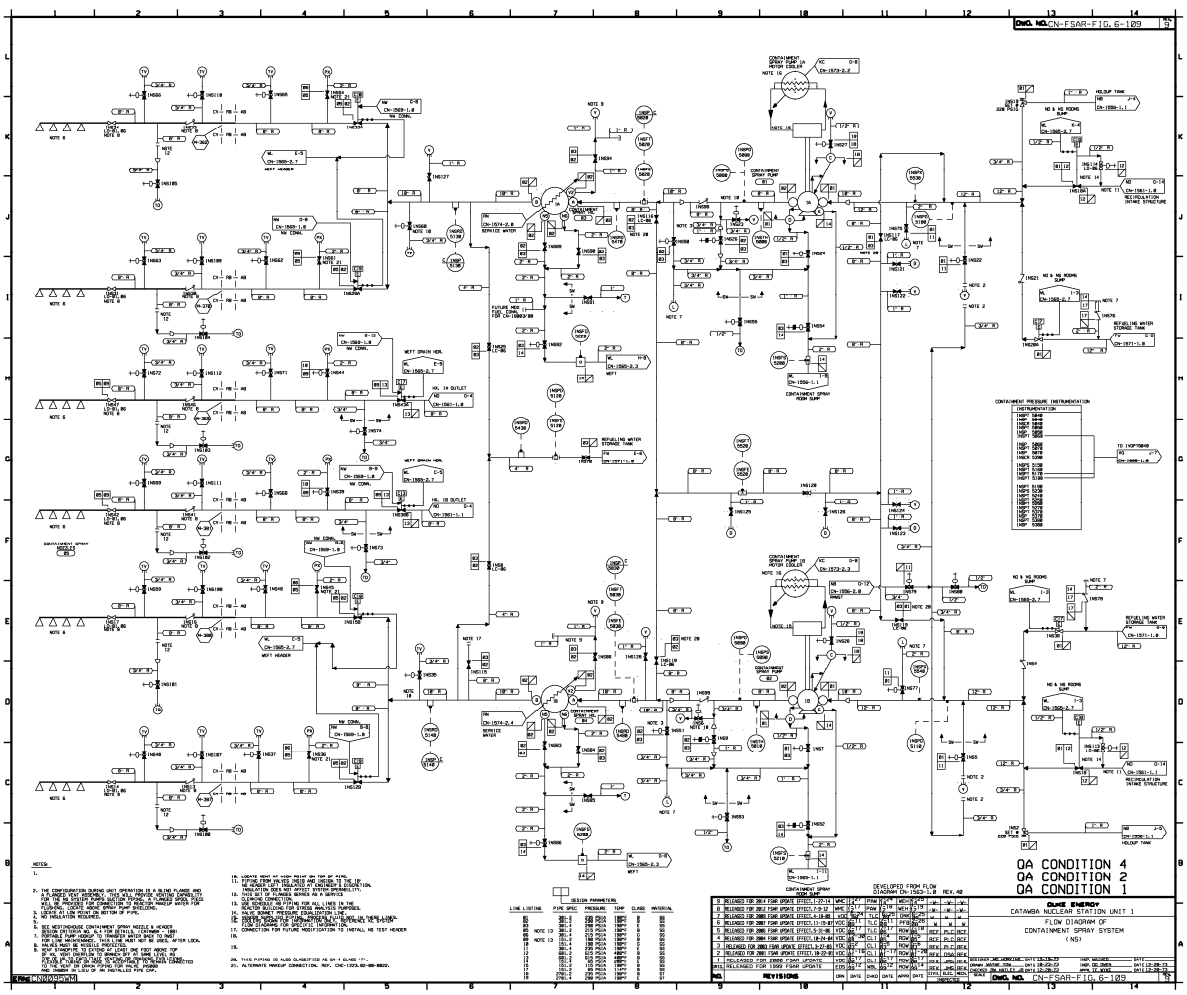

Figure 6-110. Containment Spray Pump Performance Curve

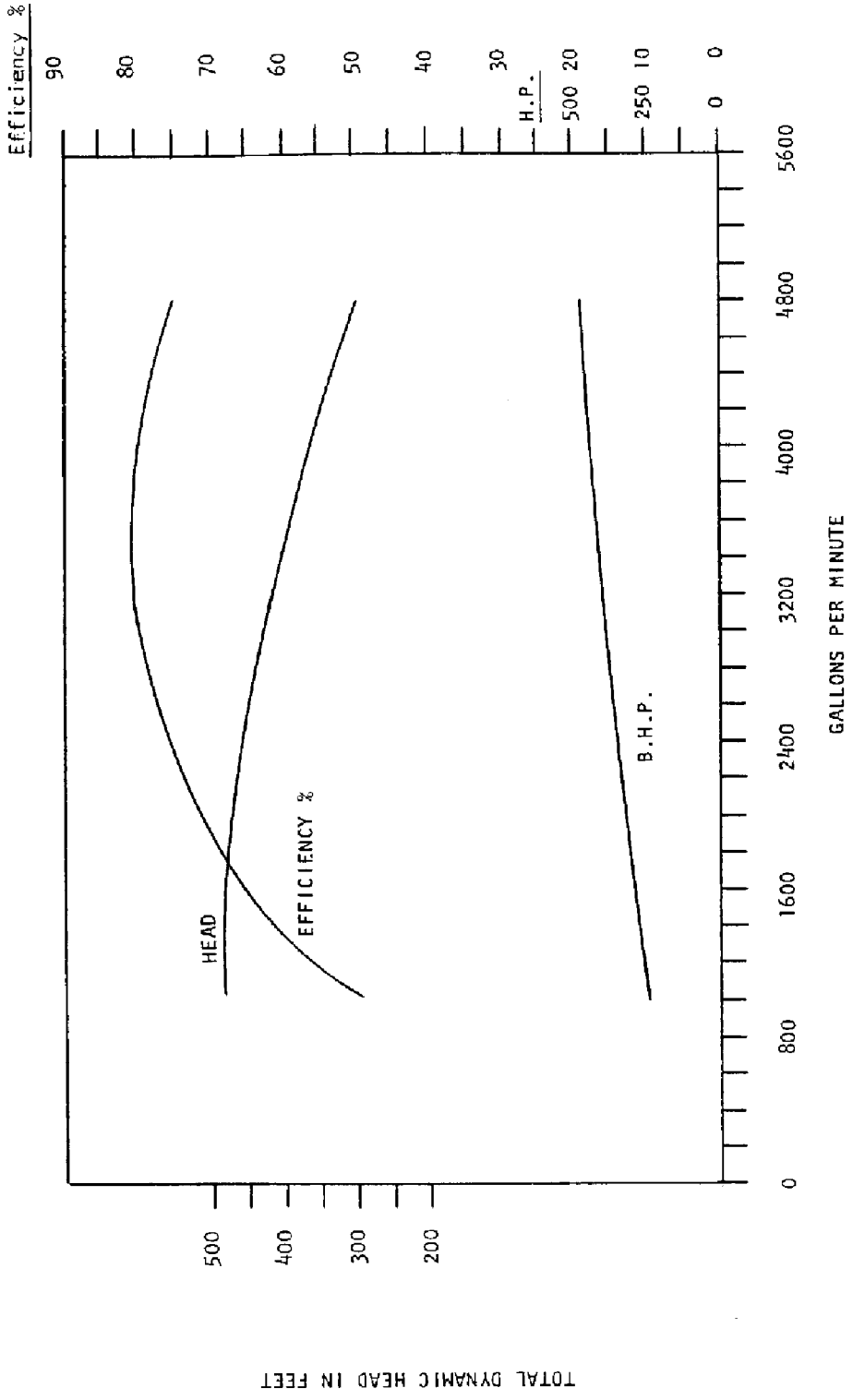

Figure 6-111. Recirculation Sump Strainer Assembly (Unit 1) (Unit 2 Similar)

Recirculation Sump Strainer Assembly

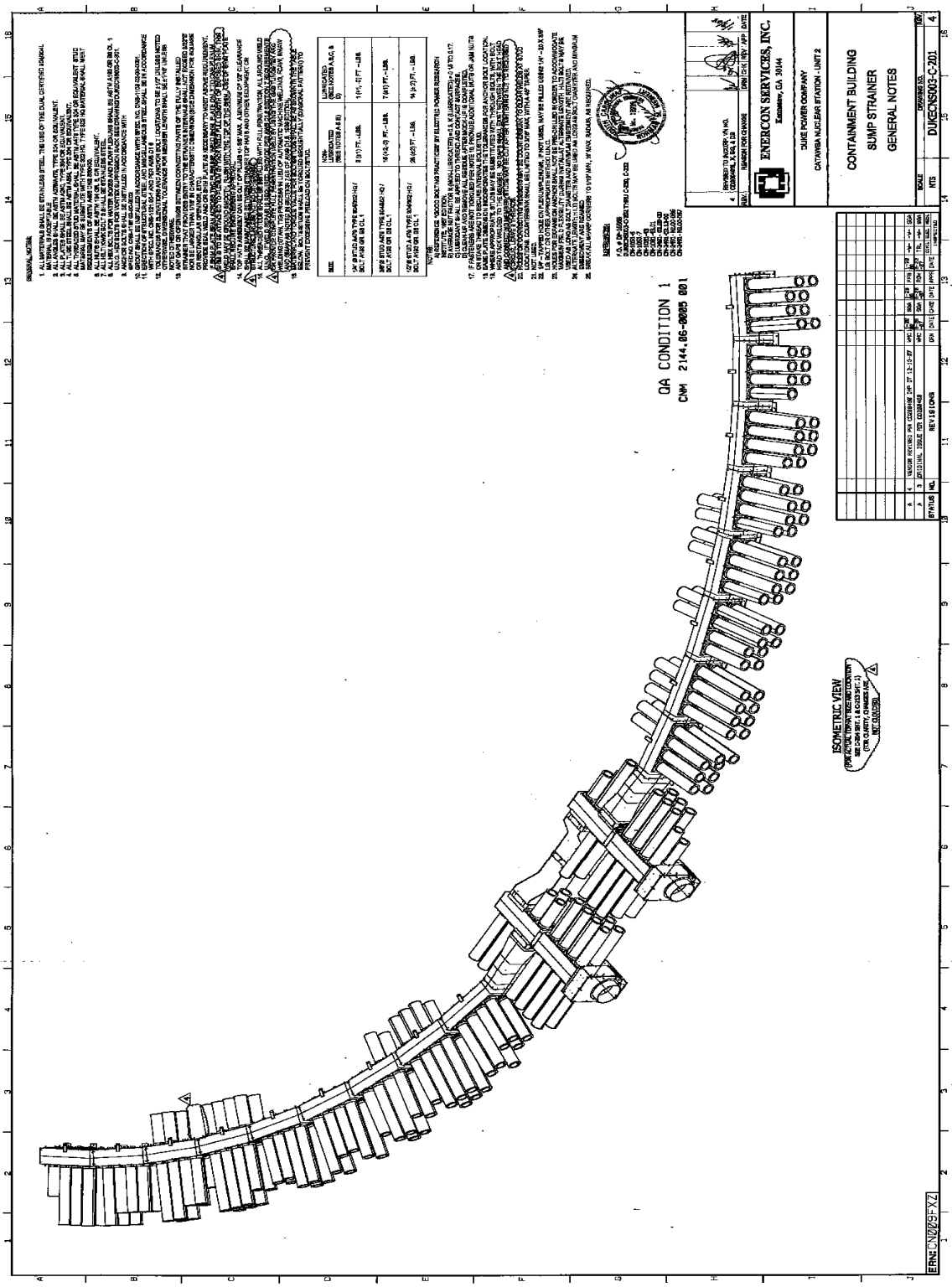

Figure 6-112. Containment Piping Penetration Valve Arrangements

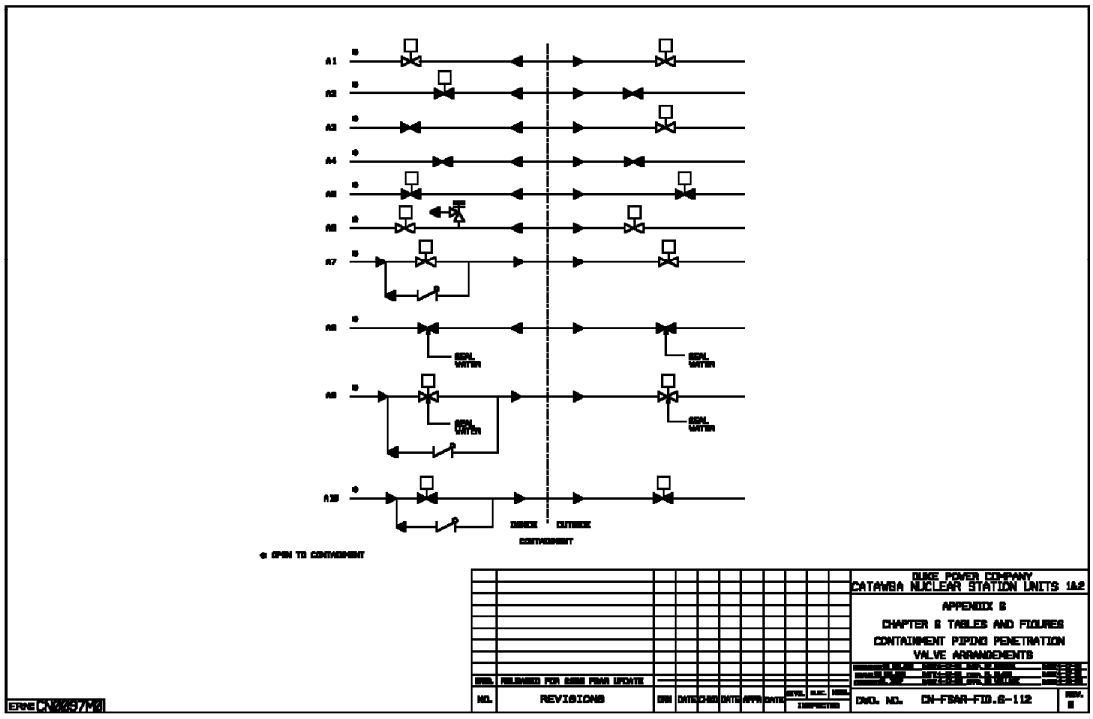

Figure 6-113. Containment Piping Penetration Valve Arrangements

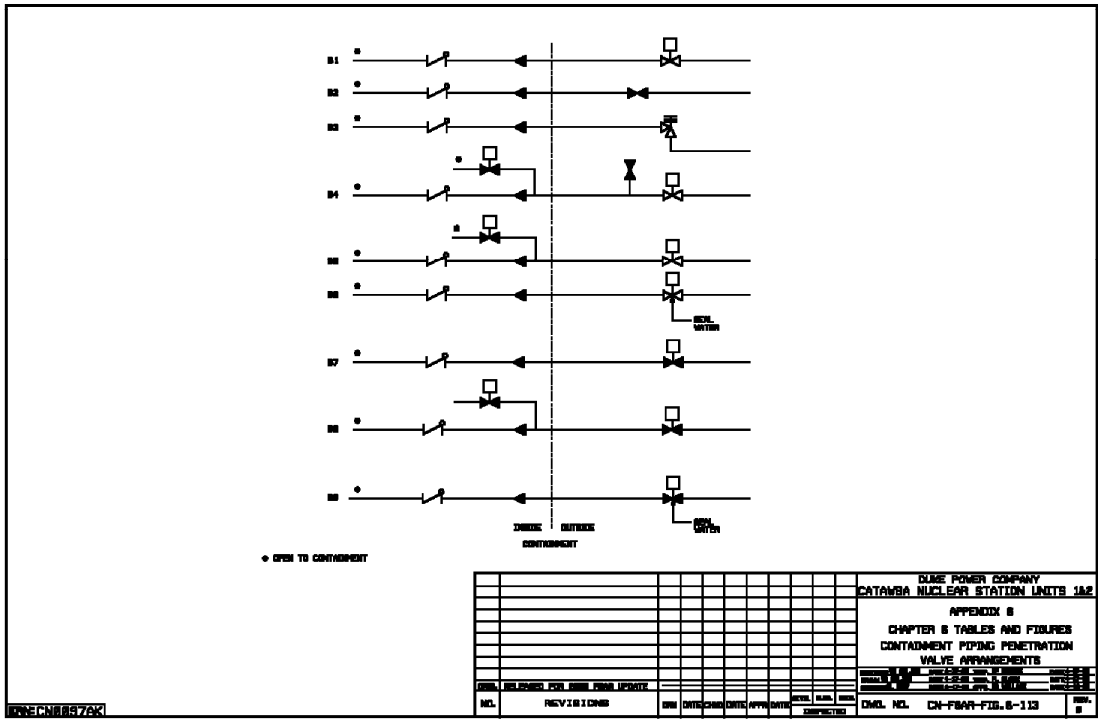

Figure 6-114. Containment Piping Penetration Valve Arrangements

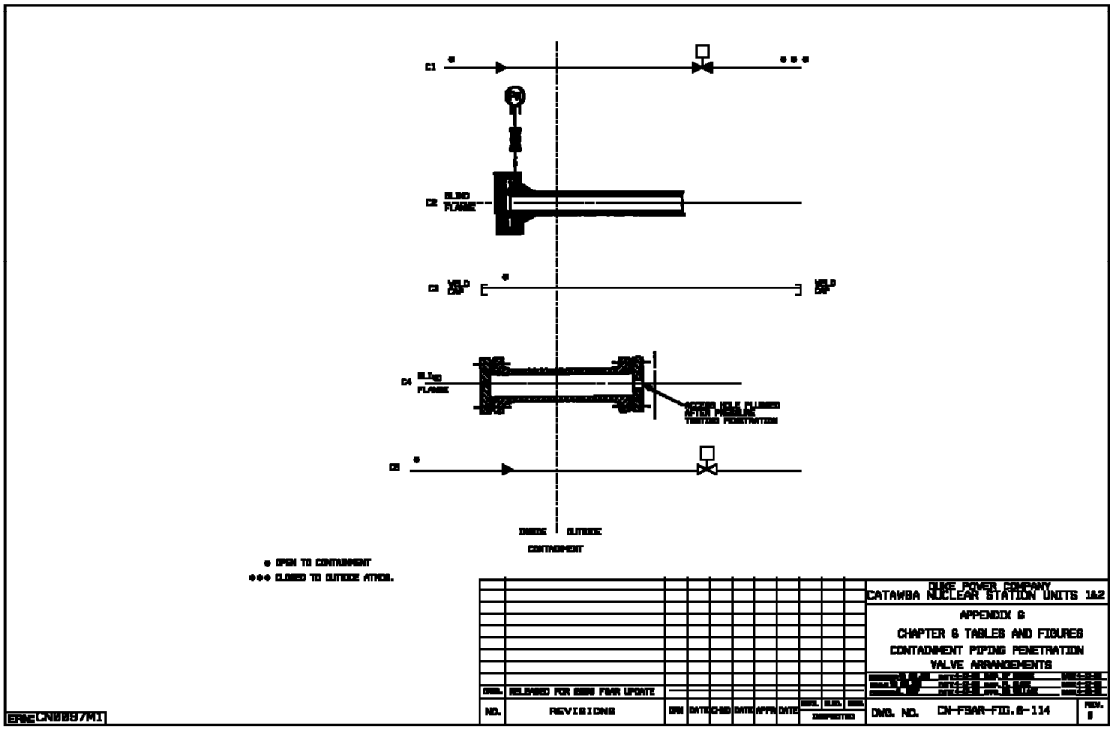

Figure 6-115. Containment Piping Penetration Valve Arrangements

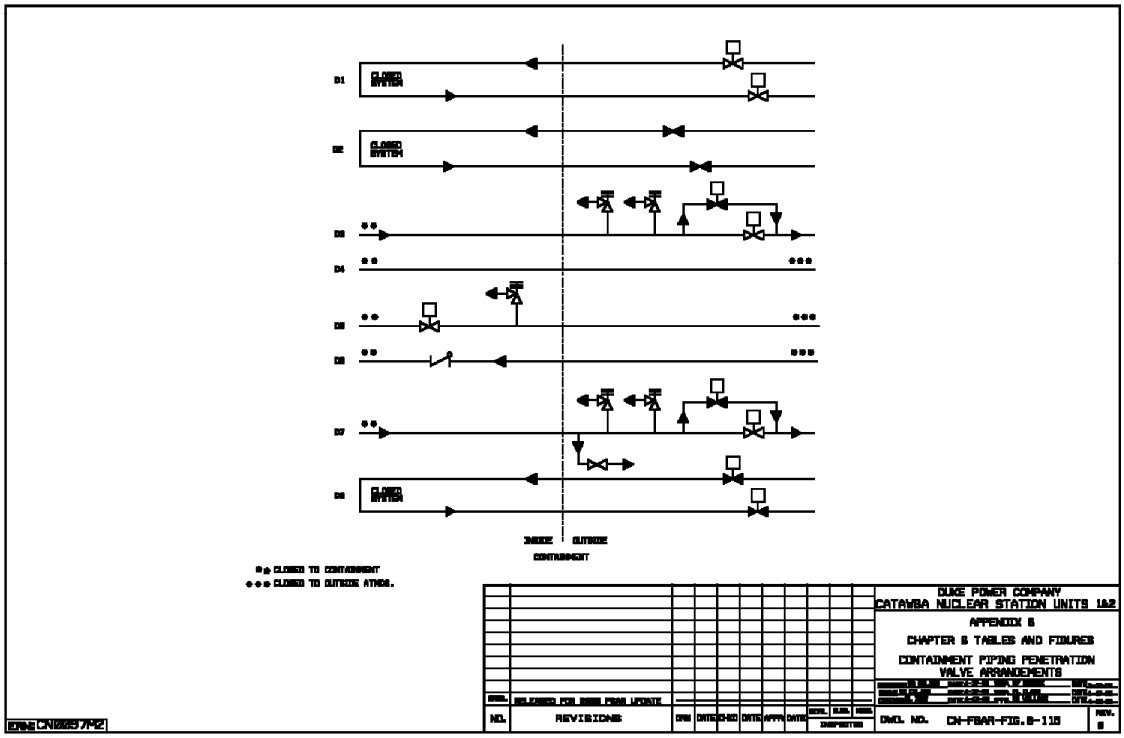

Figure 6-116. Flow Diagram of Containment Valve Injection Water System

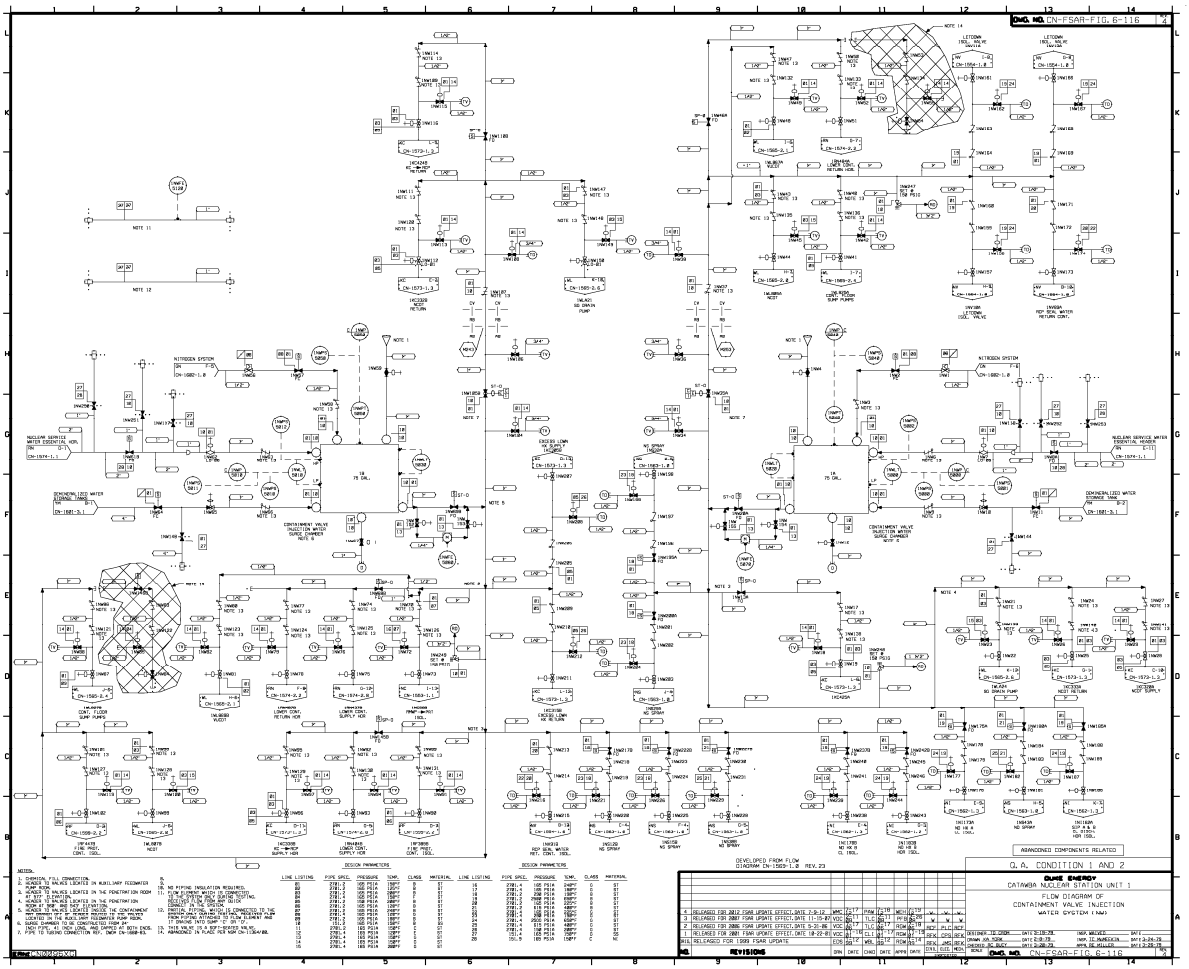

Figure 6-117. Fuel Transfer Tube

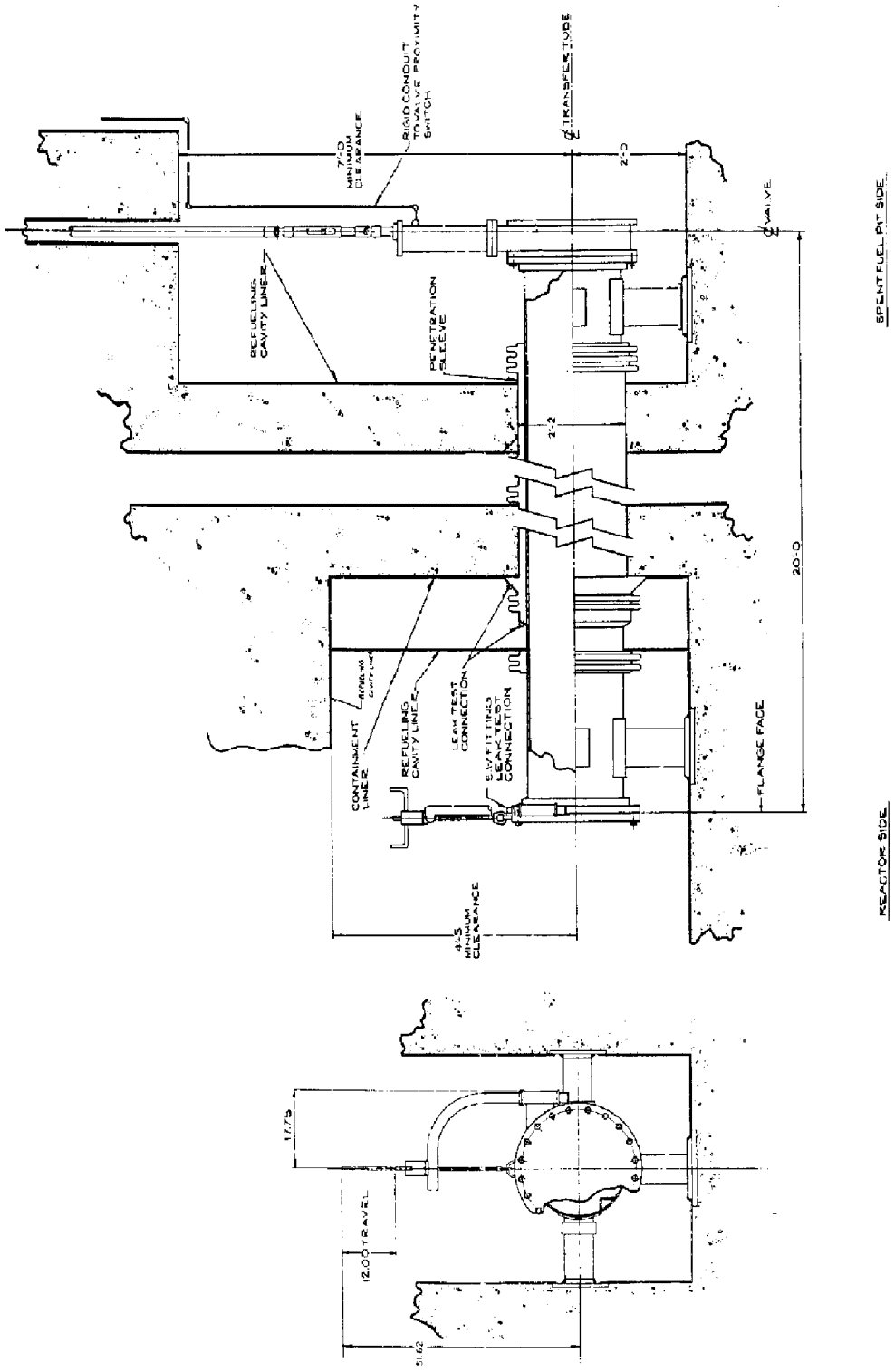

Figure 6-118. Model B Electric Hydrogen Recombiner-Cutaway

Historical information not required to be revised.

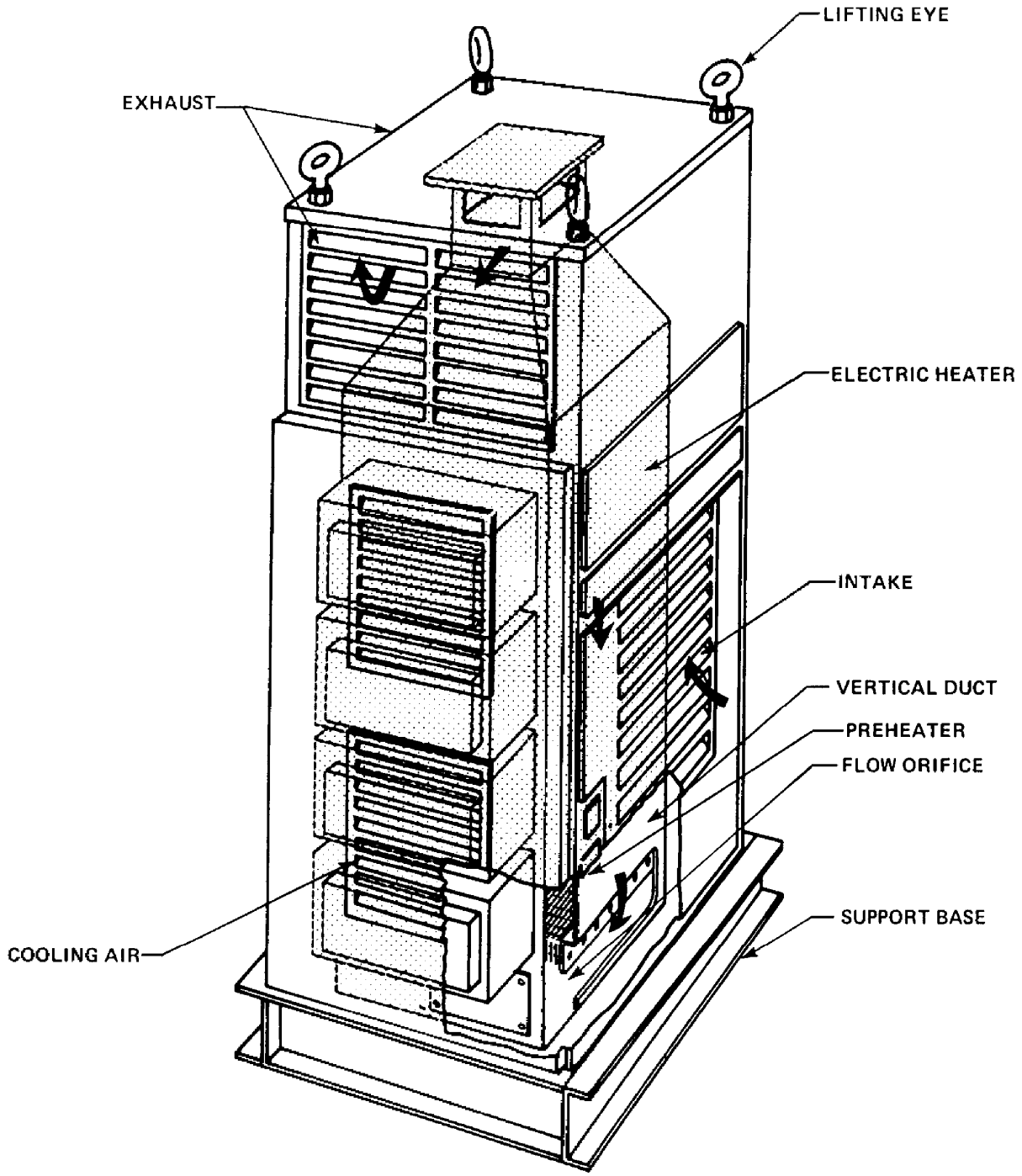

Figure 6-119. Recombiner Control System Schematic

Historical information not required to be revised.

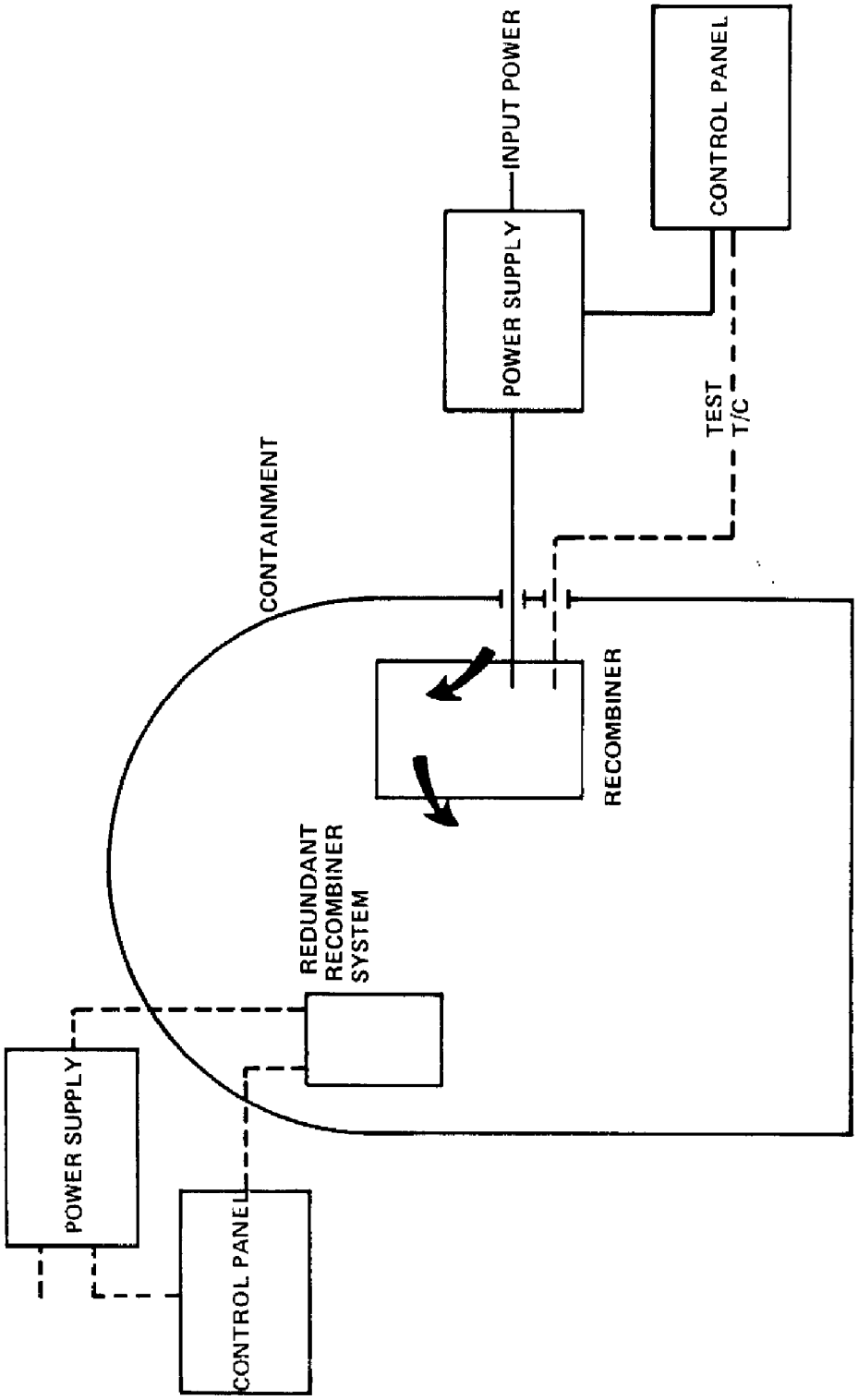

Figure 6-120. Flow Diagram of Containment Hydrogen Sample & Purge System

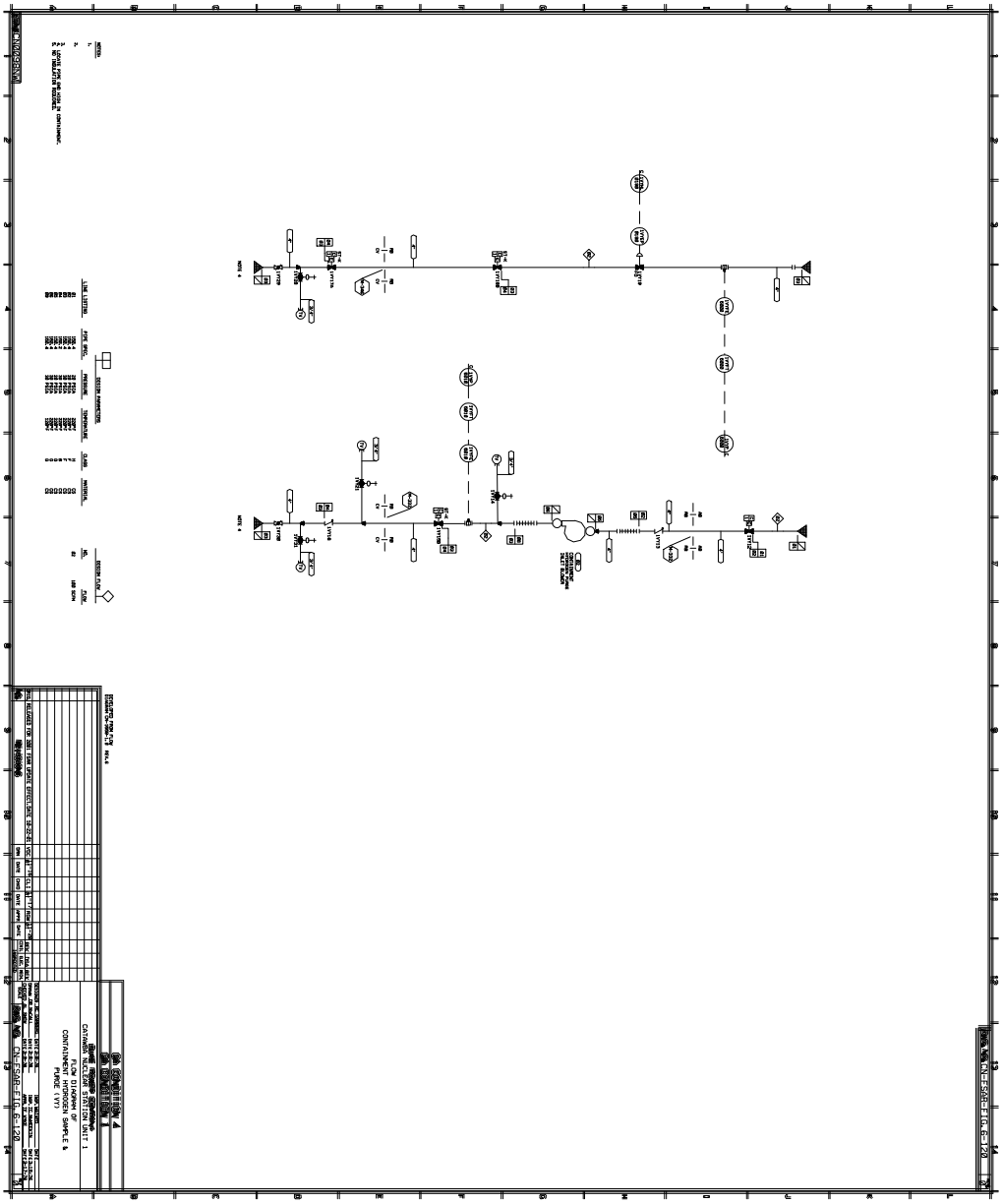

Figure 6-121. Deleted Per 1991 Update

Figure 6-122. Deleted Per 1991 Update

Figure 6-123. Deleted Per 1991 Update

Figure 6-124. Deleted Per 2004 Update

Figure 6-125. Deleted Per 2006 Update

Figure 6-126. Deleted Per 2006 Update

Figure 6-127. Deleted Per 2003 Update

Figure 6-128. Flow Diagram of Safety Injection System

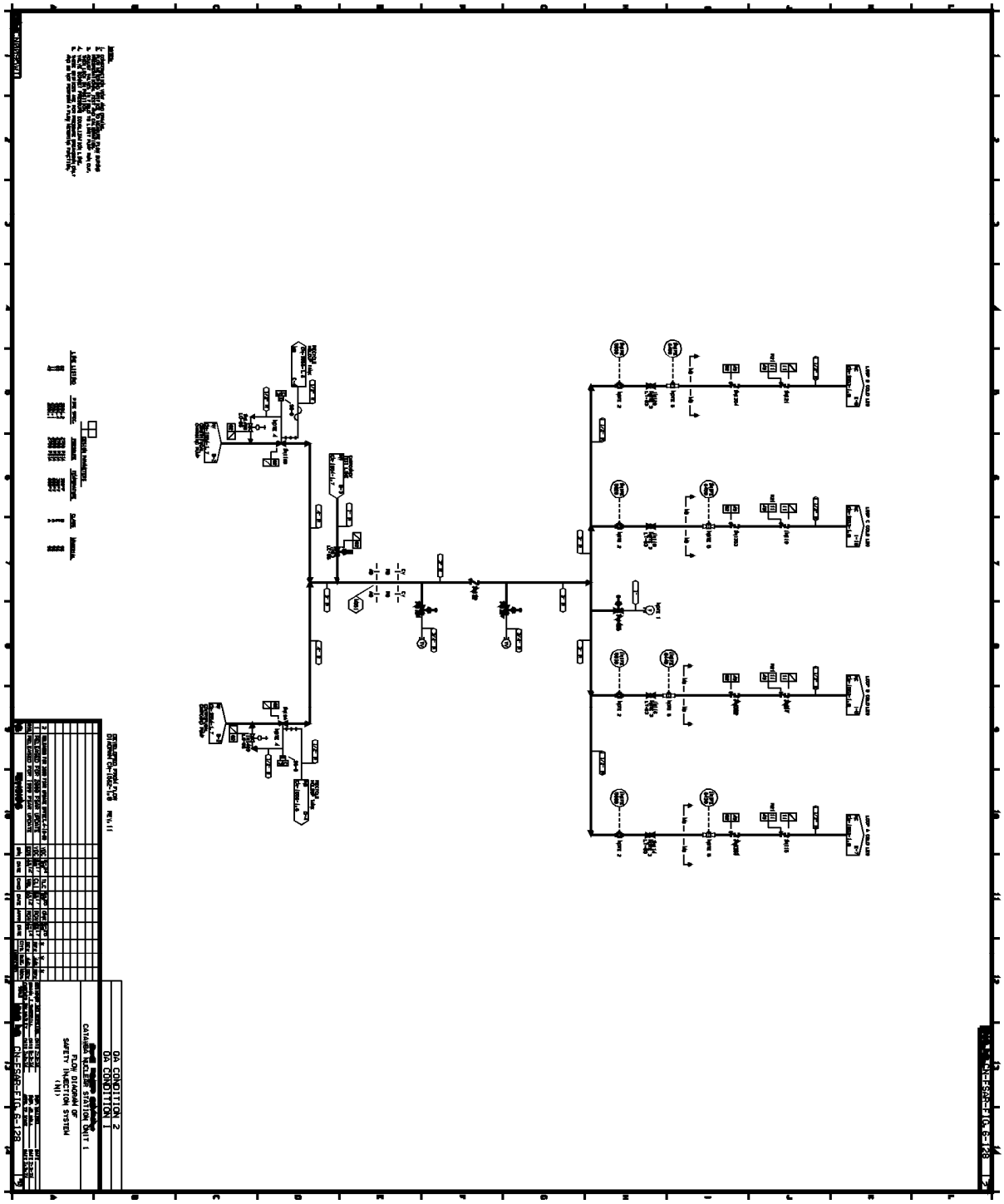

Figure 6-129. Flow Diagram of Safety Injection System

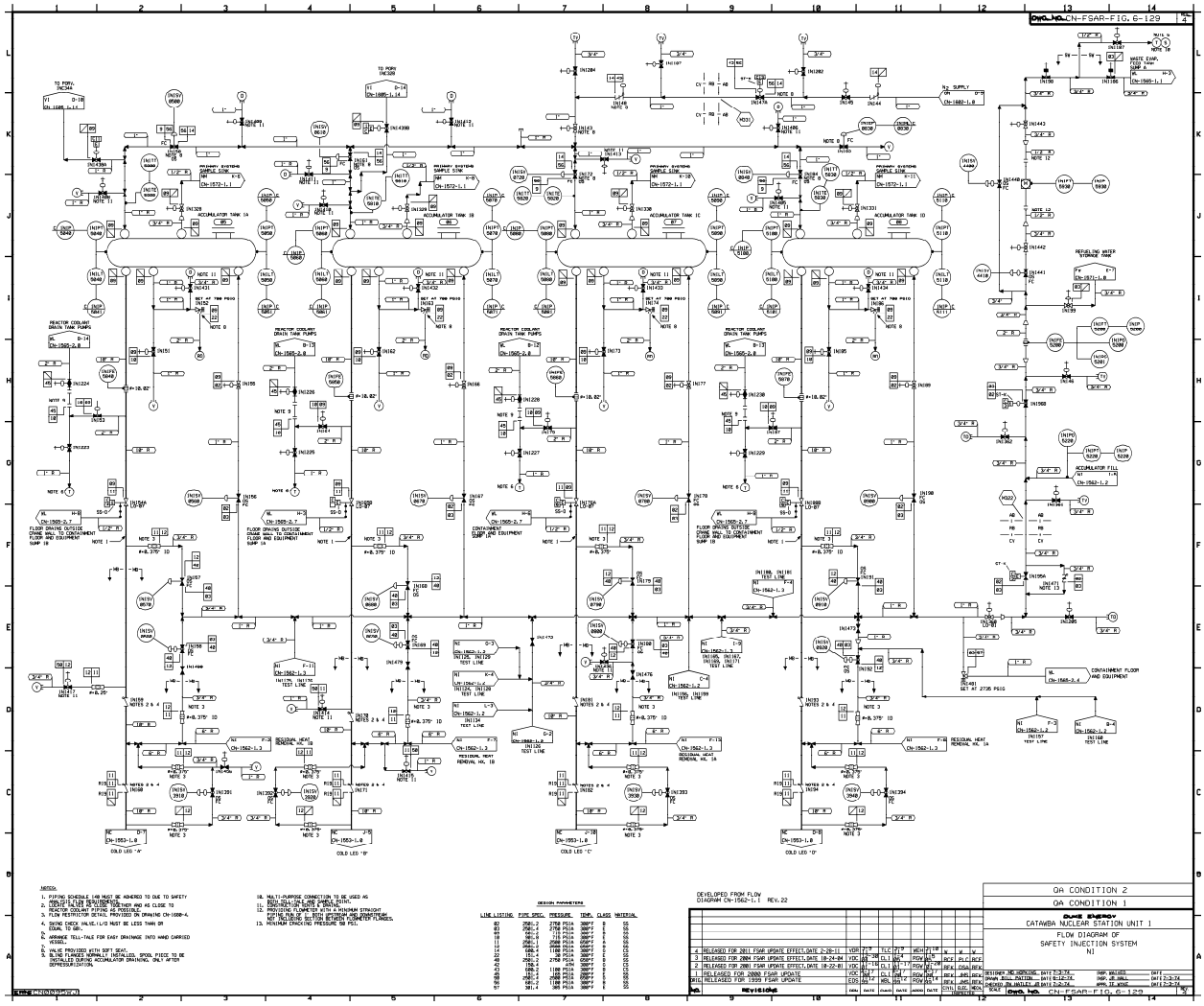

Figure 6-130. Flow Diagram of Safety Injection System

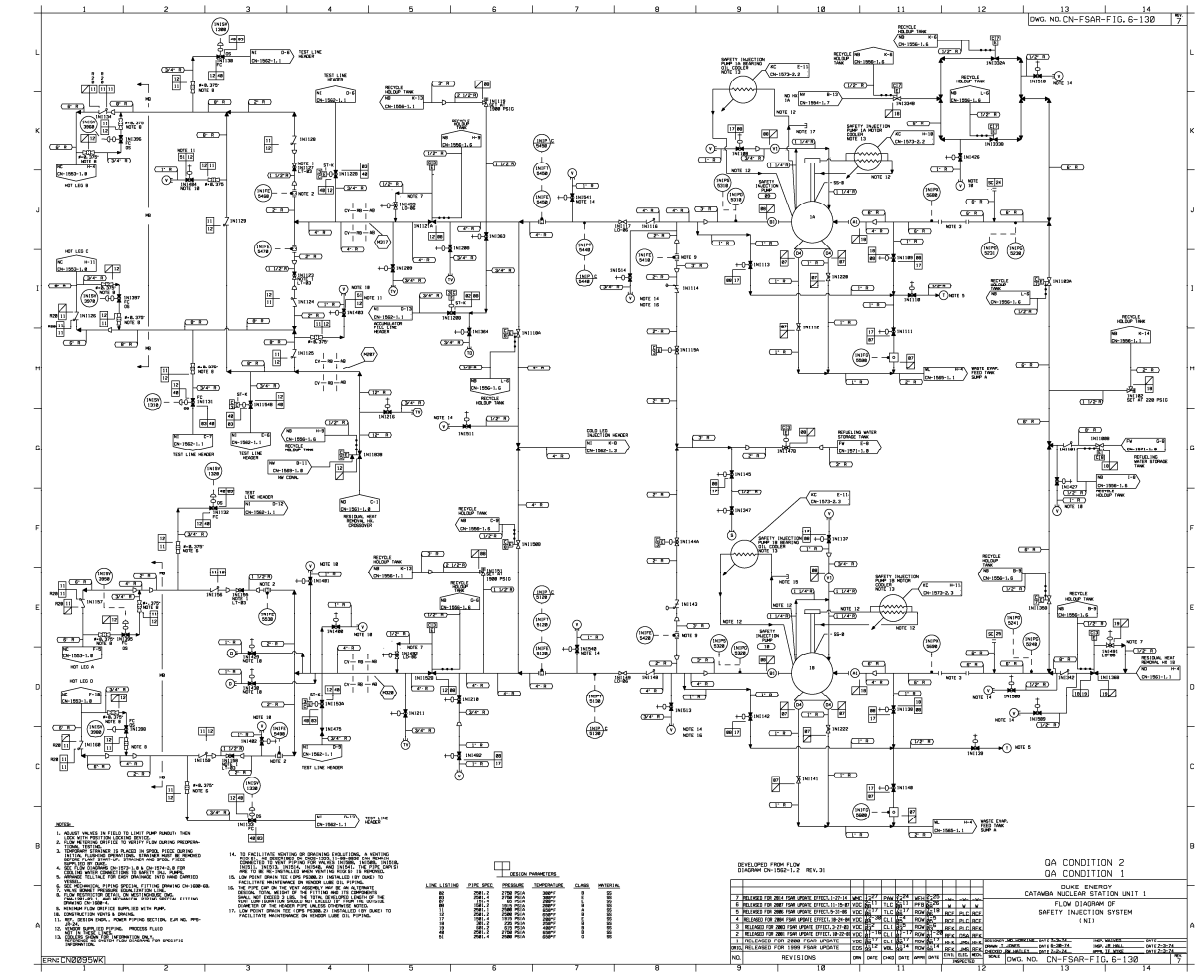

Figure 6-131. Flow Diagram of Safety Injection System

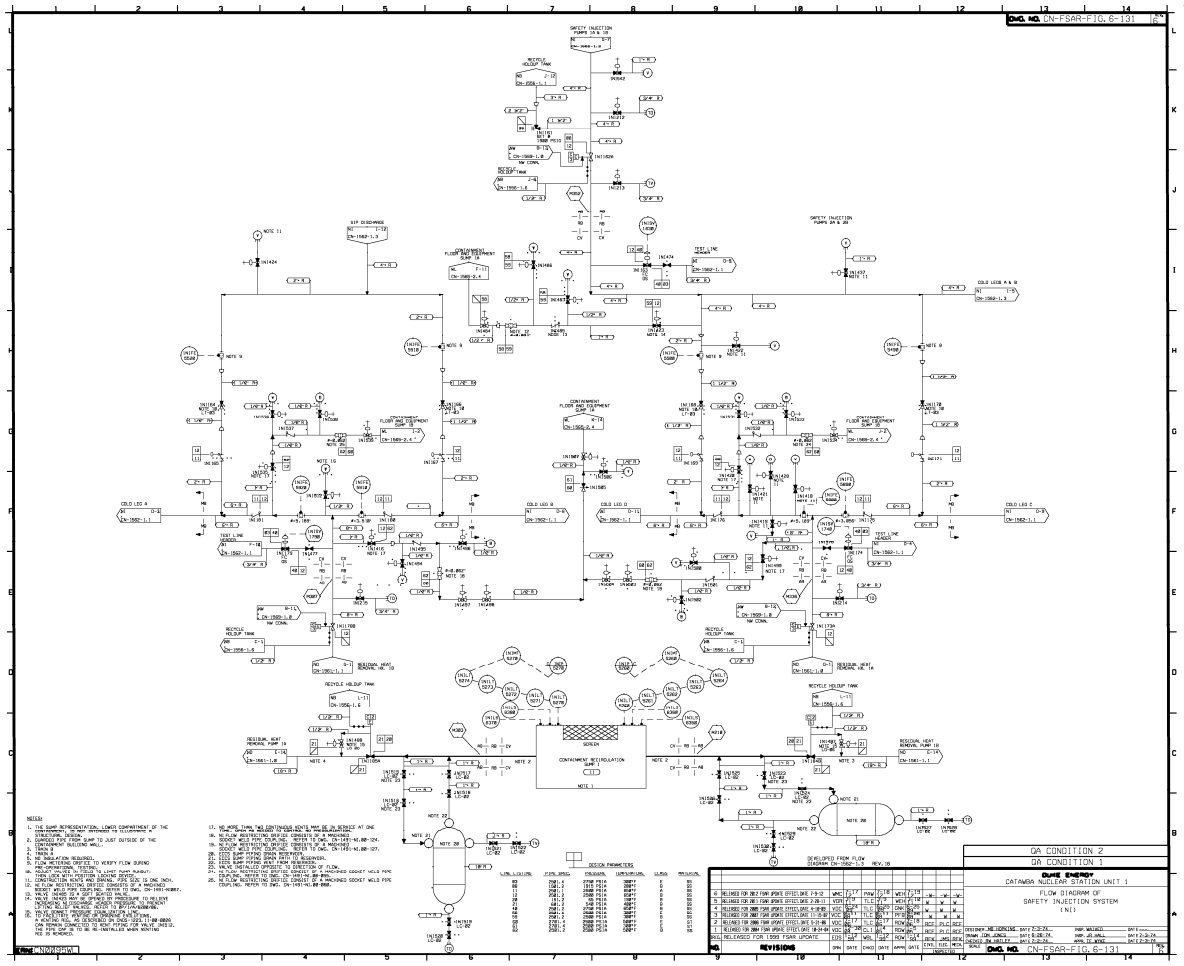

Figure 6-132. Safety Injection System

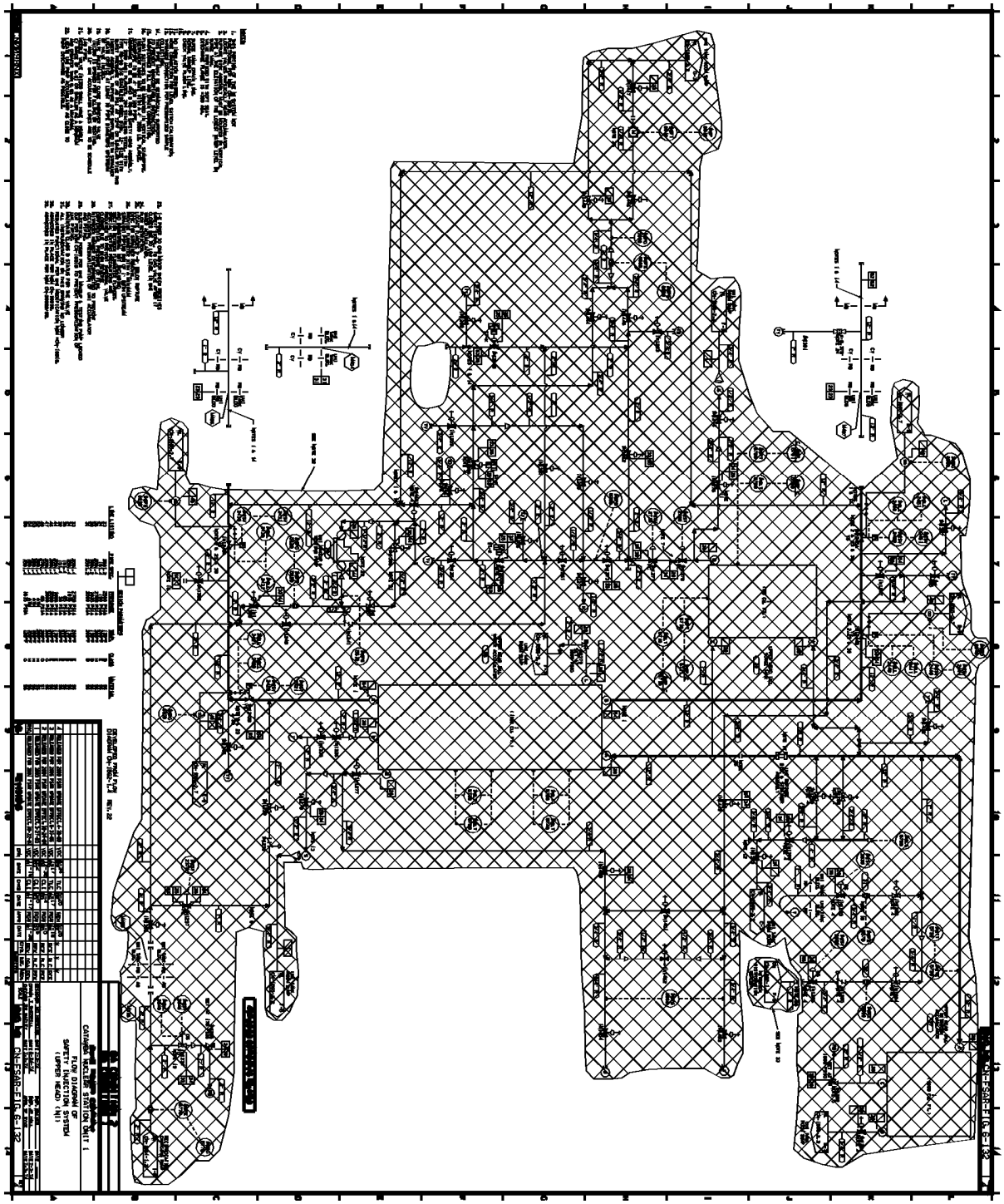

Figure 6-133. Residual Heat Removal Performance Curve

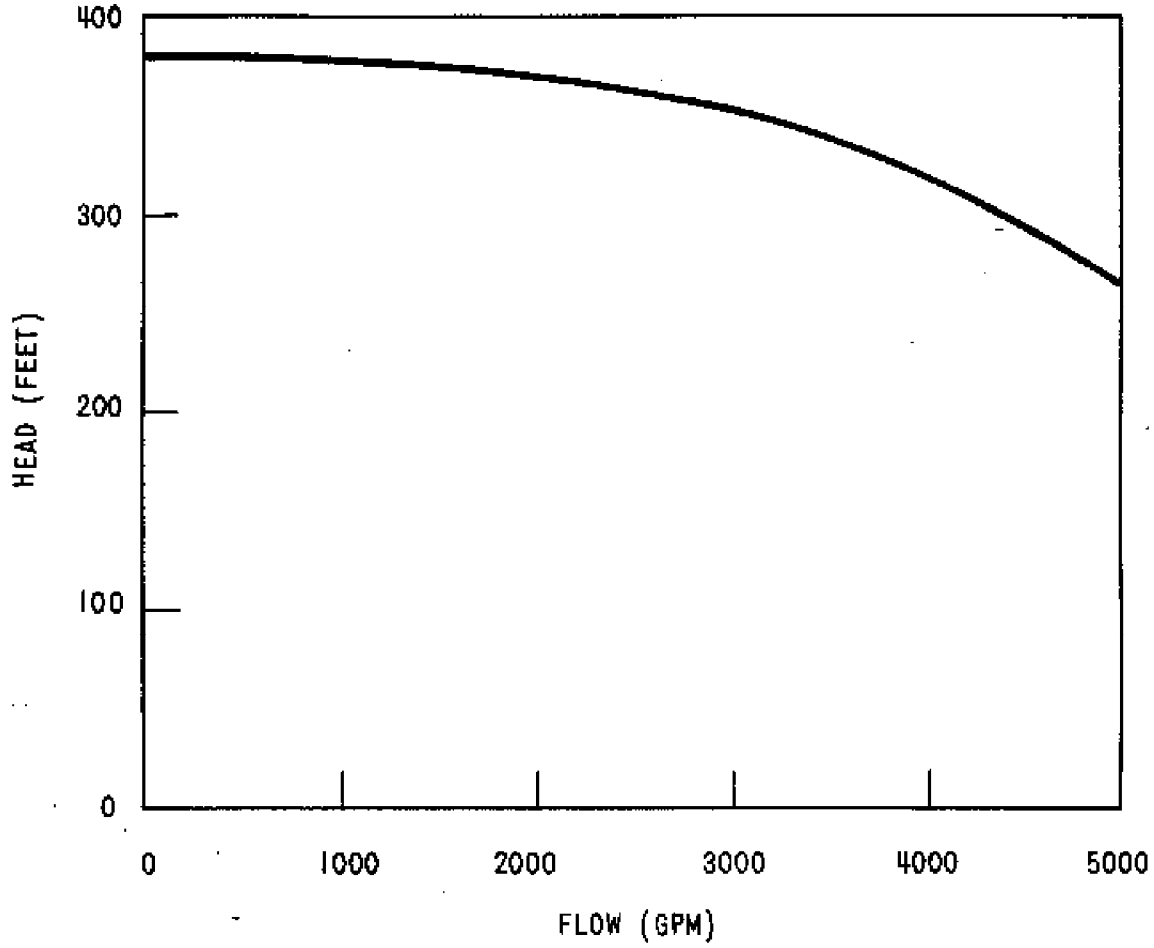

Figure 6-134. Centrifugal Charging Pump Performance Curve

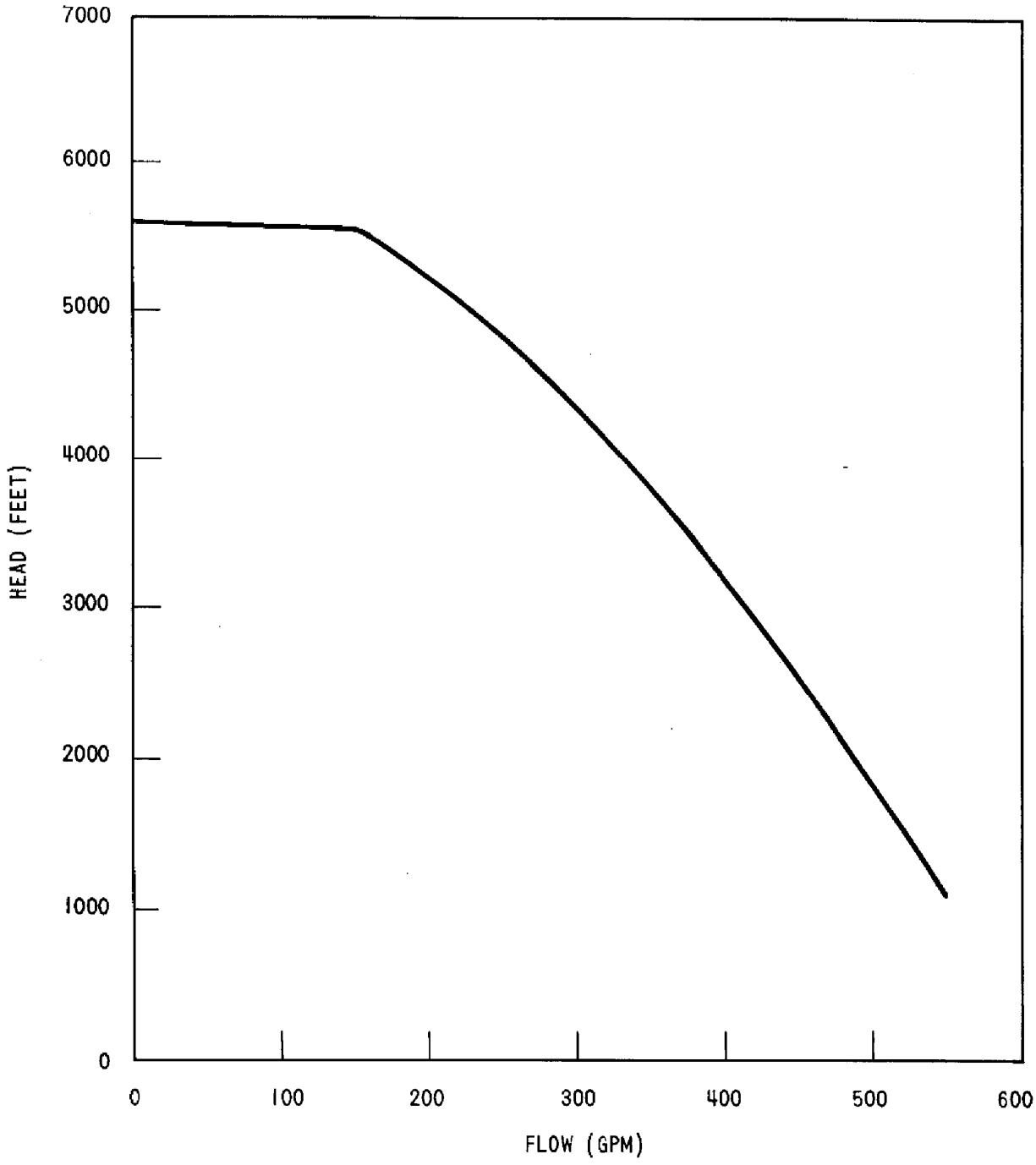

Figure 6-135. Safety Injection Pump Performance Curve

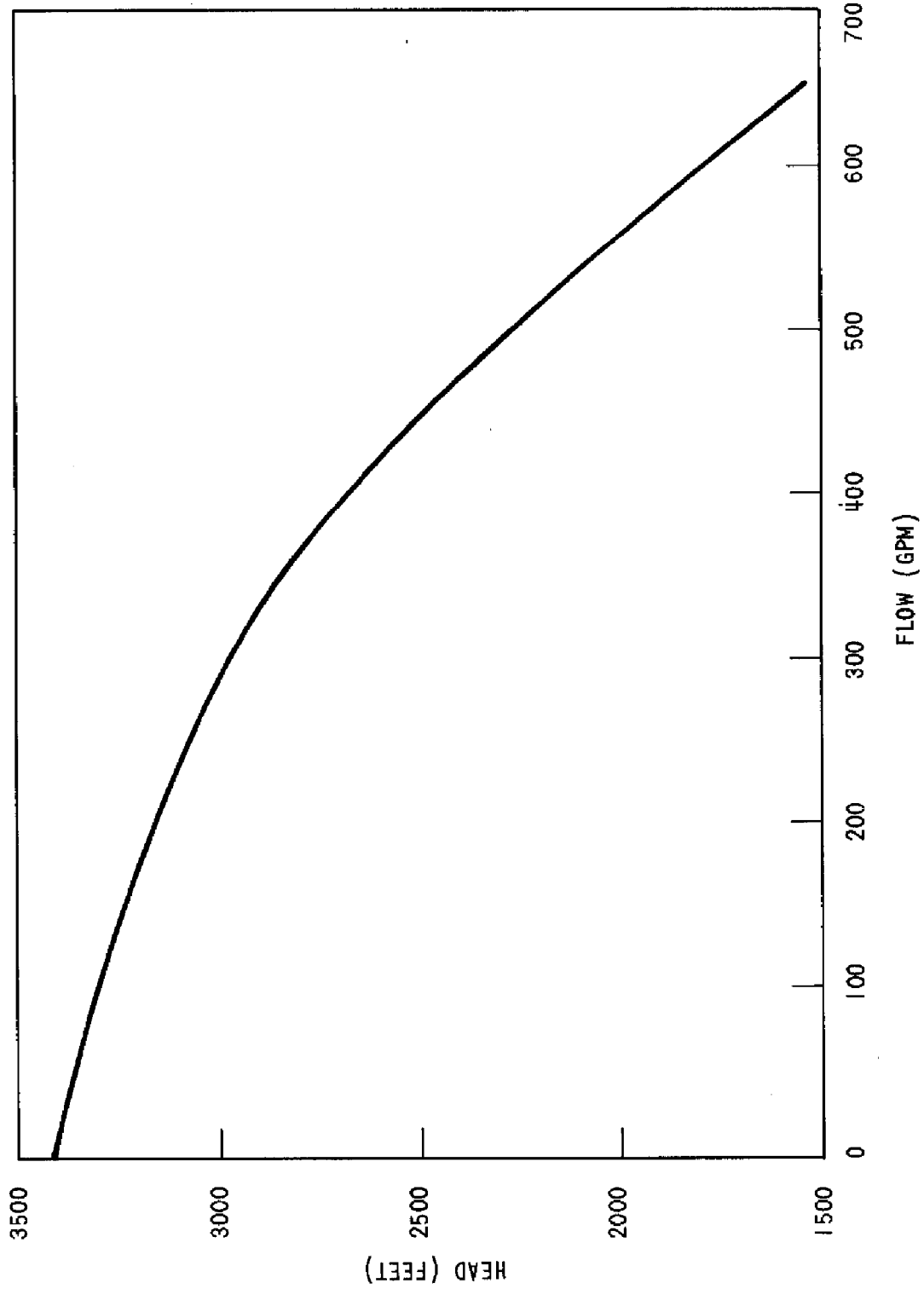

Figure 6-136. Safety Injection/Residual Heat Removal System Process Flow Diagram

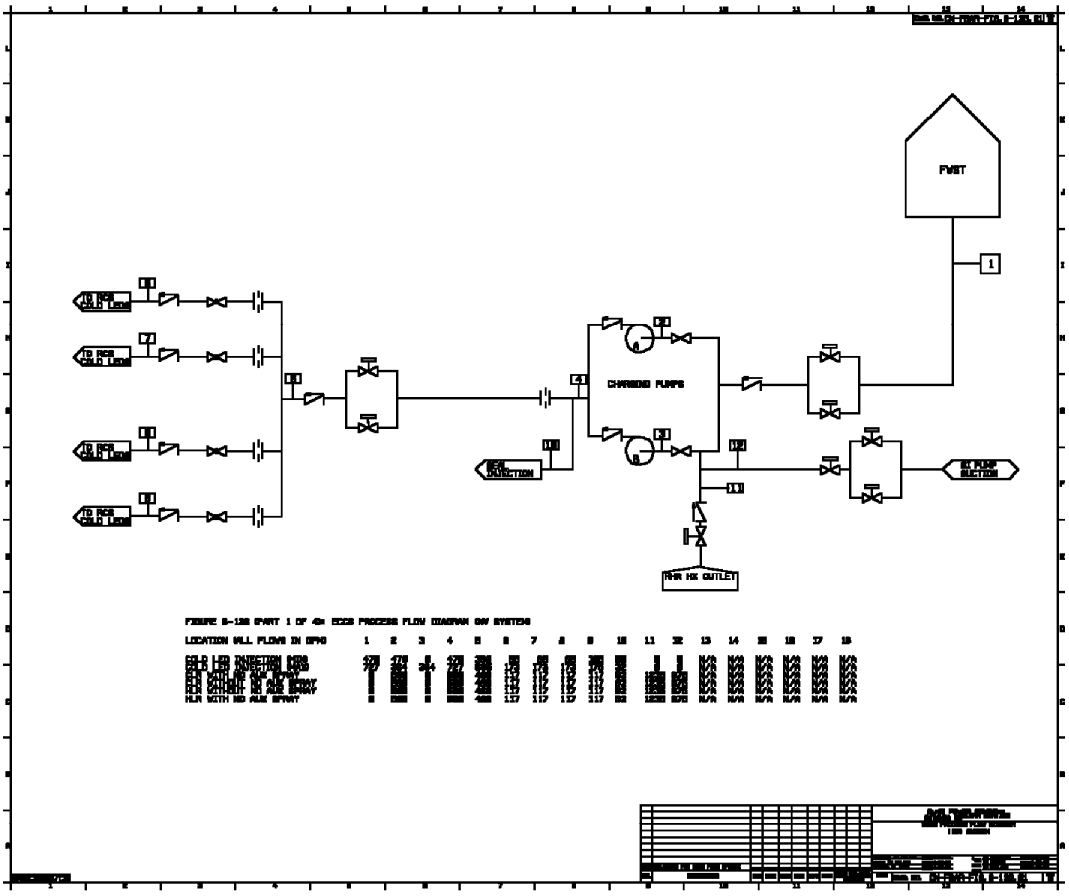

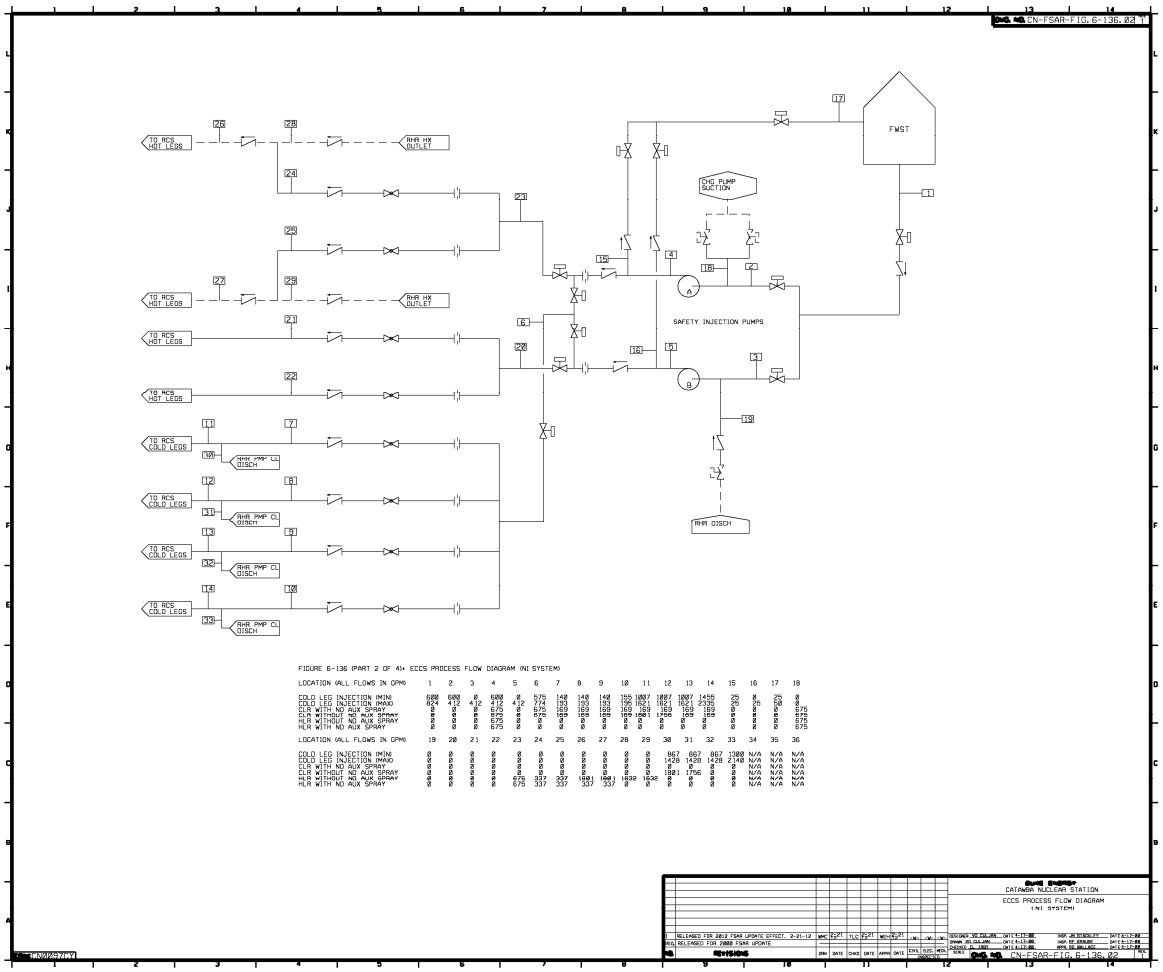

FIGURE 6-136 (PART 2 OF 4)+ ECCS PROCESS FLOW DIAGRAM (NI SYSTEM)

LOCATION (ALL FLOWS IN GPM)	1	2	3	4	5	6	7	8	9	10	11	12	13	14	15	16	17	18
COLD LEG INJECTION (MIN)	688	688	0	688	0	575	148	148	148	165	1887	1887	1887	1455	25	0	25	0
COLD LEG INJECTION (MAX)	4424	4424	4424	4424	4424	574	1425	1425	1425	1906	1825	1887	1871	2430	25	25	25	0
CLR WITH NO AUX SPRAY	0	0	0	675	0	675	169	169	169	169	169	169	169	169	0	0	0	675
CLR WITHOUT NO AUX SPRAY	0	0	0	675	0	675	169	169	169	169	1961	1756	169	169	0	0	0	675
HLR WITHOUT NO AUX SPRAY	0	0	0	675	0	0	0	0	0	0	0	0	0	0	0	0	0	675
HLR WITH NO AUX SPRAY	0	0	0	675	0	0	0	0	0	0	0	0	0	0	0	0	0	675

LOCATION (ALL FLOWS IN GPM)	19	20	21	22	23	24	25	26	27	28	29	30	31	32	33	34	35	36
COLD LEG INJECTION (MIN)	0	0	0	0	0	0	0	0	0	0	0	0	867	867	867	1388	N/A	N/A	N/A
COLD LEG INJECTION (MAX)	0	0	0	0	0	0	0	0	0	0	0	0	1428	1428	1428	2148	N/A	N/A	N/A
CLR WITH NO AUX SPRAY	0	0	0	0	0	0	0	0	0	0	0	0	0	0	0	0	N/A	N/A	N/A
CLR WITHOUT NO AUX SPRAY	0	0	0	0	0	0	0	0	0	0	0	0	1961	1756	0	0	N/A	N/A	N/A
HLR WITHOUT NO AUX SPRAY	0	0	0	0	675	337	337	1687	1687	1592	1638	0	0	0	0	0	N/A	N/A	N/A
HLR WITH NO AUX SPRAY	0	0	0	0	675	337	337	337	337	0	0	0	0	0	0	0	N/A	N/A	N/A

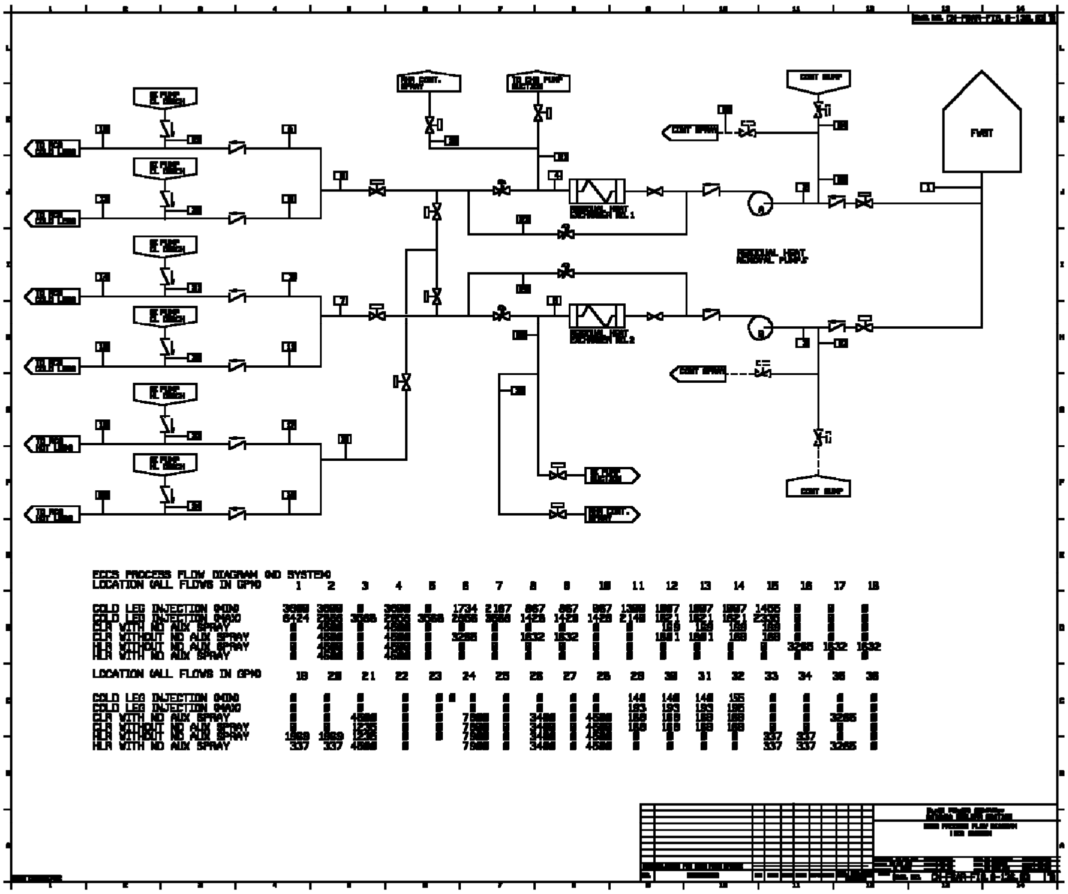
ECCS PROCESS FLOW DIAGRAM (ND SYSTEM)
LOCATION (ALL FLOWS IN GPM)
COLD LEG INJECTION (MIN)
COLD LEG INJECTION (MAX)
CLR WITH ND AUX SPRAY
CLR WITHOUT ND AUX SPRAY
HLR WITHOUT ND AUX SPRAY
HLR WITH ND AUX SPRAY
FWST
RESIDUAL HEAT REMOVAL PUMP
CONT SUMP
CONT SPRAY

NOTES TO Figure 6-136
ECCS Process Flow Diagram (Notes)

1. The cold leg injection mode of operation assumes single train ECCS operation at minimum safeguards conditions, and two train ECCS operation at maximum safeguards conditions. Minimum injection flow rates are representqative of three NV/NI lines at the minimum of the flow balance TAC windows and the single NV/NI line (attached to a broken loop) at the maximum of the flow balance TAC windows. Maximum injection flow rates are representative of all NV/NI lines at the maximum of the flow balance TAC windows.
2. Maximum water temperatures are 100°F (at the FWST) and 150°F (at the ND HX outlet) for injection and recirculation modes, respectively. Reference RCS pressure for all ECCS modes is 0 psig.
3. For minimum cold leg injection and recirculation conditions, seal injection flow rates are maximum values, thereby reducing the cold leg injection flow. For maximum cold leg injection conditions, the seal injection flow rate is a conservative nominal value of 32 gpm, thereby maximizing the cold leg injection flow rates.
4. The recirculation modes of operation assume single train ECCS operation at runout conditions. Runout flow rates are 560 gpm, 675 gpm, and 4500 gpm for a single NV, NI, and ND pump, respectively. The NV and NI injection lines are assumed to be balanced at their maximum flow balance TAC values. ND injection lines are not required to be balanced, but are assumed to be balanced equally for illustrative purposes of this diagram. The same is true for NI hot leg injection lines.
5. All flow rates are either taken directly, or indirectly determined from calculation file DPC-1552.08-00-0109, Safety Injection Flows for Safety Analysis.

Figure 6-137. Ice Condenser

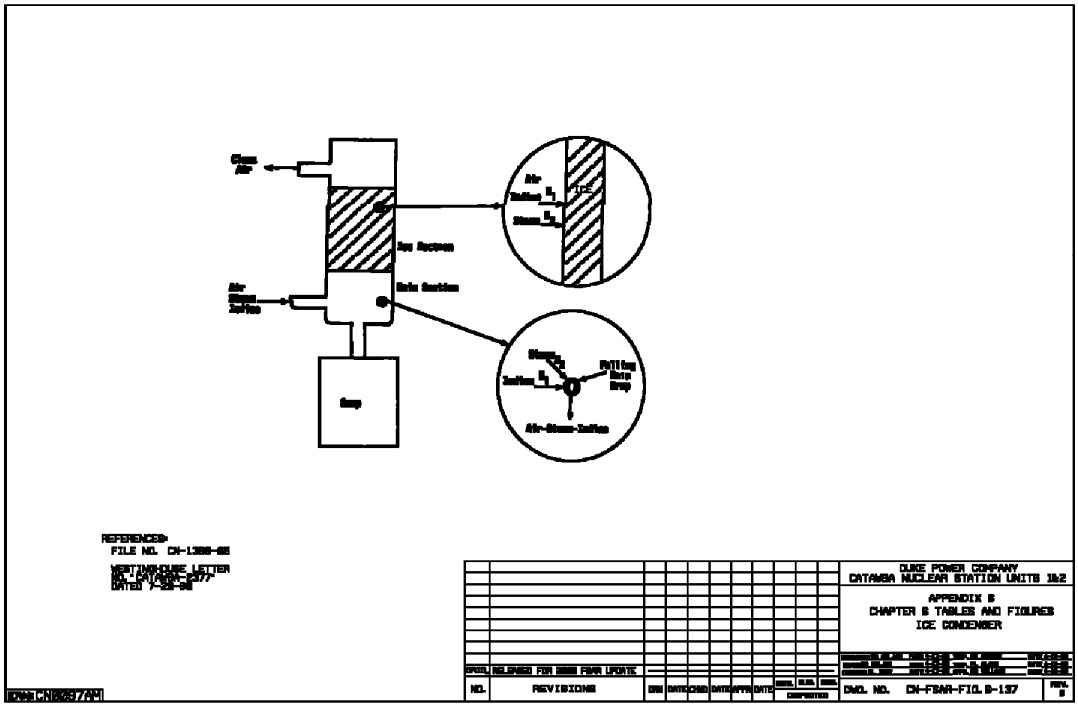

Figure 6-138. Isometric of Ice Condenser

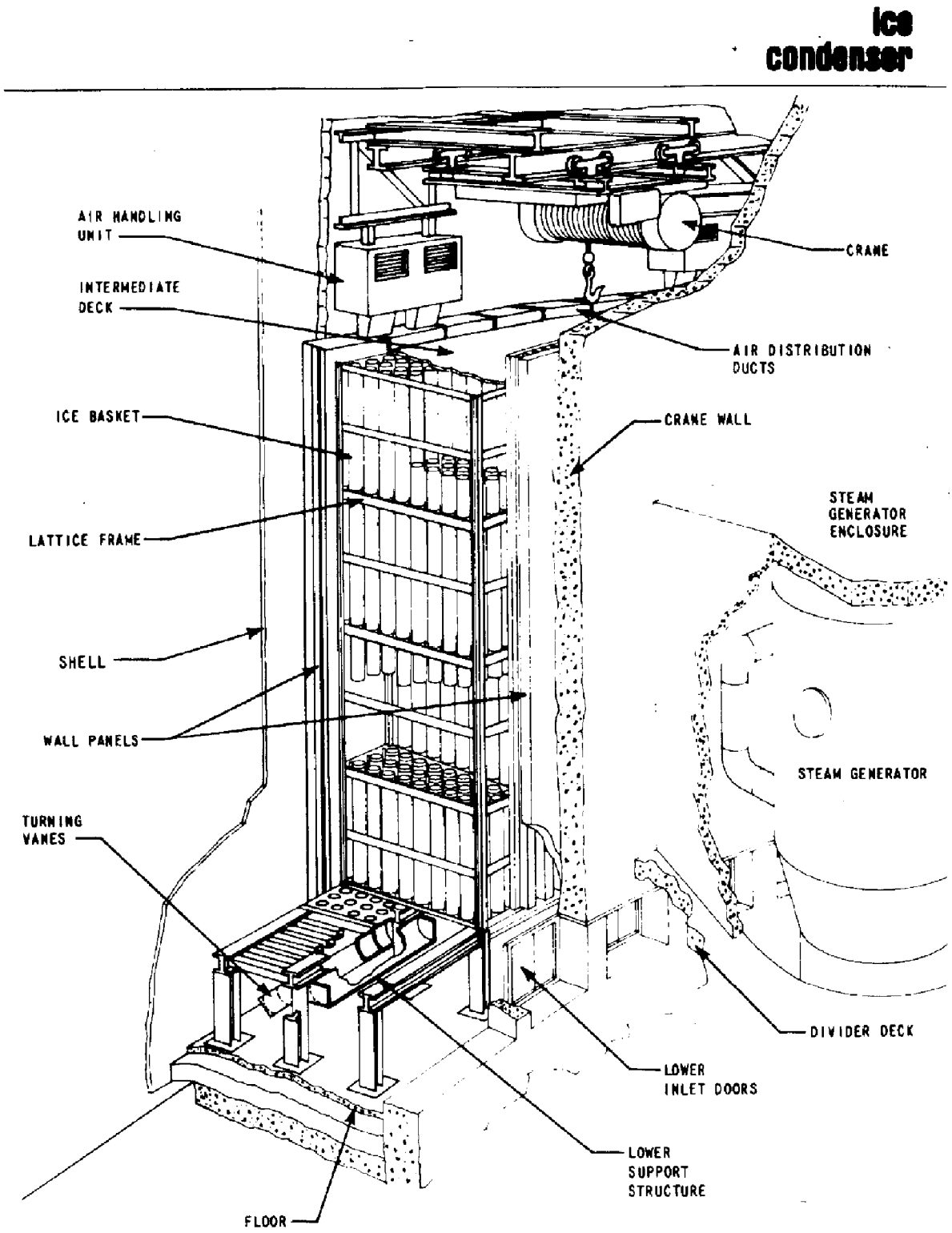

Figure 6-139. Floor Structure

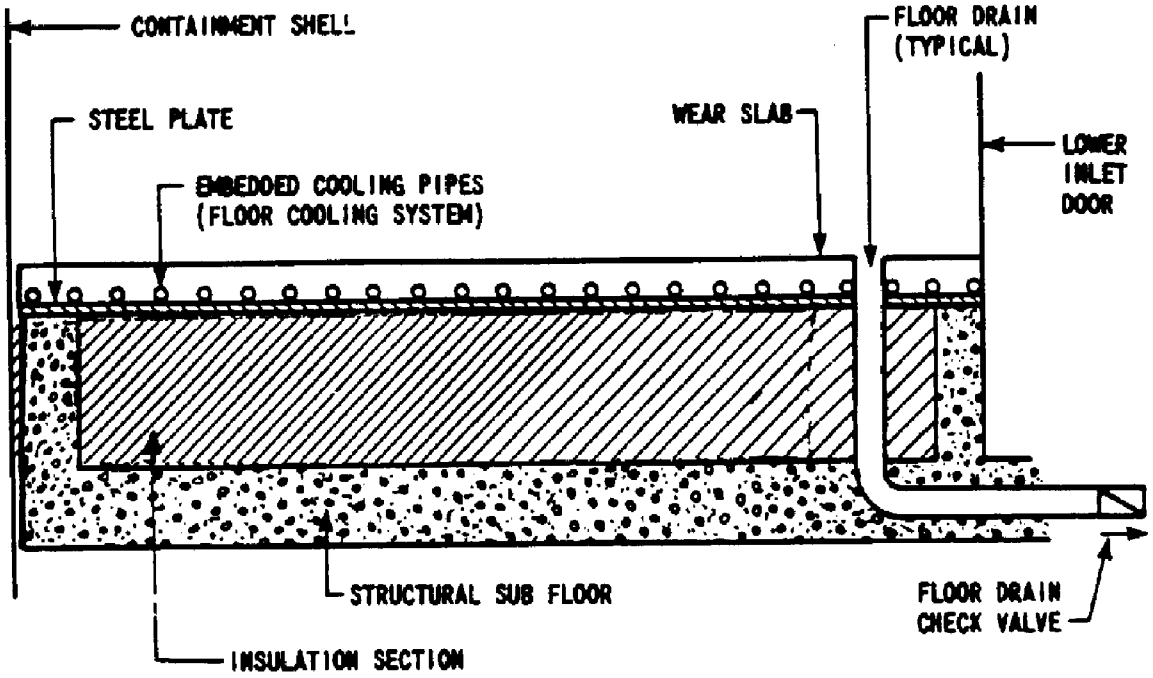

Figure 6-140. Wear Slab Top Surface Area Showing Typical Coolant Piping Layout

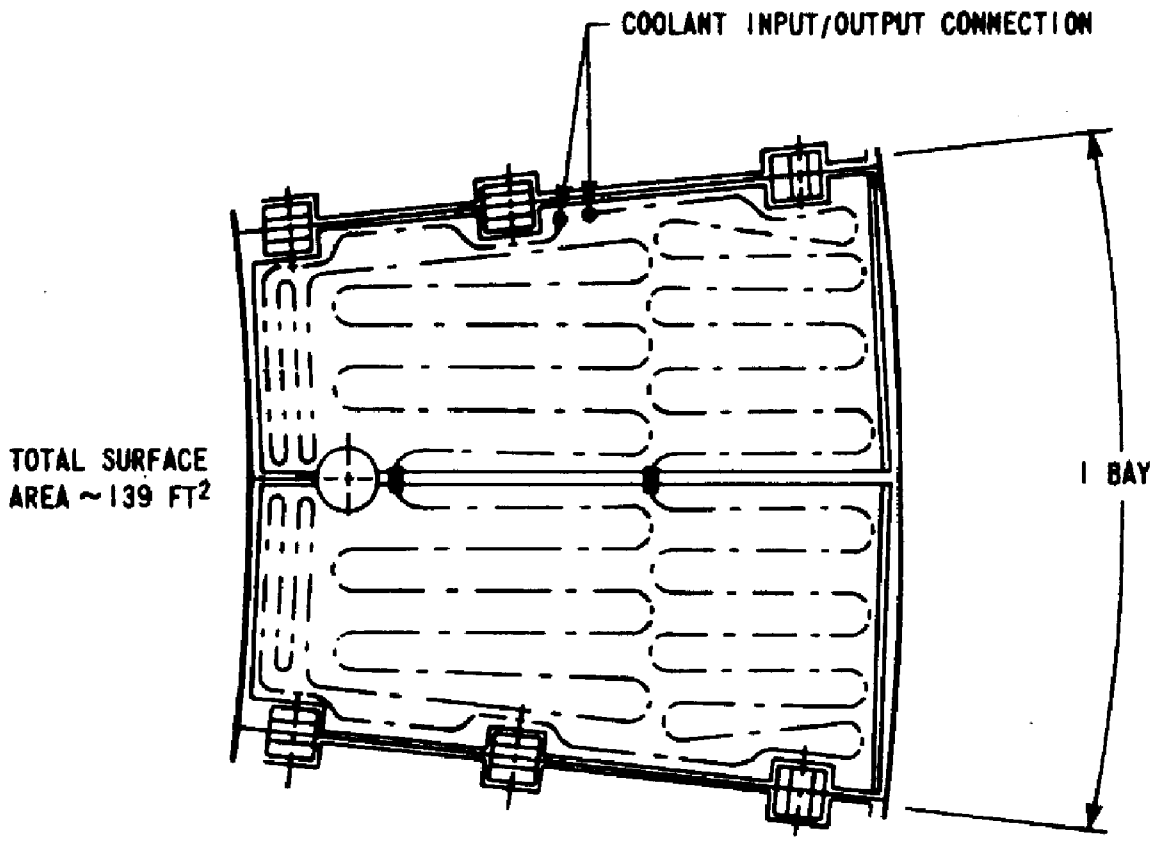

Figure 6-141. Lattice Frame Orientation

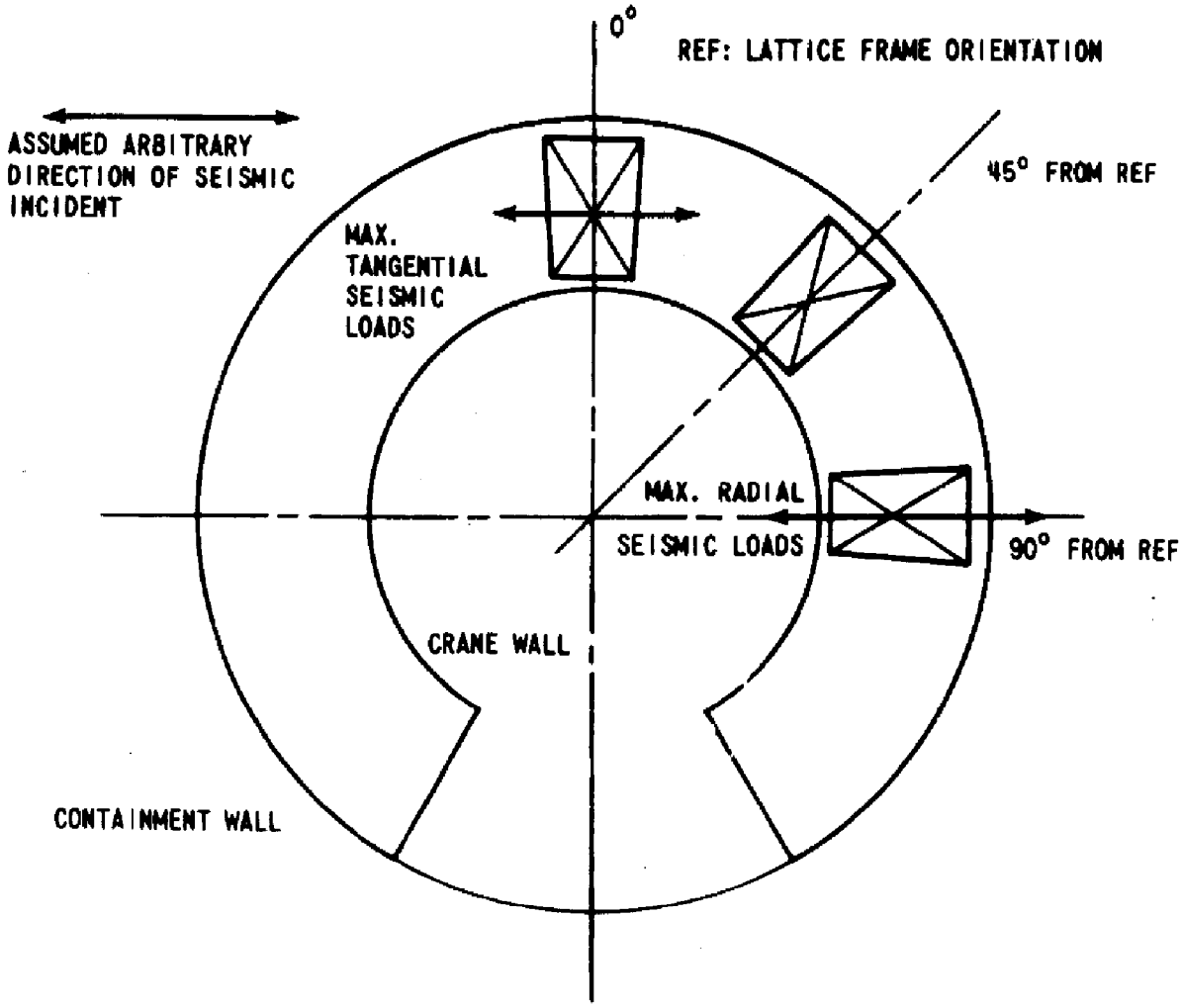

NOTES:

1. MAXIMUM TANGENTIAL AND RADIAL SEISMIC LOADS CANNOT OCCUR SIMULTANEOUSLY.
2. TANGENTIAL AND RADIAL SEISMIC LOADS 45 DEGREES FROM THE REFERENCE DIRECTION OF SEISMIC INPUT OCCUR SIMULTANEOUSLY AND THE MAGNITUDE IS THE AVERAGE OF MAXIMUM RADIAL AND MAXIMUM TANGENTIAL TIMES THE COSINE OF 45°, OR $\left(\frac{\text{RADIAL} + \text{TANGENTIAL}}{2}\right)$ .707.
3. HORIZONTAL AND VERTICAL SEISMIC LOADS CAN OCCUR HORIZONTALLY.
4. BLOWDOWN LOADS, TANGENTIAL, RADIAL AND VERTICAL CAN OCCUR SIMULTANEOUSLY. RADIAL BLOWDOWN LOADS ALWAYS OCCUR IN THE DIRECTION OF THE CONTAINMENT WALL.

* In an individual lattice frame.

Figure 6-142. Load Distribution For Tangential Seismic And Blowdown Loads In Analytical Model

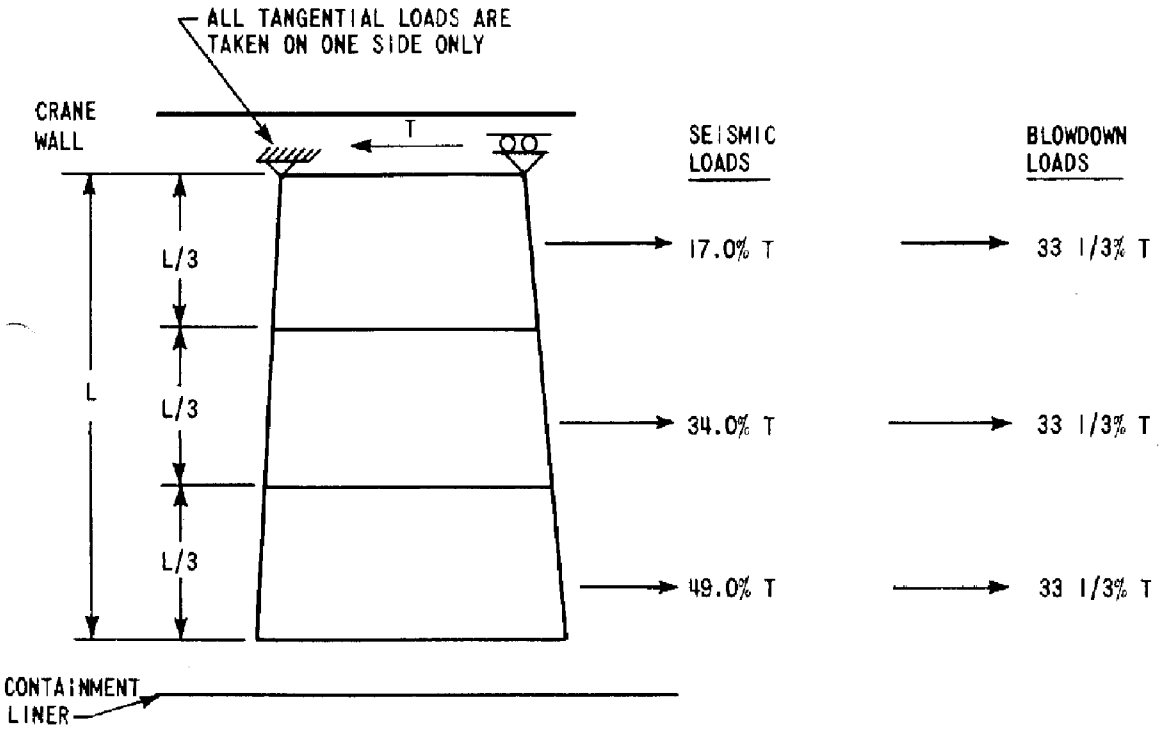

Figure 6-143. Lattice Frame

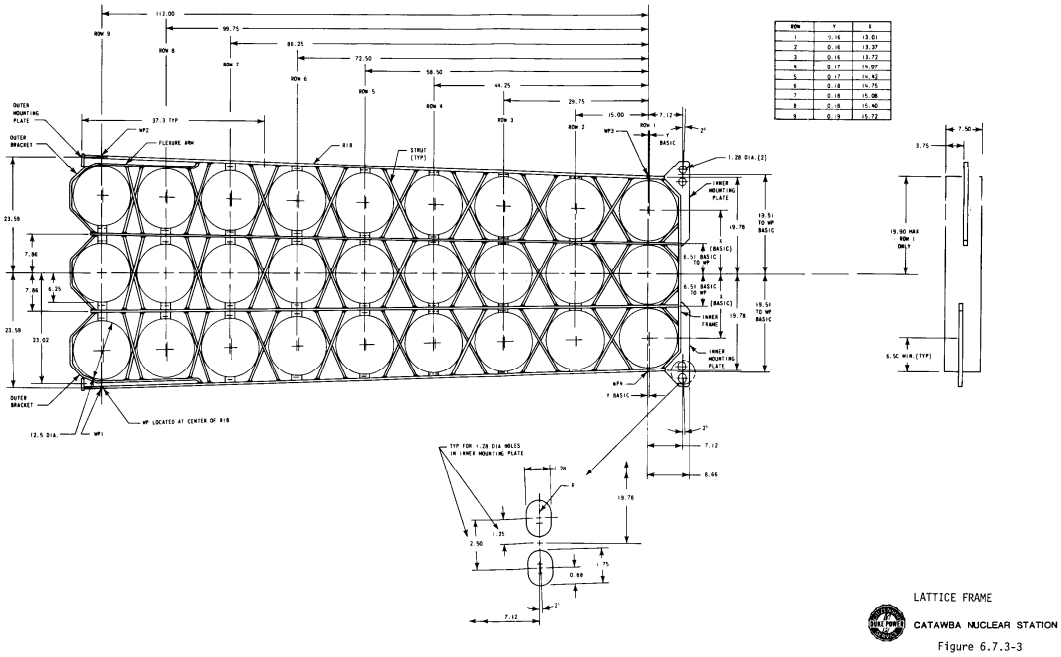

Figure 6-144. Lattice Frame Analysis Model

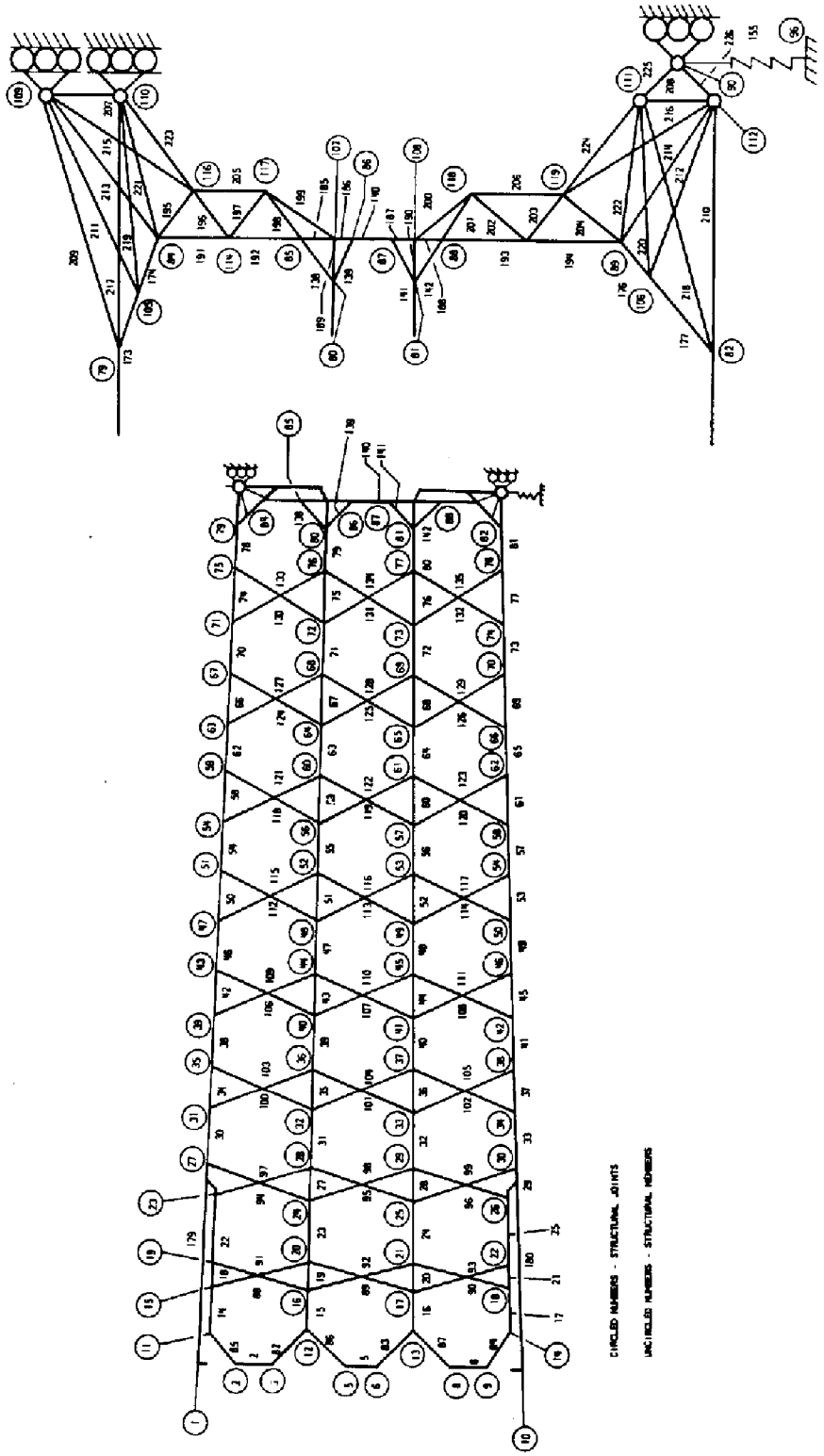

Figure 6-145. Typical Bottom Ice Basket Assembly

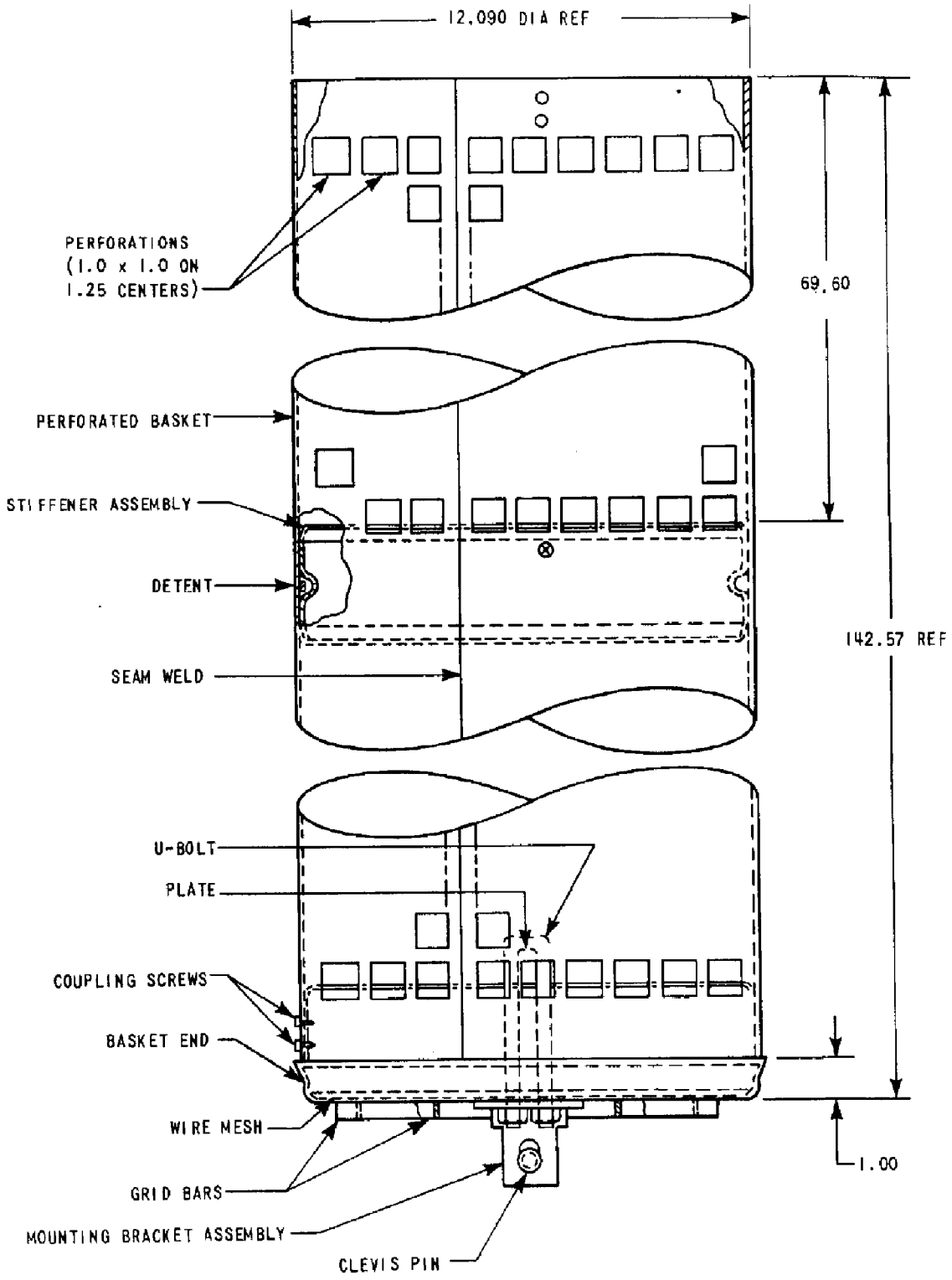

Figure 6-146. Combinations of Concentric Axial Load and Distribution Load

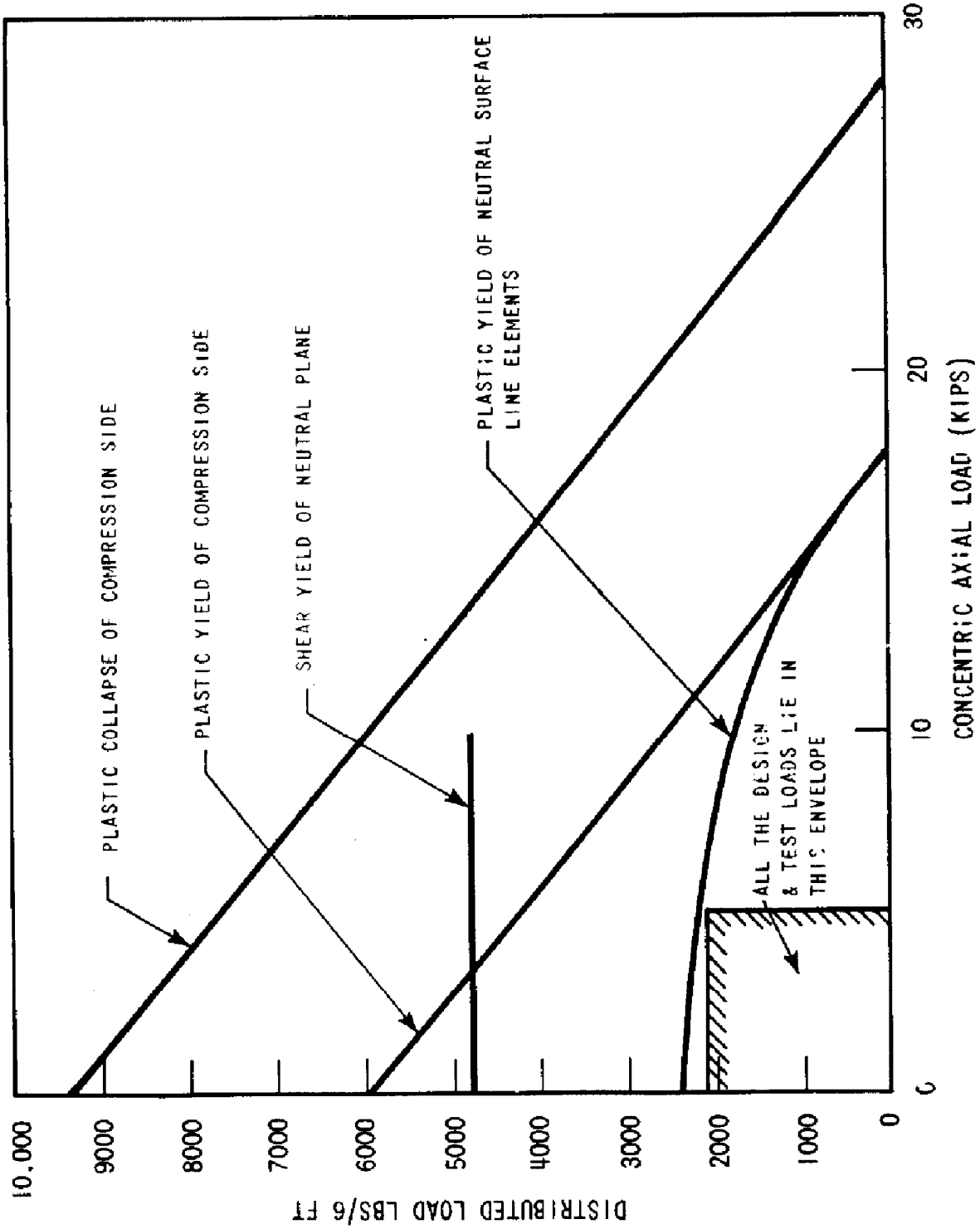

Figure 6-147. Crane Assembly

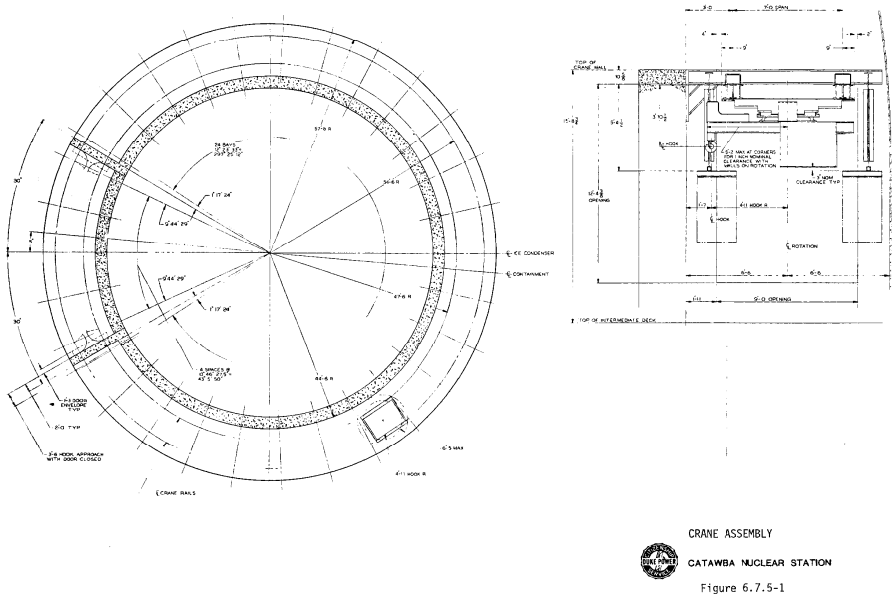

Figure 6-148. Crane Rail Assembly

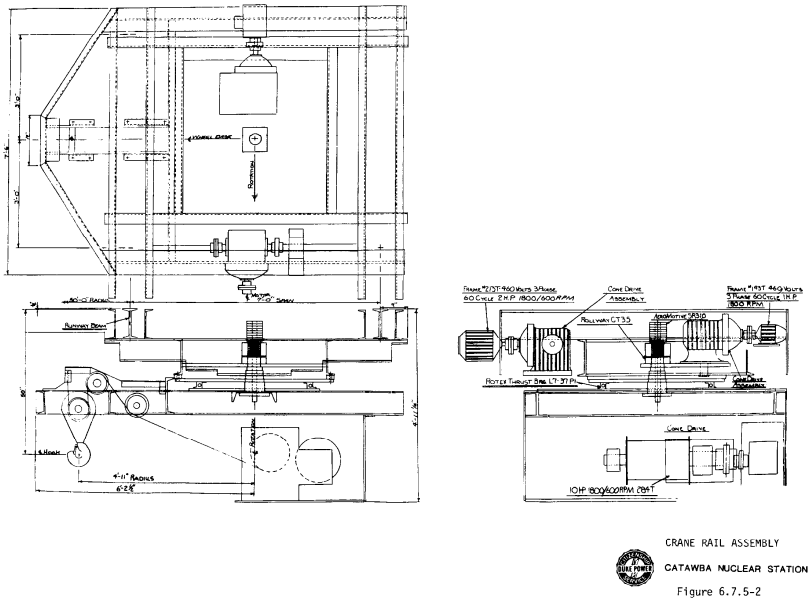

Figure 6-149. Refrigerant Cycle Diagram

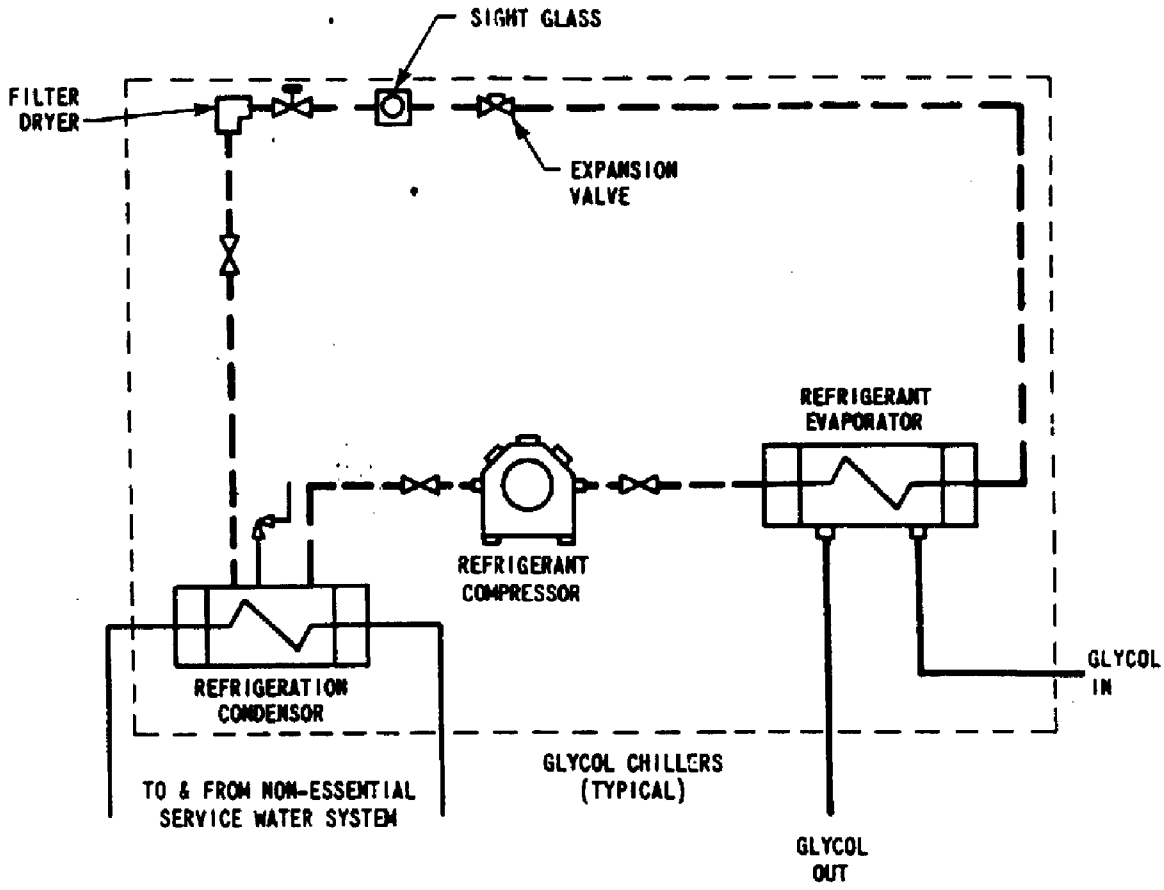

Figure 6-150. Glycol Cycle to Each Containment

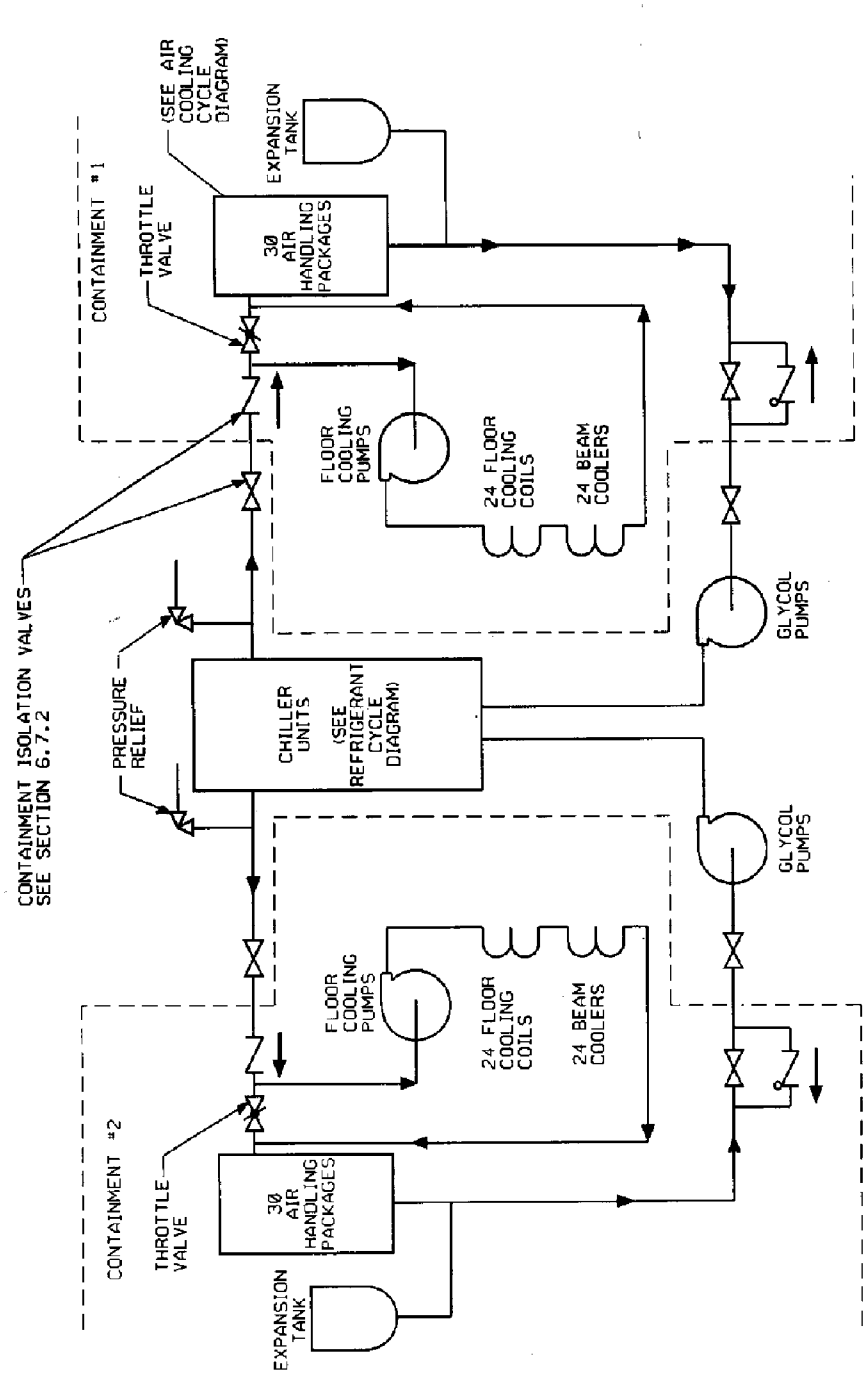

Figure 6-151. Schematic Flow Diagrams of Air Cooling Cycle

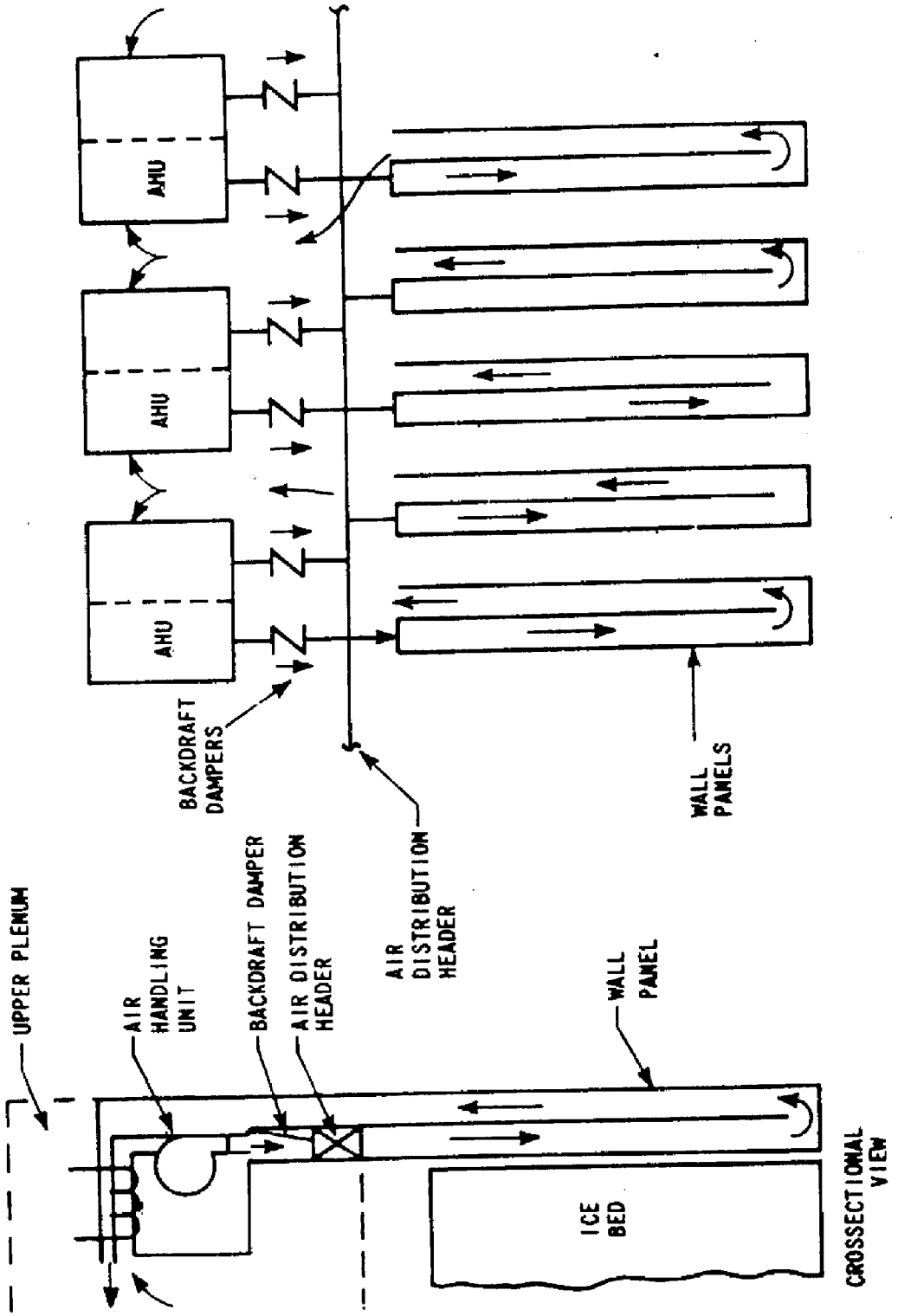

Figure 6-152. Air Handling Unit Support Structure

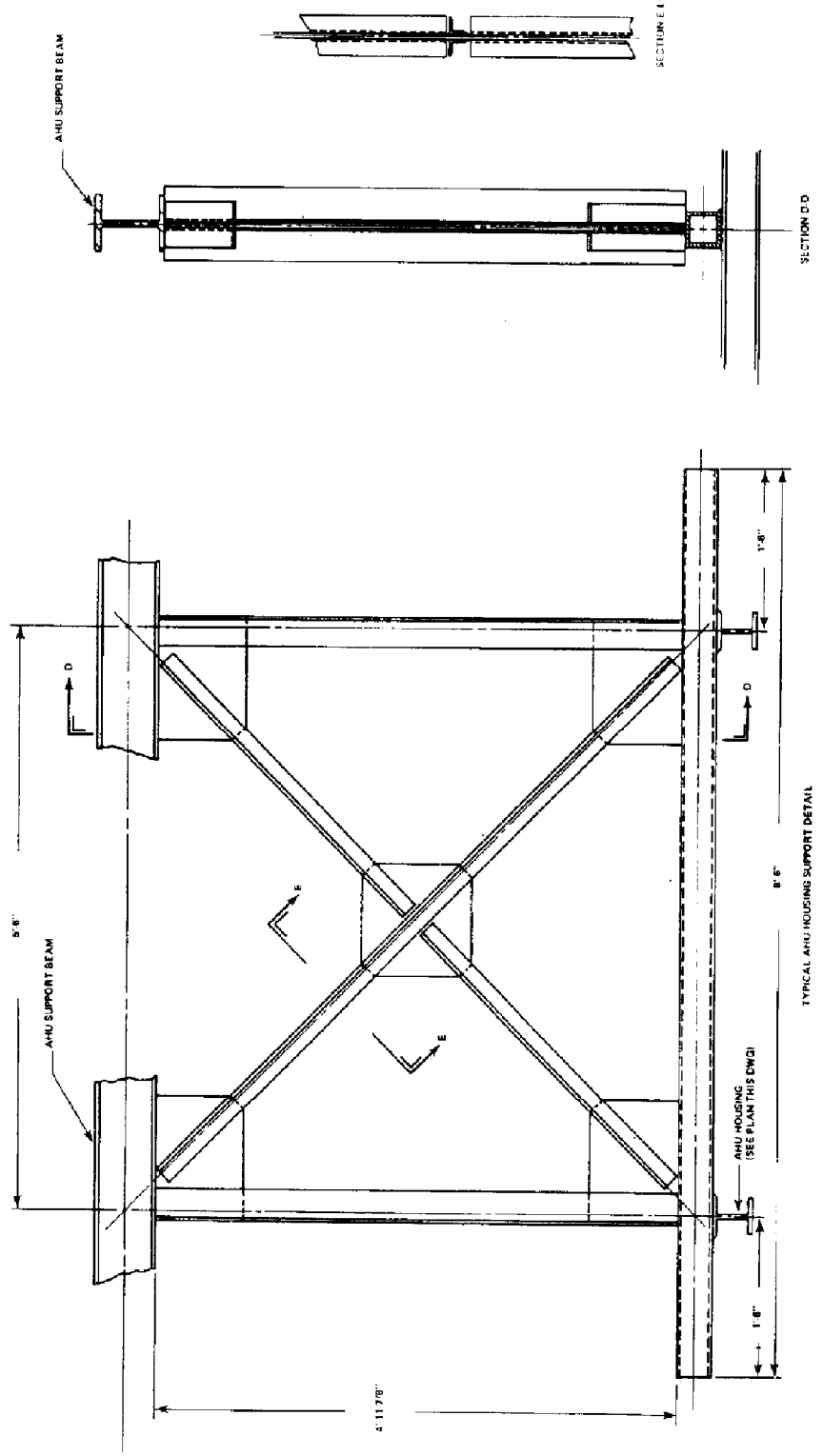

Figure 6-153. Deleted Per 2010 Update

Figure 6-154. Lower Inlet Door Assembly

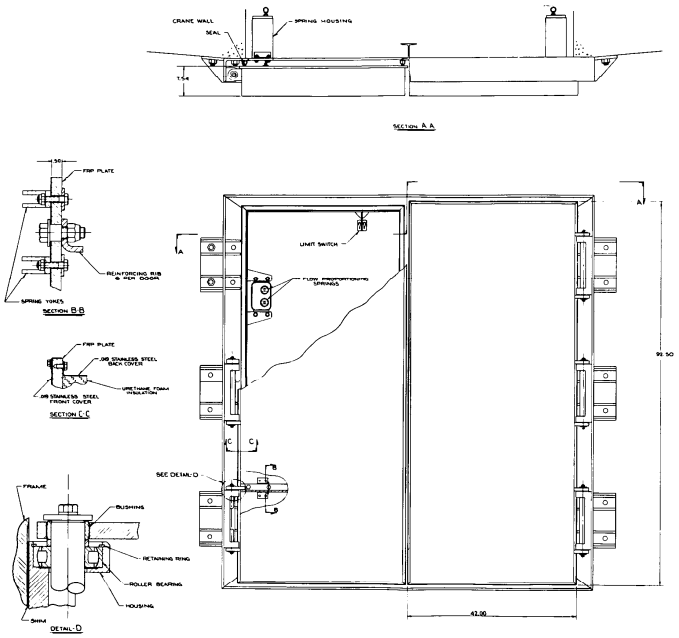

LOWER INLET DOOR ASSEMBLY
CATAWBA NUCLEAR STATION
Figure 6.7.8-2

Figure 6-155. Details of Lower Inlet Door Showing Hinge, Proportioning Mechanism Limit Switches and Seals

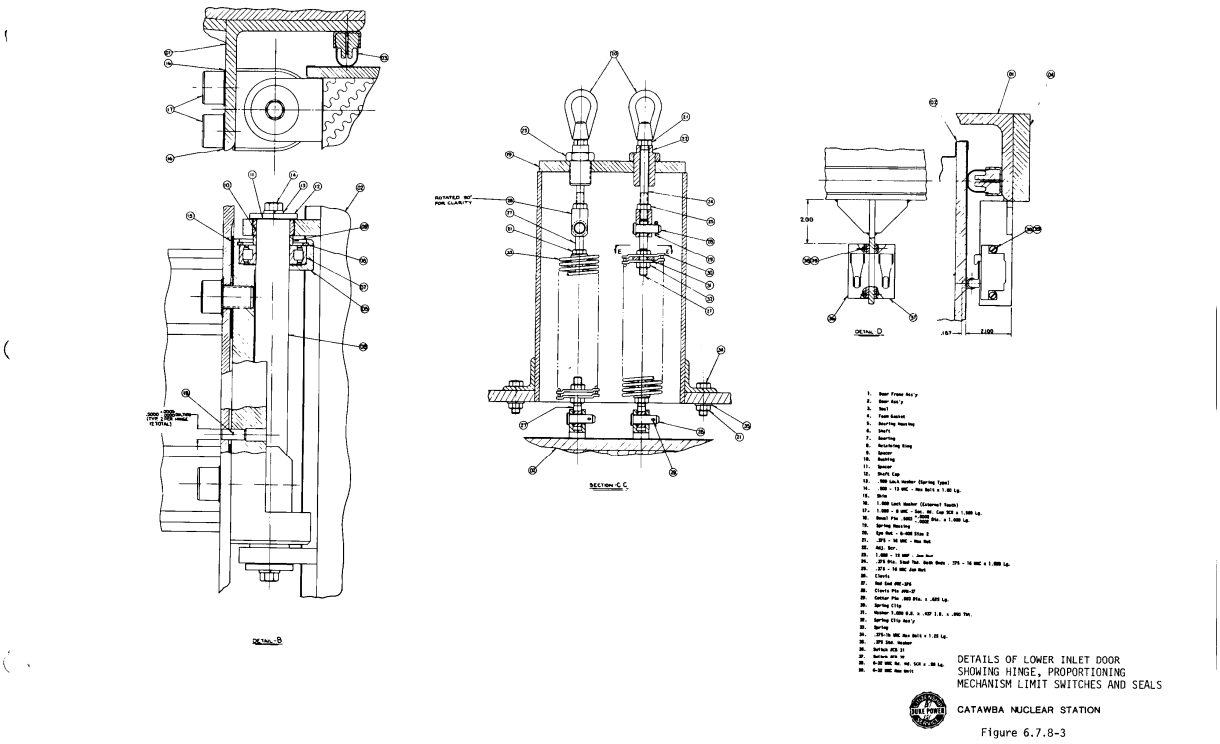

Figure 6-156. Inlet Door Frame Assembly

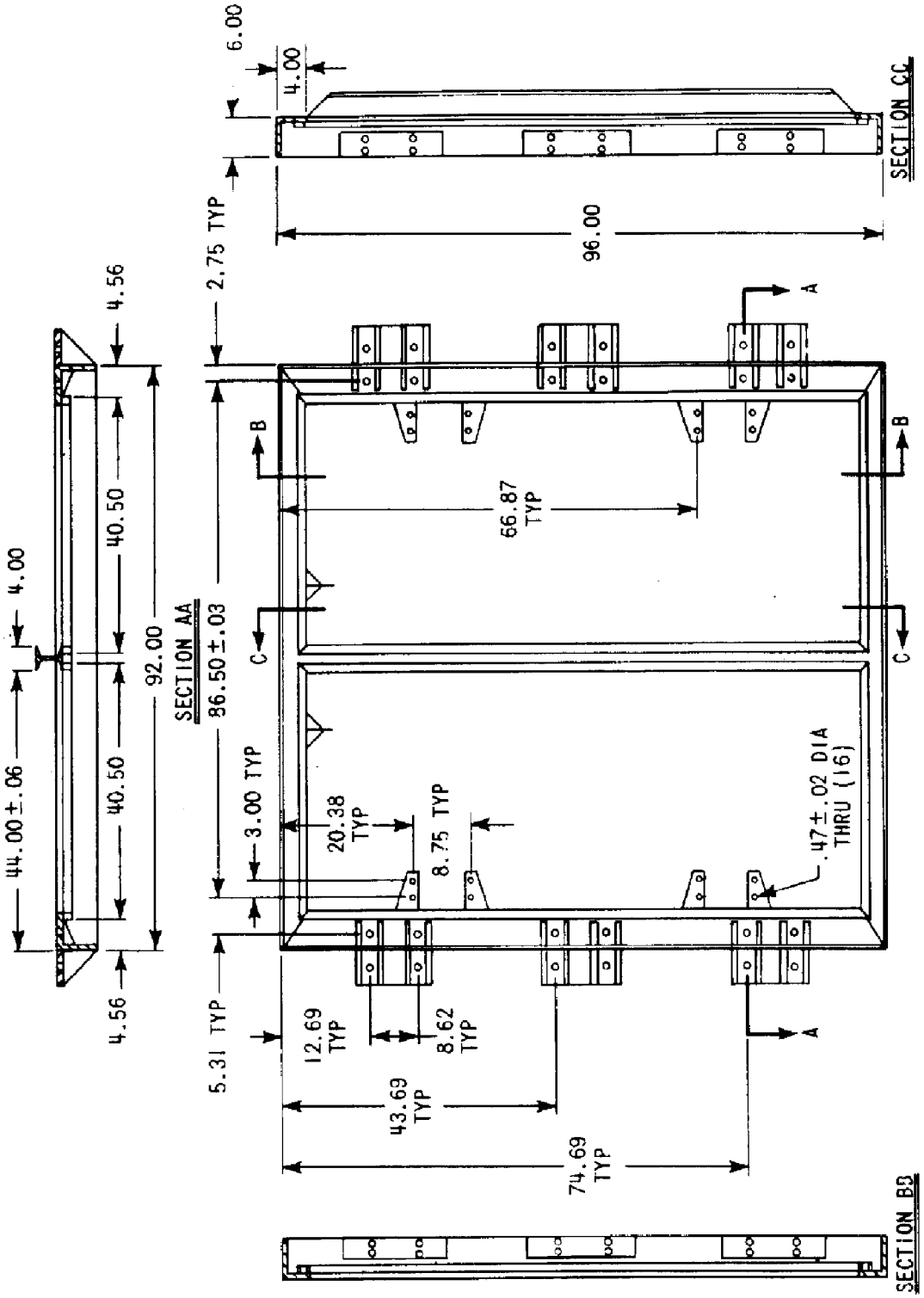

Figure 6-157. Inlet Door Panel Assembly

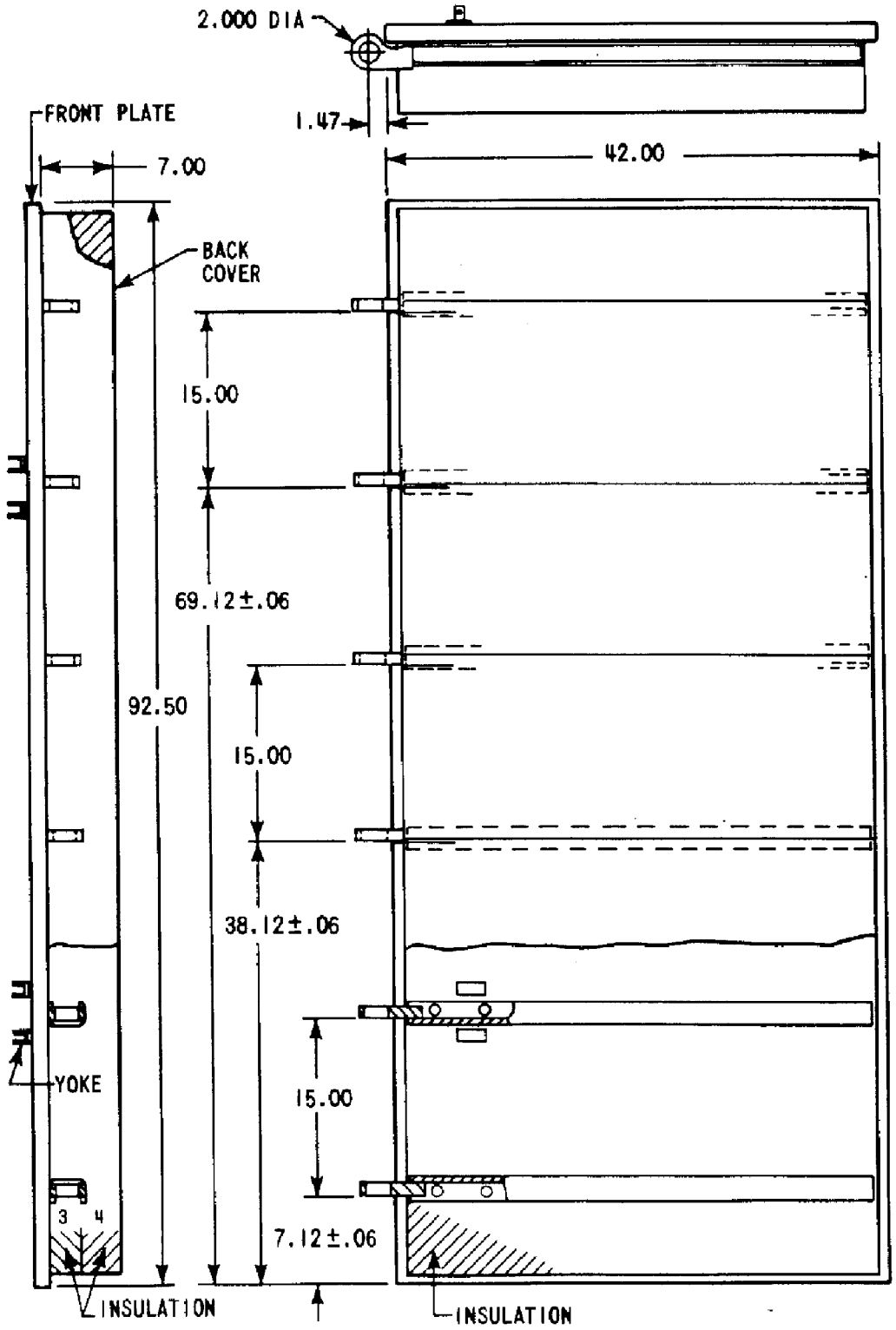

Figure 6-158. Lower Inlet Door Shock Absorber Assembly

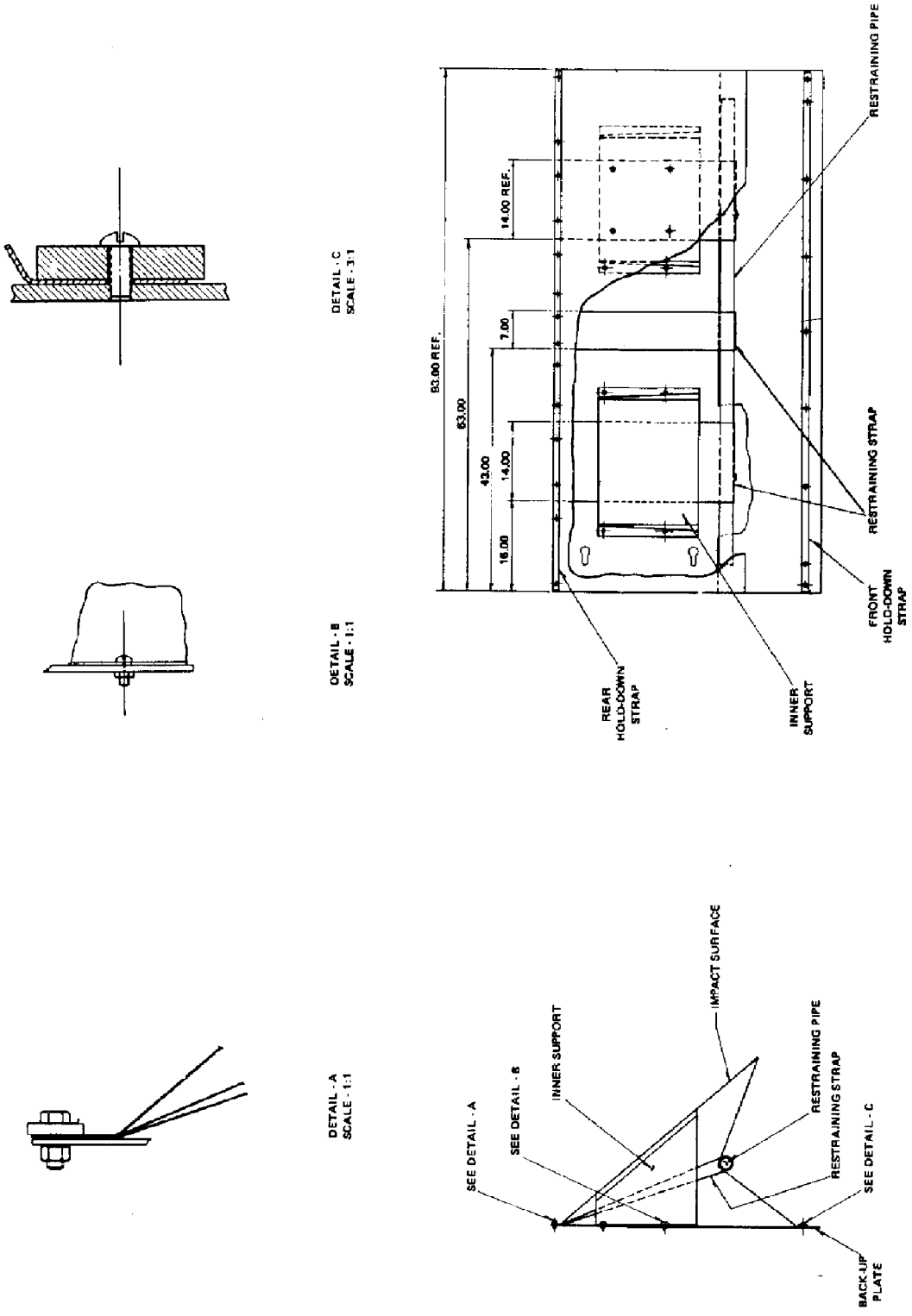

Figure 6-159. Four Loop Ice Condenser Lower Support Structure Conceptual Plan and Sections

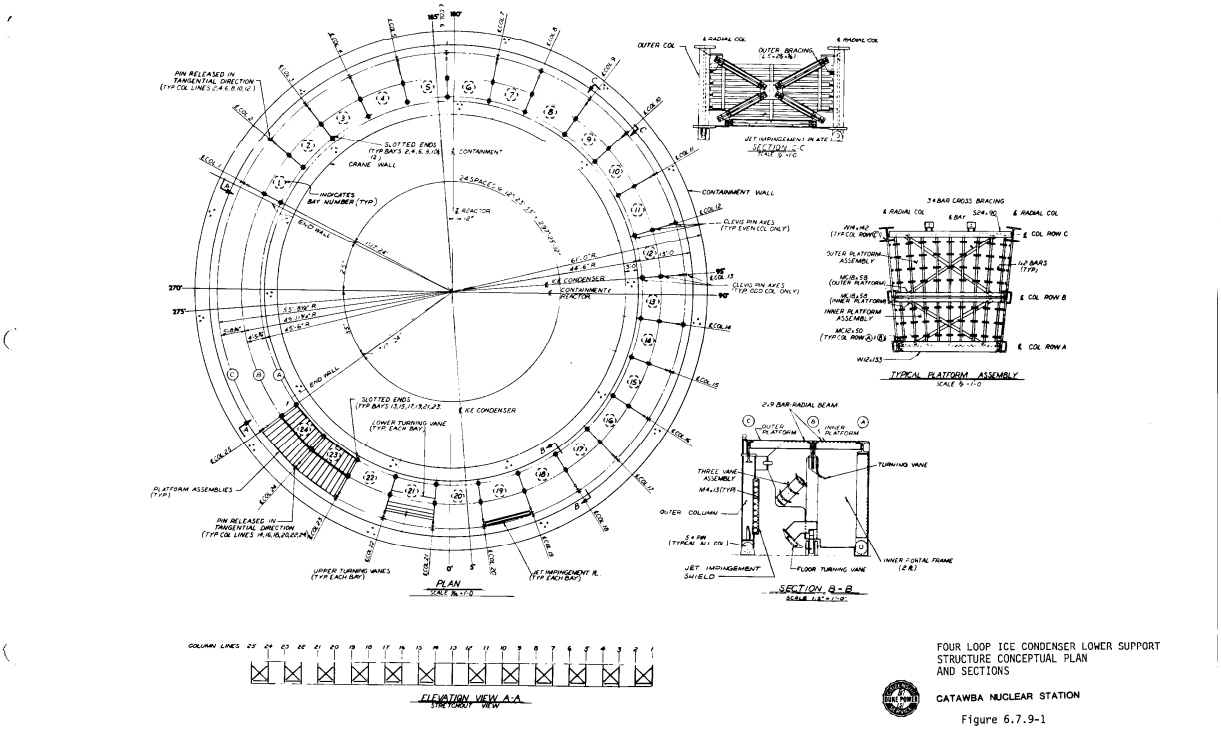

Figure 6-160. Four Loop Ice Condenser Lower Support Structure General Assembly

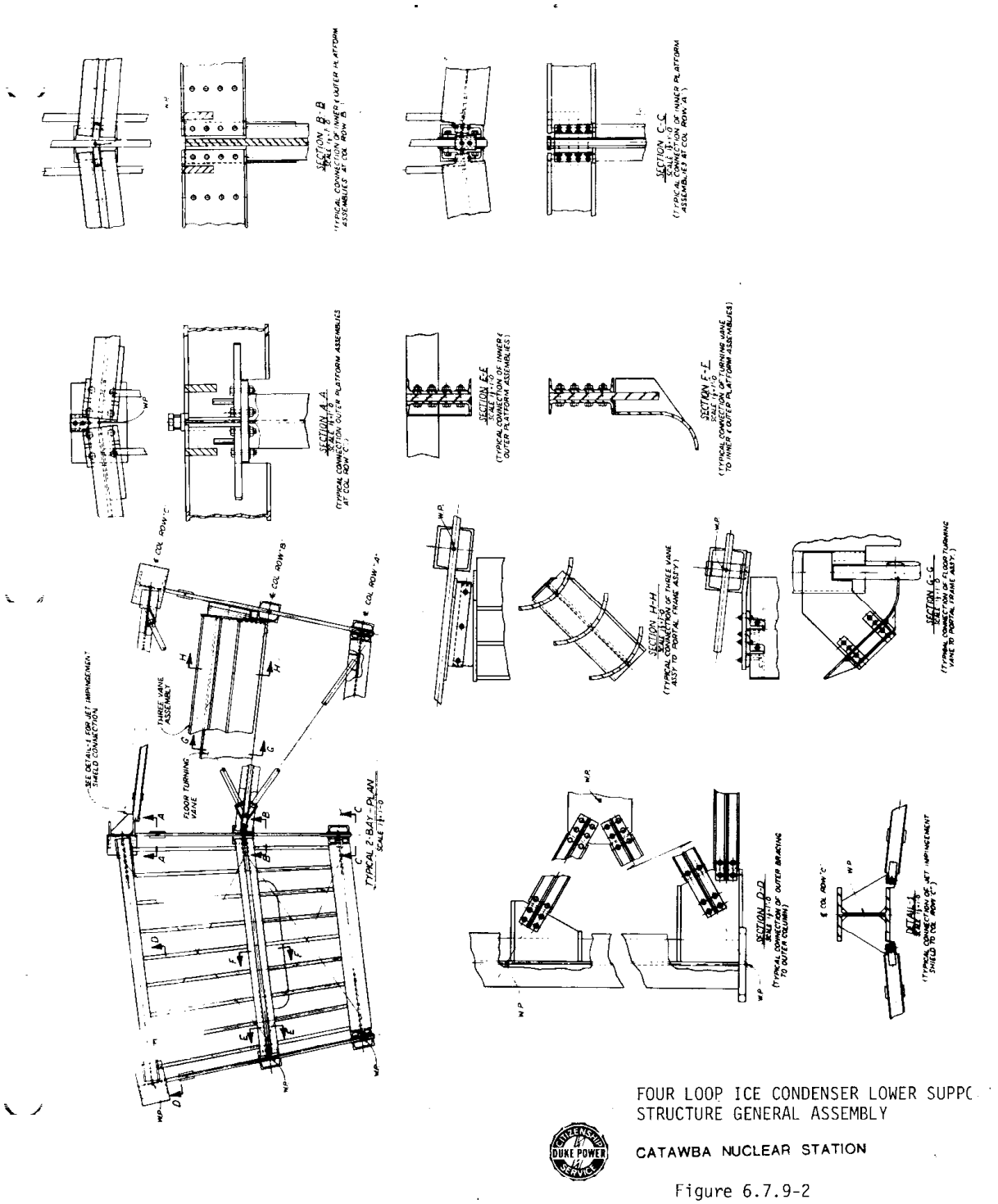

Figure 6-161. Ansys Model Assembly

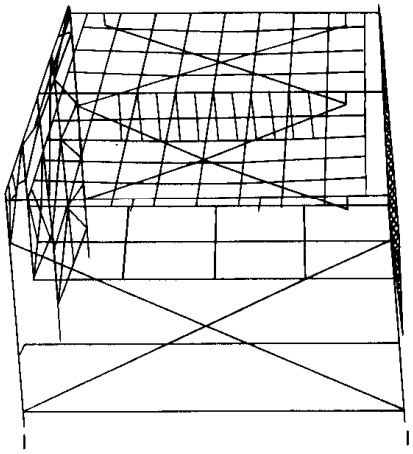

ANSYS MODEL ASSEMBLY

CATAWBA NUCLEAR STATION

Figure 6.7.9-3

Figure 6-162. Finite Element Model of Postal Frame

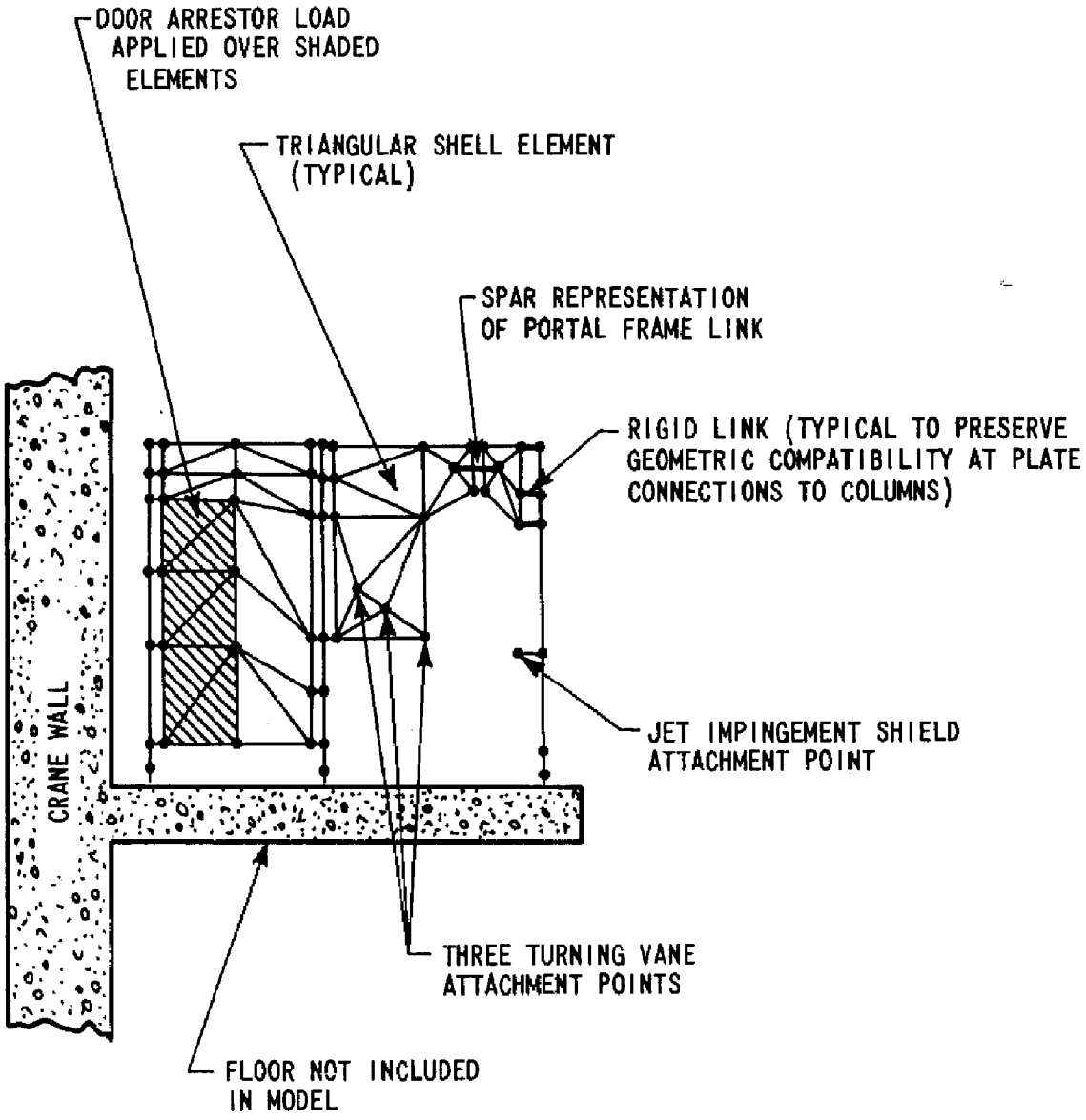

Figure 6-163. Schematic Diagram of Force Applied to Three Pier Lower Support Structure

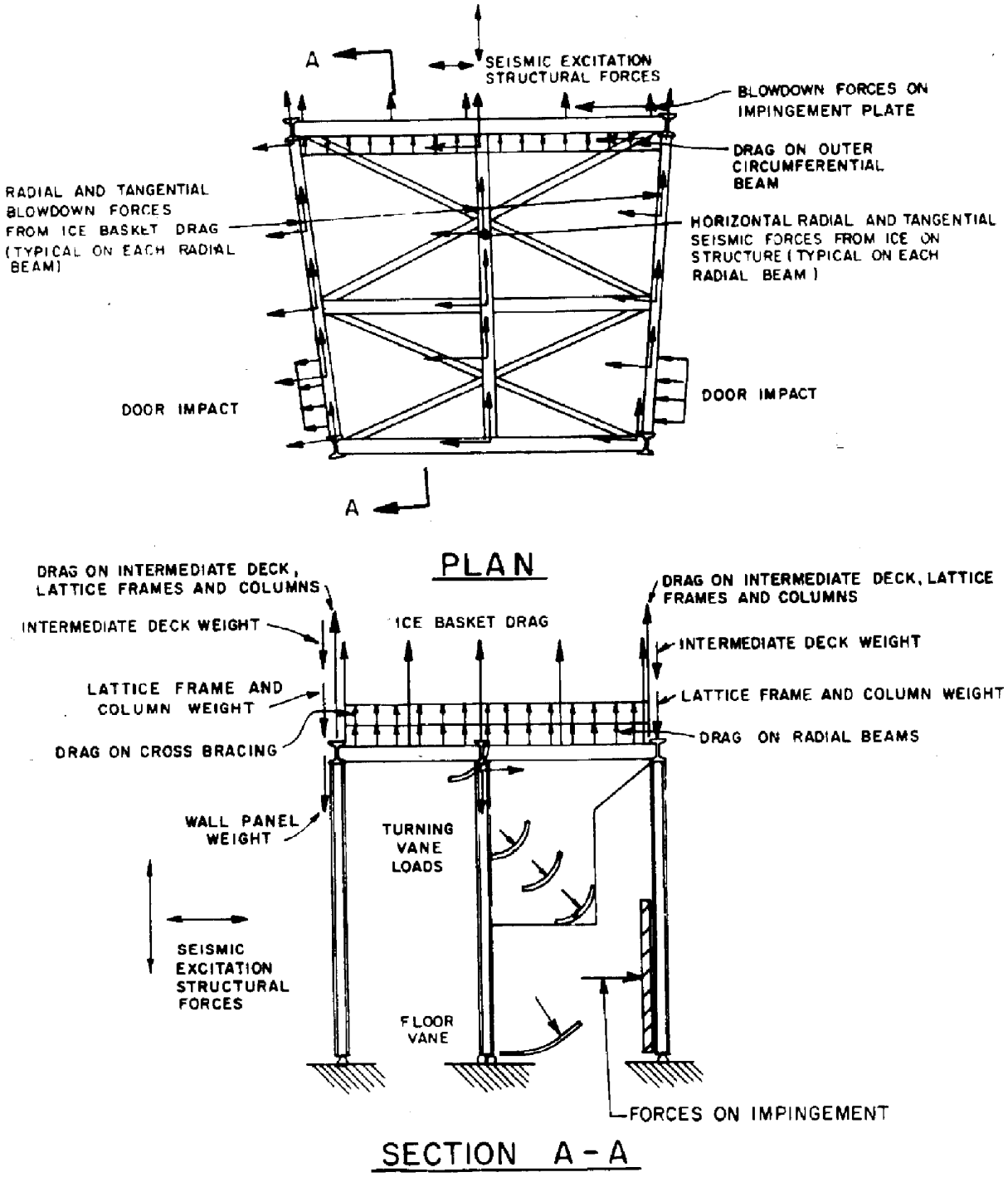

Figure 6-164. Force Transient Hot Leg Break

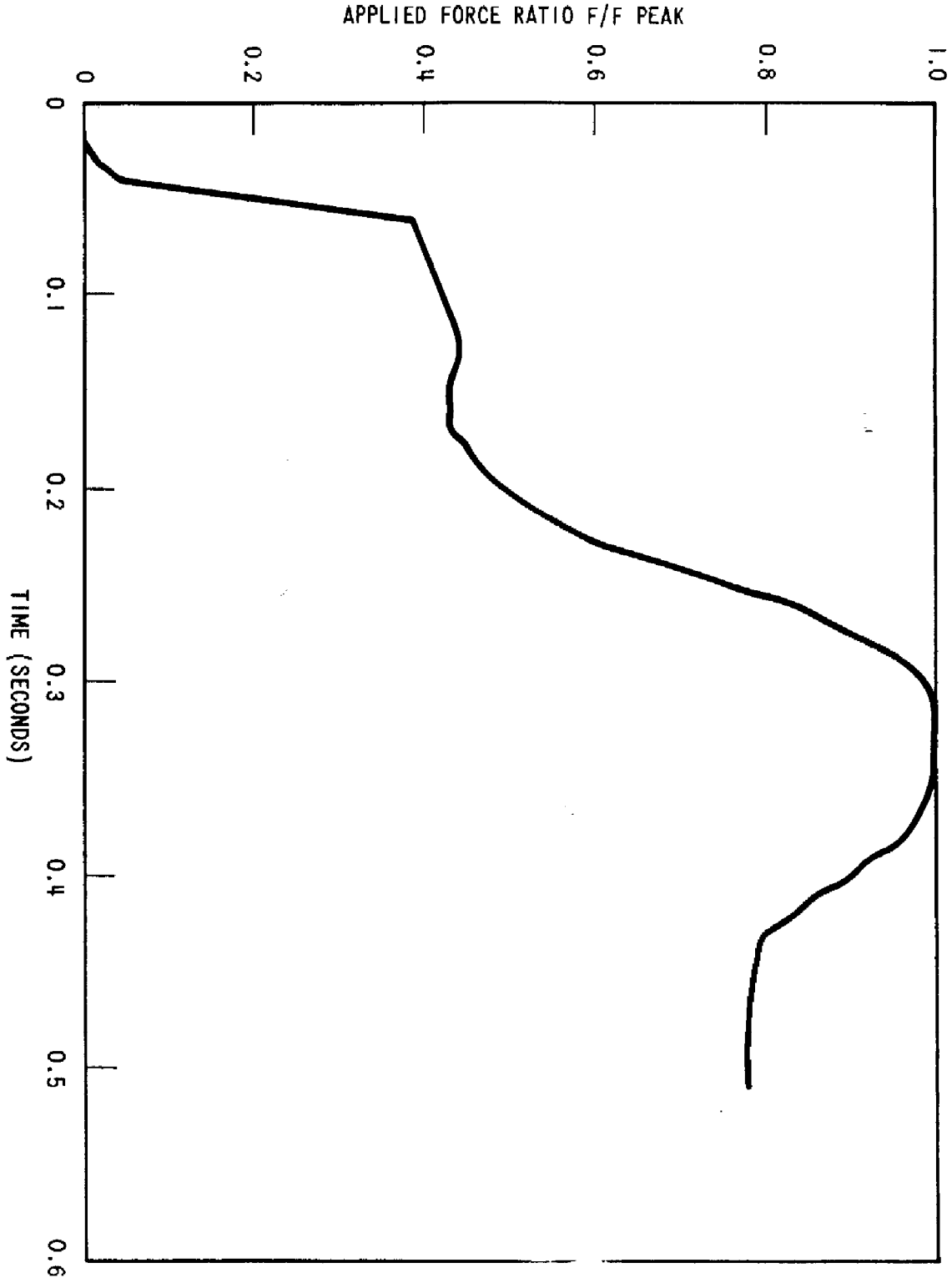

Figure 6-165. DLF Spectra Hot Leg Break Force Transient

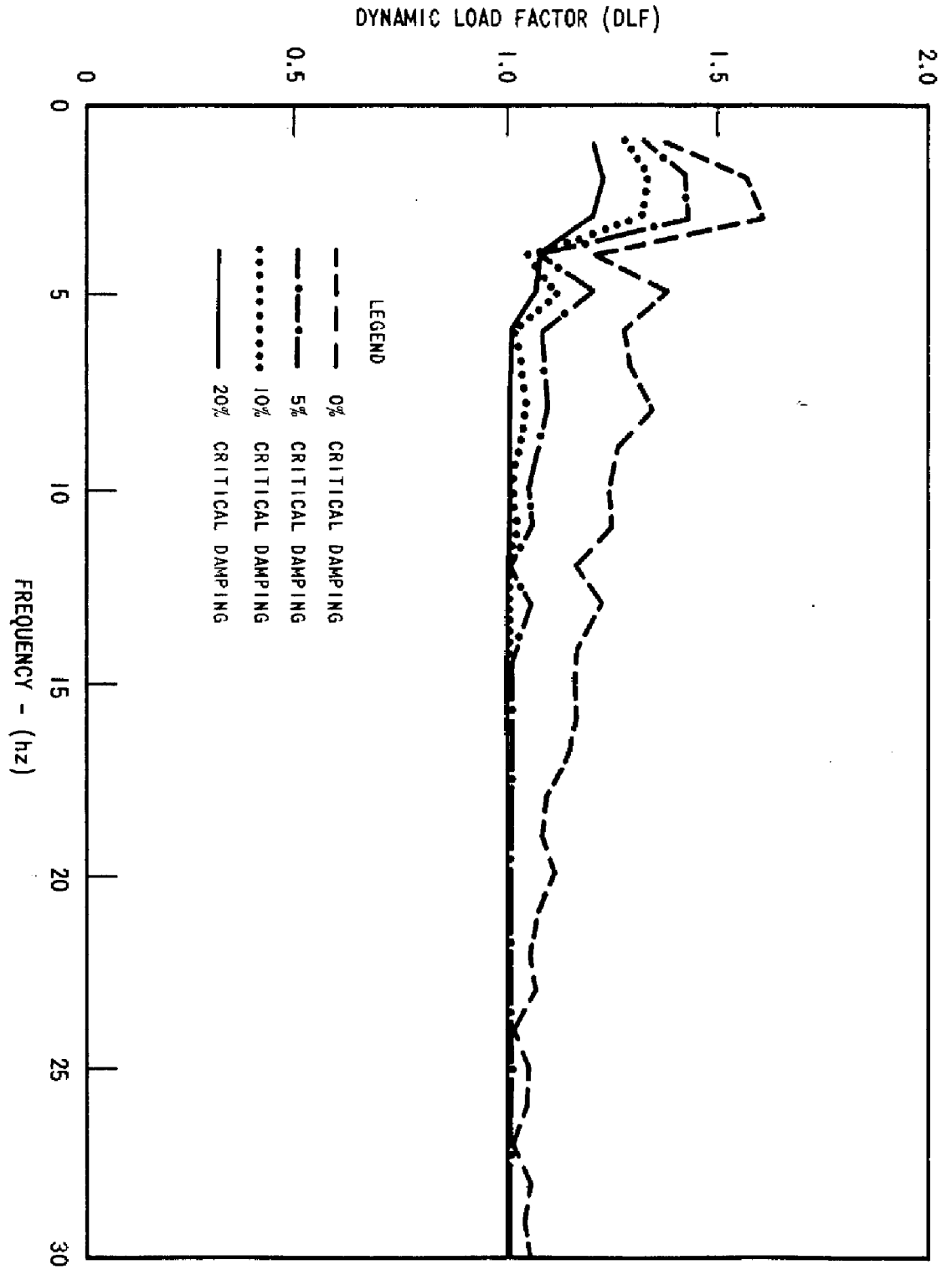

Figure 6-166. Top Deck Test Assembly

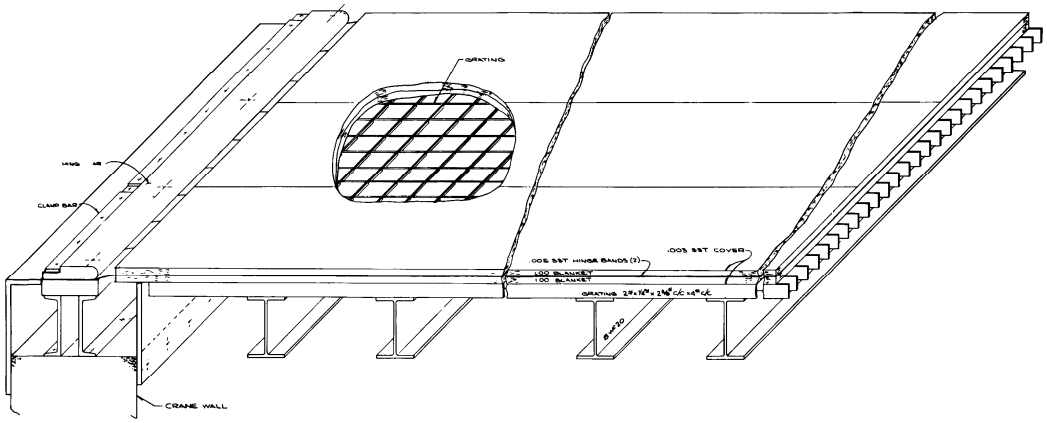

TOP DECK TEST ASSEMBLY
CATAWBA NUCLEAR STATION
Figure 6.7.10-1

Figure 6-167. Details of Top Deck Door Assembly

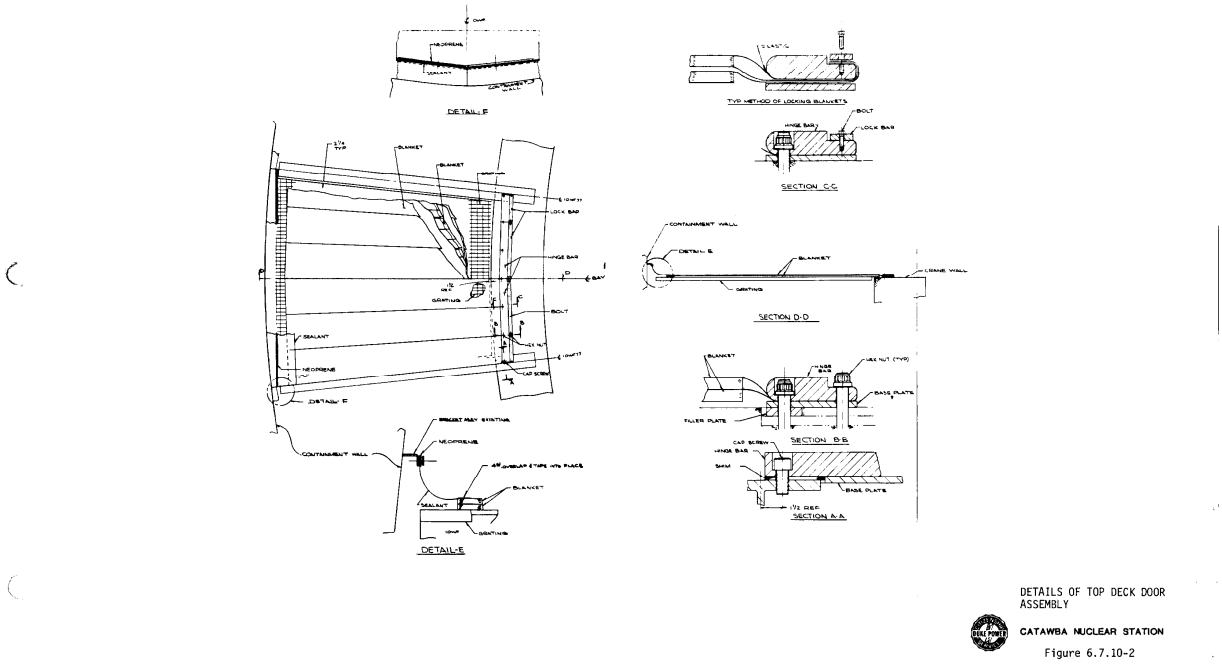

Figure 6-168. Intermediate Deck Door Assembly

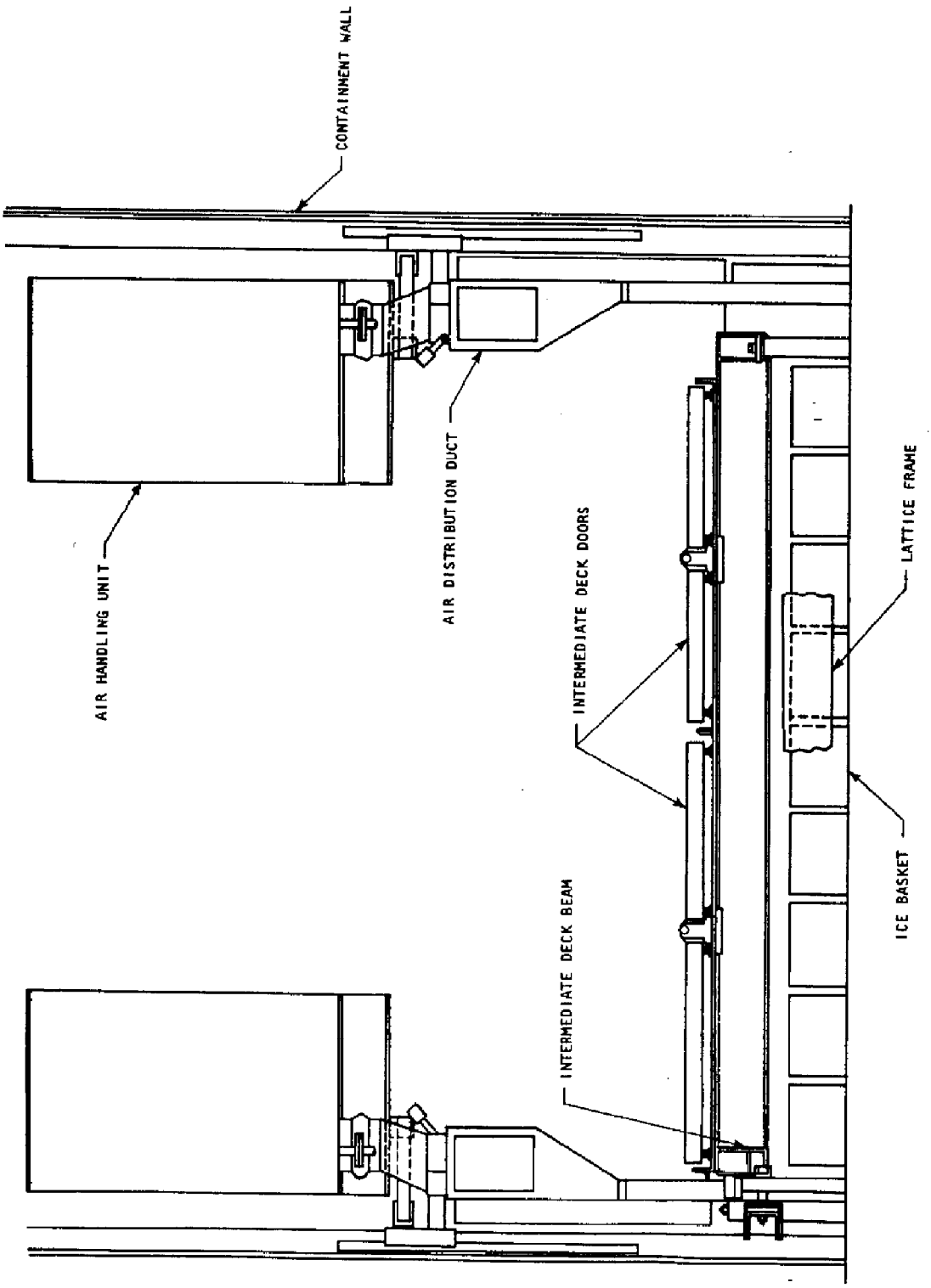

Figure 6-169. Air Distribution Duct

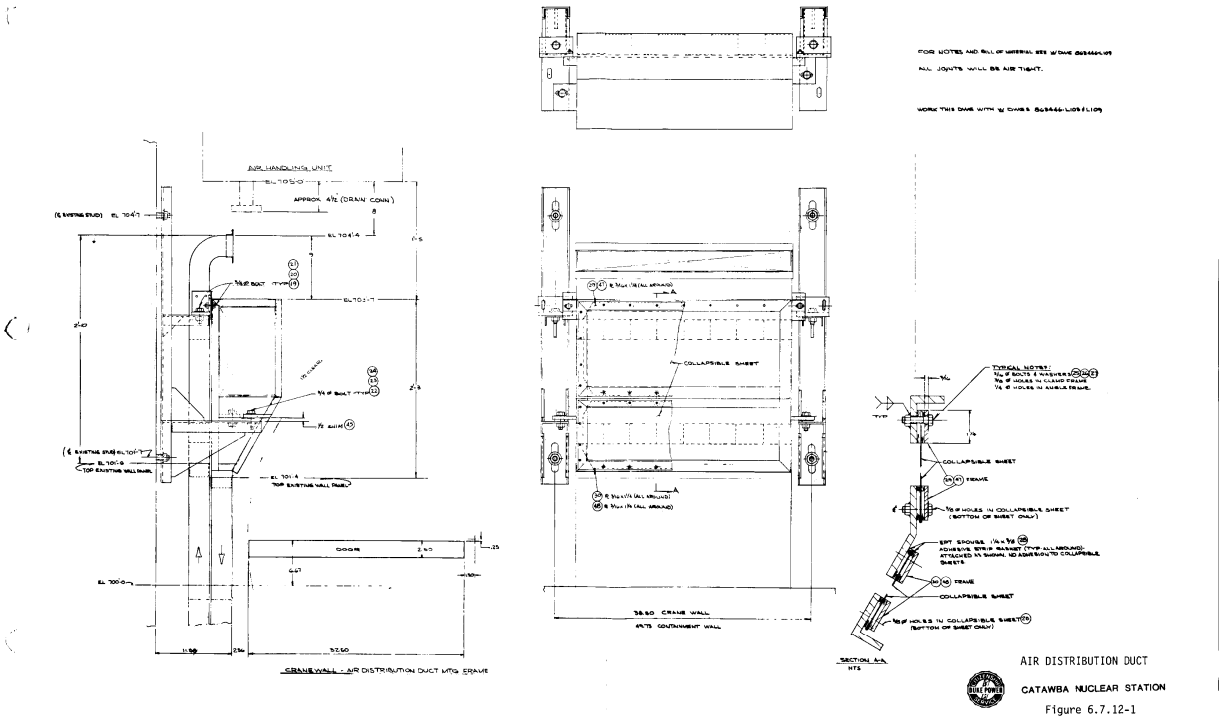

Figure 6-170. Air Distribution Duct

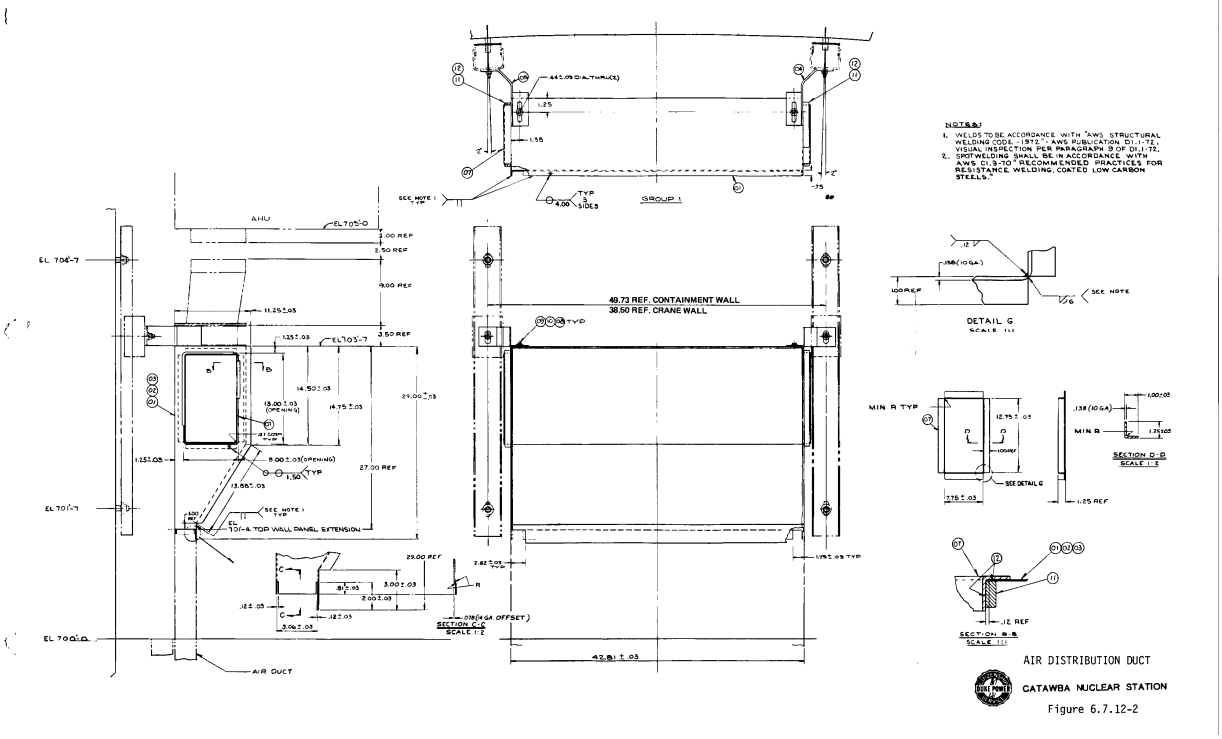

Figure 6-171. Phase Diagram for $Na_2B_4O_7$ - .10 H_20 System at One Atmosphere

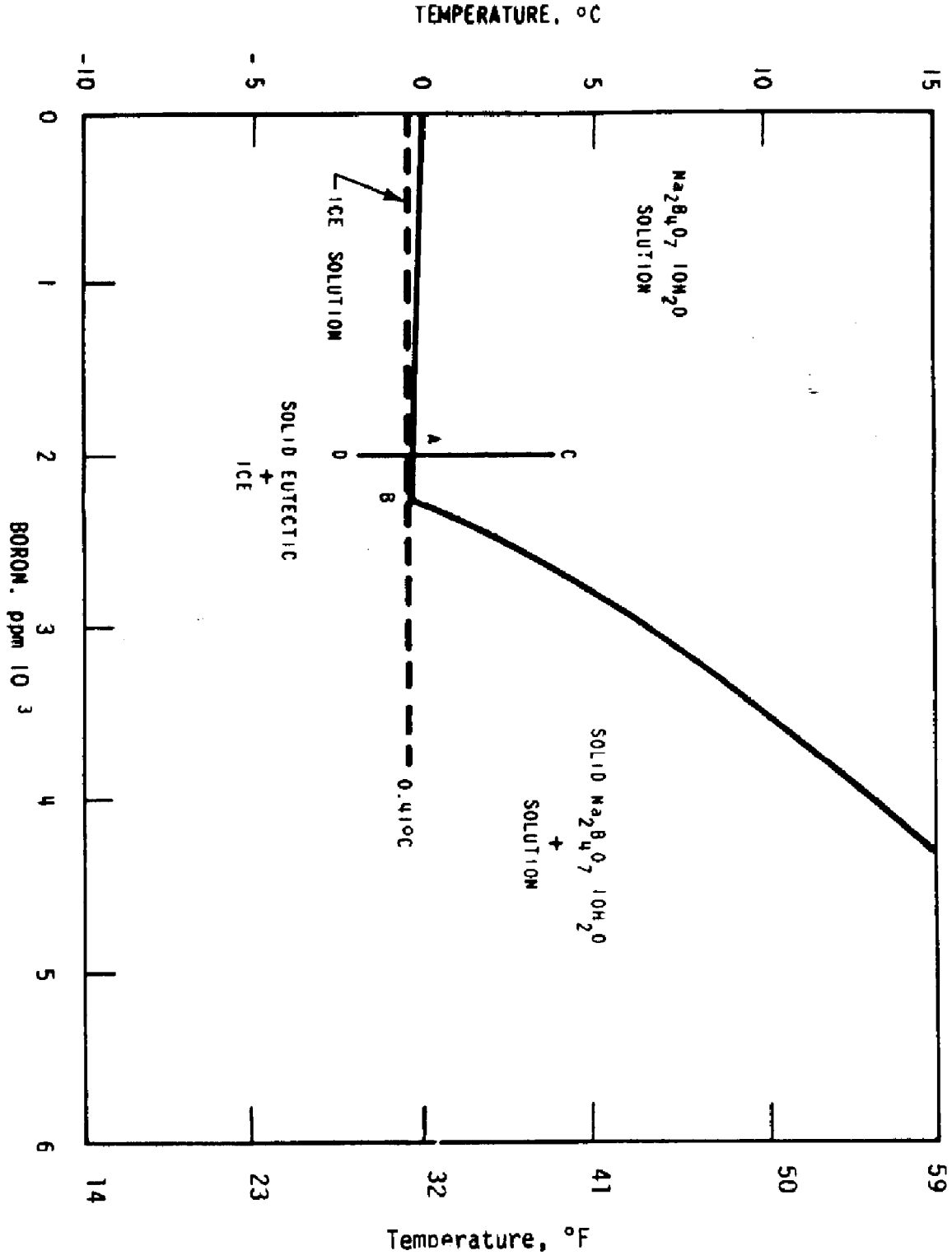

Figure 6-172. Ice Bed Compaction Versus Time

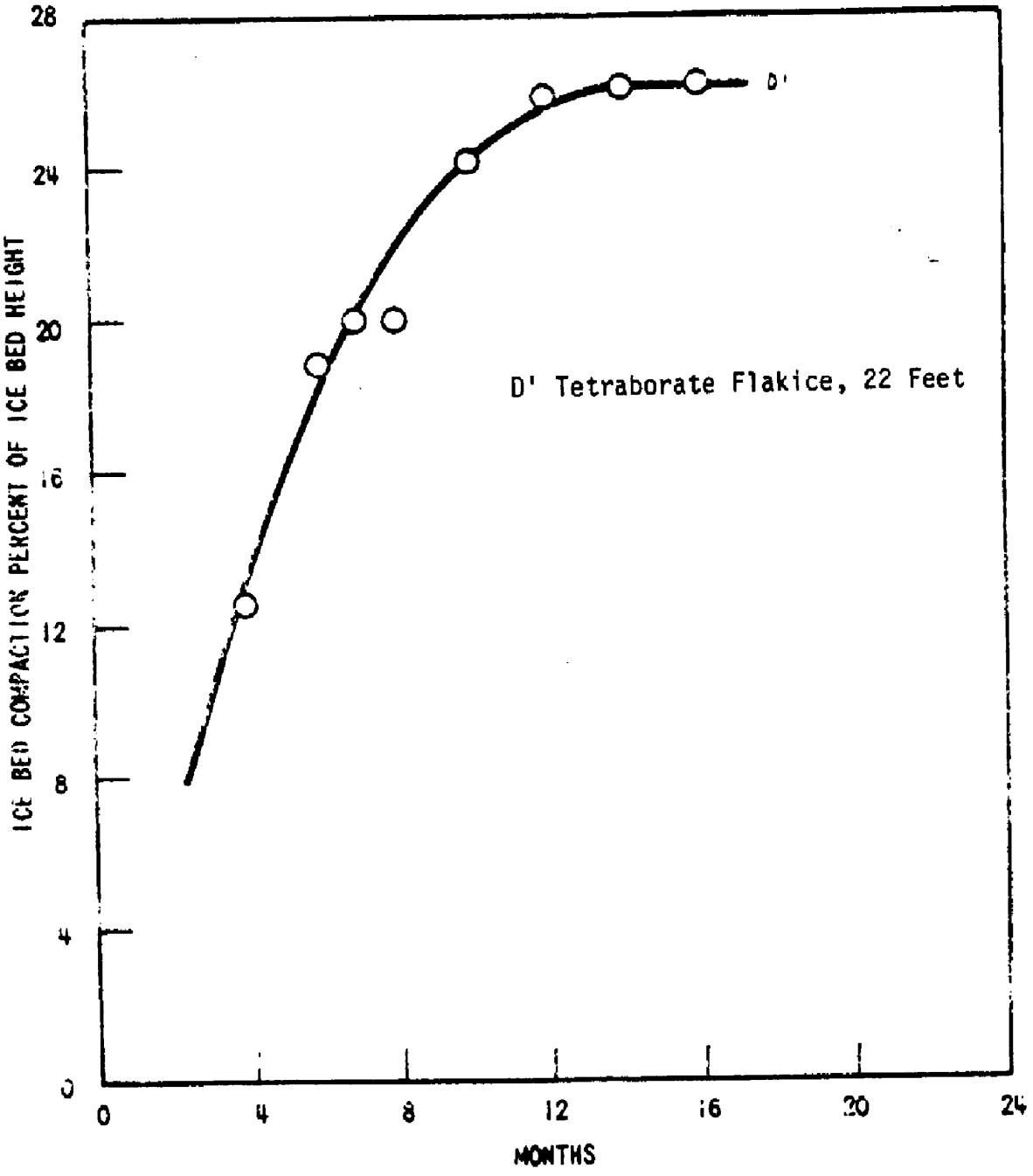

Figure 6-173. Test Ice Bed Compaction Versus Ice Bed Height

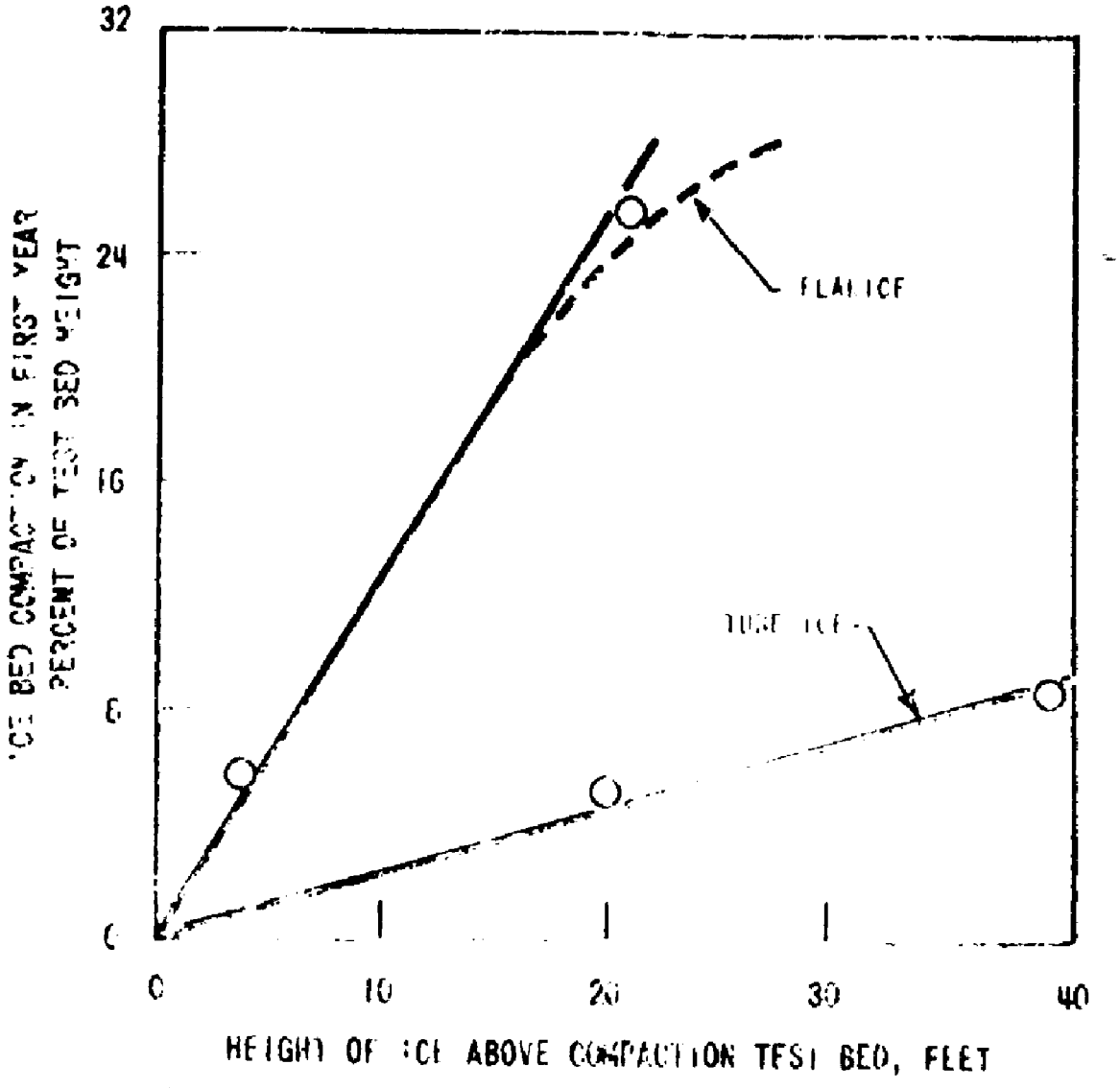

Figure 6-174. Total Ice Compaction Versus Ice Bed Height

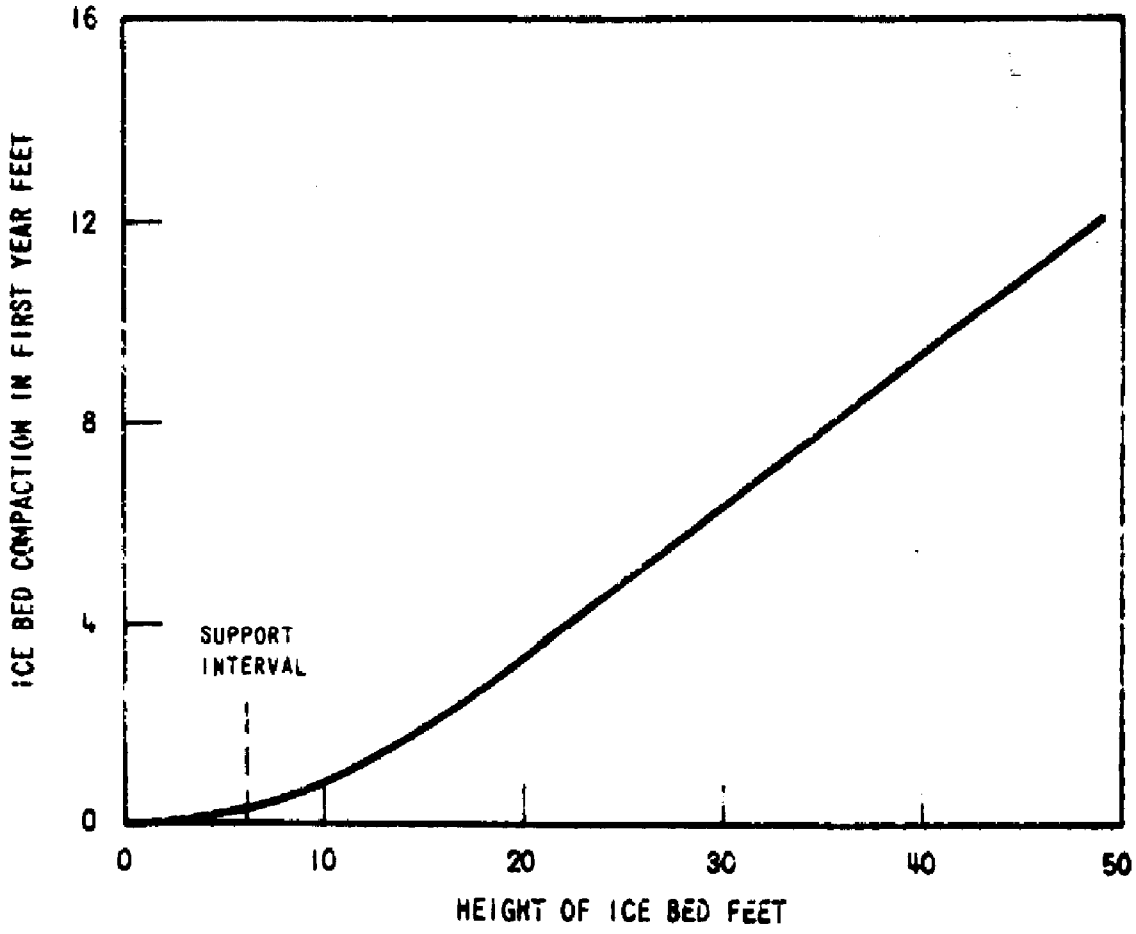

Figure 6-175. Ice Condenser RTD Location

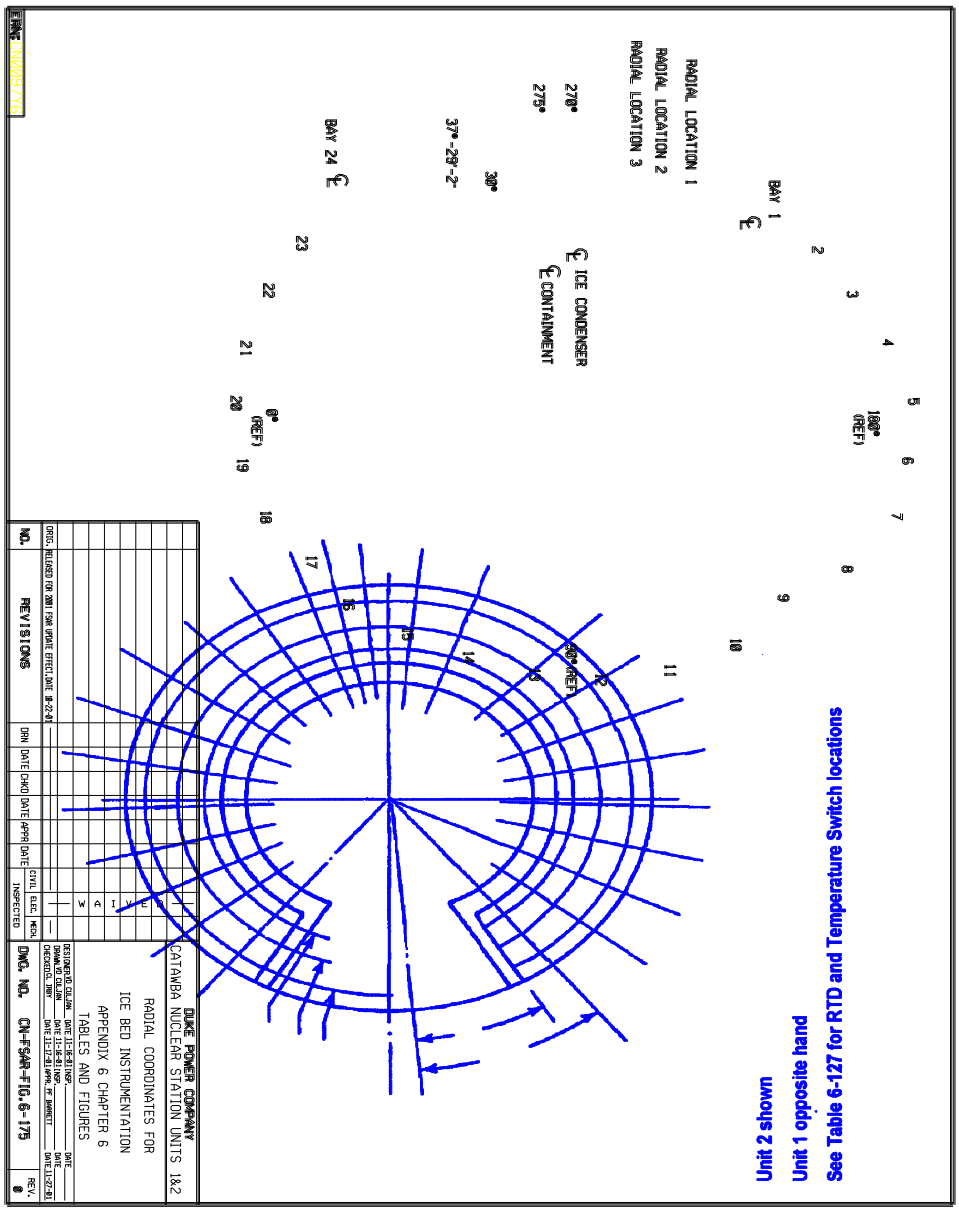

Figure 6-176. Block Diagram: Ice Condenser Temperature Monitoring System

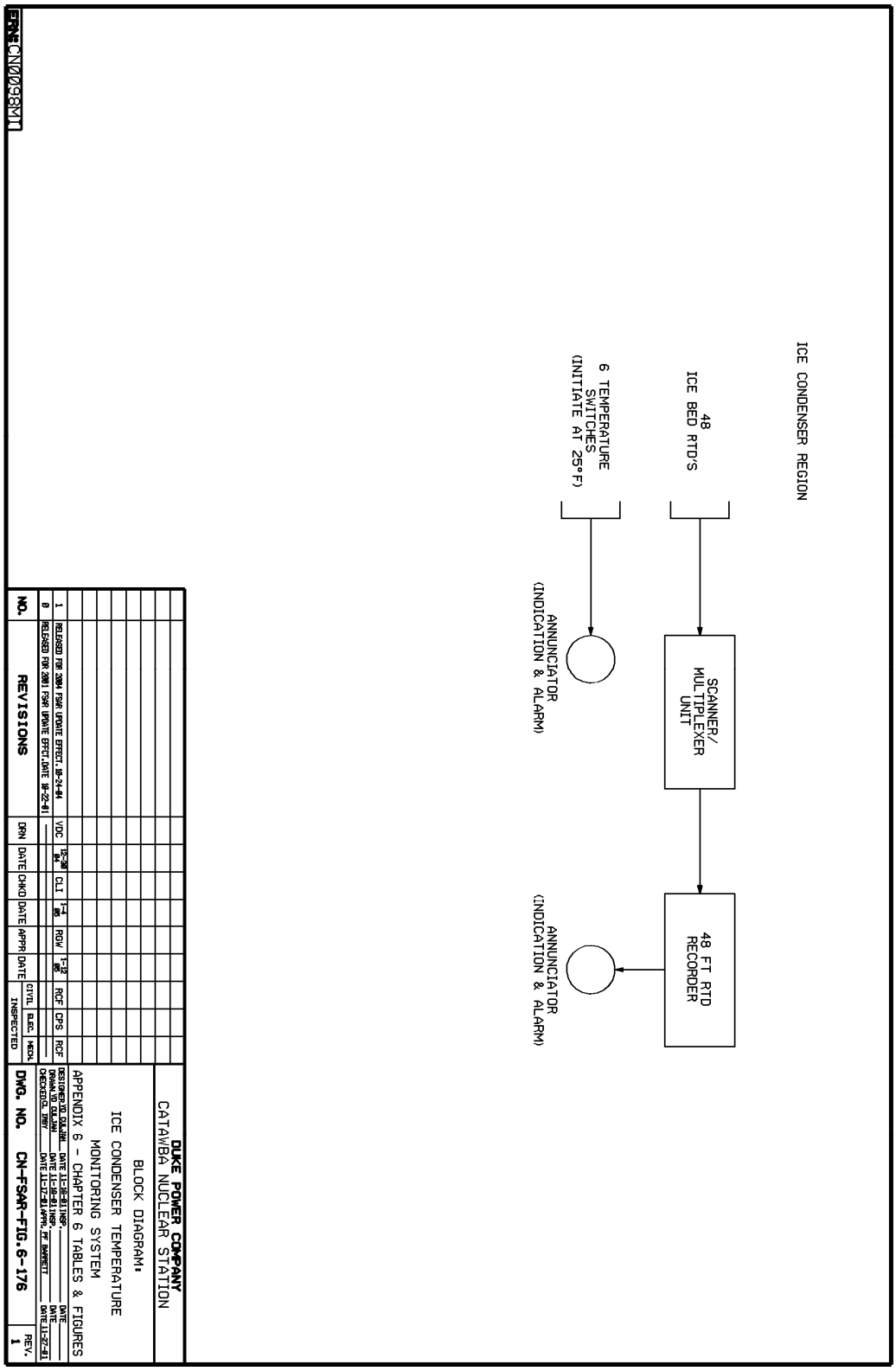

Figure 6-177. Door Monitoring Zones

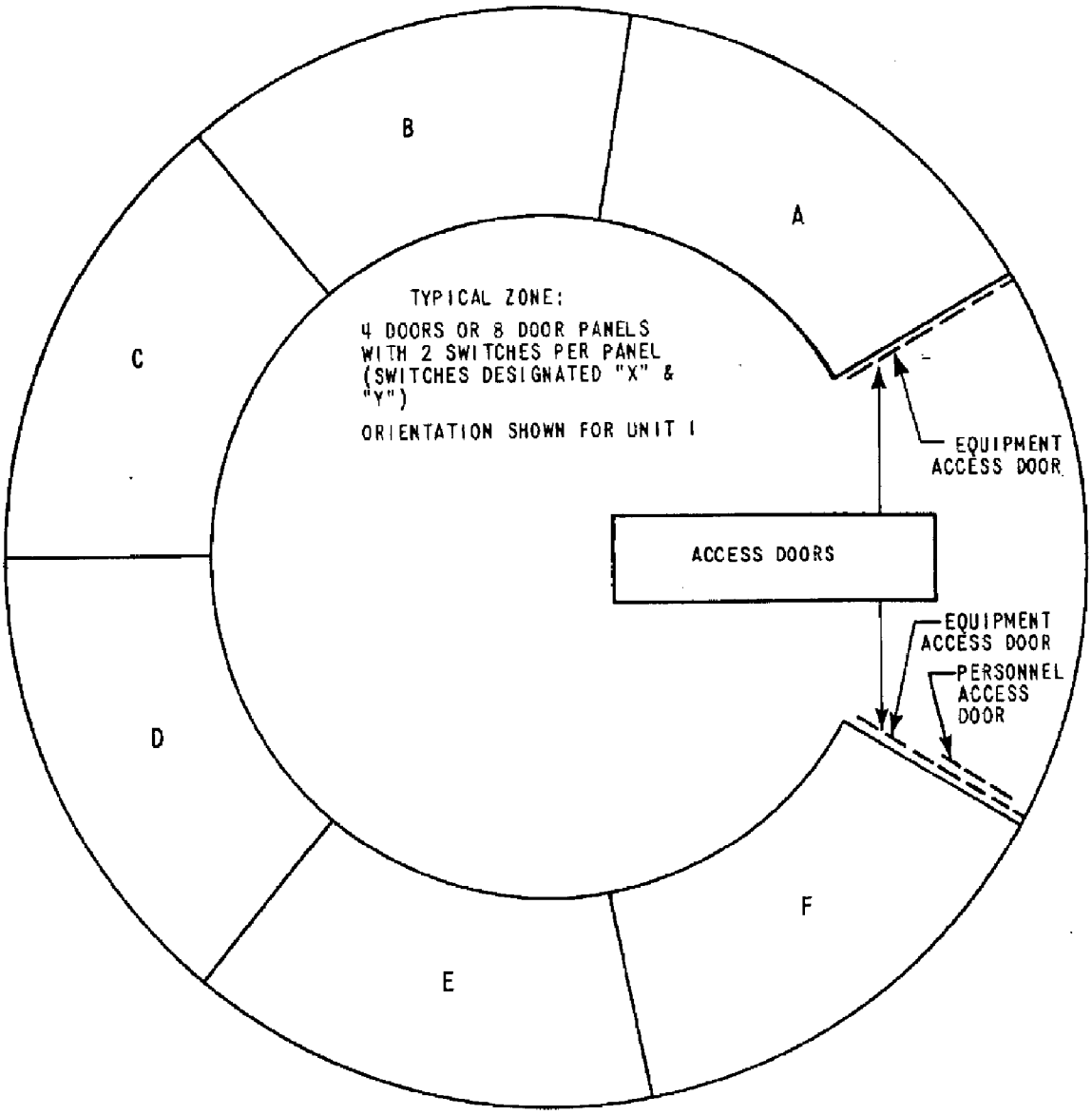

Figure 6-178. Wiring Diagram: "Y" Switch

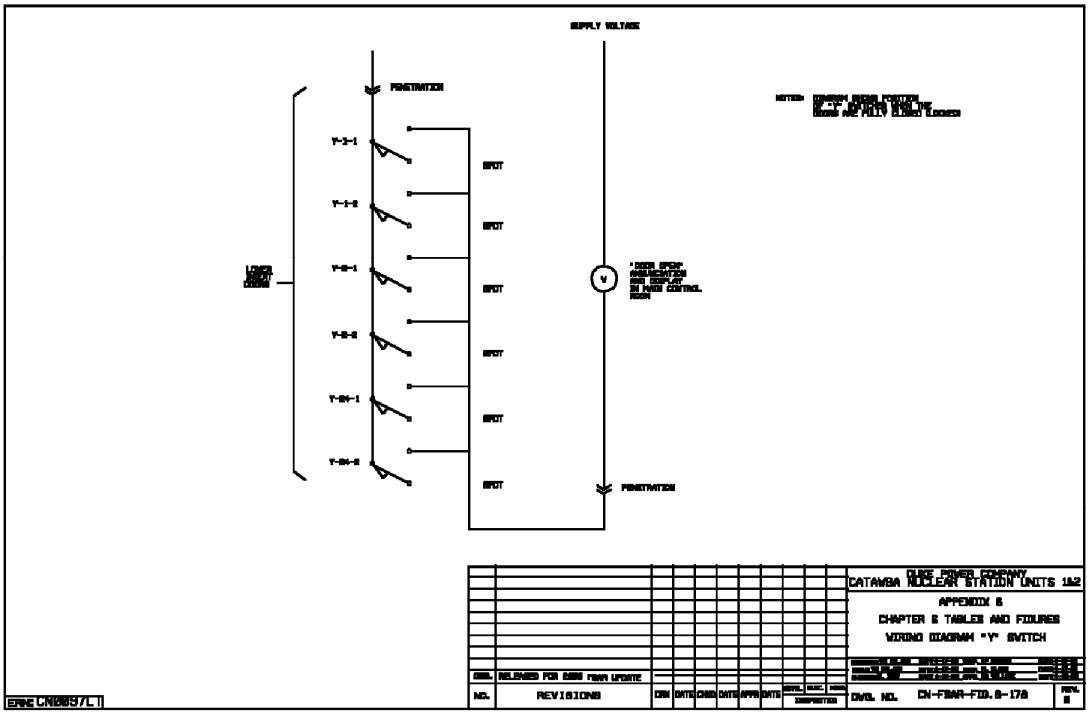

Figure 6-179. Wiring Diagram: "X" Switches Lower Inlet Doors

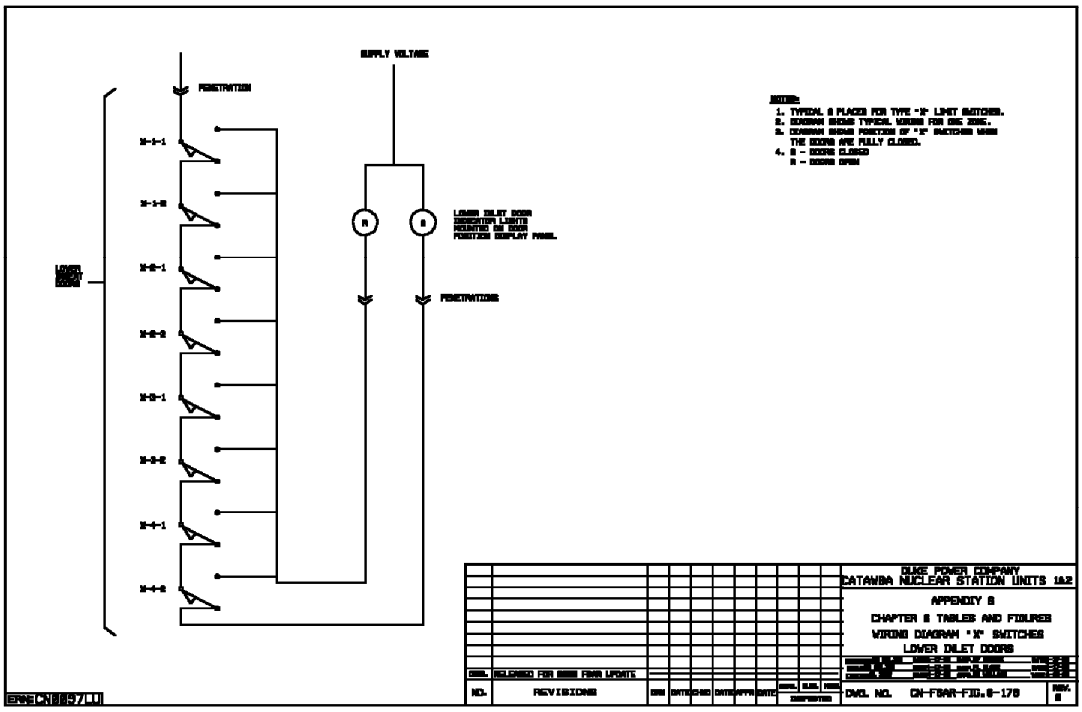

Figure 6-180. Deleted Per 2001 Update

Figure 6-181. Model of Horizontal Lattice Frame Structure

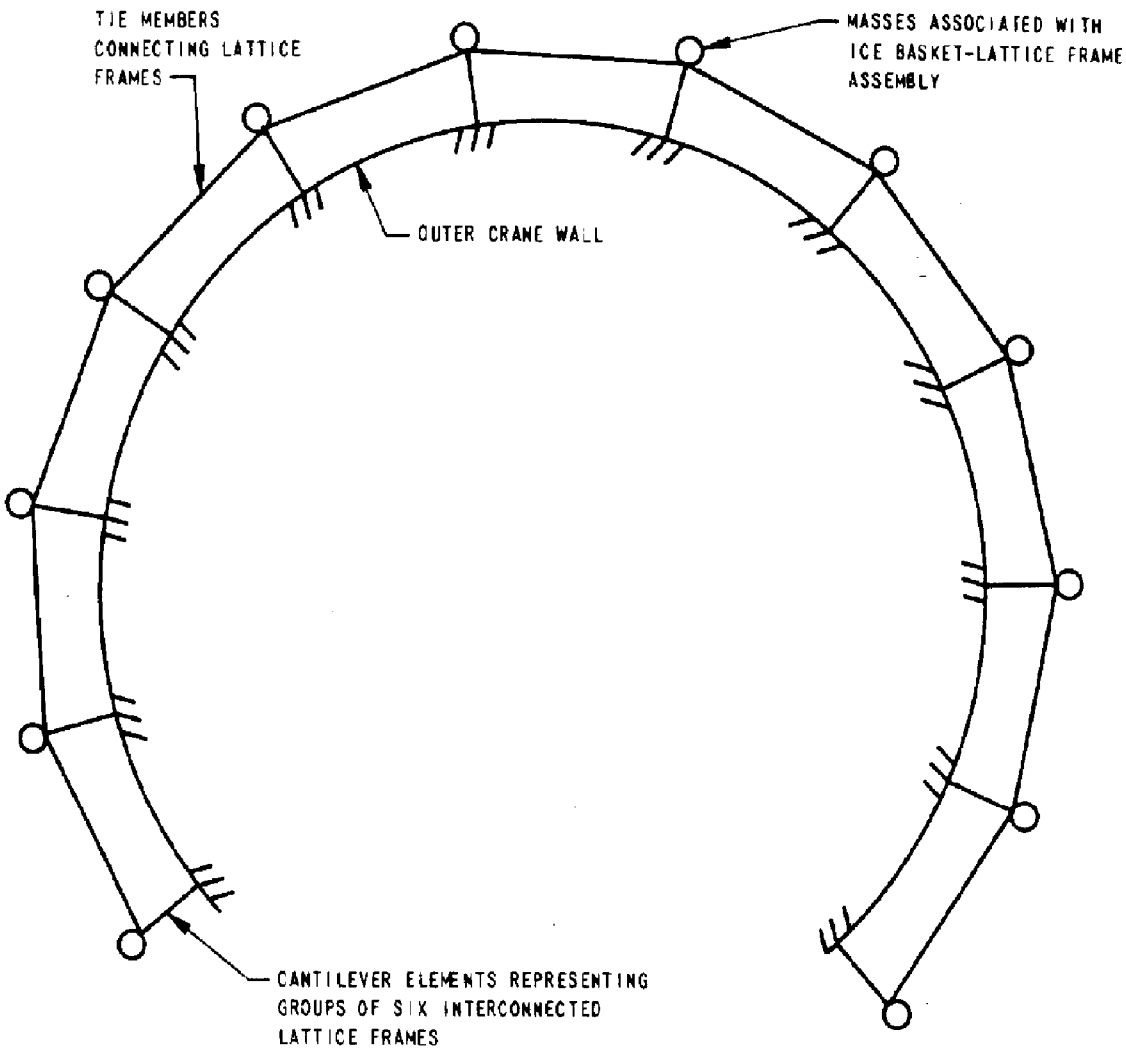

Figure 6-182. Group of Six Interconnected Lattice Frames

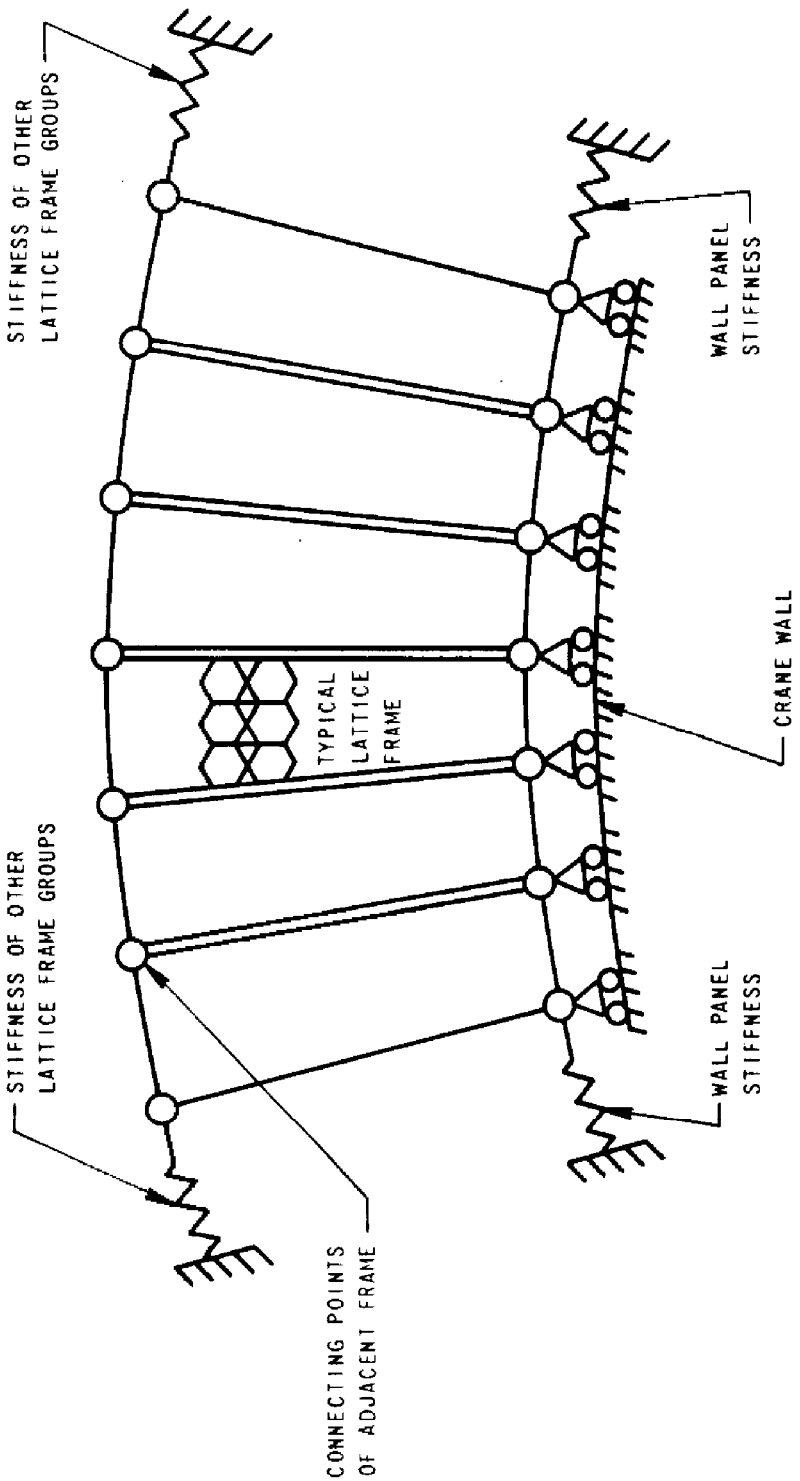

Figure 6-183. Lattice Frame Ice Basket Gap

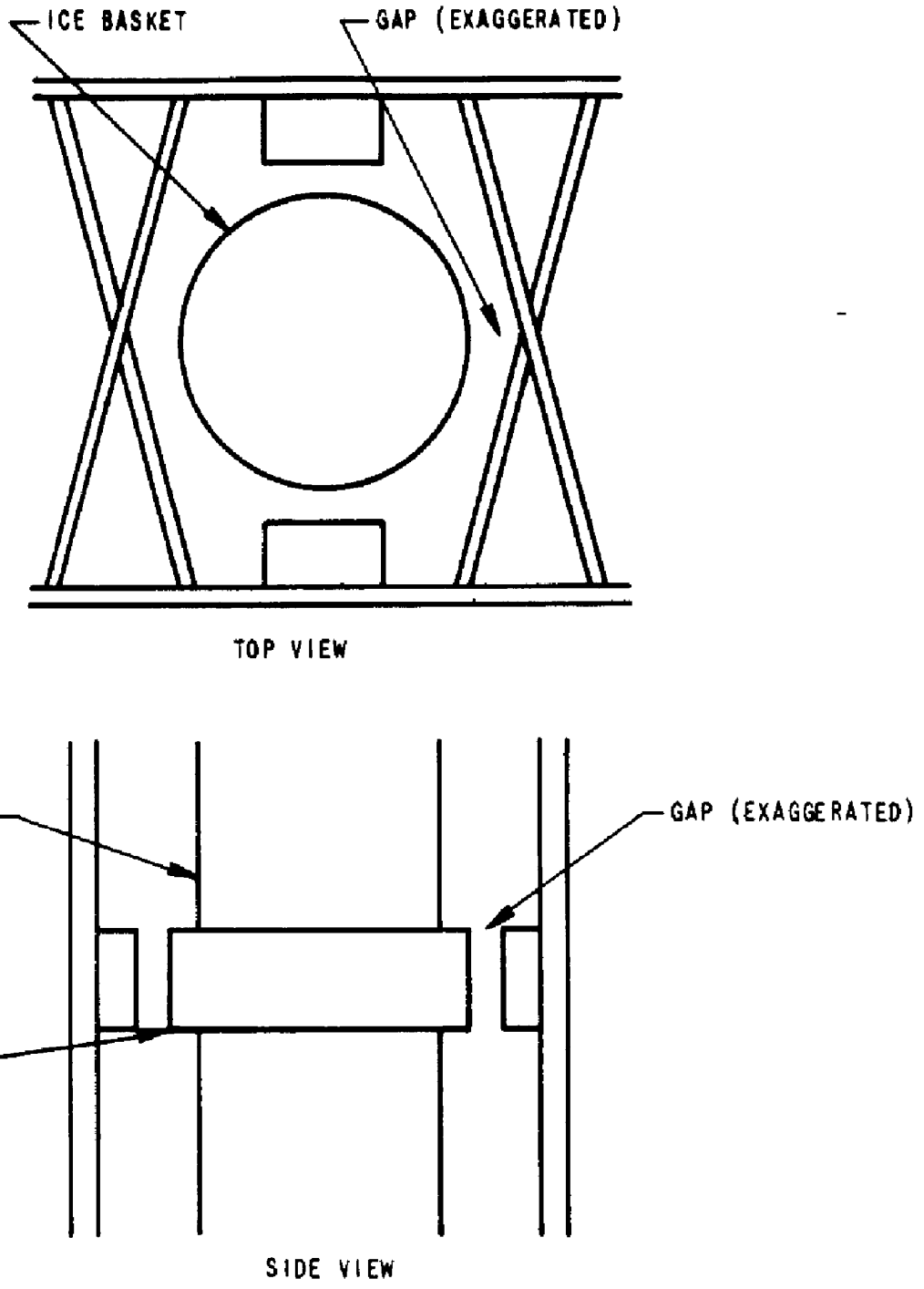

Figure 6-184. Typical Displacement Time History for 12 Foot Basket with End Supports - Pluck Test

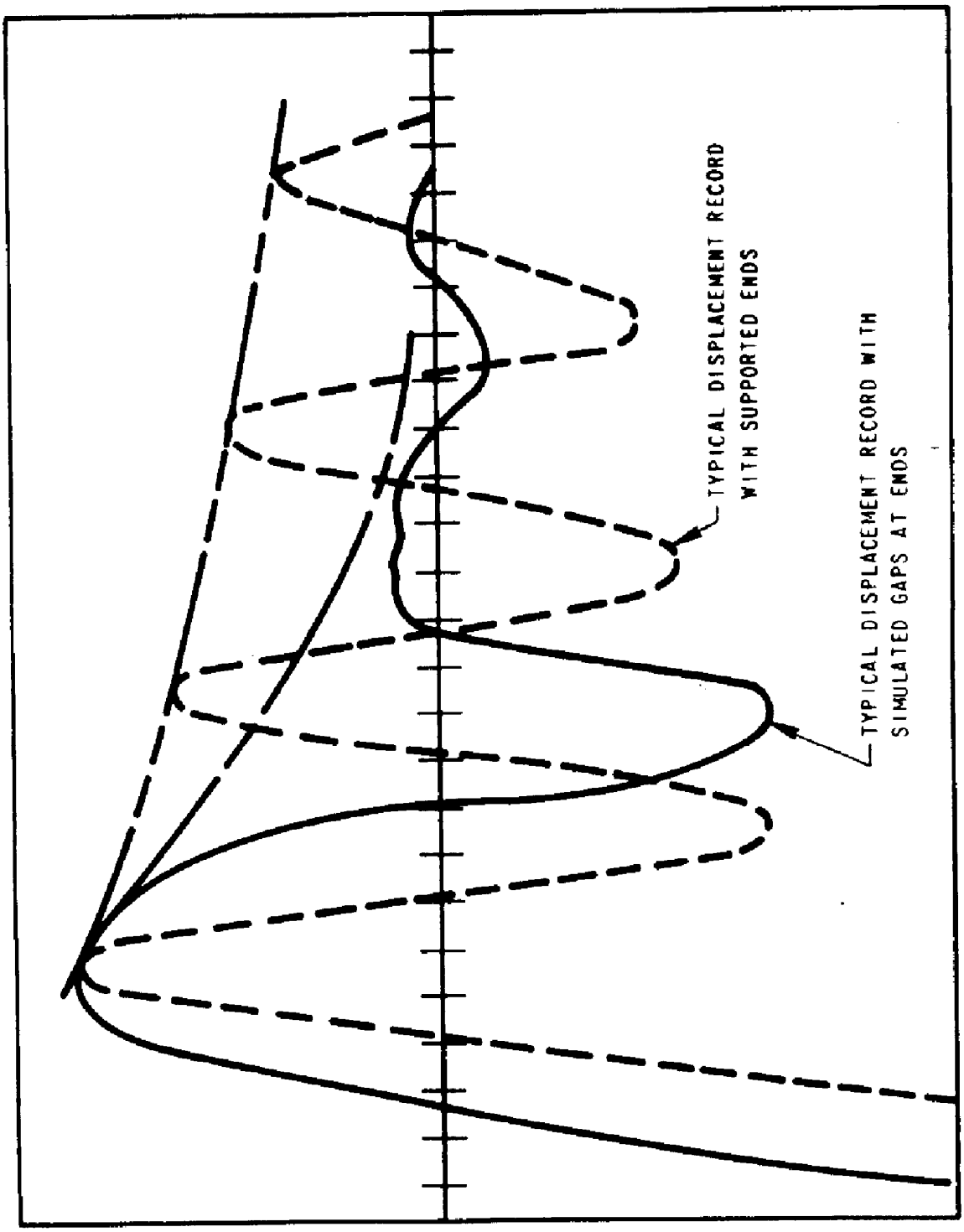

Figure 6-185. Non Linear Dynamic Model

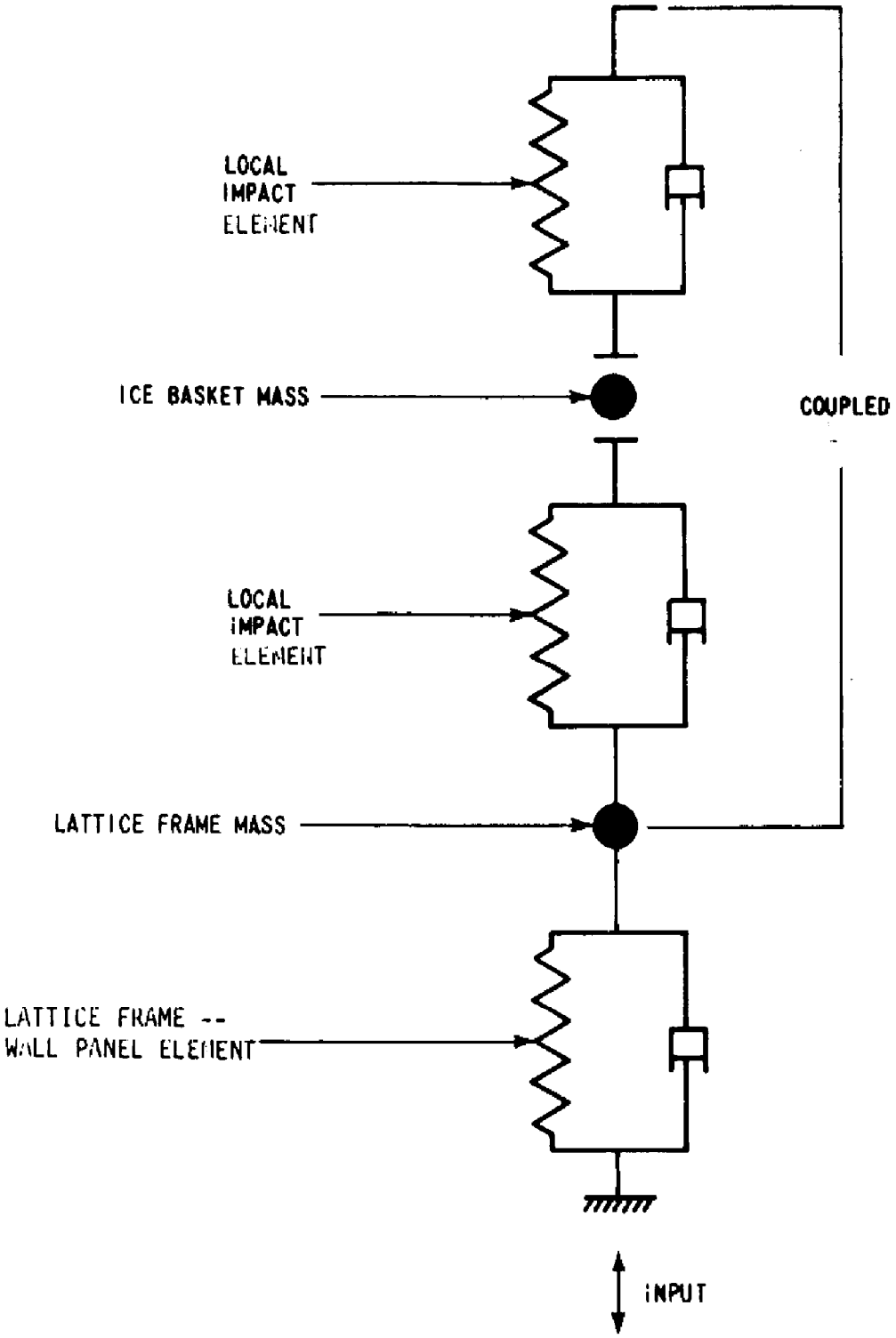

Figure 6-186. 3 Mass Tangential Ice Basket Model

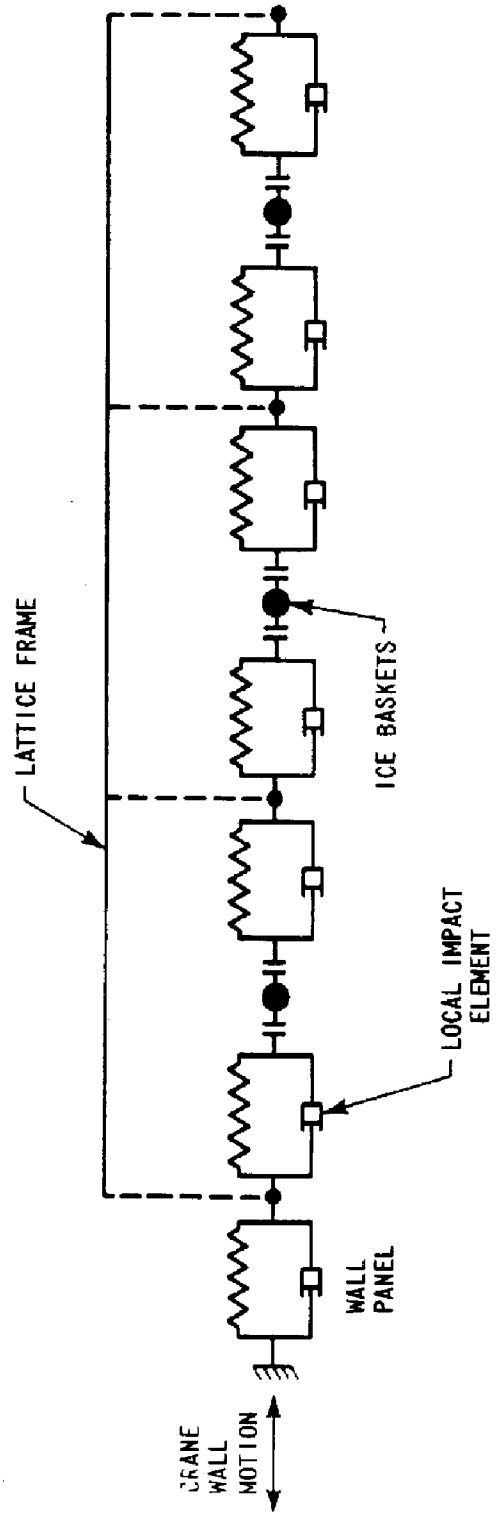

Figure 6-187. 9 Mass Radial Ice Basket Model

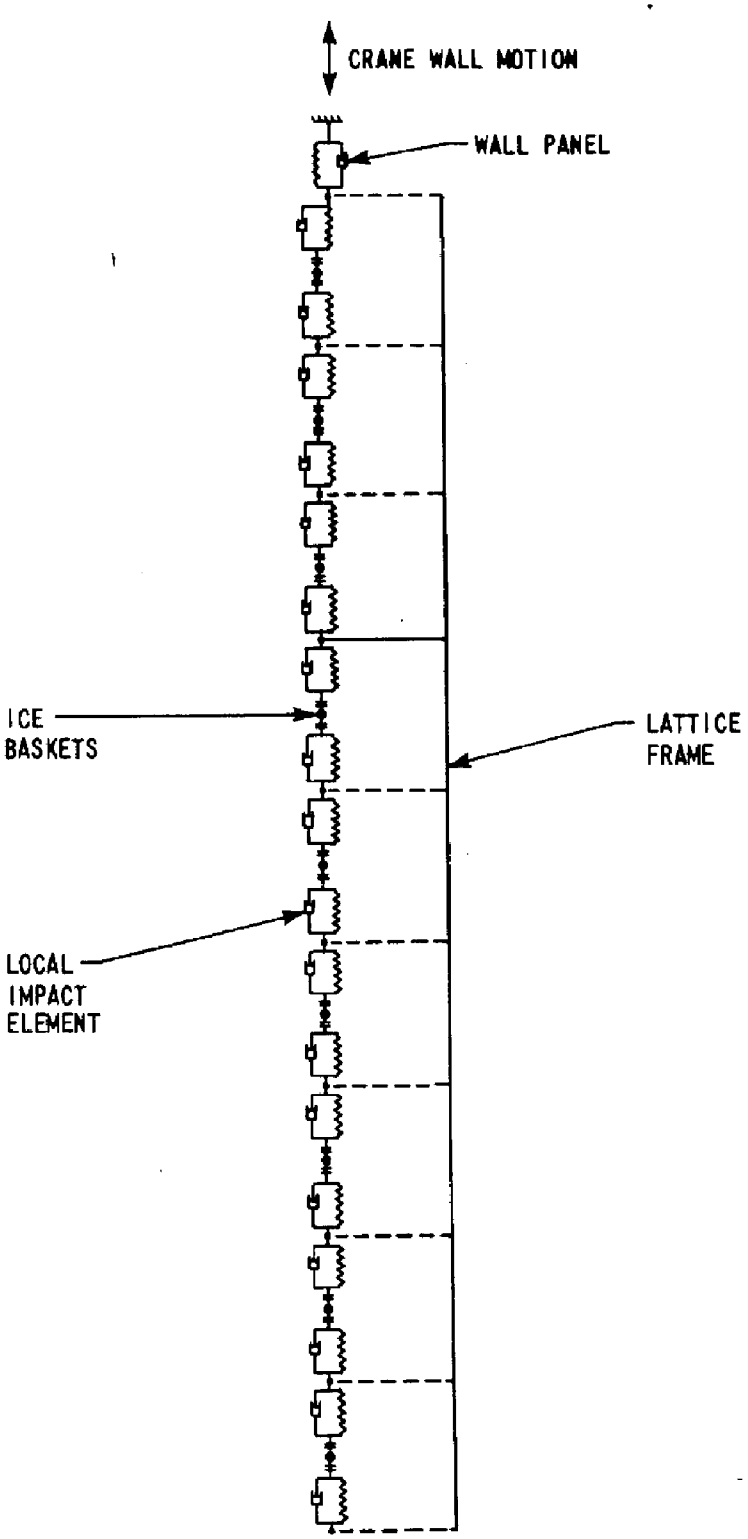

Figure 6-188. 48 Foot Beam Model

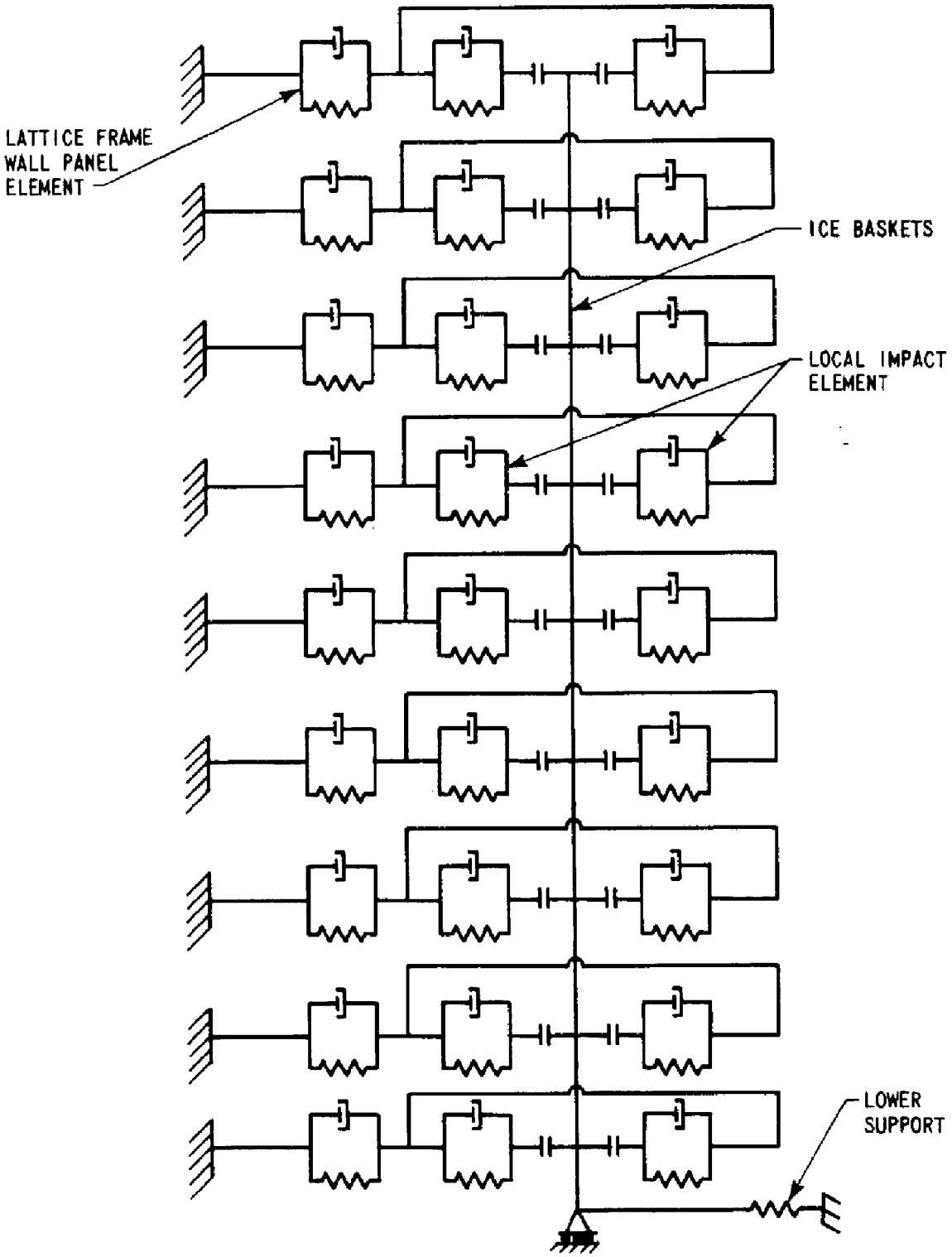

Figure 6-189. Phasing Mass Model of Adjacent Lattice Frame Bays

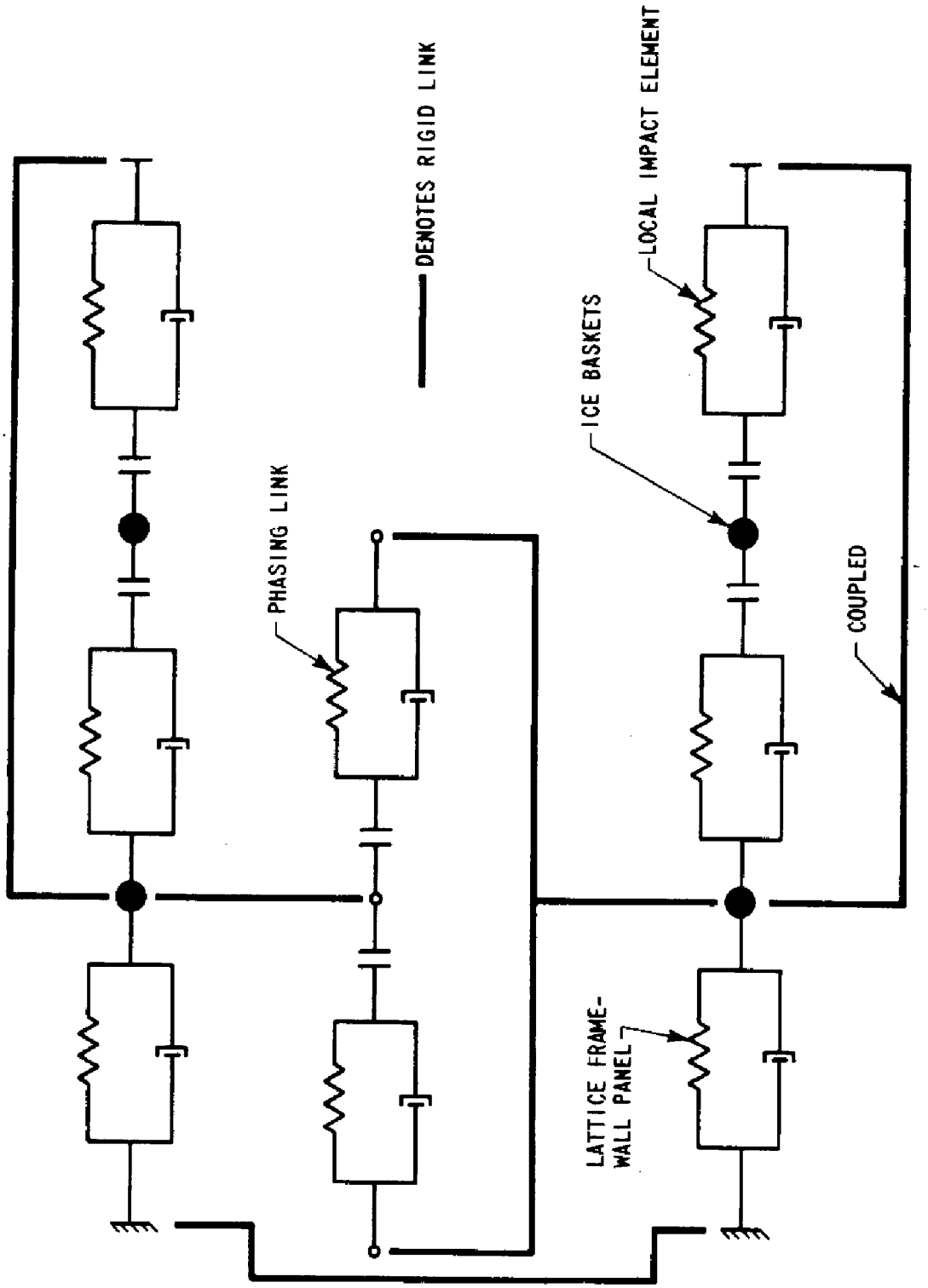

Figure 6-190. Phasing Study Model, 1 Level Lattice Frame 300 Degrees Non-Linear Model

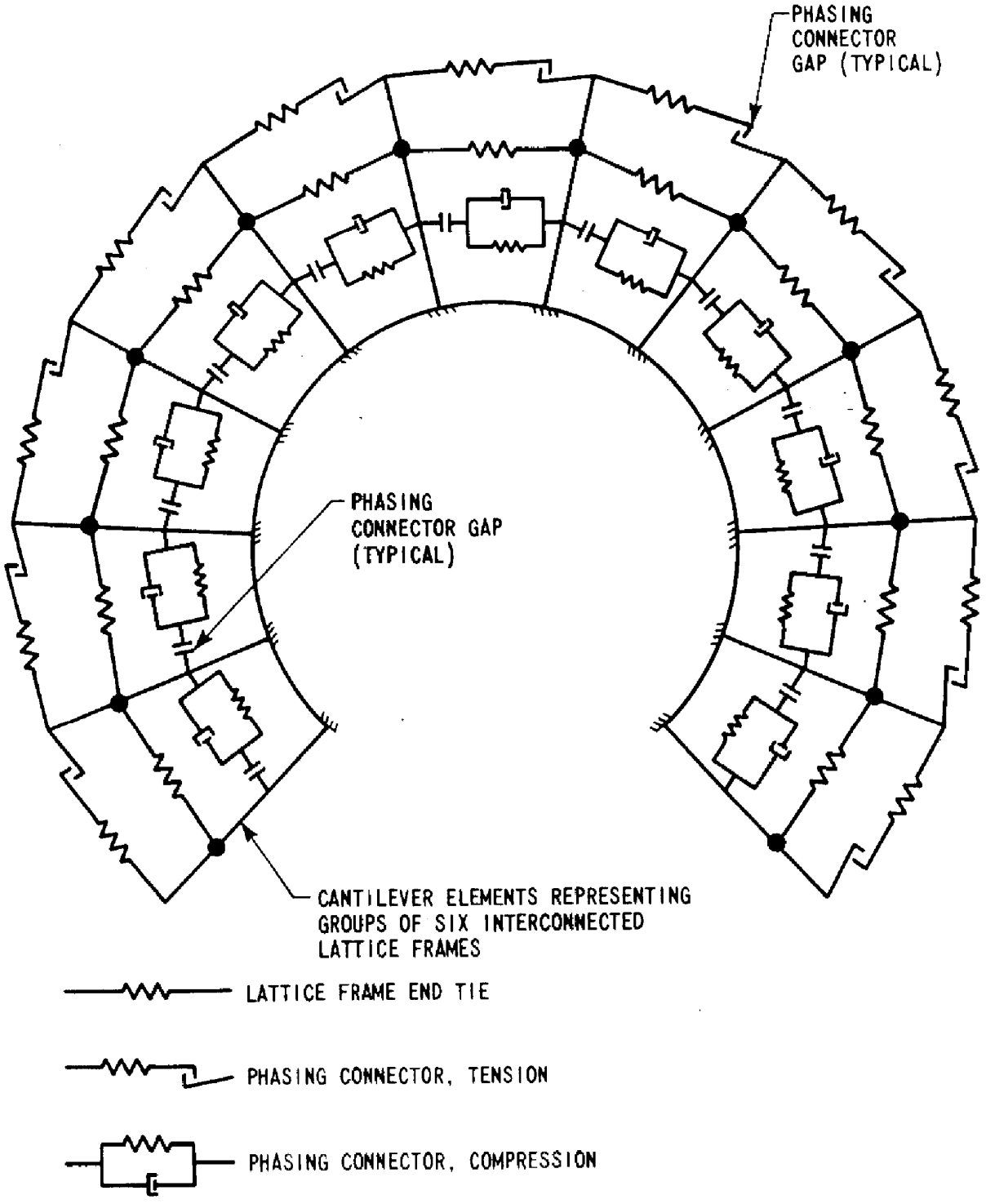

Figure 6-191. Typical Crane Wall Displacement

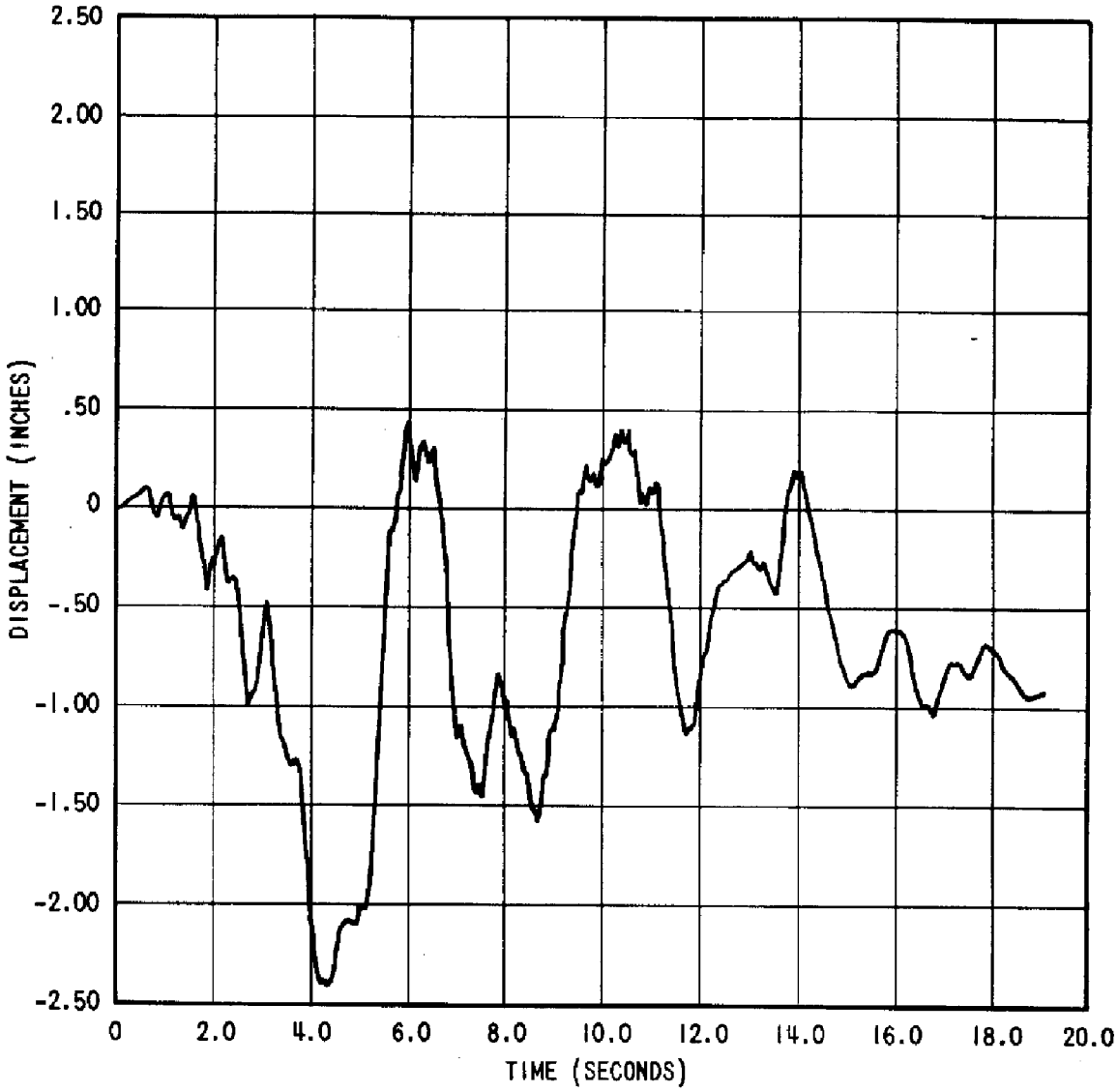

Figure 6-192. Typical Ice Basket Displacement Response

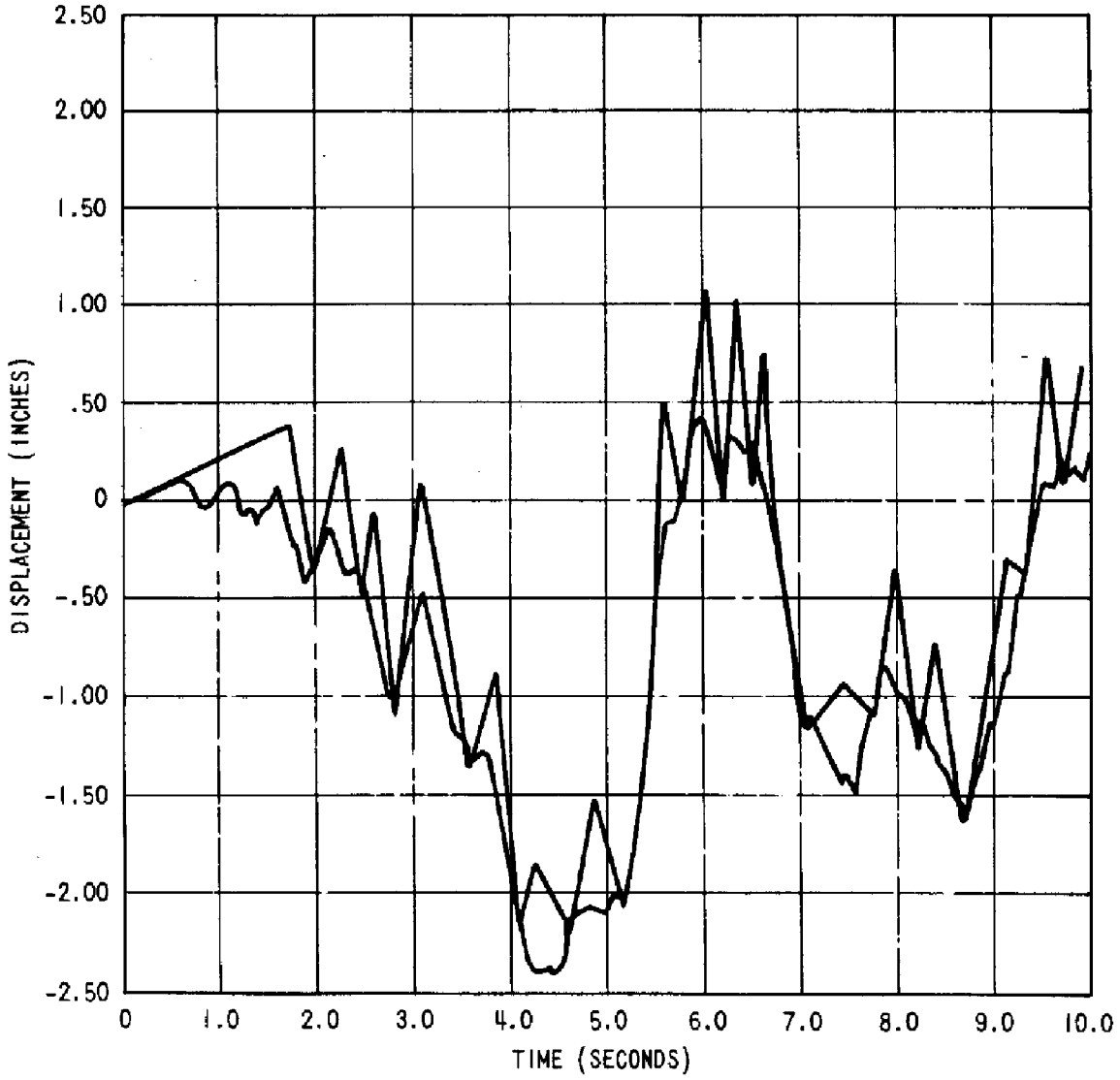

Figure 6-193. Typical Ice Basket Impact Force Response

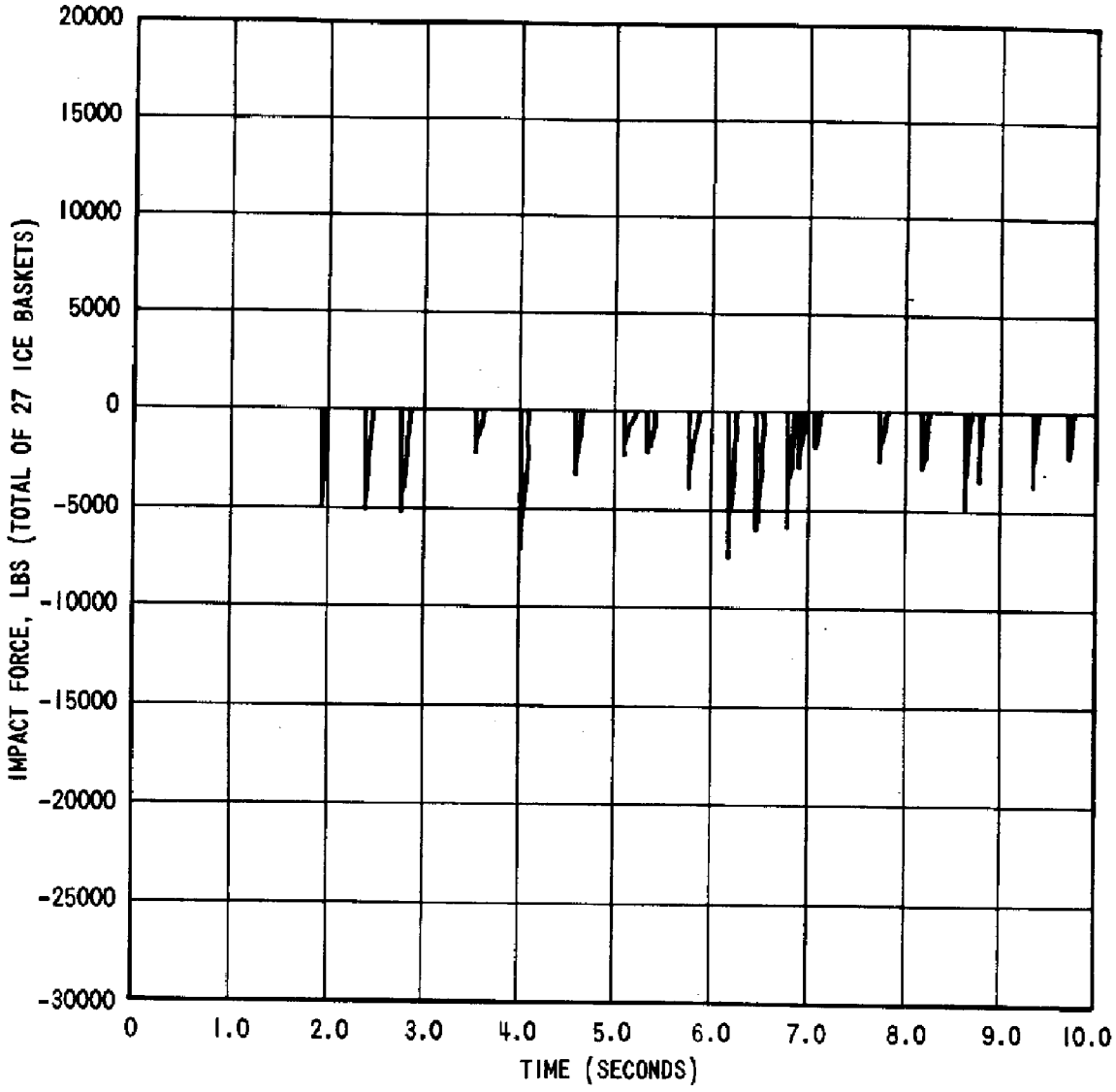

Figure 6-194. Typical Crane Wall Panel Load Response

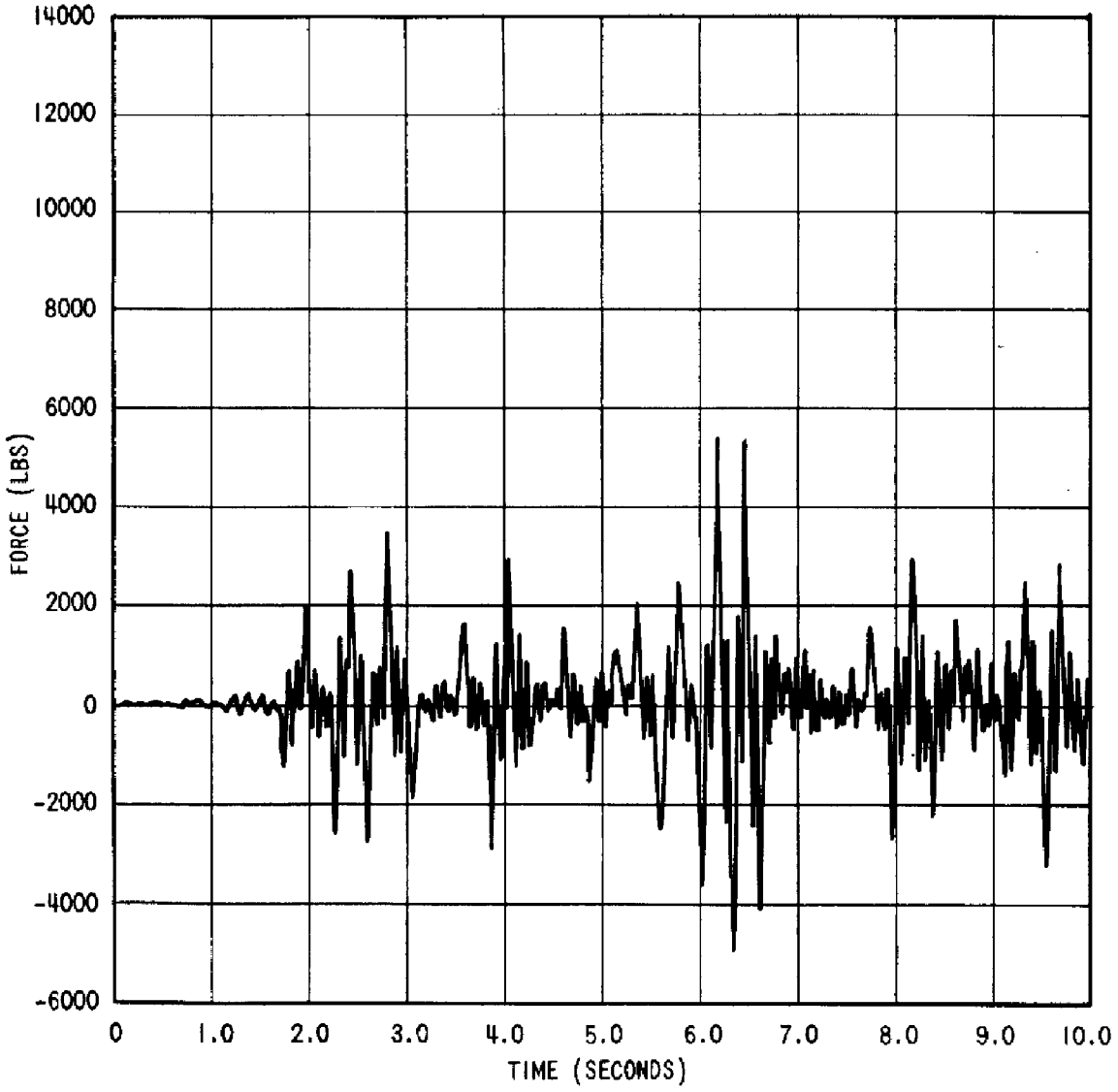

Figure 6-195. Wall Panel Design Load Distribution Obtained Using the 48-Foot Beam Model Tangential Case

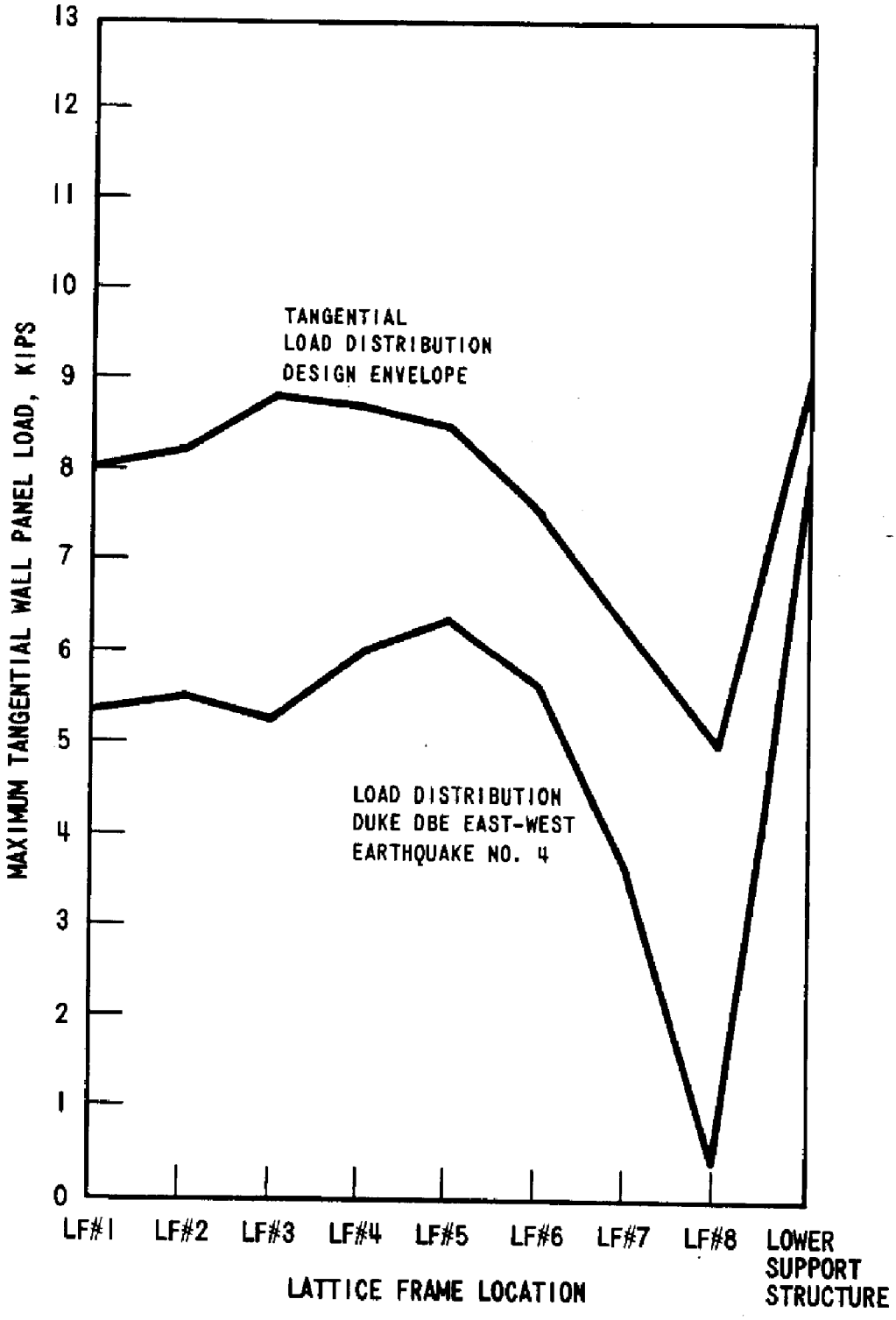

Figure 6-196. Wall Panel Design Load Distribution Obtained Using the 48-Foot Beam Model Radial Case

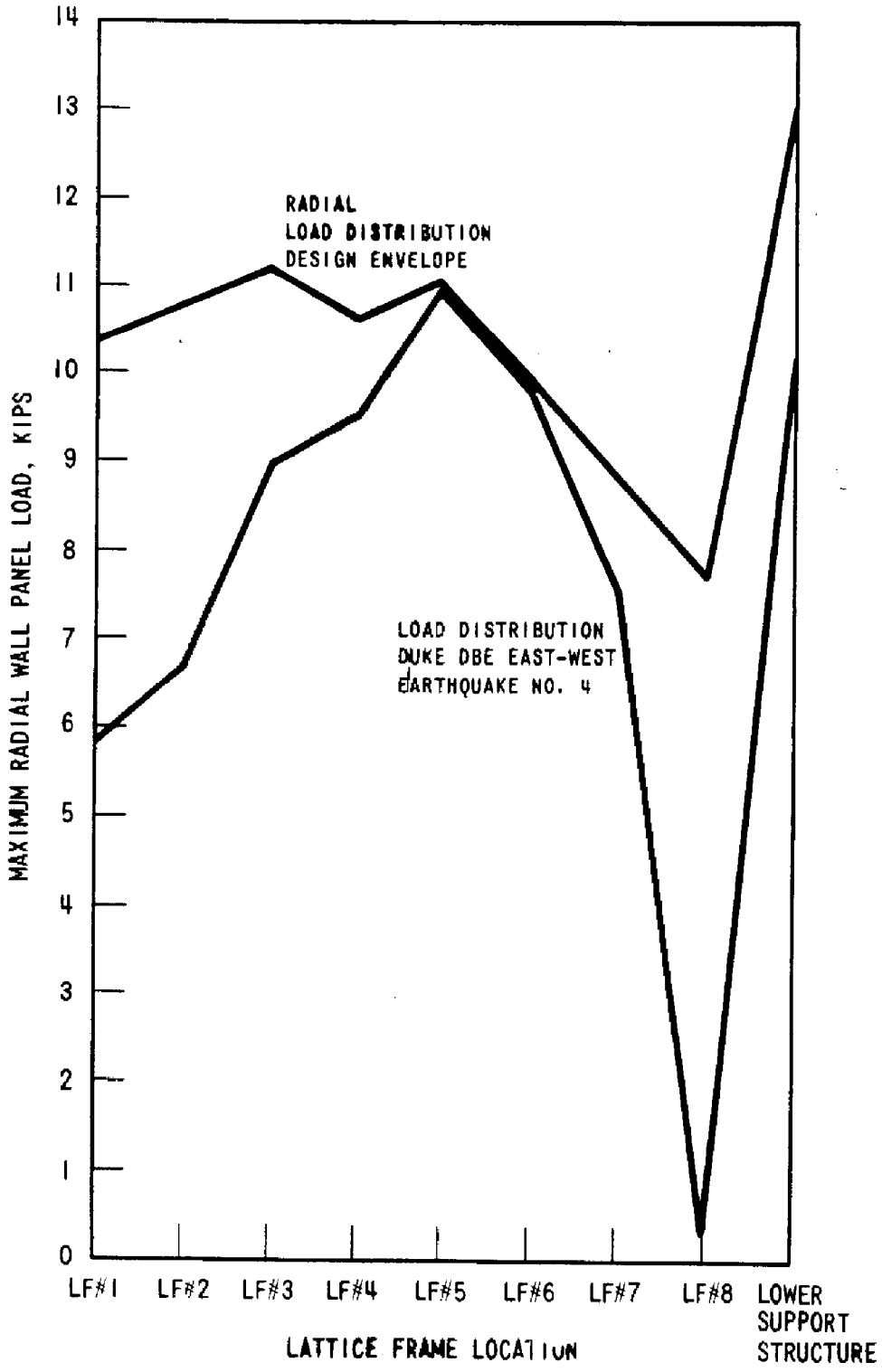

Figure 6-197. Ice Basket Swivel Bracket Assembly

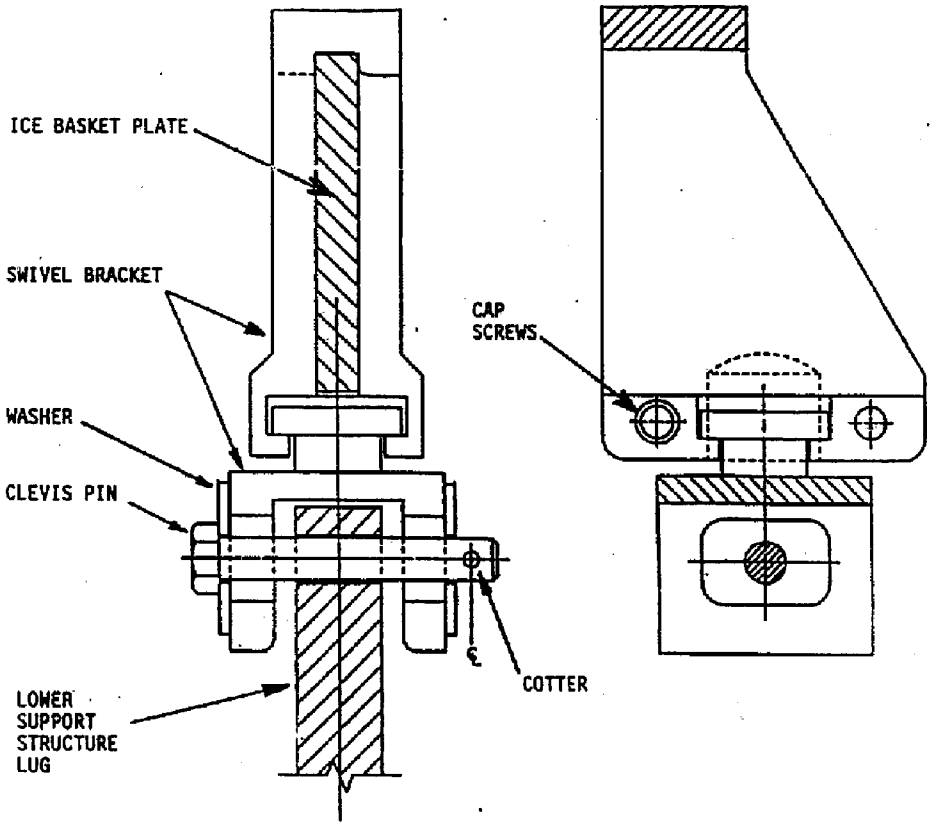

Figure 6-198. Block Ice Minimum Restriction Basket Assembly

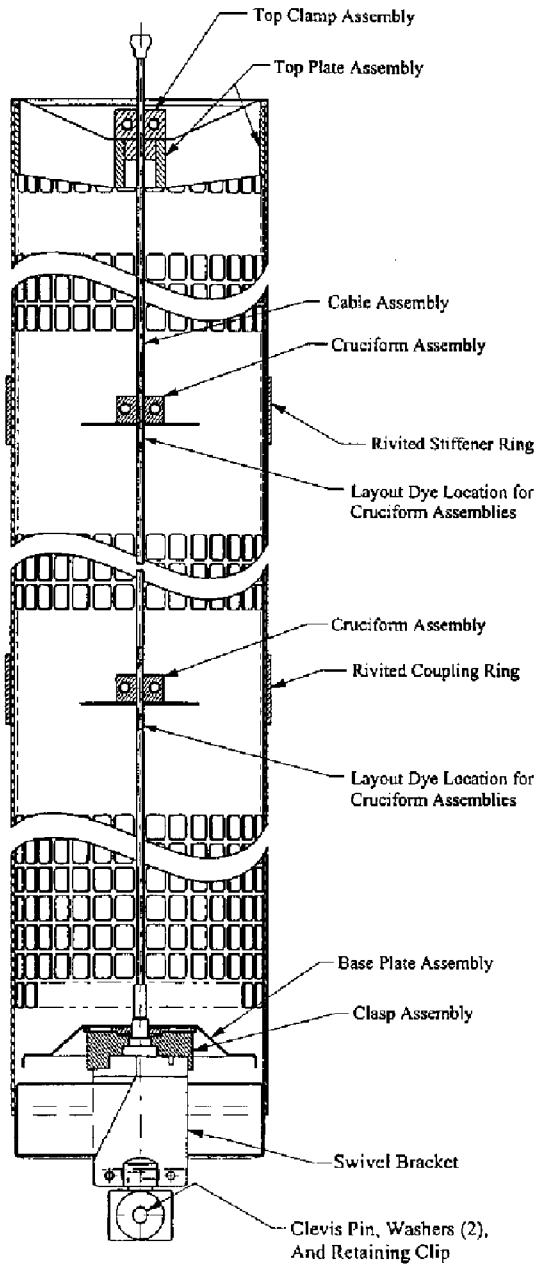

Figure 6-199. CNS-1 Double-Ended LBLOCA Mass and Energy Release Analyses

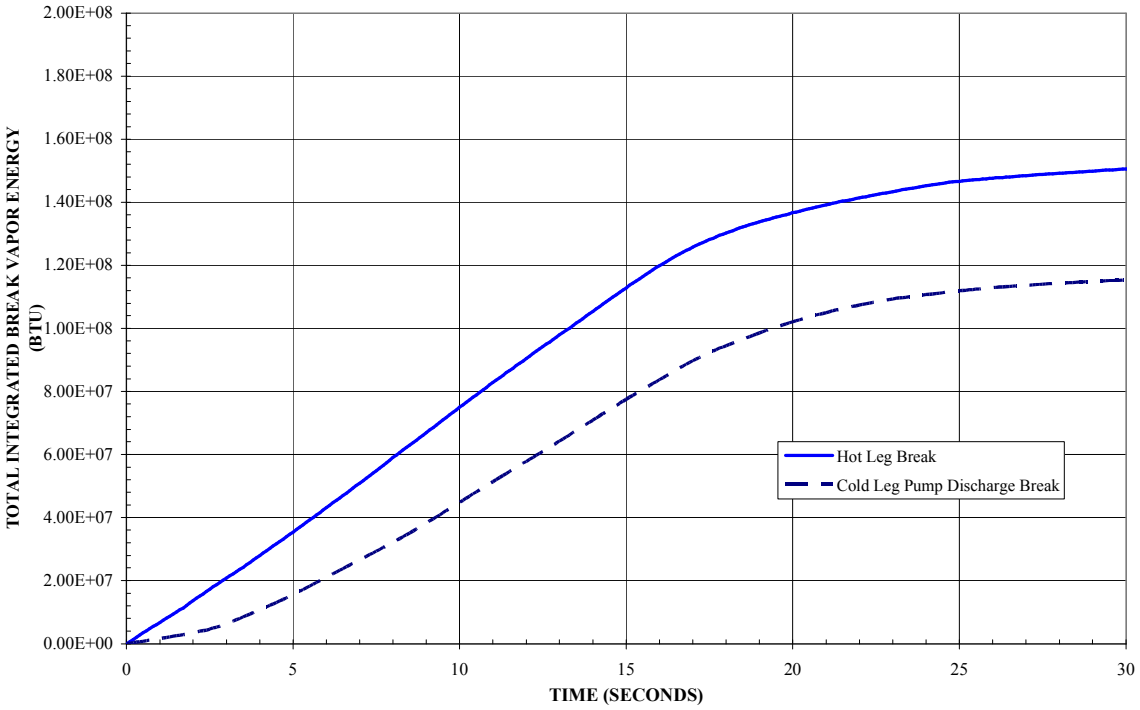

Figure 6-200. CNS-1 Double-Ended LBLOCA Mass and Energy Release Analyses

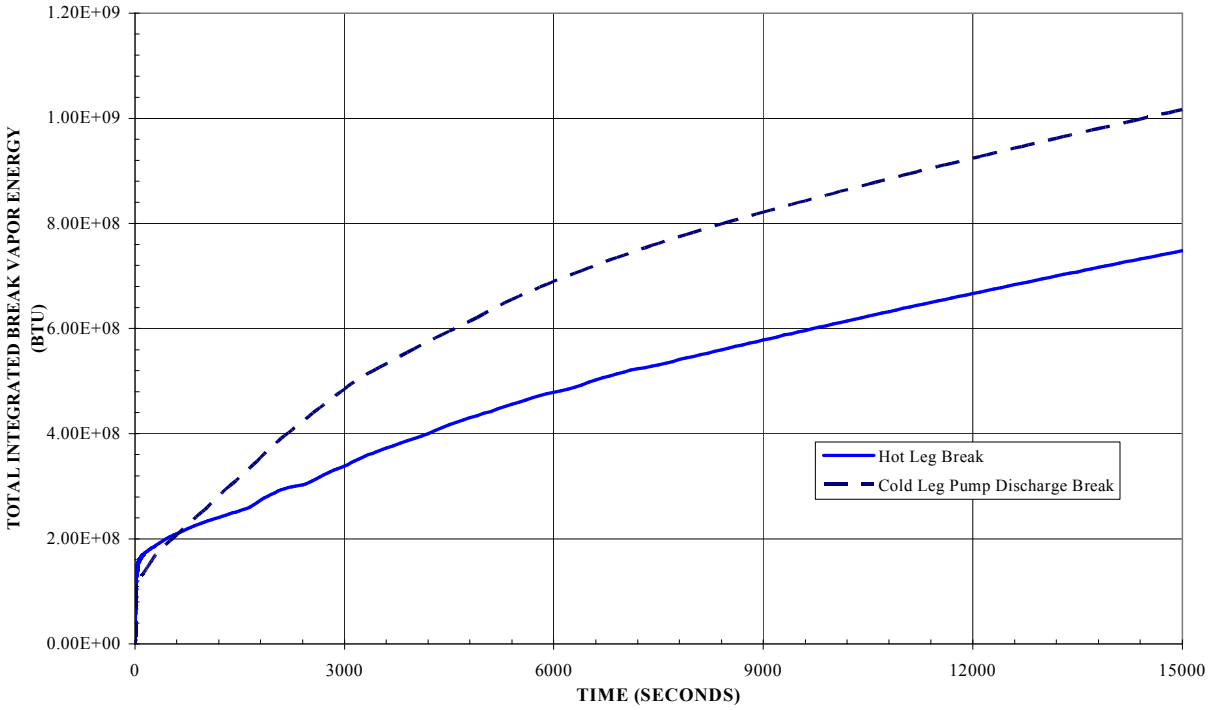

Figure 6-201. CNS-1 Double-Ended LBLOCA Mass and Energy Release Analyses

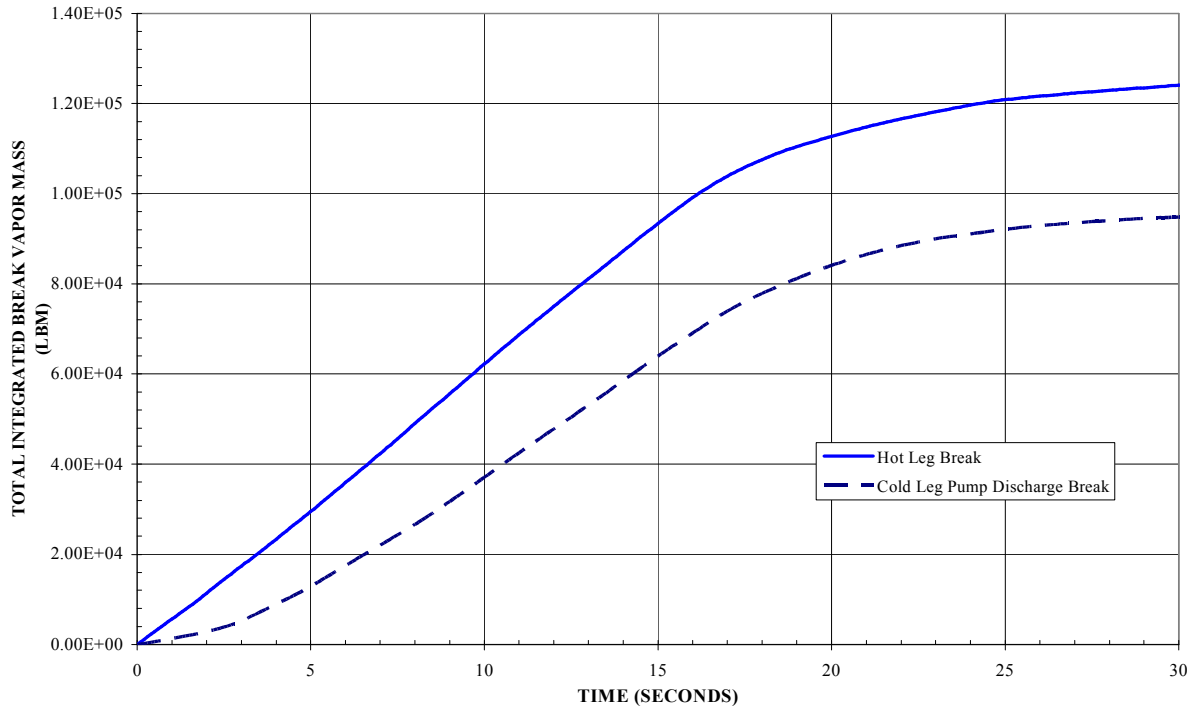

Figure 6-202. CNS-1 Double-Ended LBLOCA Mass and Energy Release Analyses

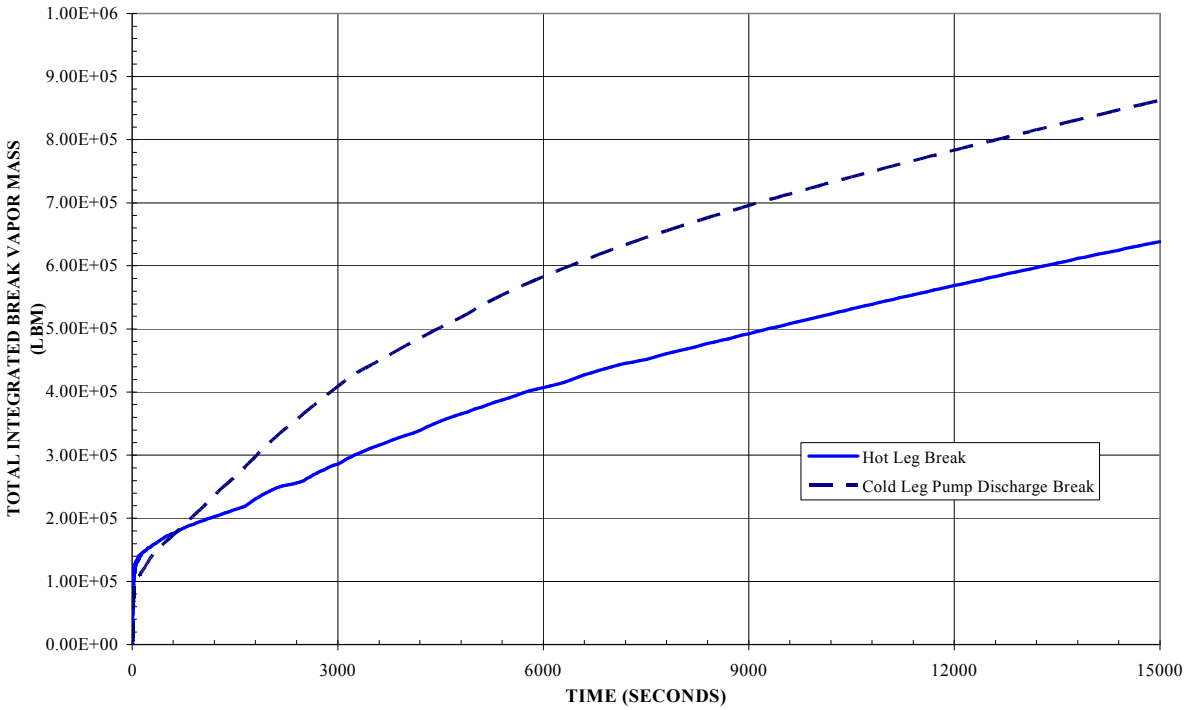

Figure 6-203. Deleted Per 2000 Update.

Figure 6-204. Upper and Lower Compartment Pressure, Min. Pressure Analysis

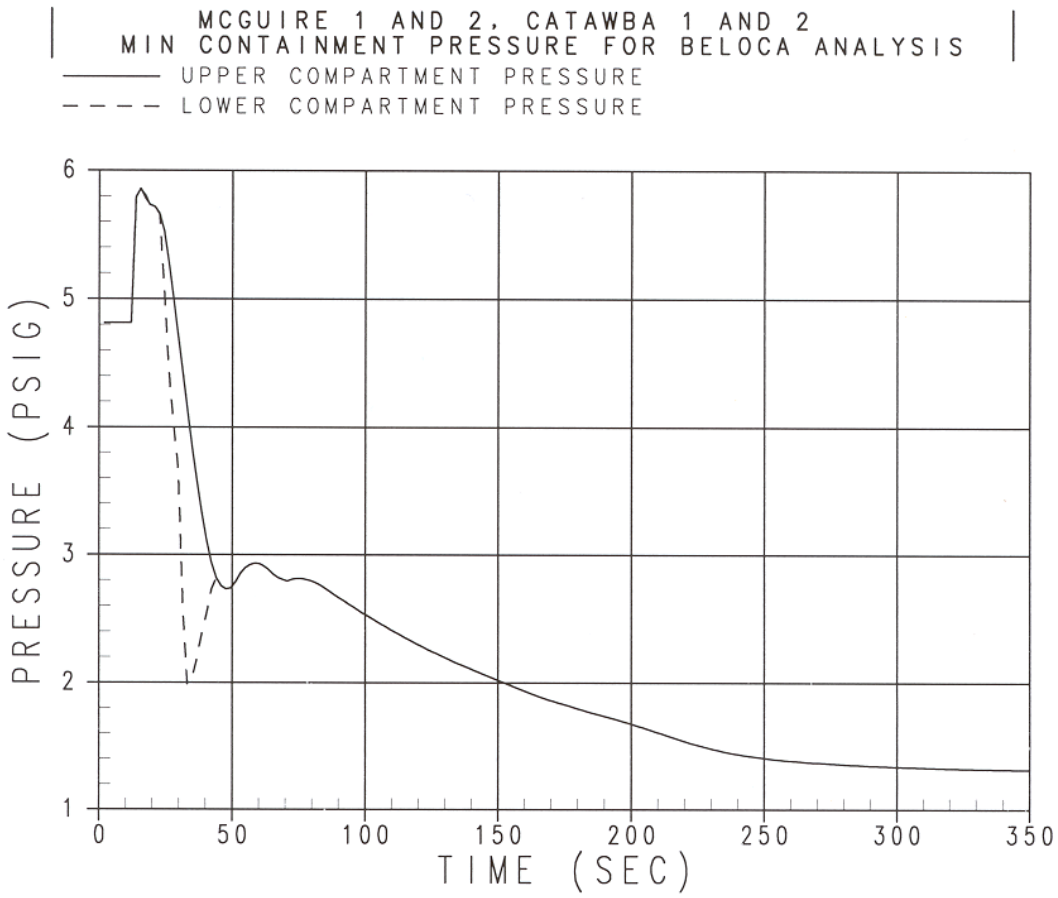

Figure 6-205. Upper Compartment Heat Removal Rate, Min. Pressure Analysis

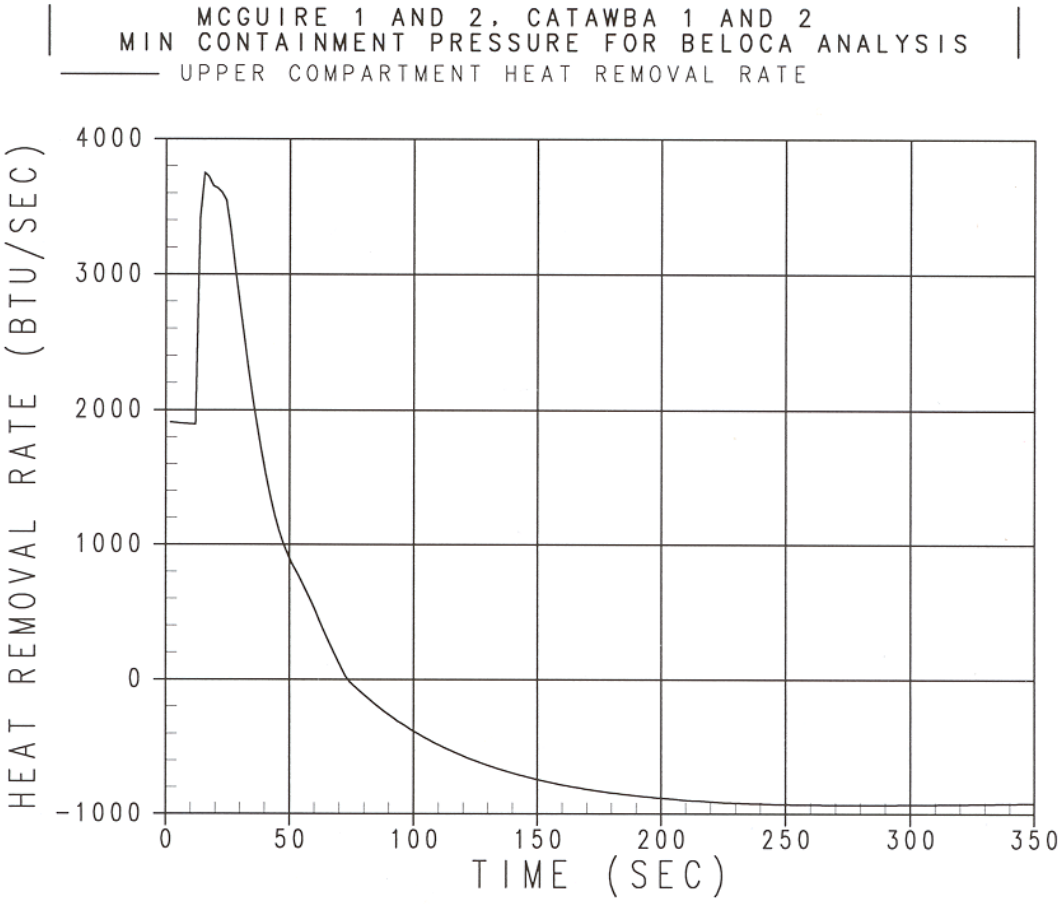

Figure 6-206. Lower Compartment Heat Removal Rate, Min. Pressure Analysis

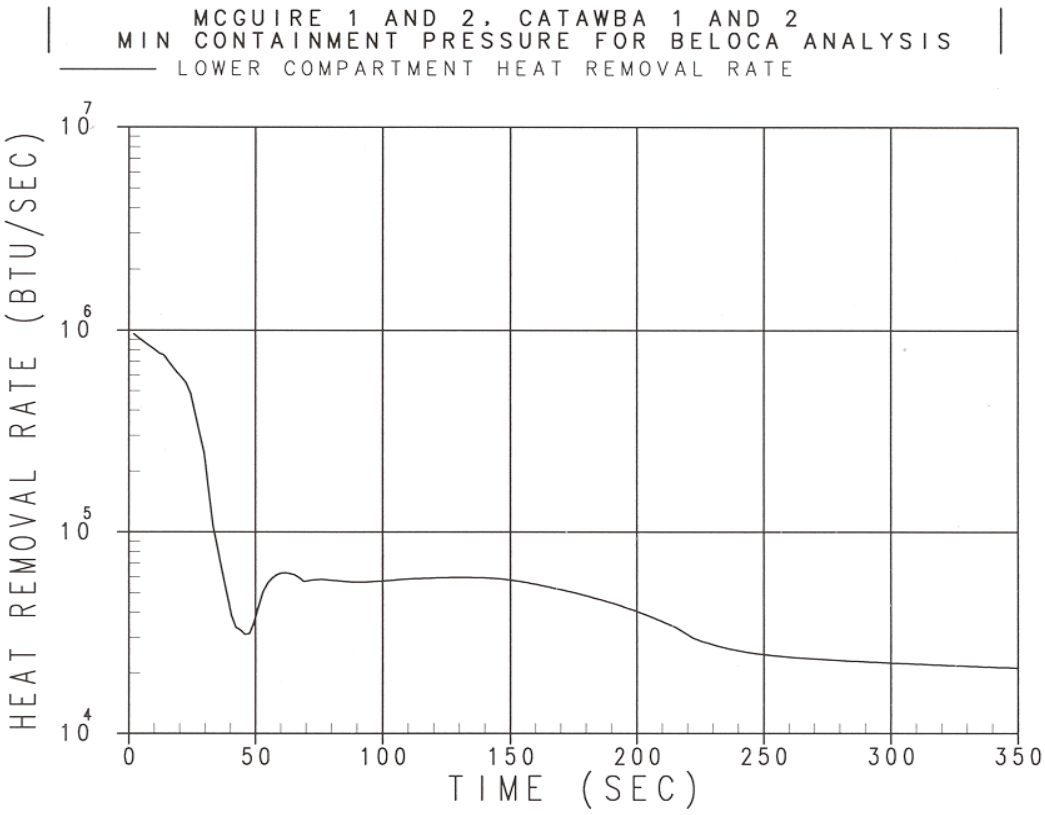

Figure 6-207. Upper and Lower Compartment Temperature, Min. Pressure Analysis

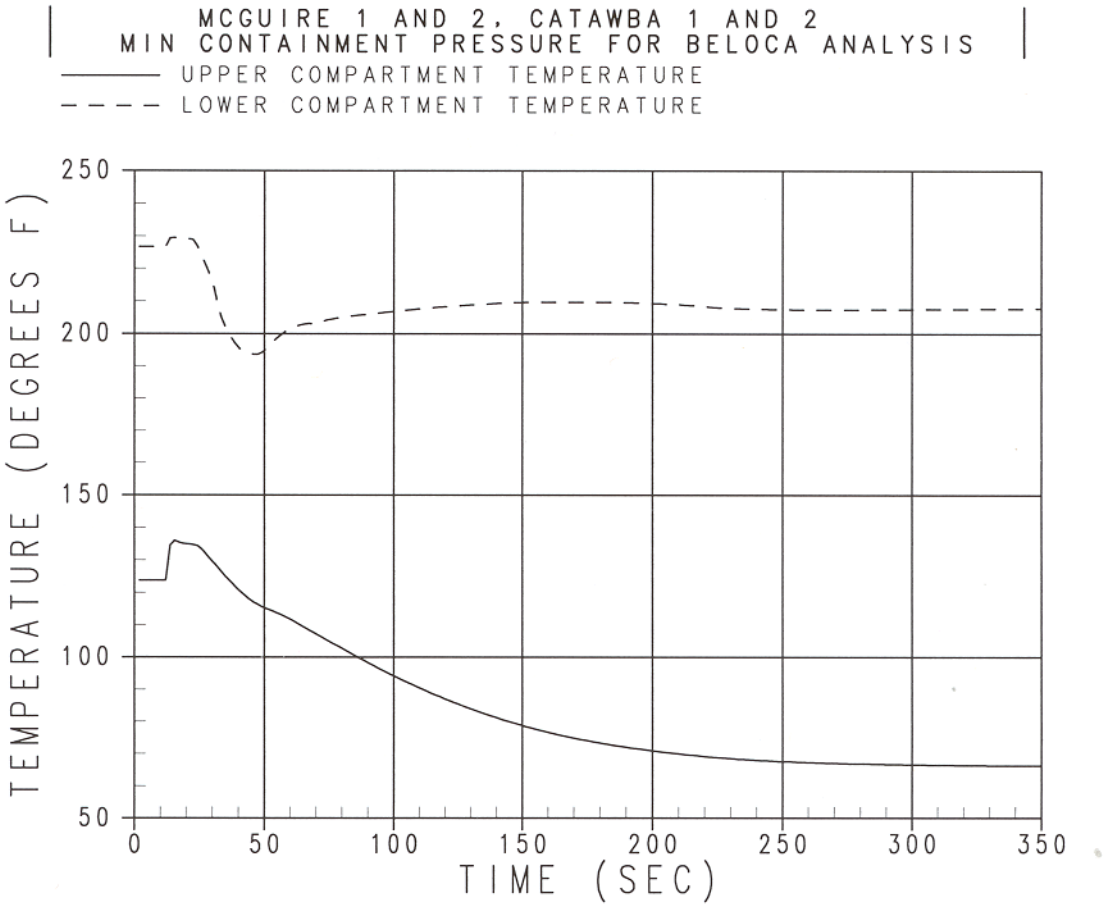

Figure 6-208. Ice Bed Heat Removal Rate, Min. Pressure Analysis

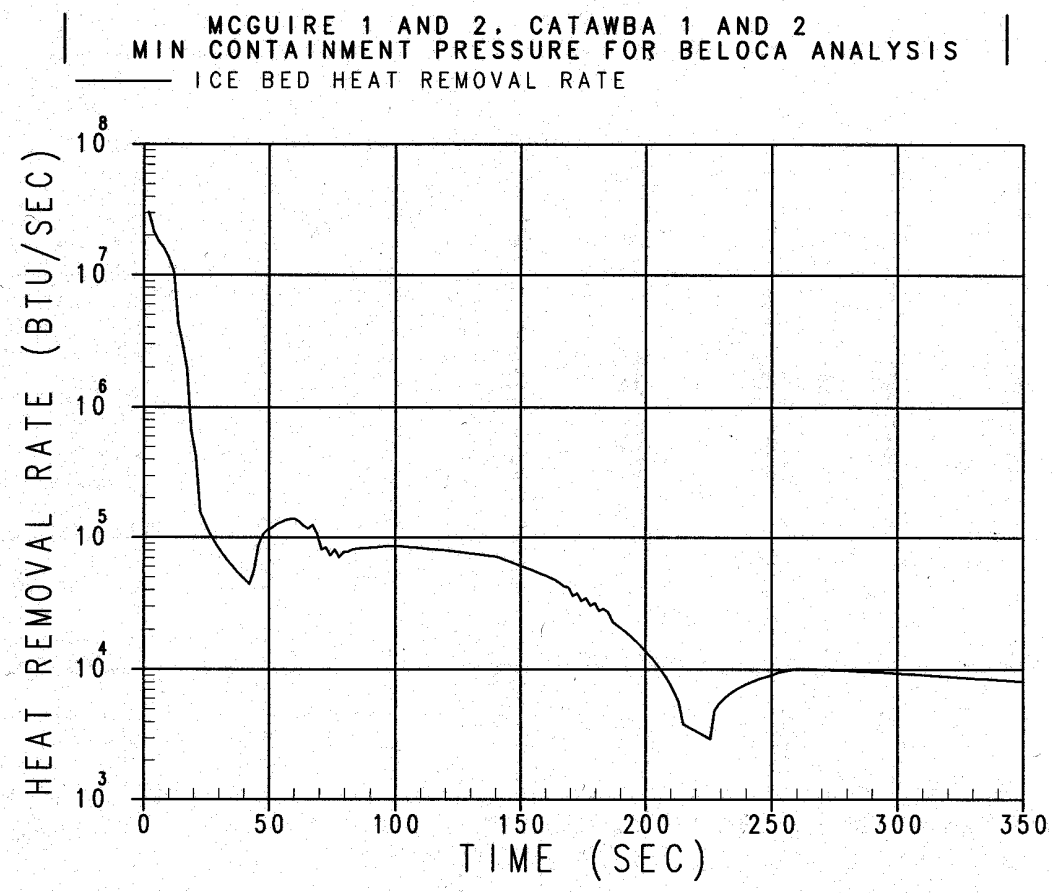

Figure 6-209. Heat Removal Rate by Lower Compartment Drain, Min. Pressure Analysis

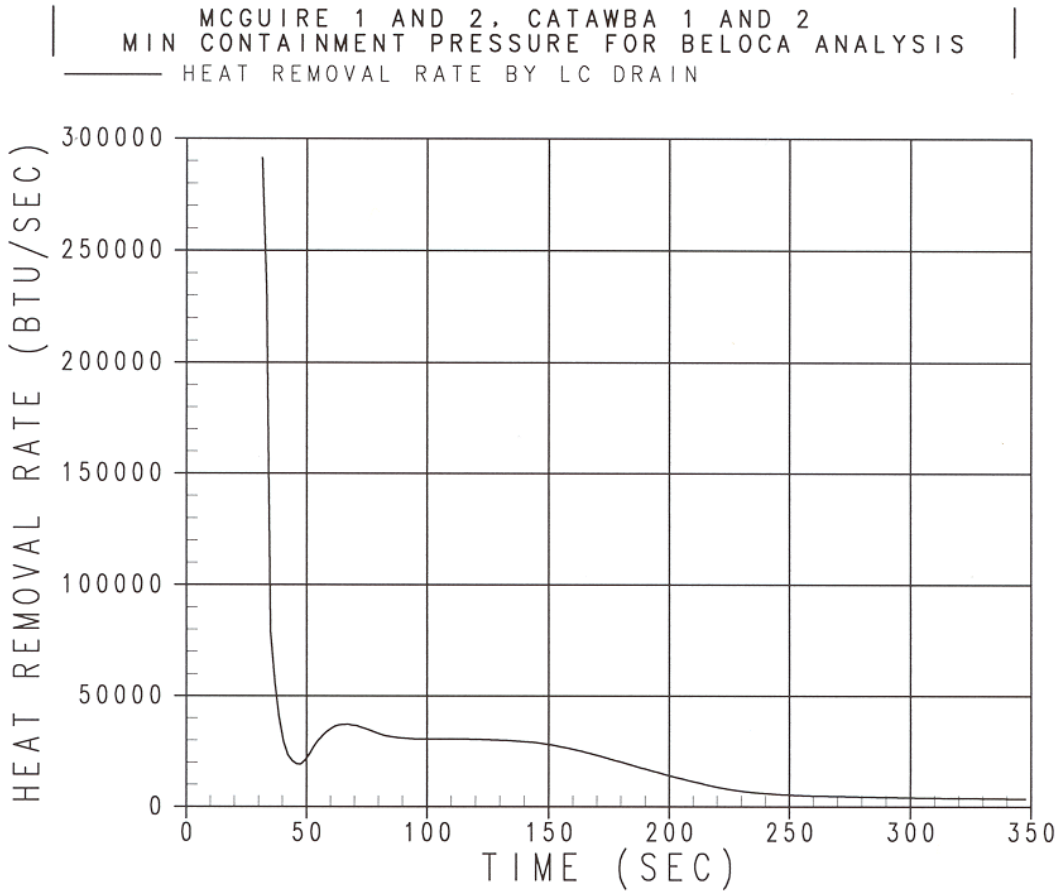

Figure 6-210. Heat Removal Rate by Sump and Spray, Min. Pressure Analysis